Role of VANGL1 as an effector of R-RAS

Nicole Hartig

A thesis submitted towards the degree of

Doctor of Philosophy

April 2013

Cell Signalling Laboratory

UCL Cancer Institute

72 Huntley Street, London

UCL Department of Biochemistry and Molecular Biology

University College London

Gower Street, London

Declaration

I, Nicole Hartig, confirm that the work presented in this thesis is my own. Where information has been derived from other sources, I confirm that this has been indicated in the thesis.

London, April 2013

In loving memory of my Mama Steffi

Abstract

The WNT pathway plays a key role in development and disease. In addition to the better studied ß-catenin dependent pathway, WNT ligands can also activate the separate 'non-canonical' or Planar Cell Polarity (PCP) pathway. Perturbations in the PCP pathway contribute to the pathogenesis of a variety of diseases including cardiac and neural tube defects, and to the invasiveness of cancer cells.

R-RAS subgroup GTPases share many of the properties of classical RAS GTPases including the ability to behave as oncogenes. However, they also have distinct functions of their own and how signalling and biological specificity is achieved is not fully understood. Using a proteomic approach to identify novel R-RAS subgroup effectors led to the identification of VANGL1, a WNT/PCP protein, demonstrated to be a novel R-RAS interacting protein.

In this thesis, I have shown that VANGL1 functions as an effector of R-RAS and TC21. Using proteomic approaches, multiple VANGL1 interacting proteins have been identified and R-RAS, as well as selected Frizzled (FZD) receptors and the tyrosine kinase ROR2 can modulate at least some of these VANGL1 interactions. Furthermore, VANGL1 leads to the protein degradation of PRICKLE by a mechanism that remains to be determined, and R-RAS GTPases are able to inhibit this effect.

Using RBD pulldown assays, I was able to show that WNT ligands and ROR2 can lead to the activation of R-RAS, and that R-RAS and TC21 are key mediators of RHO activation by WNT5a. Finally, I demonstrated that R-RAS/TC21 and VANGL1 are critically required for directed migration.

The identification of R-RAS activation by WNT ligands and its interaction with VANGL1 provides an exciting new link between the R-RAS subgroup of the RAS family and the WNT/PCP pathway.

Acknowledgments

First and foremost I would like to thank my supervisor Pablo Rodriguez-Viciana for giving me the opportunity to work in his laboratory, the supervision and guidance throughout my PhD studies and the final push during writing this thesis. I also want to thank my thesis examiners for their interest and time, and I am looking forward to our discussion.

I truly enjoyed my PhD time, thanks to an amazing group of work colleagues and students. In particular, I would like to thank Kristina for helpful discussions, interest and encouragement throughout my project. Work would have not been the same without Lucy, my partner in crime, who is a great team mate and friend. Thanks to Berna, even long days went by fast and never got dull due to creation of a fun work environment and her entertaining personality.

I also want to thank Marta, Ariadna, Giammy and Konstantinos for helpful experimental discussions and conversations about (PhD) life in general and guidance through the last 4 years.

A very warm thank you goes to Michiru Nishita and Prof Yasuhiro Minami and the rest of the very hardworking laboratory members at Kobe University for the wonderful and unique time in Japan, and especially for the experimental assistance during my stay.

A specific thank you goes to my family, who supported me all along during my studies and their interest in my work. Especially my beloved mum, who unfortunately is not able to experience this day – I miss you very much.

And last but not least, without my second family, the Jhalas, a big, fun and loving part of my life in London would be missing – I love you all!

The biggest gratitude I want to express is for Shiv, who supported me through the last three years, is always there for me, and is simply a wonderful person. Thank you for being at my side.

Thank you all for being part of my long and interesting PhD journey.

Table of Contents

List of Figures

List of Tables

Abbreviations

aa	amino acid
AF6	Acute lymphoblastic leukaemia-1 Fused gene on chr. 6
AMBRA	Activating Molecule Beclin-Regulated Autophagy
AP-1	Activator Protein-1
APC	Adenomatous Polyposis Coli
aPKC	atypical Protein Kinase C
ATGs	autophagy regulators
BBS	Bardet-Biedl Syndrome
BCR	B-Cell antigen Receptor
BGH	Bovine Growth Hormone
BSA	Bovine Serum Albumin
C17ORF62	Chromosome 17 Open Reading Frame 62
CamKII	Calcium/calmodulin-dependent Kinase II
CASK	CAlcium/calmodulin-dependent Serine protein Kinase
CBP	Calmodulin Binding Peptide
CE	Convergent Extension
CELSR	Cadherin, EGF LAG Seven-pass G-type receptor 1
CK	Casein Kinase
CM	Conditioned Media
CMV	Cytomegalovirus
CQ	Chloroquine
CRD	Cysteine Rich Domain
C-terminal	Carboxy-terminal
CTGF	Connective Tissue Growth Factors
CTHRC1	Collagen Triple Helix Repeat-Containing 1
CXCR2	CXC-motif chemokine Receptor 2
DAAM	DVL Associated Activator of Morphogenesis 1
DAB2IP	Doc-2/DAB2 Interactive Protein
DAG	Diacylglycerol
DAPI	4',6-diamidino-2-phenylindole

DEPC	Diethylpyrocarbonate
Dgo	Diego
DH	Dbl Homology
Dkk	Dickkopf
DLG1	Disks Large homolog 1
DMSO	Dimethyl Dulfoxide
DPI	Dots Per Inch
DTT	Dithiothreitol
DVL/Dsh	Dishevelled
ECM	Extracellular Matrix
E.coli	*Escherichia coli*
EGF	Epidermal Growth Factor
ERK	Extracellular signal Regulated Kinase
ETS	E26-Transcription factor proteins
FAK	Focal Adhesion Kinase
FBS	Foetal Bovine Serum
FL	Full Length
FLNa	Filamin A
FTase	Farnesyl Transferase
FZD	Frizzled
GAP	GTPase Activating Protein
GEF	Guanine nucleotide Exchange Factor
GMP-PNP	5'-Guanylyl imidodiphosphate
GPC3	Glypican 3
GPCR	G Protein Coupled Receptor
GSK3	Glycogen Synthase Kinase 3
GST	Glutathione S-Transferase
GTP	Guanosintriphosphat
GTPases	Guanosine Triphosphatases
HEK293T	Human Embryonic Kidney 293 T cells
HSPGs	Heparansulfate Proteoglycans
HVR	Hypervariable Region

ICMT1	Isoprenylcystein Carboxymethyltransferase 1
JNK	c-Jun NH2-terminal Kinase
KAI1/CD82	Kangai1/Cluster of Differentiation 82
LB	Luria Bertani
LiCl	Lithium Chloride
LIM	LIN-11, Isl1 and MEC-3
LC3	microtubule-associated protein 1 Light Chain 3
LDLR	Low-Density Lipoprotein Receptor
Lp	*loop tail*
LPHN2	Latrophilin 2
LRP	Low density lipoprotein-Related Protein
Ltap	Loop-Tail-Associated Protein
MAP	Mitogen-Activated Protein
MINK1	Misshapen-like Kinase 1
MMP	Matrix Metalloprotease
MOPS	3-(N-morpholino)propanesulfonic acid
MS	Mass Spectrometry
MST	Mammalian Sterile-20-like protein kinase-1
MTOC	Microtubule-Organizing Center
Myr	myristolated
NDFIP1	Nedd4 Family Interacting Protein 1
NF-AT	Nuclear Factor of Activated T cells
NMDAR	*N*-methyl-D-aspartate glutamate ligand-gated ion channel receptors
NMT	N-Myristoyltransferase
NTD	Neural Tube Defect
O/N	Overnight
PAK	p21-activated kinases
PBS	Phosphate Buffered Saline
PCP	Planar Cell Polarity
PCR	Polymerase Chain Reaction
PDZ	PSD-95-Discs-large-ZO-1;

PE	Phosphatidylethanolamine
PET	Polyethylene terephthalate
PI3K	Phosphatidylinositide 3-Kinases
PFA	Paraformaldehyde
PH	Pleckstrin Homology
PIP2	Phosphatidylinositol 4,5-bisphosphate
PIP3	Phosphatidylinositol (3,4,5)-triphosphate
PK	PRICKLE
PKA	cAMP-dependent Protein Kinase A
PKC	Protein Kinase C
PLC	Phospholipase C
PTM	Post Translational Modification
PP1	Protein Phosphatase 1
PP2A	Protein Phosphatase 2A
PRD	Proline Rich Domain
PTK7	tyrosine-Protein Kinase-like 7
PTKR	Protein Tyrosine Kinase Receptor
PTase	Palmitoyltransferase
PVDF	Polyvinylidene Fluoride
R1A	Protein Kinase A type 1 regulatory subunit alpha
RA	RAS Associating
RAB3GAP1	Rab3 GTPase-activating protein catalytic subunit
RAL	RAS-like
RALBP1	RAL-Binding Protein-1
RALGDS	RAL Guanine nucleotide Dissociation Stimulator
RASAL	RASGAP-Activating-Like
RASGRF	RAS-specific Guanine-nucleotide-Releasing Factor
RASGRP	RAS-specific Guanine-nucleotide-Releasing Protein
RASIP1	RAS Interacting Protein 1
RASSF	RAS Association domain-containing Family
RBD	RAS/RHO Binding Domain
RCE1	RAS Converting Enzyme-1

REM	RAS Exchange Motif
RHO	RAS Homologous
RHOGDI	RHO GDP Dissociation Inhibitor
RIN	RAS interaction/interference protein
RLIP76	76 kDa RAL-Interacting Protein
RFG	RAS Family GTPases
ROCK	Rho Associated Kinase
ROR2	Receptor tyrosine kinase-like Orphan Receptor
R-RAS	Related RAS
RSPO	R-Spondins
RT	Room Temperature
RT-PCR	Reverse Transcript PCR
RTK	Receptor Tyrosine Kinase
RYK	Receptor related to tyrosine Kinase
SBP	Streptavidine Binding Peptide
Scr	Scramble
SCRIB	SCRIBBLE
SDC	Syndecan
SEM	Standard Errors of the Means
SF9	*Spodoptera frugiperda*
sFRP	secreted Frizzled-Related Proteins
SH	SRC homology
SHOC2	soc-2 suppressor of clear homolog
SOS	Son of Sevenless
SOST	Sclerostin
Stbm	*Strabismus*
SYNJ2BP	Synaptojanin 2 Binding Protein
TAP	Tandem Affinity Purification
TAE	Tris-Acetate-EDTA buffer
TE	Tris-EDTA buffer
TCA	Trichloroacetic Acid
TCF	T-Cell Factor

TCR	T-Cell Receptor
TF8	Transcription Factor 8
TFF	Trefoil Family Factors
TIAM	T-cell lymphoma Invasion And Metastasis 1
TK	Tyrosine Kinase
TM4SF	Tetra Membrane Spanning Family
TM	Transmembrane domain
tri	trilobite
Ub	Ubiquitin
UFD1L	Ubiquitin Fusion Degradation 1-Like
UTR	Untranslated Region
VANGL1	Vang-like
WD40	WD40 repeat protein
Wg	Wingless
WGEF	Weak similarity GEF
WIF	WNT Inhibitory Factor
WNT	Wingless/Int-1
wt	Wild Type
YIF	Yip1 Interacting Factor

CHAPTER 1

INTRODUCTION

1 Introduction

Cancer is a diverse disease affecting one out of four people and is characterised among others by uncontrolled cell growth, evasion of apoptosis and invasion (Hanahan and Weinberg 2000; Hanahan and Weinberg 2011).
RAS proteins play critical roles in multiple biological processes including proliferation, differentiation and survival, and are one of the most frequently mutated oncogenes detected in human cancer with an incidence of about 30% (Barbacid 1987; Bos 1989; Campbell and Der 2004; Karnoub and Weinberg 2008).
Consequently, considerable efforts have been made to understand how RAS proteins work and how their transforming activity can be blocked therapeutically (Kloog and Cox 2000; Rodriguez-Viciana et al. 2005; Baines et al. 2011). In addition, a better understanding of the full spectrum of effector pathways regulated by RAS proteins is critical for comprehension of their many biological functions and their contribution to human disease in order to develop more specific treatment options (Rodriguez-Viciana et al. 2004).

1.1 RAS superfamily

The RAS superfamily of small guanosine triphosphatases (GTPases) consists of over 150 human members and is subdivided into at least five major branches based on structural homology, sequence and function (RAS, RHO, RAB, ARF, and RAN subfamilies) (Figure 1.2A) (Wennerberg et al. 2005; Karnoub and Weinberg 2008).

GTPases act as nucleotide driven switches, cycling between an inactive GDP-bound and an active GTP-bound state (Figure 1.1). The transition from an inactive to active conformation is achieved by guanine nucleotide exchange factors (GEFs), which stimulate the dissociation of GDP and subsequent exchange to GTP (Schmidt and Hall 2002). This in turn induces a conformational change, enabling the respective GTPase to recognise downstream targets, termed effector proteins. The active state is terminated by the antagonising effect of GTPase activating proteins (GAPs), which accelerate the intrinsic GTPase activity of RAS proteins by several orders of magnitude, rendering the GTPase GDP-bound, and consequently inactive (Takai et al. 2001; Bernards and Settleman 2004).

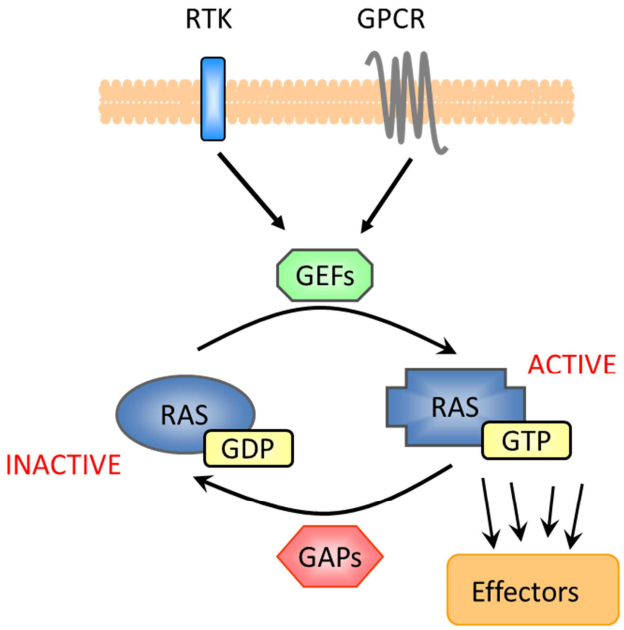

Figure 1.1: RAS proteins cycle between a GTP-bound active and a GDP-bound inactive state. Receptor tyrosine kinases (RTK), G-protein coupled receptors (GPCR) and other types of membrane receptors (not shown) are able to activate guanine exchange factors (GEFs), which in turn stimulate GDP release and GTP exchange. Binding of GTP induces a conformational change within the switch 1 and switch 2 region of RAS proteins, enabling effector interaction. This state is terminated by GTPase activating proteins, enhancing RAS poor intrinsic GTPase activity, rendering the protein GDP-bound and thus inactive.

1.2 RAS subfamily

RAS proteins are highly conserved and are found in all organisms from yeast to human (DeFeo et al. 1981; Chang et al. 1982; Takai et al. 2001; Wennerberg et al. 2005). Within the RAS superfamily, RAS lends its name to a subgroup consisting of at least 39 members encoded by 36 genes in the human genome (Figure 1.2). The best-studied genes of this family are the classical RAS proteins encoded by *H-RAS, K-RAS*, and *N-RAS* genes (Figure 1.2B, blue square).

RAS proteins serve as signalling hubs, activated in response to a wide range of extracellular stimuli, regulate cytoplasmic signalling networks that control gene expression and regulation of cell proliferation, differentation and survival (Wennerberg et al. 2005; Karnoub and Weinberg 2008). Because of their critical

roles in human oncogenesis they are the focus of intense research (Downward 2003; Repasky et al. 2004; Roberts and Der 2007).

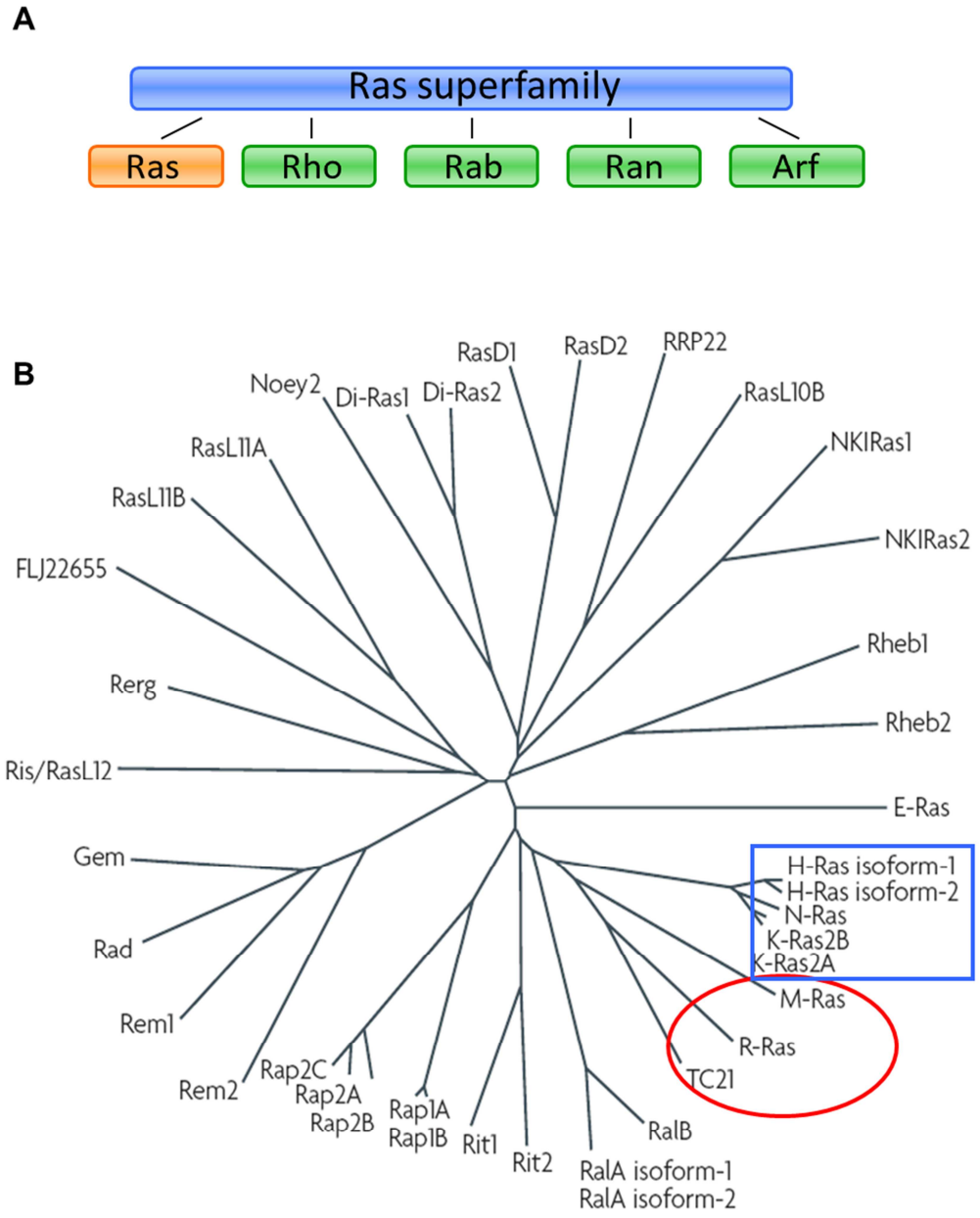

Figure 1.2: Overview of RAS subfamily proteins. (A) The RAS superfamily is divided in five major families based on structure homology and function. **(B)** To date, 39 RAS proteins are known, encoded by 36 genes in the human genome. Blue square highlights the classical H-, K-, and N-RAS proteins. Red circle indicates the RAS related subgroup (R-RAS branch), which share many biological functions with classical RAS proteins such as the ability to act as oncogenes. Parts of the figure were taken from Karnoub and Weinberg, 2008.

1.2.1 RAS regulatory proteins: GEFs and GAPs

RAS signalling activity is regulated by RASGEFs and RASGAPs, mediating RAS GDP/GTP bound state. Eight RASGEFs are encoded by mammalian genomes and include two isoforms of Son of Sevenless (SOS), two RAS specific guanine-nucleotide releasing factor (RASGRF) proteins and four RAS specific guanine nucleotide releasing protein (RASGRP) members (Figure 1.3 and Figure 1.4A) (Vigil et al. 2010).

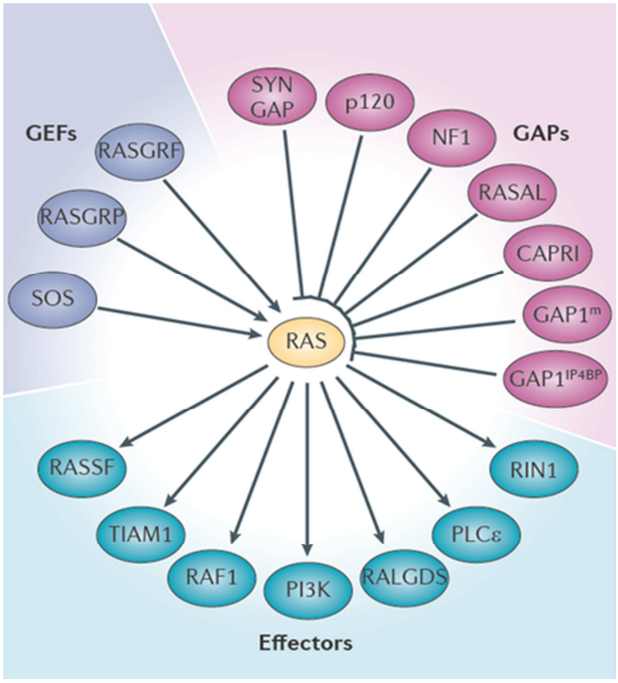

Figure 1.3: RAS regulatory proteins and effectors. RAS proteins are activated through guanine exchange factors (GEFs) of the Son of Sevenless (SOS), RAS-specific guanine-nucleotide-releasing protein (RASGRP) and RAS-specific guanine-nucleotide-releasing factor (RASGRF) families. GEFs facilitate the exchange from GDP to GTP and thus render RAS GTP bound, which then interacts with various downstream effectors modulating cellular processes such as gene expression, proliferation, survival, cell cycle entry, cytoskeletal dynamics and differentiation. Termination of the signal is achieved by RAS GTPase activating proteins (GAP), strongly enhancing RAS protein intrinsic GTPase activity and thus rendering RAS GDP-bound and thus inactive. For more details see text. CAPRI-calcium-promoted RAS inactivator, $GAP1^{IP4BP}$-GAP1 InsP4-binding protein, MEK-MAPK/ERK kinase; NF1-neurofibromin 1, PLCε-phospholipase Cε, PI3K-phosphoinositide 3-kinase, RALGDS-RAL guanine nucleotide dissociation stimulator, RASAL-RASGAP-activating-like, RASSF-RAS association domain-containing family, RIN1-RAS and RAB interactor 1, SYNGAP-synaptic RASGAP, TIAM1-lymphoma invasion and metastasis-inducing 1. Figure taken from Ahearn et al., 2012.

The best characterised GEF is SOS due to its role downstream of receptor tyrosine kinases (RTKs) (Figure 1.7) (Yang et al. 2013). Each GEF contains a CDC25 homology catalytic domain, which stimulates the release of GDP, and is flanked by at least one adjacent RAS exchange motif (REM) (Figure 1.4A). The Dbl homology domain (DH) mediates GDP/GTP exchange on RHO GTPases (Rossman et al. 2005), and is located adjacent to the pleckstrin homology (PH) domain, which facilitates membrane association. SOS specific histone homology domains interact with negatively charged phospholipids (Figure 1.4A) (Yadav and Bar-Sagi 2010).

Similar to SOS, RASGRFs also contain tandem REM-CDC25 and DH-PH domains, in addition to calmodulin-binding motif containing conserved I and Q residues (Figure 1.4A). RASGRF promotes RAS activation downstream of *N*-methyl-D-aspartate glutamate ligand-gated ion channel receptors (NMDARs) through receptor stimulated Ca^{2+} influx (Krapivinsky et al. 2003; Tian et al. 2004).

Both SOS and RASGRF exhibit a dual specificity for RAS and RAC GTPases, providing a link between RAS activation and the function of RAS and RHO proteins (Fan et al. 1998; Kiyono et al. 1999; Kiyono et al. 2000; Wennerberg and Der 2004).

RASGRPs, also termed CalDAG-GEFs, form a group which is activated by diacylglycerol (DAG) and phorbol ester. They share a common domain architecture of a REM-CDC25 tandem domain, followed by a pair of Ca^{2+} binding atypical EF hands and C1-protein kinase C conserved region 1, able to bind DAG and phorbol esters (Figure 1.4A) (Mitin et al. 2006). Among the four members, variations in GTPase specificity, expression, subcellular localisation and signal regulation have been observed. RASGRP3 is reported to exhibit the broadest GTPase substrate specificity, including RAP1 and RAP2 (Figure 1.5) (Mitin et al. 2006).

RAS activity is negatively regulated through GAPs, stimulating RAS poor intrinsic GTPase activity by several orders of magnitude through stabilising the transition state of the nucleophilic attack of water, mediated by insertion of an 'Arg finger', thus terminating signalling (Bernards 2003; Bernards and Settleman 2004).

RASGAPs share a common ~250 amino acid RASGAP catalytic domain, but otherwise do not shows sequence similarity or consistent domain structures in the adjacent RASGAP flanking regions (Figure 1.4B) (Bernards and Settleman 2004).

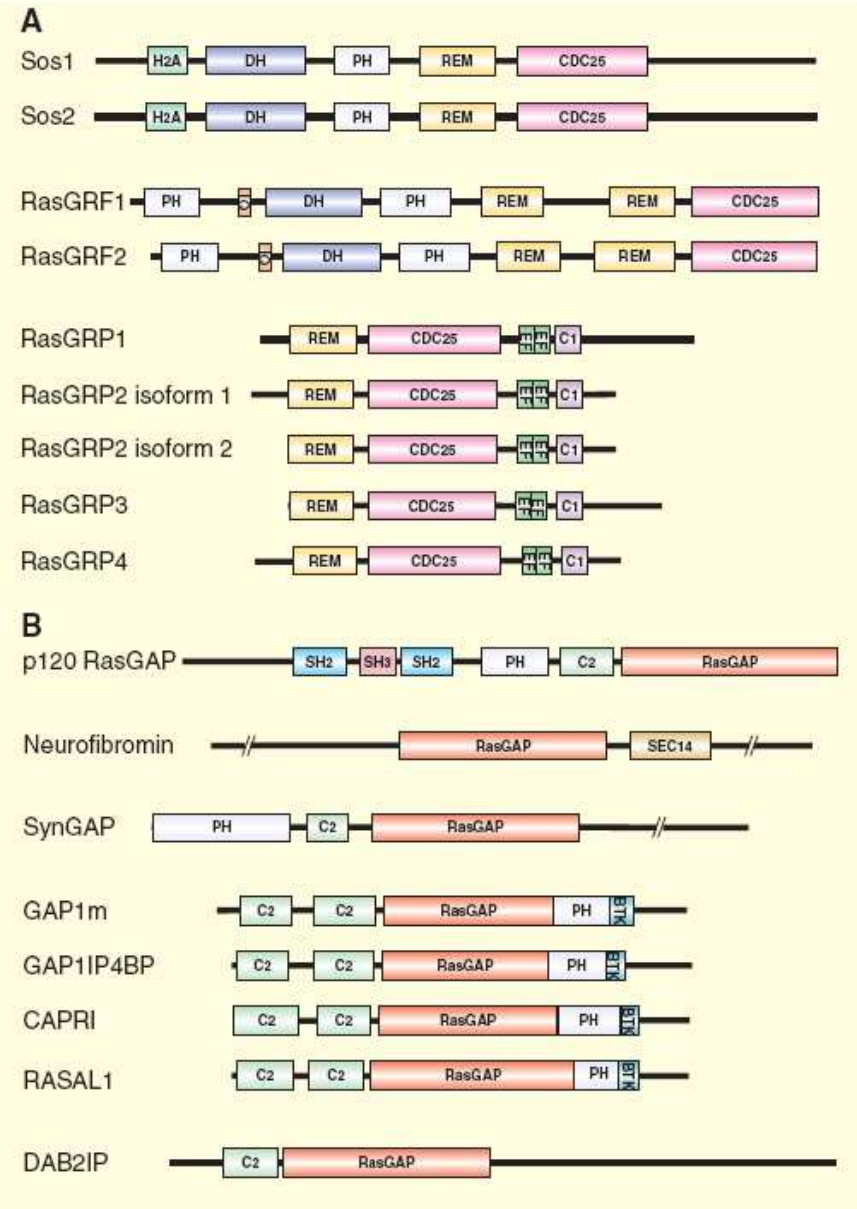

Figure 1.4: Domain overview of RAS regulatory proteins. (A) RAS specific GEFs. In addition to the CDC25 domain, SOS and RASGRF contain Dbl homology (DH) and pleckstrin (PH) domains. Other domains found in RASGEFs include: H2A-histone 2A homology, IQ-short calmodulin-binding motif containing conserved I and Q residues, EF-Ca^{2+}-binding EF hand, and C1-protein kinase C conserved region 1, which binds DAG and phorbol esters. **(B)** RAS specific GAPs. RASGAPs have a common ~250 amino acid α-helical catalytic domain (RasGAP). Other RASGAPs domains include: SH2-Src homology 2, SH3-Src homology 3, PH, C2-protein kinase C conserved region 2, serving as a Ca^{2+}-dependent lipid-binding motif, Sec14-Sec14p-like lipid-binding domain and BTK-Bruton's tyrosine kinase cysteine-rich zinc-binding motif. Figure from Mitin et al, 2005.

There are eight RAS specific GAPs known, of which p120 RASGAP/RASA1 and the tumour suppressor neurofibromin are the best studied (Dasgupta and Gutmann 2003; Bernards and Settleman 2004). Others are the synaptic RASGAP/SYNGAP, $GAP1^{m}$/RASA2, $GAP1^{IB4BP}$/RASA3, and the two calcium activated GAPs CAPRI/RASA4 and RASGAP-activating-like (RASAL) (Figure 1.4B) (Mitin et al. 2006; Rojas and Santos 2006).

Despite the similar domain structure of $GAP1^{m}$, $GAP1^{IB4BP}$, CAPRI and RASAL, these RASGAP members exhibit different modes of regulation and plasma membrane association. $GAP1^{m}$ exhibits a distinct perinuclear and cytosolic localisation, which translocates to the plasma membrane upon EGF stimulation. In contrast, $GAP1^{IB4BP}$ displays a constitutive plasma membrane association (Lockyer et al. 1997; Cozier et al. 2000), and its RASGAP activity might be regulated through inositol 1,3,4,5 tetrakisphosphate (Cullen et al. 1995).

Both CAPRI and RASAL undergo Ca^{2+} stimulated C2-dependent plasma membrane association (Lockyer et al. 2001; Walker et al. 2004). In summary, Ca^{2+} regulation is able to control activities of RASGAPs and RASGEFs.

Protein	Other activities	Substrates
GEFs		
Sos1	RacGEF	H-Ras, N-Ras, K-Ras, R-Ras2, R-Ras3, Rac1; not R-Ras
Sos2	RacGEF	H-Ras
Ras-GRF1	RacGEF	H-Ras, K-Ras[1], N-Ras[1], R-Ras, R-Ras2, R-Ras3, Rac1; not K-Ras[1], N-Ras[1], Rap1
Ras-GRF2	RacGEF	H-Ras, Rac1; not R-Ras
RasGRP1 (CalDAG-GEFII)	DAG-, Ca^{2+}-binding	H-Ras, N-Ras, R-Ras, R-Ras2, R-Ras3; not Rap1A
RasGRP2 (CalDAG-GEFI)	DAG-, Ca^{2+}-binding	N-Ras, K-Ras, R-Ras, R-Ras2, Rap1A, Rap2A; not H-Ras
RasGRP3 (CalDAG-GEFIII)	DAG-, Ca^{2+}-binding	H-Ras, R-Ras, R-Ras2, R-Ras3, Rap1A, Rap2B
RasGRP4	DAG-, Ca^{2+}-binding	H-Ras
GAPs		
p120 RasGAP	p190 RhoGAP-binding	H-Ras, N-Ras, R-Ras, R-Ras2, R-Ras3, Rab5; not Rap proteins
Neurofibromin		H-Ras, K-Ras, N-Ras, R-Ras, R-Ras2, R-Ras3; not Rap1A
SynGAP		H-Ras
$GAP1^{IP4BP}$ (R-Ras GAP)	Inositol 1,3,4,5-tetrakisphosphate-binding	H-Ras, R-Ras, R-Ras2, Rap1A
$GAP1^{m}$	PIP_3-binding; Ga_{12}	H-Ras, R-Ras, R-Ras2, R-Ras3; not Rap1A
RASAL1	Ca^{2+}-binding	H-Ras
CAPRI	Ca^{2+}-binding	H-Ras
DAB2IP (DIP1/2)	DOC-2/DAB2-binding	H-Ras, K-Ras, R-Ras, R-Ras2; not Rap1A

Figure 1.5: Overview of RASGEF and RASGAP GTPase substrate specificity. [1]Conflicting reports for substrate specificity have been made. Figure from Mitin et al, 2006.

SYNGAP is expressed primarily in the brain and localises to glutamatergic synapses and is positively regulated through phosphorylation of calcium/calmodulin-dependent kinase II (Oh et al. 2004).

Doc-2/DAB2 interactive protein (DAB2IP) has been demonstrated to exhibit RASGAP activity *in vitro*, and its gene expression has been reported to be reduced in certain cancers (Wang et al. 2002).

1.2.2 RAS protein effectors

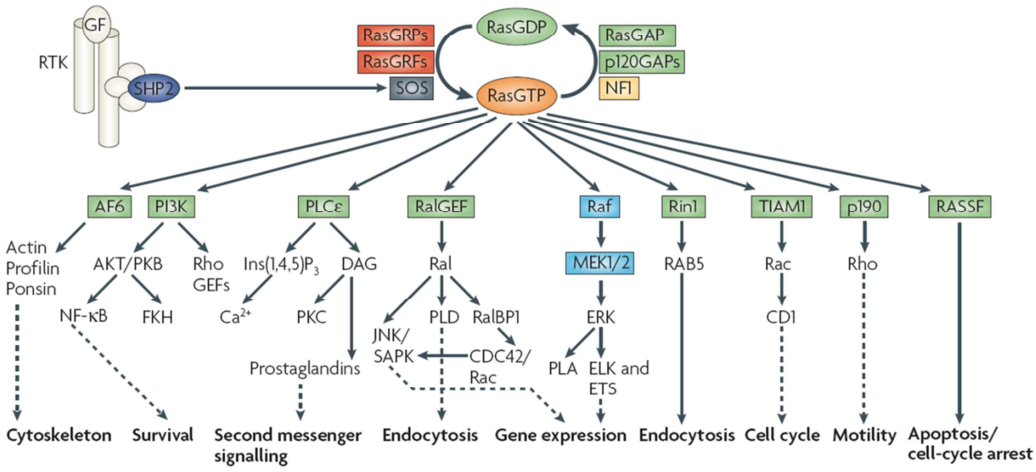

Figure 1.6: RAS effector pathways. Upon stimulation, RAS proteins interact with a multitude of effector proteins involved in various cellular processes. See section 1.2.1 and 1.2.2 for details. Abbreviations are: AF6-acute lymphoblastic leukaemia-1 fused gene on chromosome 6, CD1-cadherin domain-1, CDC42-cell division cycle-42, ELK-ETS-like protein, ERK-extracellular signal regulated kinase, ETS-E26-transcription factor proteins, Ins(1,4,5)P3-inositol-1,4,5-trisphosphate, JNK-Jun N-terminal kinase, MEK-mitogen-activated protein kinase/ERK kinase, NF-κB-nuclear factor-κB, PI3K-phosphoinositide 3-kinase, PKB/C-protein kinase B/C, PLA/Cε/D- phospholipase A/Cε/D, RalBP1-Ral-binding protein-1, RASSF-RAS association domain-containing family, Rin1-RAS interaction/interference protein-1, SAPK-stress-activated protein kinase, SHP2-Src-homology 2 domain-containing protein Tyr phosphatase-2, TIAM1-T-cell lymphoma invasion and metastasis-1. Figure from Karnoub and Weinberg 2008.

The first identified and also best characterised RAS effectors were RAF serine/theonine kinases (Moodie et al. 1993; Vojtek et al. 1993; Warne et al. 1993; Zhang et al. 1993; Wellbrock et al. 2004), through which RAS activates the growth-regulatory mitogen-activated protein (MAP) kinase cascade and the E26-transcription factor proteins (ETS) (Figure 1.7) (Ahearn et al. 2012). This pathway has been demonstrated to be necessary and sufficient for RAS induced transformation of murine cells (Leevers et al. 1994; Stokoe et al. 1994; Khosravi-Far et al. 1995; White et al. 1995). The identification of *BRAF* mutations in cancers, generally in a mutually exclusive manner with *RAS* mutations, underscores the importance of a this pathway downstream of RAS function and in oncogenesis (Rajagopalan et al. 2002).

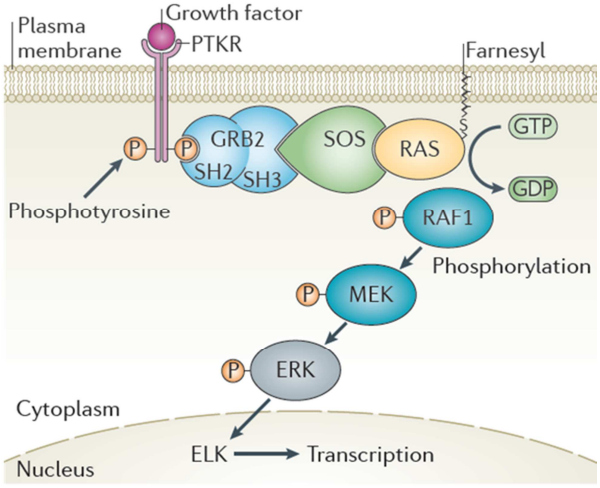

Figure 1.7: The RAS-RAF-ERK signalling pathway. Upon stimulation of a protein tyrosine kinase receptor (PTKR) with growth factors, the cytoplasmic GRB2-SOS complex is recruited to the plasma membrane through association of the GRB2-SH2 domain to phosphorylated residues of the activated receptor. Interaction of the PH domain of SOS with phospholipids induces a conformational change which allows binding of membrane localised RAS and leads to its activation through GTP loading. RAS then initiates downstream signalling through recruitment of RAF1 to the membrane and stimulation of its kinase activity. RAF kinases then phosphorylate and activate MEK, which then activates ERK, followed by phosphorylation and activation of multiple transcription factors including ELK. Figure from Ahearn et al, 2012.

The second best characterised RAS effectors are the p110 (α, β, γ and δ) catalytic subunit of class I Phosphoinositide 3-kinases (PI3K) (Rodriguez-Viciana et al. 1994; Castellano and Downward 2010). PI3K signalling mediates cell

growth, proliferation, differentiation, motility, survival and intracellular trafficking, which if deregulated, results in cancer (Cain and Ridley 2009; Vanhaesebroeck et al. 2012).

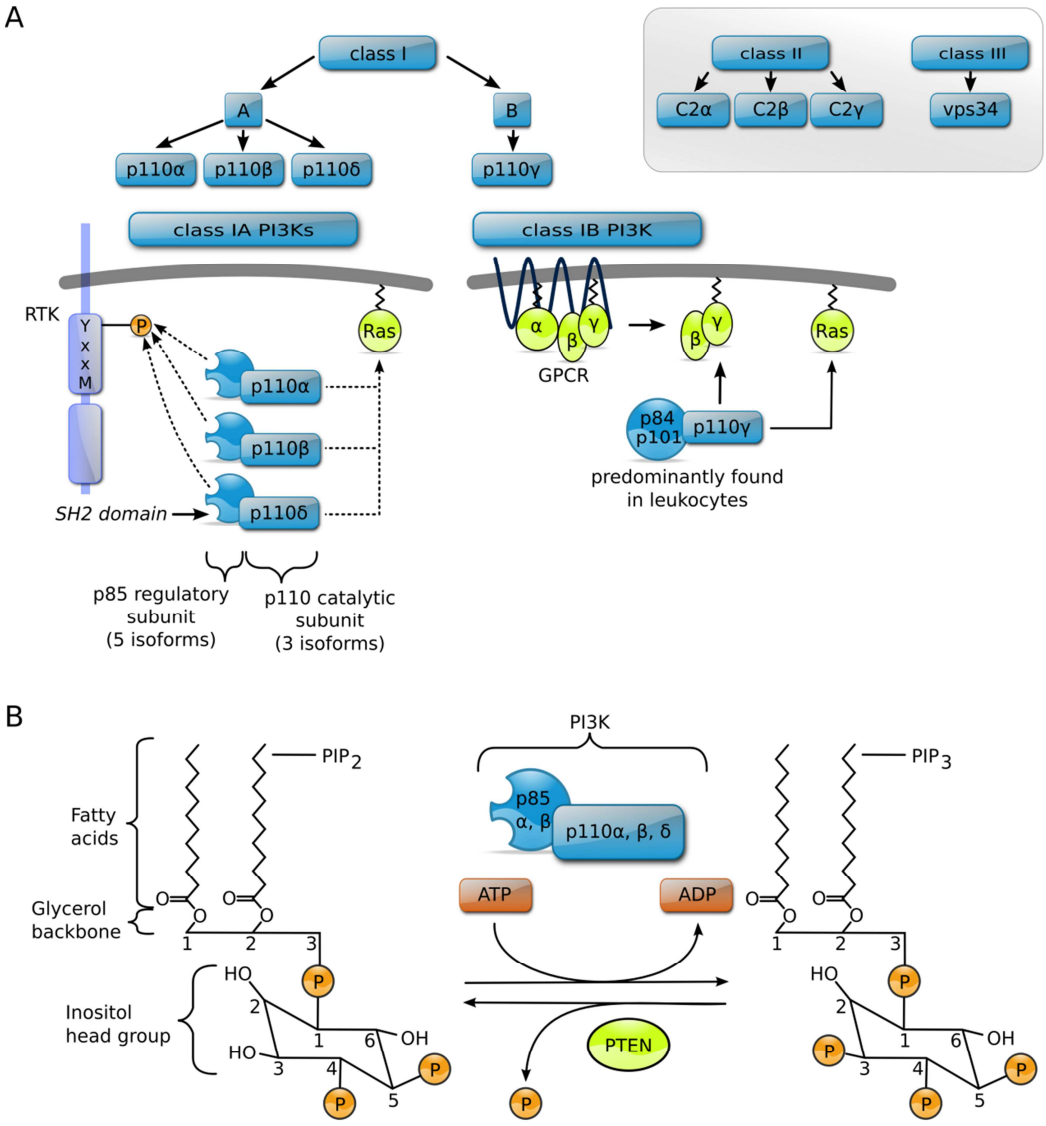

Figure 1.8: Phosphoinositide 3-kinases are RAS effectors. (A) PI3K are activated through binding of the regulatory p85 subunit the SRC homology (SH2) domain to the phosphorylated receptor YxxM motif or through RAS binding of the catalytic subunits in a GTP dependent manner. Class IA PI3Ks are activated through receptor tyrosine kinases (RTKs), whereas Class IB PI3K are either G-protein couple receptor (GPRC) or RAS activated. **(B)** The catalytic subunit of PI3K comprises a lipid kinase activity and catalyses phosphorylation of Phosphatidylinositol 4,5-bisphosphate (PIP2) to Phosphatidylinositol (3,4,5)-triphosphate (PIP3). PTEN- Phosphatase and tensin homologue.

PI3Ks generate lipid second messengers by phosphorylation of phosphoinositides at the 3' position (Class I: phosphatidylinositol (3,4,5)-triphosphate) (Figure 1.8), which then recruit and bind downstream effectors such as AKT or lead to stimulation of RAC and RHO through respective GEF activation (Welch et al. 2003; Costa et al. 2007; Cain and Ridley 2009).

Both described pathways, MAPK and PI3K, display a critical role in RAS mediated oncogenesis, supported by the frequent mutational activation of *BRAF* (13%, COSMIC database, www.sanger.ac.uk/genetics/CGP/cosmic) and *PIK3CA* (19%).

RAL guanine nucleotide dissociation stimulator (RALGDS) was the first of RAL (RAS-like) exchange factors (RALGEFs) identified to be RAS effector proteins (Kikuchi et al. 1994; Spaargaren and Bischoff 1994). RALGDS possesses sequence homology with the REM and CDC25 domains found in RASGEFs. However, studies revealed that RALGDS does not display an exchange activity for RAS and rather is selective for RALA and RALB (Neel et al. 2011).

RAL interacts with multiple, functionally divergent downstream effector proteins involved in endocytosis, exocytosis, actin organisation, phosholipid metabolism and second messenger generation (Figure 1.9) (Neel et al. 2011). Effectors are RALBP1 (Ral binding protein 1)/RLIP76 (76 kDa Ral-interacting protein) (Cantor et al. 1995; Jullien-Flores et al. 1995), the octameric exocyst complex including Sec5 and Exo84 (Moskalenko et al. 2002; Moskalenko et al. 2003), Phospholipase C delta 1 (PLCδ1) (Sidhu et al. 2005), or the actin filament crosslinking protein FilaminA required for RALA induced filopodium formation (Ohta et al. 1999; Ohta et al. 2006).

In addition, RAS GTPases interact with a wide array of other effectors that are less well characterised. RAS interaction/interference protein 1 (RIN1) has been described as a GEF for RAB5-like proteins, implicated in endocytosis downstream of RAS stimulating growth factors such as EGF (Han and Colicelli 1995; Tall et al. 2001).

T-cell lymphoma invasion and metastasis 1 (TIAM1) has been described as a RAS effector and acts as a RAC specific GEF, that links RAS signalling to RAC, which regulates the actin cytoskeleton and stimulates p21-activated kinases (PAK) and c-JUN activated kinase (JNK) (Lambert et al. 2002). TIAM deficient

mice displayed a resistance to RAS induced skin carcinogenesis, suggesting that TIAM activity is required for RAS transformation (Malliri et al. 2002).

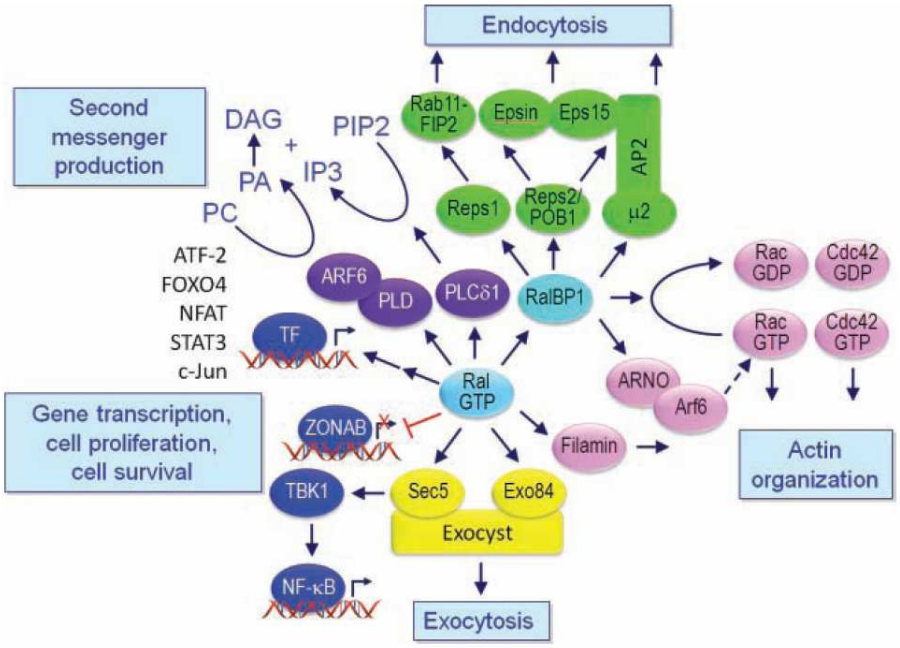

Figure 1.9: Overview of RAL effectors and associated signalling pathways. RAL downstream effectors mediate endocytosis, exocytosis, actin re-organisation, phospholipid metabolism and generation of second messengers. Also, RAL has been shown to activate various transcription factors and to regulate gene expression. PC-phosphadidylcholine, PA-phosphatidic acid. Figure from Neel et al., 2011.

ALL (acute lymphoblastic leukaemia) 1 fused gene on chromosome 6 (AF6) or AFADIN was identified by RAS-GTP affinity chromatography (Kuriyama et al. 1996), and has been characterised to contain both microtubule and actin binding motifs, suggesting that AF6 might participate in cytoskeletal processes downstream of RAS (Ponting and Benjamin 1996). Indeed, studies suggest that AF6 associates with proteins that are involved in regulation of polarity, and to localise to adherens junctions (Mandai et al. 1997).

Activation of the RAS effector Phospholipase C-ε (PLCε) leads to generation of diacylglycerol through the cleavage of Phosphatidylinositol 1,4,5-bisphosphate into Phosphatidylinositol (4,5)-triphosphate. This in turn promotes the release of Ca^{2+} and the activation of PKC (Kelley et al. 2001; Song et al. 2001).

RAS association domain-containing family 5 (RASSF5) also known as NORE1 has been identified as a RAS effector protein (Vavvas et al. 1998), which possesses pro-apoptotic functions (Khokhlatchev et al. 2002; Vos et al. 2003) and a potential involvement in cell migration (Dallol et al. 2005). Although the functional mechanism is not fully elucidated yet, preliminary evidence links RASSF proteins to the mammalian sterile-20-like protein kinase-1 (MST1) and MST2, and to the Hippo signalling pathway (Tommasi et al. 2005; Cho et al. 2006; Varelas et al. 2010; Heallen et al. 2011).

In mitogenically stimulated cells, a complex formation of a RASGAP and the cellular protein p190 has been observed (Moran et al. 1991). p190 contains a carboxy-terminal domain that functions as a GAP for the RHO family GTPases, and thus the RASGAP-p190 complex may serve to couple RAS- and RHO-mediated signalling pathways.

More recent and less well characterised RAS effectors are the RAS interacting protein 1 (RASIP1), also known as RAIN, which is required for endothelial cell motility, angiogenesis and vessel formation (Xu et al. 2009; Xu et al. 2011). The regulator of G-protein signalling 14 (RGS14) has been demonstrated to facilitates the formation of a selective RAS-GTP/RAF/MEK/ERK multi-protein complex to promote sustained ERK activation, which regulates H-RAS dependent neuritogenesis (Willard et al. 2007; Willard et al. 2009). The protein impedes mitogenic signal propagation (IMP1A) E3 ligase member acts as a steady-state resistor within the RAF/MEK/ERK kinase module, and is directly regulated by RAS (Matheny et al. 2004; Matheny and White 2009).

1.2.3 Structural features of RAS proteins

RAS proteins share a highly conserved G domain, involved in Mg^{2+} and nucleotide binding and nucleotide hydrolysis (residues 1-164). The exchange of GDP to GTP leads to conformational changes in two stretches of the protein, the switch I (Asp30 - Asp38) and switch II (Gly59 – Glu67) regions, located close to the γ-phosphate group of the activating GTP. The third structurally important element of RAS GTPases is the P-loop (Gly10 – Ser17), which winds around the β- and γ-phosphates and contributes to most of the required energy for GTP binding (Figure 1.10) (Milburn et al. 1990).

Overlapping with switch I is the core RAS effector domain (Tyr32 - Tyr40), also known as effector loop, which is important for downstream interactions with effectors or inactivating proteins like GAPs (Figure 1.10) (Wennerberg et al. 2005).

Single amino acid activating mutations in *RAS* genes are frequently detected in human cancers (Cox and Der 2010). For example, replacement of P-loop located Gly12 residue in H-RAS with any other amino acid except proline results in an increased tumour transforming potential due to its importance for GTP binding (Clark et al. 1985).

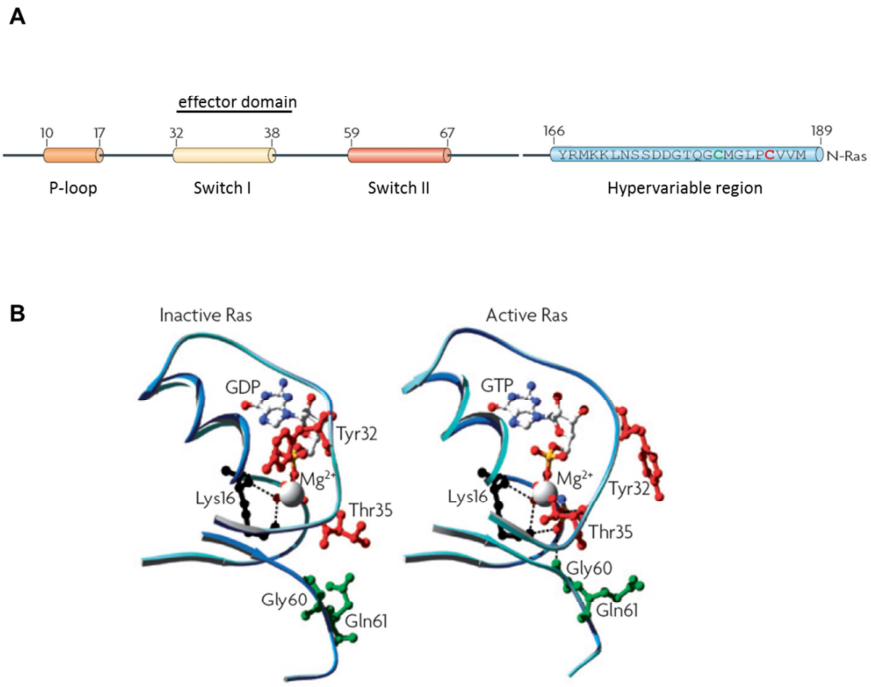

Figure 1.10: Structure of RAS proteins. **(A)** RAS proteins consist of a GTP binding domain (residues 1-164) and a C-terminal hypervariable region (amino acids 166-189) that contains isoform-specific membrane binding and trafficking determinants. Further strutural motifs include the phosphate binding motif P-loop, switch I and II regions as well as a C-terminal targeting sequence (CAAX motif). **(B)** Nucleotide-dependent structural rearrangements. The differences between the inactive GDP bound and the active GTP-bound RAS are confined to mainly in two regions, termed switch I and switch II, both of which are required for the interactions of RAS with its regulators and effectors. The γ-phosphate induces significant changes in the orientation of the switch II region through the interactions that it establishes with Thr35 and Gly60. Notably, these two residues are among the most conserved residues in the GTPase family, suggesting that the mechanisms of GTP binding (and hydrolysis) are essentially the same among various members. Figure adapted from Karnoub and Weinberg, 2008.

The oncogenic mutation Gln61Leu positioned in switch II, impairs GTP hydrolysis as a result of its catalytically essential residue involved in GAP interaction (Resat et al. 2001; Karnoub and Weinberg 2008; Cox and Der 2010).

1.2.4 Post translational modification of RAS proteins

RAS proteins are post-translational modified (PTM) through hydrophobic groups, dictating specific subcellular localisations, that are essential for biological activity (Hancock 2003; Hancock and Parton 2005; Wright and Philips 2006; Ahearn et al. 2012).

RAS proteins terminate with a CAAX tetrapeptide, were C represents a cysteine residue, A - any aliphatic amino acid and X symbolises any residue, which in conjunction with immediate upstream cysteine residues form the membrane targeting sequence, dictate interaction with distinct membrane compartments and subcellular localisations (Figure 1.11A) (Wright and Philips 2006; Eisenberg et al. 2013).

Notably, all CAAX proteins still require a second signal for trafficking to the plasma membrane (Hancock et al. 1990). In case of H-RAS, N-RAS and K-RAS4A, the second signal is comprised of Cys residues that are palmitoylated, a process also known as acylation (Resh 1999). For K-RAS4B, the second signal consists of a polybasic Lys-rich region with a net positive charge that is believed to form an eloctrostatic interaction with the negatively charged phospholipids at the plasma membrane (Figure 1.11A).

The CAAX motif recognition sequence is modified by the enzyme farnesyl transferase (FTase), which attaches a farnesyl group to the cysteine residue via a thioester bond. Next, the last three amino acids (AAX) are proteolytic cleaved, catalysed by the RAS converting enzyme-1 (RCE1) and the now C-terminal cysteine residue undergoes a methylesterification mediated by isoprenylcystein carboxymethyltransferase 1 (ICMT1). In addition, RAS proteins are further modified with palmitoyl groups at different cysteine residues in the vicinity of the C-terminus performed through palmitoyltransferase (PTase), which is required for membrane association (Figure 1.11B) (Wright and Philips 2006).

Besides attachment of polyisoprenoid lipids, RAS GTPases are found to be further post translationally modified through phosphorylation, nitrosylation,

ubiquitinylation and peptidyl-prolyl isomerisation, which are conditional upon cell activation, redox state or microbial pathogenesis (Figure 1.12) (Ahearn et al. 2012).

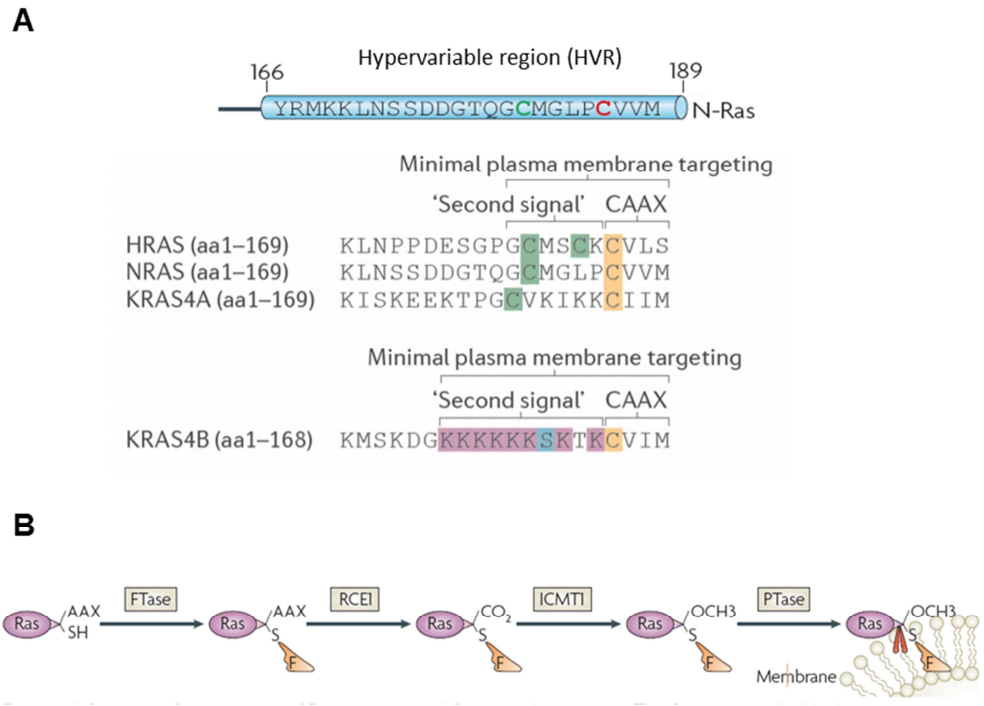

Figure 1.11: C-terminal RAS membrane targeting signals. (A) This figure illustrates the hypervariable region (HVR) of H-, K- and N-RAS proteins. Highlighted in yellow is the first post translational modification (PMT) motif, the cysteine residue forming the membrane targeting CAAX motif, which is farnesylated. An additional upstream 'second' signal is required for plama membrane targeting, shaded in green. For H-RAS, N-RAS and K-RAS4A, the second signal consists of Cys residues that are palmitoylated. For K-RAS4B, the second signal consists of a polybasic region with a net positive charge of eight (pink) and Ser181 residue, which is the principal site of phosphorylation is highlighted in blue. Figure adapted from Ahearn et al, 2012. **(B)** C-terminal processing of RAS proteins. Membrane association is absolutely required for RAS GTPase function and takes place through C-terminal modification of the CAAX motif. Farnesyltransferase (FTase) covalently attaches a farnesyl group (F, orange) to the final cysteine residue, followed by protealytic cleavage of the last three amino acids (AAX) by RAS converting enzyme-1 (RCEI). The now terminal farnesylated cysteine is carboxymethylated by isoprenylcystein carboxymethyltransferase 1 (ICMT1). RAS proteins are further modified (with the exception of K-RAS-4B) through attachment of palmitoyl groups (red lines) catalysed through palmitoyltransferase (PTase). Figure taken from Karnoub and Weinberg, 2008.

A recent study showed that the cis–trans prolyl isomerase 12 kDa FK506-binding protein (FKBP12) functions in the regulation of RAS depalmitoylation (Ahearn et al. 2011) through isomerization of the Gly–Pro peptidyl-prolyl bond at position 178–179. This constitutes a molecular timer for acylation and therefore this modification gained more appreciation for signalling purposes (Lu et al. 2007).

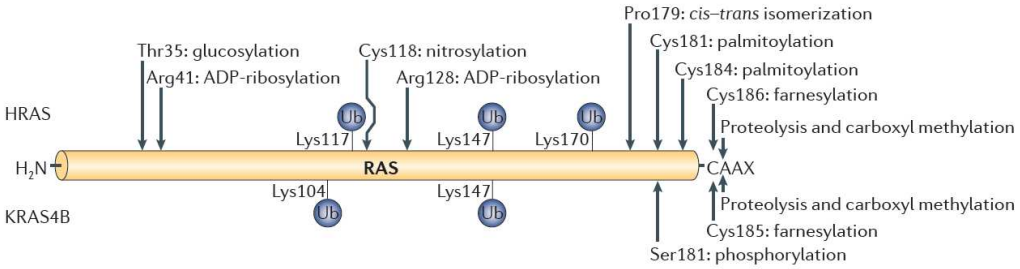

Figure 1.12: Post translational modifications of RAS proteins. Overview of reported post-translational modifications (PTMs) for H-RAS (top) and K-RAS4B (bottom). Sites of mono-ubiquitylation and di-ubiquitylation are indicated with blue spheres (Ub-ubiquitin). Note that glucosylation and ADP-ribosylation modifications have been only observed in cells intoxicated with bacterial virulence factors. All other PTMs are intrinsic to all eukaryotic cells, which have been implicated in RAS trafficking and signalling. Figure from Ahearn 2012.

H-RAS, N-RAS and K-RAS4B were recently shown to be substrates for mono-ubiquitination and di- ubiquitination modifications (Jura et al. 2006; Sasaki et al. 2011). The responsible E3 ligase was identified as rabaptin 5-associated exchange factor for RAB5 (RABEX5), which requires RIN for RABEX5-dependent RAS ubiquitination (Xu et al. 2010). RIN1, through its function as a GEF for RAB5, is believed to promote the RAB5-dependent recruitment of RABEX5 to endosomal sites, where H-RAS ubiquitination takes place. Thus, ubiquitination regulates trafficking of H-RAS to and from endosomes, indicating that this modification poses an additional way to regulate RAS compartmentalisation, and the spatial control of its signalling output.

Similarly, phosphorylation of K-RAS at Ser181 by PKC reduces the net charge of the polybasic region, thus leading K-RAS4B to lose affinity for plasma membrane association and to accumulate on endomembranes (Ballester et al. 1987; Bivona et al. 2006).

The RAS Cys118 residue is highly conserved among RAS isoforms, and it is the most surface-exposed Cys on these GTPases. Studies revealed that Cys118 could be nitrosylated when exposed to nitric oxide (NO) (Lander et al. 1995b; Lander et al. 1996). Even though S-nitrosylation does not alter the structure of RAS, this modification leads to enhanced guanine nucleotide exchange (Lander et al. 1995a; Williams et al. 2003), which promotes more efficient RAS activation.

Once the ER localised CAAX processing is complete, RAS isoforms diverge into their subsequent trafficking routes (Wright and Philips 2006). Palmitoylated RAS proteins (H-RAS, N-RAS and K-RAS4A) travel to the Golgi, where they get acylated. This step traps them into the Golgi, and leads to incorporation into transport vesicles and to enter the secretory pathway.

In contrast, K-RAS4B does not shuttle to the Golgi but instead associates directly with the plasma membrane. Whether this is achieved through diffusion or by an as yet unknown mechanism remains elusive (Figure 1.13) (Choy et al. 1999; Apolloni et al. 2000).

On the membrane, RAS proteins are able to become enriched with the cholesterol-binding protein caveolin and localise to specific plasma membrane micro-domains (lipid raft or non-raft domains) (Simons and Ikonen 1997; Prior et al. 2001) (Figure 1.12). It seems that functional activation of RAS depends on its release from lipid-raft micro-domains in the plasma membrane and its redistribution to nearby sites thus enabling interaction with various downstream effectors (Prior et al. 2001).

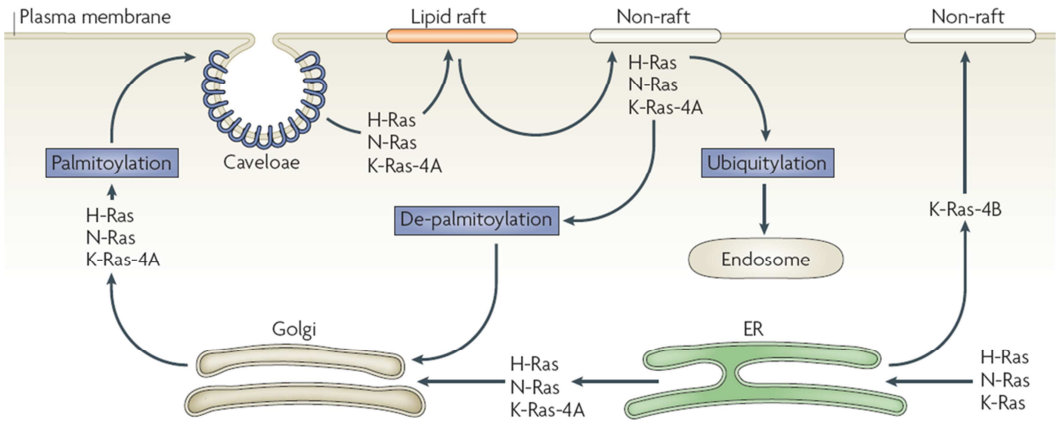

Figure 1.13: RAS post translational modifications lead to various subcellular localisations. See text for details. Figure from Karnoub 2008.

1.3 The R-RAS subgroup

Within the Ras subfamiliy, the related Ras (R-RAS) subgroup shares the highest similarity with classical Ras proteins (H-, K- and N-RAS) and exhibits significant oncogenic potential (Figure 1.2B, red circle) (Saez et al. 1994; Graham et al. 1999; Movilla et al. 1999; Erdogan et al. 2007; Erdogan et al. 2008). Three R-RAS family members have been characterised, R-RAS (Lowe et al. 1987), TC21 (R-RAS2)(Drivas et al. 1990) and M-RAS (R-RAS3) (Matsumoto et al. 1997). Although, this subgroup shares many biochemical and biological properties with classical Ras proteins such as an identical effector domain, overlapping GEFs and GAPs and the ability to act as oncogenes, evidence suggest that R-RAS GTPases have distinct properties and functions to classical RAS proteins (Zhang et al. 1996; Huff et al. 1997; Self et al. 2001) (Figure 1.14).

1.3.1 R-RAS

The founding member R-RAS shares a 55% aa identity with H-RAS and was discovered using a low stringency hybridisation probe of *H-RAS*, underscoring the high similarity to the classical H-, K- and N-RAS proteins (Lowe et al. 1987) (Figure 1.14). Accordingly, R-RAS and RAS share at least two GAPs, p120RASGAP and neurofibromin, the exchange factor RASGRF and effectors RAF, PI3K, RalGDS, RIN and AF6 (Rey et al. 1994; Spaargaren and Bischoff 1994; Spaargaren et al. 1994; Gotoh et al. 1997; Marte et al. 1997; Ebinu et al. 1998).

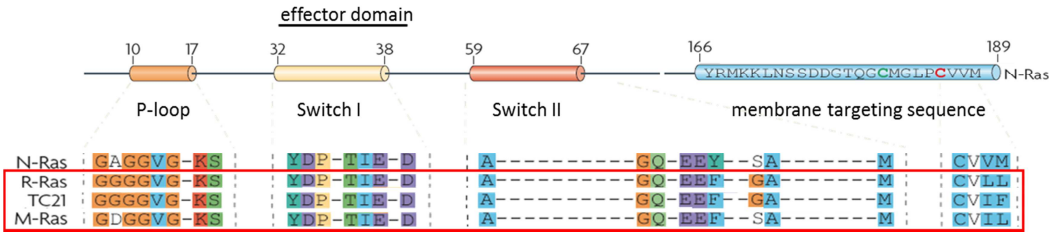

Figure 1.14: Oncogenic classical Ras proteins are structurally highly similar to R-RAS proteins. R-RAS displays a 55% amino acid homology to H-RAS, and structural conserved features such as the effector loop mediating downstream effector binding, are entirely identical between classical RAS proteins and the members of the R-RAS branch. Figure adapted from Karnoub and Weinberg, 2008.

Further, oncogenic activating mutants in human cancers analogous to those of found in the H-RAS oncogenes, have been identified for R-RAS GTPases (COSMIC database).

Despite the fact that R-RAS proteins share many regulatory and effector proteins with RAS proteins (Ehrhardt et al. 2002), R-RAS causes a transformed phenotype which is distinct from that induced by RAS (Self et al. 2001). Therefore, it is likely that R-RAS controls signalling and cellular processes which are distinct from classical RAS proteins. Indeed, R-RAS does not activate MAP kinase pathways and is only weakly oncogenic (Self et al. 2001). Furthermore, R-RAS activates α5β1 integrin independently of PI3K, through a different mechanism to H-RAS (Zhang et al. 1996; Sethi et al. 1999; Kinashi et al. 2000). RALBP1 also termed RLIP76, is the only effector known to date exclusive to R-RAS that is not shared with other classial RAS family members, and mediates adhesion-dependent RAC activation and cell migration (Goldfinger et al. 2006).

R-RAS differs from classical RAS proteins structurally through e.g. an N-terminal 26 amino acid extension, and differs at nine amino acids within the extended effector region across amino acids 23-46 (Lowe et al. 1987; Self et al. 1993; Holly et al. 2005). N-terminal truncated R-RAS failed to activate RAC and resulted in reduced cell spreading compared to full length R-RAS protein in 32D mouse myeloid cells, whereas adhesion or subcellular localisation was not affected (Holly et al. 2005).

Active R-RAS was demonstrated to increase ligand binding activity of integrins and to stimulate the adhesive properties of suspension cells (Zhang et al. 1996). In this context it has been further shown that R-RAS is able to antagonise H-RAS mediated integrin activation suppression (Sethi et al. 1999). R-RAS integrin regulation seems to be mediated through the effector loop and prenylation site of R-RAS (Oertli et al. 2000) possibly through a distinct plasma membrane micro-domain distribution (Hansen et al. 2003). Further, it has been demonstrated that R-RAS effects on integrin activation are negatively regulated through phosphorylation of the effector domain tyrosine residue Tyr66 by Eph receptor kinase EphB2 (Zou et al. 1999) or c-SRC, measured by cell adhesion reducing effects (Zou et al. 2002). Notably, it has been reported that R-RAS activation of integrin signalling could be a bi-directional system, since R-RAS has been observed to be activated downstream of integrin-mediated adhesion (Wozniak et al. 2005).

Studies focussing on R-RAS C-terminal sequences employing R-RAS/RAS chimeras, showed that the last 53 amino acids are necessary and sufficient to specify the contrasting biological activities beween R-RAS and RAS. Identified properties included H-RAS induced integrin suppression, reactive oxygen species production and morphological effects of transformed cells (Hansen et al. 2002).

R-RAS acts as a regulator of cell adhesion through effects on integrin affinity (Keely et al. 1999; Hansen et al. 2003), and focal adhesion formation (Berrier et al. 2000; Kwong et al. 2003). For example, in T47D breast cells active R-RAS strongly stimulates focal adhesion kinase (FAK) and p130Cas phosphorylation by an unknown mechanism (Kwong et al. 2003). Using a H-RAS/R-RAS chimera approach mapped the focal adhesion targeting signal to the C-terminal end of R-RAS (Furuhjelm and Peranen 2003). It is further known that R-RAS promotes adhesion-induced activation of RAC through its effector PI3K (Marte et al. 1997; Berrier et al. 2000; Holly et al. 2005).

R-RAS has been found to interact with Oxysterol-binding protein (OSBP)-related protein 3 (ORP3) (Goldfinger et al. 2007; Lehto et al. 2008). ORP3 is highly expressed in epithelial, neuronal and hematopoietic cells and has been described to be involved in integrin signalling and organisation of the actin cytoskeleton (Lehto et al. 2001). Therefore it has been proposed that R-RAS – ORP3 interaction is able to regulate cell-cell and cell-matrix adhesion (Lehto et al. 2008).

As noted above, the exclusively R-RAS binding protein RLIP76 (does not bind H-RAS or RAP1) mediates the R-RAS induced effect on cell spreading and migration through ARF6 (Goldfinger et al. 2006). Activated ARF6 stimulates adhesion-induced RAC1 activation, leading to lamellipodium formation and cell migration (Radhakrishna et al. 1999; Santy and Casanova 2001; Goldfinger et al. 2006). Additional studies confirm a role of R-RAS in cell migration through the spatial regulation of RAC and RHO (Wozniak et al. 2005; Shang et al. 2011). Consistent with this, activated R-RAS has been shown to promote cell migration of breast (Keely et al. 1999; Jeong et al. 2005) and cervical epithelial cells (Rincon-Arano et al. 2003; Mora et al. 2007) and has been identified as a cancer linked gene (Nishigaki et al. 2005). In the latter study using gastric cancer samples, it was discovered that gene demethylation of specific CpG sites within the first intron of R-RAS causes activation in more than half of the tested samples (Nishigaki et al. 2005).

Further evidence for a role of R-RAS in actin cytoskeleton re-modelling and cell migration stems from interaction with the actin-binding scaffolding protein FilaminA (FLNa), which also binds to integrin β1, β2, β7 tails. FLNa is necessary for tumour cell metastasis and vascular remodelling (Ott et al. 1998; de Curtis 2001; Yamazaki et al. 2005; Feng et al. 2006). Studies in human melanoma cells M2 showed that R-RAS functionally associates with FLNa and thereby regulates integrin dependent migration (Gawecka et al. 2010) or maintenance of endothelial barrier function in human coronary artery endothelial cells (Griffiths et al. 2011).

R-RAS was found enriched on both early and recycling endosomes, and displayed a higher activity if endosome located compared to the plasma membrane, resulting in RGL2 effector recruitment (a GEF for RALA) (Takaya et al. 2007).

Active R-RAS lengthened the duration of initial membrane protrusion and promoted the formation of ruffling lamellipodia and the lack of filopodia structures, which might be mediated through activity of PLCε, (Ada-Nguema et al. 2006). Consistently, studies in COS-7 cells showed that R-RAS localises to the leading edge of migrating cells, where it regulates membrane protrusion and ruffle formation (Conklin et al. 2010). Furthermore, it has been demonstrated that endogenous R-RAS co-localises with β-integrin in ruffles and endocytic vesicles and R-RAS is required for integrin accumulation into ruffles (Conklin et al. 2010). In addition, it has been described that active R-RAS is able to convert RIN2 from a GEF to an adaptor protein which preferentially binds RAB5. Active RAB5 then triggers the endocytosis of ECM bound/active integrins and active R-RAS to early endosomes, which then mediates the TIAM-mediated activation of RAC1 (Sandri et al. 2012).

Semaphorins are large secreted and transmembrane molecules involved in axon guidance, which are modulated by plexins and signal to the cytoskeleton in a RHO and RAC dependent manner (Kolodkin et al. 1993; Tamagnone et al. 1999). Plexins have been proposed to behave as GAPs specific for R-RAS and M-RAS, suggesting a selective role for R-RAS proteins in plexin-regulated signalling pathways, involved in cell migration and axon guidance (Oinuma et al. 2004; Kruger et al. 2005; Pasterkamp 2005; Saito et al. 2009; Oinuma et al. 2010). However, a more recent paper suggested that Plexins are GAPs for RAP1 rather than R-RAS (Bos and Pannekoek 2012).

R-RAS null mice are viable and fertile with no obvious abnormalities and normal tissues upon histologic examination (Komatsu and Ruoslahti 2005). However, R-RAS deficient mice exhibited exaggerated neointimal thickening in response to arterial injury and increased angiogenesis in implanted tumours (Komatsu and Ruoslahti 2005). Expression of R-RAS is mainly restricted to endothelial cells and vascular smooth muscle cells, where is has been found to regulate blood vessel remodelling, through to integrin-mediated cell adhesion to ECM components (Zhang et al. 1996; Kinbara et al. 2003; Komatsu and Ruoslahti 2005). Moreover, a recent study confirmed this observation and established R-RAS as a critical regulator of vessel integrity and function during tumour vascularisation (Sawada et al. 2012).

1.3.2 TC21

TC21 was initially cloned from a human teratocarcinoma cDNA library using oligonucleotides corresponding to the conserved region of RAS genes (Drivas et al. 1990). TC21 shows similar transformation ability than H-RAS (Graham et al. 1999) and mutated TC21 has been found in human tumours (Chan et al. 1994; Huang et al. 1995; Barker and Crompton 1998) and COSMIC database. Moreover, overexpression of TC21 has been associated with oral, breast, hepatocellular and esophagous carcinoma (Clark et al. 1996; Arora et al. 2005; Sharma et al. 2005; Luo et al. 2010; Macha et al. 2010).

TC21 has been found to be essential for survival and maintenance of B- and T lymphocytes, through linking respective antigen receptors to PI3K-mediated survival pathways (Delgado et al. 2009). Moreover, TC21 and RHOG mediate T cell receptor internalisation from the immunological synapse through phagocytosis (Alarcon and Martinez-Martin 2011; Martinez-Martin et al. 2011).

TC21 deficient mice do not display major alterations in viability, growth rates, cardiovascular parameters, or fertility but exhibit a delay in mammary gland development (Larive et al. 2012). TC21 is expressed in the same cell types as R-RAS (Kozian and Augustin 1997; Komatsu and Ruoslahti 2005; Larive et al. 2012) and they share overlapping regulatory proteins, and thus might mediate similar cellular functions (Ohba et al. 2000; Self et al. 2001; Ehrhardt et al. 2002).

1.3.3 M-RAS

The last identified R-RAS member is M-RAS (208aa) or R-RAS3, which was first cloned from mouse skeletal muscle myoblasts and rat brain (Matsumoto et al. 1997). M-RAS is predominantly expressed in the central nervous system, and is implicated in re-organisation of the actin cytoskeleton and promotes neurite outgrowth in PC12 cells (Matsumoto et al. 1997; Kimmelman et al. 2002; Nunez Rodriguez et al. 2006; Sun et al. 2006). Plexins also function as GAPs for M-RAS and thereby suppress dentritic outgrowth and branching (Saito et al. 2009). Further, the *MRAS* gene has been identified by genome wide associated studies to be a new susceptibilty locus for coronary heart disease (Erdmann et al. 2009).

Despite the high homology of M-RAS and R-RAS, these GTPases perform different functions due to differential effector coupling (Marte et al. 1997; Nunez Rodriguez et al. 2006). M-RAS activates MAPK signalling through BRaf, stimulating neurite outgrowth, even though activation by EGF seems to be more sustained compared to prototypic RAS. Furthermore, phosphatase holoenzyme comprised of Shoc2/Sur8 and the catalytic subunit of PP1 functions as a highly specific M-RAS effector to modulate RAF activity (Rodriguez-Viciana et al. 2006).

M-Ras null mice appeared phenotypically normal, including lack of detectable morphological and neurological defects, or alteration of MAPK/PI3K signalling (Nunez Rodriguez et al. 2006).

1.4 RHO GTPases

Ras HOmologous (RHO) GTPases form another subgroup of the RAS superfamily and regulate cytoskeletal architectures associated with cell migration and polarity, adhesion, proliferation and differentiation (Figure 1.2A and Figure 1.15) (Etienne-Manneville and Hall 2002; Raftopoulou and Hall 2004; Ridley 2006; Heasman and Ridley 2008; Vega and Ridley 2008).

RHO family small GTPases act as molecular switches and are activated by GEFs and inhibited by GAPs as described earlier for RAS proteins (Figure 1.1). A third level of regulation is provided by the stoichiometric binding of RHO GDP dissociation inhibitor (RHOGDI), masking prenyl modification and promoting cytosolic sequestration (DerMardirossian and Bokoch 2005; Cherfils and Zeghouf 2013).

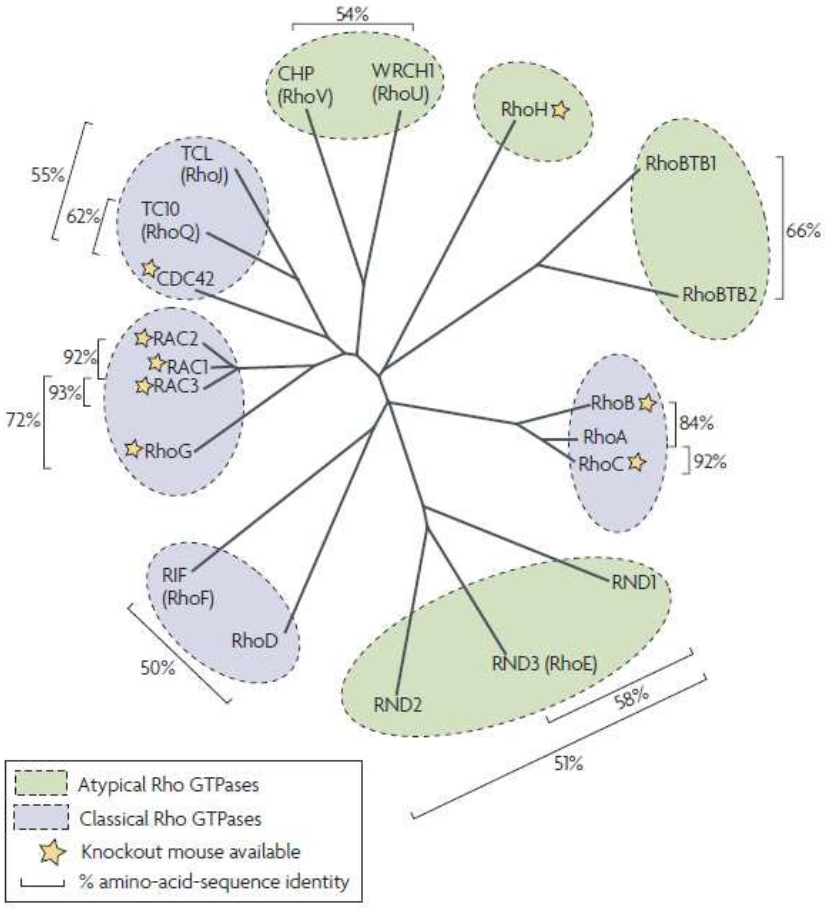

Figure 1.15: Overview of RHO GTPase family. The RHO GTPase group consists of 20 members subdivided into eight branches. High sequence similarity is found between proteins within the RAC and RHO subfamilies. Figure taken from Heasman and Ridley, 2008.

The RHO GTPase familiy is comprised of more than 20 distinct proteins with the best characterised members RHOA, RAC1 and CDC42, acting as regulators of actin cytoskeleton re-arrangements (Heasman 2008 #482). In addition to the wide range of cellular processes from cell polarity and movement, cell shape, cell-cell and cell-matrix interactions (Etienne-Manneville and Hall 2002; Raftopoulou and Hall 2004; Ridley 2006), RHO familiy proteins play additional roles in a variety of cellular processes, including secretion, smooth muscle contraction, migration, neurite retraction and gene transcription (Etienne-Manneville and Hall 2002; Jaffe and Hall 2002; Jaffe and Hall 2005).

1.4.1 RHO regulatory proteins: GEFs, GAPs and GDIs

About 71 different GEFs for RHO family members (RhoGEFs) belonging to the Dbl protein family, which share the typical tandem motif consisting of a Dbl homology (DH) domain, responsible for exchange activity, and a pleckstrin homology (PH) domain, involved in subcellular localisation of the GEFs (Blomberg et al. 1999; Zheng 2001; Schmidt and Hall 2002; Hall 2012). In addition to this tandem motif, RhoGEFs often contain one or more additional signal transduction domains, like SH2, SH3, PDZ and additional PH domains. Therefore, they often function as molecular bridges between different signal transducion pathways (Zheng 2001; Schmidt and Hall 2002).

In addition, characterisation of a protein DOCK and its orthologues led to the identification of a second sequence-unrelated family of GEFs, which consist of 11 members in the mammalian genome (Meller et al. 2005). The substrates of DOCK family proteins appear to be RAC and CDC42 GTPases only (Hall 2012).

So far, 67 RHO family GAPs within the mammalin genome have been reported. RHOGAPs harbour a bcr homology (BH) domain (Diekmann et al. 1991; Hall 2012). In addition, three RHO family GDIs have been identified, which inhibit the dissociation of GDP from RHO (Matsui et al. 1990).

Identification of RHO family GTPase effectors is hard due to the lack of CRIB domains. Nonetheless, more than 100 targets have been reported to interact with the RHO family (Bishop and Hall 2000). About one third are kinases and a large number are scaffold or adaptor proteins. Analysis of RHO GTPases signalling pathways is a challenging task due to the fact that RHO, RAC and CDC42 are able to interact with 20 or 30 different proteins in a GTP dependent

manner. This led to the hypothesis that each of the mentioned small GTPases is able to regulate numerous distinct signalling transduction pathways.

1.4.2 RHO proteins

RAS homologue gene family member A (RHOA), RHOB and RHOC are highly homologous, but appear to have divergent biological functions (Wheeler and Ridley 2004). Carboxy-terminal modifications and differences in subcellular localisation allow these three proteins to respond to and act on distinct signalling molecules (Wennerberg and Der 2004; Wheeler and Ridley 2004).

RHOA, the best studied member of the three has been demonstrated to function in regulation of actomyosin contractility, cytokinesis, focal adhesion assembly and cell polarity (Barry and Critchley 1994; Kimura et al. 2000; Bi et al. 2005; Van Keymeulen et al. 2006).

RHOB is involved in regulation of cell shape, migration and adhesion, but also has been discovered to play a role in protein trafficking and in CXC-motif chemokine receptor 2 (CXCR2)-mediated chemotaxis (Neel et al. 2007; Sandilands et al. 2007; Wheeler and Ridley 2007). Recent studies showed that RHOB is able to differentially control Akt function in endothelial cells during breast tumourigenesis, and that RHOB regulates cell migration through altered focal adhesion dynamics (Witze et al. 2008; Vega et al. 2012; Kazerounian et al. 2013).

1.4.3 RAC and CDC42

RAC and CDC42 play key signalling roles in cytoskeletal re-organisation, membrane trafficking, transcriptional regulation, cell growth and development (Ridley 2001c; Wennerberg and Der 2004; Heasman and Ridley 2008).

RAC1 promotes lamellipodium formation and membrane ruffling, whereas CDC42 stimulates filopodia and actin microspike formation (Ridley 1999; Ridley 2001a).

1.5 WNT signalling branches

The WNT pathway regulates vital developmental processes during embryogenesis, including cell-fate specification, tissue patterning, cell polarity, and cell movements during morphogenesis. In addition, this pathway plays key roles in adult tissue homeostasis, stem cell renewal and has been implicated in tumourigenesis (Veeman et al. 2003a; Logan and Nusse 2004; Reya and Clevers 2005; Zallen 2007).
Notably, the WNT signalling pathway comprises a complex network of ligands, cognate receptors and co-receptors and agonistic/antagonistic modulators acting to activate a vast intracellular downstream signalling network (Niehrs 2012), which will be discussed in more detail in the following section 1.6.

The best studied branch of the signaling network is commonly known as canonical signalling pathway and results in ß-catenin dependent gene transcription and regulation of cell fate decisions (Logan and Nusse 2004; Kikuchi et al. 2009; MacDonald et al. 2009). Less well-defined cascades, known as ß-catenin independent or non-canonical pathways, include the WNT/Ca^{2+} pathway and the planar cell polarity branch, involved in cytoskeletal rearrangements and cell movements (Veeman et al. 2003a; Zallen 2007). Overall, these pathways collectively regulate cell survival, cell proliferation, cell fate determination, cell polarity, tissue patterning, and tissue homeostasis (Veeman et al. 2003a; Reya and Clevers 2005; Zallen 2007; MacDonald et al. 2009). These three major signalling pathways associated with WNT-receptor interaction, are outlined in more detail below.

1.5.1 β-catenin (canonical) WNT-signalling pathway

Canonical β-catenin WNT signalling is highly conserved across species, and carries out essential roles in cell proliferation, survival and cell fate specification. In addition, this signalling cascade is associated with tumourigenesis, in particular with colorectal cancer (Giles et al. 2003; Logan and Nusse 2004; Reya and Clevers 2005; MacDonald et al. 2009; Clevers and Nusse 2012; Niehrs 2012).

In the unstimulated state (in the absence of WNT ligands), β-catenin - the fundamental player of the pathway (Willert and Nusse 1998), is phosphorylated and targeted for proteasomal degradation. Cytosolic β-catenin is bound to a

destruction complex formed by several proteins including the scaffolding protein AXIN, adenomatous polyposis coli (APC), casein kinase 1 alpha (CK1α) and glycogen synthase kinase 3 beta (GSK3β) (Aberle et al. 1997; Ikeda et al. 1998; Kishida et al. 1998; Kitagawa et al. 1999; Liu et al. 2002; Hino et al. 2003). CK1α phosphorylates β-catenin at Ser45 (Amit et al. 2002). This phosphorylation event primes β-catenin for subsequent phosphorylation by GSK3β at residues Ser33, Ser37, and Thr42 (Yost et al. 1996; Liu et al. 2002; Yanagawa et al. 2002). This N-terminal phosphorylation pattern is recognised by the E3 Ubiquitin ligase β-TRCP, which performs ubiquitination of β-catenin, leading to subsequent proteasomal degradation (Marikawa and Elinson 1998; Stamos and Weis 2013).

Activation of canonical signalling is triggered by WNT proteins (section 1.6.1) and is further modulated through agonists/antagonists of WNT ligands or cognate receptors (section 1.6.2). Binding of WNT ligands (such as WNT1, WNT3a or WNT8) to Frizzled (FZD) receptors lead to plasma membrane recruitment and association of the cytoplasmic destruction complex with phosphorylatyed LRP5/6, which loses its ability to target β-catenin for proteasomal degradation (Figure 1.16). This in turns results in an increase of cytoplasmic β-catenin levels and subsequent translocation to the nucleus, where it associates with transcriptional co-activators like CREB-binding protein (CBP/p300), BRG1 and CDC73. Binding of β-catenin to T-cell factor (TCF) transcription factor displaces Groucho, and the β-catenin complex can then stimulate WNT target gene transcription (Figure 1.16B). WNT responsive genes include among others *c-Myc*, *cyclinD1* and *Axin2* (Hurlstone and Clevers 2002; Clevers and Nusse 2012).

Notably, mutations at phosphorylation sites targeted by the destruction complex lead to the stabilisation of β-catenin protein levels and have been found in many tumour cell lines (Morin et al. 1997).

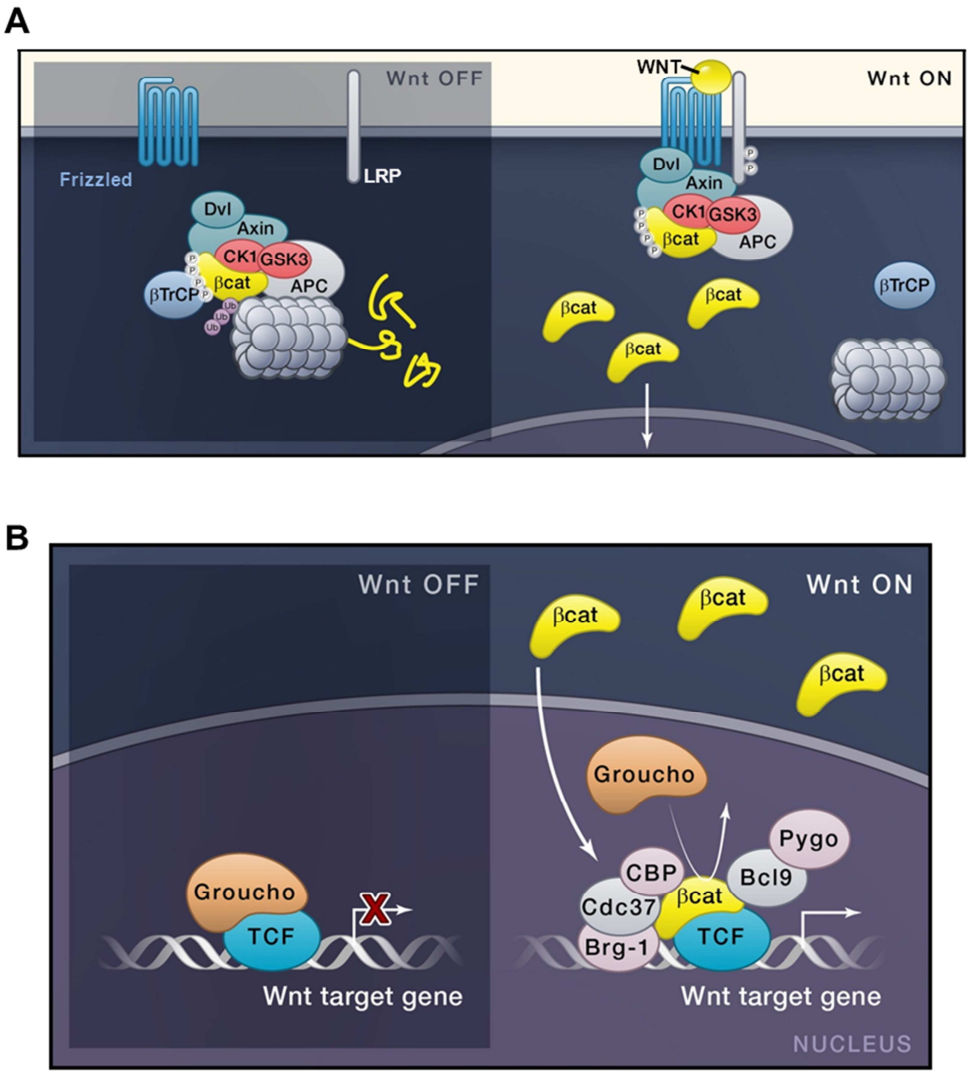

Figure 1.16: β-catenin (canonical) WNT signalling. (A) In the unstimulated (WNT off) state, a destuction complex is formed of DVL, AXIN, CK1, GSK3β, APC and β-catenin, which leads to phosphorylation and subsequent ubiquitination of β-catenin through the E3 Ubiquitin ligase β-TRCP. β-catenin is then degraded by the proteasome. WNT signalling is initiated (WNT on) through WNT ligand binding to Frizzled receptors and co-receptors LRP5/6. This pathway stimulation leads to association of the intact degradation complex with phosphorylated LRP, which still is able to capture and phosphorylate β-catenin, but the ubiquitination by β-TRCP is blocked. This leads to β-catenin accumulation in the cytoplasm, and eventually nuclear translocation. **(B)** In the absence of WNT ligands, TCF occupies and represses its target genes, assisted by transcriptional co-repressors such as Groucho. Upon WNT activation, nuclear translocated β-catenin replaces Groucho from TCF and recruits transcriptional co-activators and histone modifiers such as BRG1, CBP, CDC73, BCL9, and Pygopus to drive target gene expression. APC - adenomatous polyposis coli, CK1-Caseine kinase 1, DVL – Dishevelled, GSK3β – glycogen synthase kinase 3β, LRP5/6 - LDL receptor-related proteins 5&6, TCF - T-cell factor. Figure taken from Clevers and Nusse, 2012.

1.5.2 Planar Cell Polarity (PCP) pathway

Planar Cell Polarity (PCP) was originally identified in insects and then extensively studied in *Drosophila* (Lawrence and Shelton 1975; Gubb and Garcia-Bellido 1982). This pathway regulates the polarity of epithelial cells within a plane orthogonal to their apical – basal axis, thus resulting in uniform coordinated polarised cells and cellular behaviour across a field (Tree et al. 2002; Jenny 2010). In multicellular organisms, PCP is required for establishment and co-ordination of cell polarities and regulation of directional morphogenesis during embryonic development and tissue morphogenesis. Studies in mammalian model systems elucidated that PCP is involved in neural tube closure through convergent extension movements, asymmetric cell division, orientation of cilia and sensory hair cells, axon guidance and cell motility (Tissir and Goffinet 2005; Seifert and Mlodzik 2007; Zallen 2007; Rida and Chen 2009; Jenny 2010; Goodrich and Strutt 2011; Gray et al. 2011).

Genetic studies in *Drosophila* identified a group of core PCP genes, in which mutations caused misorientation of bristles of the *Drosphila* wing and disarrangement of the ommatidia in the *Drosophila* eye (Figure 1.18B and F) (Adler 2002; Tree et al. 2002; Seifert and Mlodzik 2007; McNeill 2010). These include the membrane-spanning Frizzled proteins (Vinson and Adler 1987; Adler et al. 1997), Strabismus (VANGL) (Taylor et al. 1998; Wolff and Rubin 1998), Flamingo (CELSR) (Chae et al. 1999; Usui et al. 1999) and the cytoplasmic proteins Dishevelled (Theisen et al. 1994), Prickle (Gubb et al. 1999) and Diego (Inversin) (Feiguin et al. 2001).

The hallmark of the PCP activation in Drosophila is the asymmetric distribution of the aforementioned PCP proteins (Figure 1.17). Frizzled, Dishevelled and Diego preferentially localise to the distal side and Strabismus and Prickle to the proximal side of the cell. Thus, Frizzled and Strabismus complexes are asymmetrically localized in a mutually exclusive manner, whereas the atypical cadherin Flamingo localises both distally and proximally (Usui et al. 1999; Axelrod 2001; Strutt 2001; Tree et al. 2002; Lawrence et al. 2004; Chen et al. 2008). This asymmetric membrane localisation is presumed to lead to polarised localisation and/or activation of associated components and downstream effectors and thereby elicit tissue-specific responses (Adler 2002; Tree et al. 2002; Seifert and Mlodzik 2007; Vladar et al. 2009; McNeill 2010).

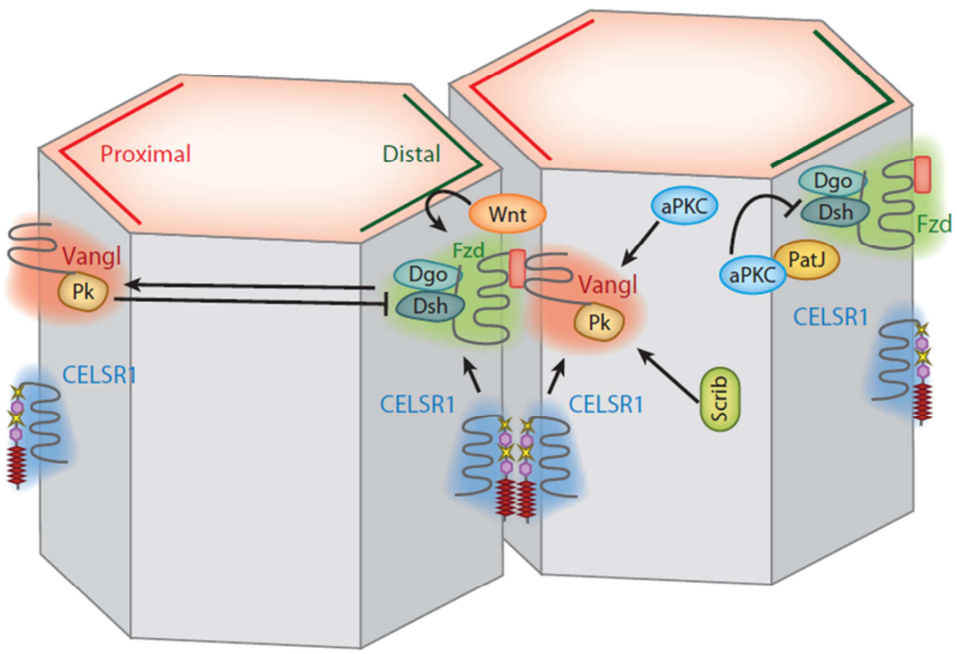

Figure 1.17: Asymmetrical distribution of planar cell polarity proteins in *Drosophila.* The hallmark of PCP activity is asymmetric distribution of PCP core proteins along the proximal-distal axis. Vangl proteins binds to Prickle (Pk) and form a complex at the proximal end of the cell. Whereas the Wnt receptor Frizzled (Fzd) binds to Diego (Dgo) and Dishevelled (Dsh) to form a complex at the distal site of the cell. CELSR1 localises both distally and proximally and recruits Vangl or Fzd to the membrane. Abbreviations: aPKC - atypical protein kinase C, CELSR1 - Cadherin, EGF LAG seven-pass G-type receptor 1, PATJ - Pals1-associated tight junction protein, Scrib – Scribble. Figure taken from Muthuswamy and Xue, 2012.

The PCP pathway is well conserved across species (Figure 1.18), but differences have been observed between *Drosophila* and vertebrate model systems. For example, additional proteins have been identified in vertebrates, which are proposed to function in PCP signalling (Wang and Nathans 2007). SCRIB and PTK7 mutants exhibit classic PCP phenotypes and they show genetic interaction with VANGL2 (Murdoch et al. 2003; Lu et al. 2004b). Furthermore, to date no WNT ligand has been identified to initate PCP signalling in *Drosophila* (Wu and Mlodzik 2009), whereas in vertebrates WNT ligands WNT11 (Zhou et al. 2007), WNT5a (Qian et al. 2007), and possibly WNT9b (Karner et al. 2009) have been shown to be required for PCP activation (Mlodzik 2002; Fanto and McNeill 2004; Simons and Mlodzik 2008; Wallingford 2012).

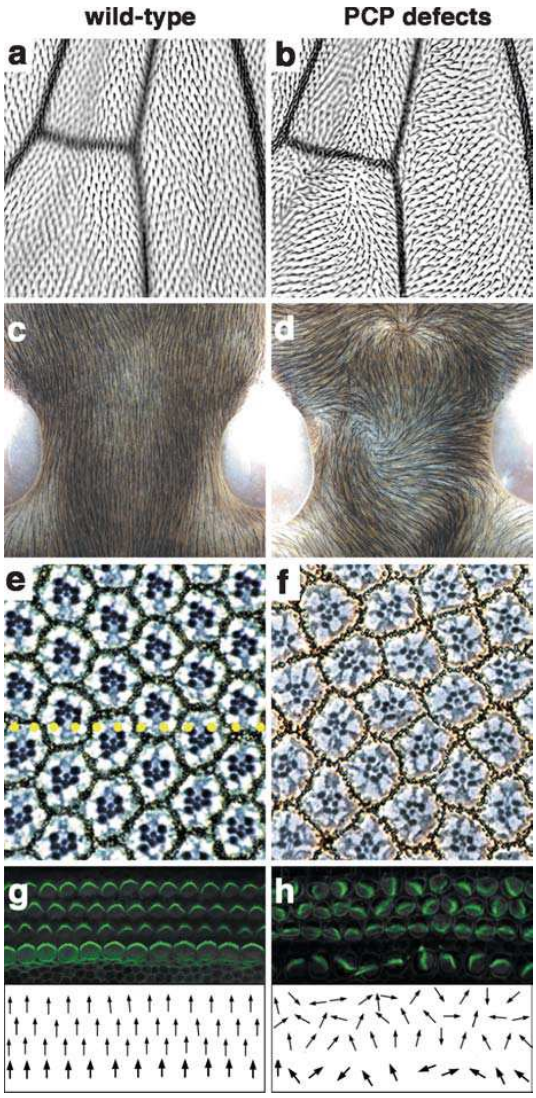

Figure 1.18: PCP phenotype examples in Drosophila and mammals. The left hand side column displays wild type appearance, compared to the right hand column side, demonstrating a PCP defect in the respective tissue. (a,b) *Drosophila* wing hair patterns, (c,d) mouse skin hairs (in dorsal view of neck), (e,f) *Drosophila* eye neuroepithelium, (g,h) mouse inner ear neuroepithelium. Orientation of inner ear sensory cells is representated as arrows in the schematic below. Figure from Klein and Mlodzik, 2005.

In contrast to β-catenin signalling (section 1.5.1), β-catenin independent/PCP signalling is much less understood. This is further hampered by the fact that Frizzled receptors and Dishevelled proteins participate in all known WNT signalling cascades, complicating PCP signalling analysis (Figure 1.19). In addition, PCP studies mostly rely on *in vivo* phenotypic analysis, due to the lack of convenient biochemical reporter assays such as the TCF/LEF based luciferase assay (TOPFLASH).

Even though Frizzled receptors and DVLs are shared upstream components of various WNT pathways, different ligands and co-receptors might be involved in activation of specific WNT branches (see section 1.6) (van Amerongen et al. 2008; Niehrs 2012).

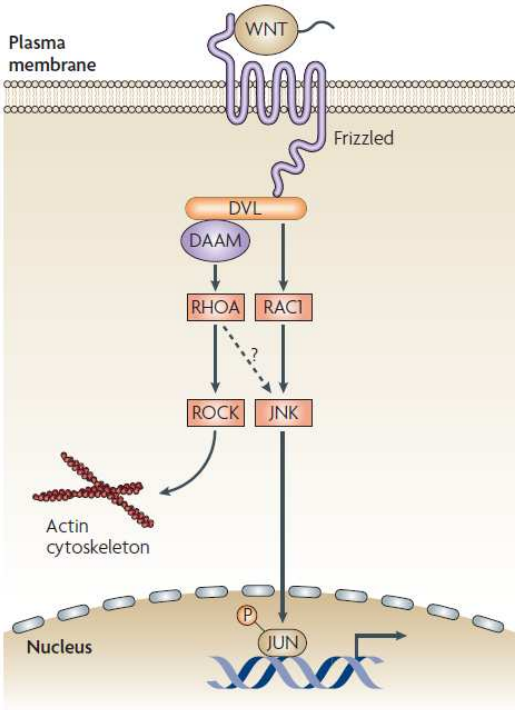

Figure 1.19: WNT/Planar Cell Polarity signalling. The Planar Cell Polarity (PCP) pathway is stimulated by WNT ligands such as WNT5a or WNT11, which bind to Frizzled receptors or (co)-receptors such as ROR2 or RYK (not displayed). The WNT-Frizzled complex recruits DVL, which then associates with DAAM. This in turn stimulates RHO GTPases such as RHOA, which subsequently activates RHO associated kinase (ROCK). DVL is also able to activate RAC, resulting in c-Jun N-terminal kinase (JNK) signalling. Both RHO GTPases RHO and RAC modulate actin cytoskeletal rearrangements thus regulating cellular polarity and migration. DAAM - DVL associated activator of morphogenesis 1, ROR2 – RTK-like orphan receptor. Figure taken from Staal et al, 2008.

Genetic and biochemical studies in flies and vertebrates have shown that the WNT/PCP branch regulates cytoskeletal rearrangements and thereby controls processes like epithelial cell polarisation, directed cell migration and oriented cell divisions (Figure 1.19) (Bellaiche et al. 2001; Jessen et al. 2002; Wallingford et al. 2002; Ciruna et al. 2006).

This is achieved, at least partly, through DVL mediated activation of RHO subfamiliy GTPases RHO and RAC, which in turn stimulates RHO associated

kinase (ROCK) activity and activation of JNK (Figure 1.19) (Winter et al. 2001; Marlow et al. 2002; Habas et al. 2003; Jaffe and Hall 2005). Furthermore, PRICKLE or VANGL proteins have been reported to be instrumental in this context (Park and Moon 2002; Takeuchi et al. 2003; Veeman et al. 2003b; Phillips et al. 2005; Gao et al. 2011).

Perturbations in the PCP pathway contribute to the pathogenesis of a variety of diseases including cardiac and neural tube defects, the two most common types of birth defects (Ciruna et al. 2006; Wen et al. 2010; Bartsch et al. 2012; Tada and Kai 2012).

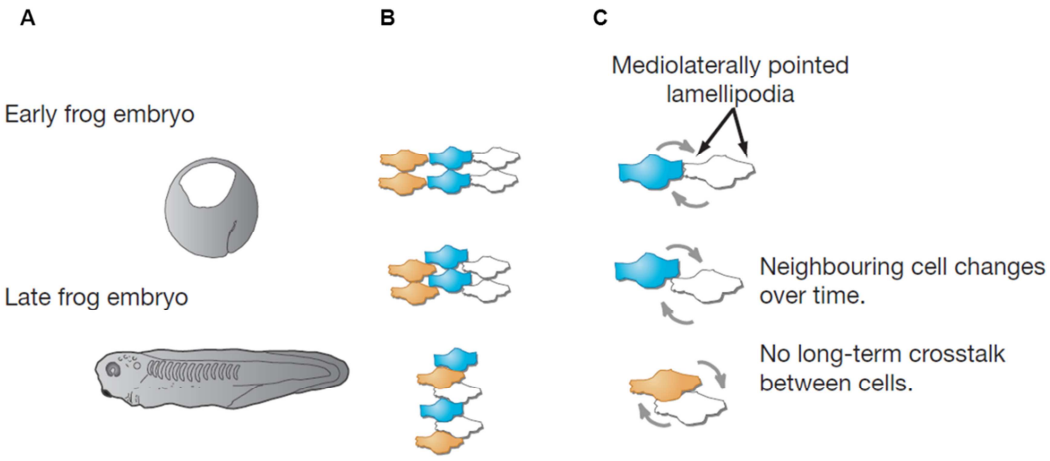

Figure 1.20: Convergent extension and planar polarity. (A) Vertebrate embryos convert from spherical eggs into elongated animals by a process called convergent extension (CE). **(B)** In the frog, convergent extension is achieved through cell intercalation. This process requires co-ordinated migration towards each other (convergence), intercalating along a single axis and a mediolateral extension, yielding a cell population which shaped a short and wide arrangement into along and narrow one. **(C)** This process involves stabilisation of lamellipodia specifically on the mediolateral faces, and it is thought that crosstalk between neighbouring cells is critical to the positioning of lamellipodia. The control of this process is complicated by the fact that cells are constantly changing neighbours. Figure from Wallingford 2004.

Another observed PCP-linked disorder is the genetic disorder Bardet-Biedl syndrome (BBS) (Fliegauf et al. 2007), which is a ciliopathic disorder, characterised principally by obesity, retinitis, polydactyly, hypogonadism and pigmentosa (Beales et al. 1999). Affected gene products are the BBS proteins,

which are found in the basal body and cilia of the cell (Ansley et al. 2003). BBS proteins are involved in intraflagellar transport, a bi-directional transportation activity along the long axis of the ciliary shaft that is essential for ciliogenesis and the maintenance of cilia (Blacque et al. 2004). PCP has been linked to BBS since it was demonstrated that PCP signalling is essential for directional beating of motile cilia, which play a crucial role in the movement of materials and cells (Vladar et al. 2009; Wallingford 2010; Wallingford and Mitchell 2011). Further, PCP controls tissue level of multi-ciliated cells through VANGL2, CELSR2, and CELSR3, which are required for establishment of rotation (Mitchell et al. 2009; Guirao et al. 2010; Tissir et al. 2010; Wallingford and Mitchell 2011)

Aberrant regulation of planar cell polarity has further been linked to polycystic kidney disease (Simons and Mlodzik 2008; Luyten et al. 2010) and Nephronophthisis type 2, a renal cystic disease cause by a mutation in the PCP component Inversin (Otto et al. 2003; Simons et al. 2005).

Overall, the β-catenin (canonical) pathway has been linked to carcinogenesis, while the planar cell polarity (PCP) pathway is implicated in cell motility and metastasis (Clevers and Nusse 2012; Muthuswamy and Xue 2012).

1.5.3 The WNT/Ca^{2+} pathway

The non-canonical WNT/Ca^{2+} pathway is stimulated by a distinct group of WNT ligands like WNT5a or WNT11 (Slusarski et al. 1997a; Slusarski et al. 1997b; Westfall et al. 2003; Wang et al. 2010) and Frizzled receptors such as FZD2 (Slusarski et al. 1997a; Niu et al. 2012), leading to an intracellular increase of the second messenger Ca^{2+} (Figure 1.21). This in turn leads to activation of calcium/calmodulin-dependent kinase II (CamKII) (Kuhl et al. 2000a) and protein kinase C (PKC) (Sheldahl et al. 1999). PKC then translocates to the plasma membrane where it interacts with target proteins (Sheldahl et al. 1999).

The calcium responsive factor nuclear factor of activated T-cells (NF-AT) acts downstream of CamKII and is involved in the development of cardiac, skeletal muscle, and nervous systems (Kuhl et al. 2000b; Kohn and Moon 2005). Furthermore, the WNT/Ca^{2+} pathway mediates cell migration and has been

implicated in the promotion of malignant progression and cell invasiveness of cancer cells (Weeraratna et al. 2002; Kuhl 2004).
WNT5a induced PKC signalling has been shown to increase melanoma cell motility through elevated Snail and Vimentin and decreased E-cadherin expression (Dissanayake et al. 2007).

Thus, WNT/Ca^{2+} signalling modulates cell movement and behaviour and induces structural changes similar to PCP (Torres et al. 1996; Kuhl et al. 2001; Okamoto et al. 2007; Witze et al. 2008); but the extent, to which this pathway overlaps with PCP still remains uncertain (Bryja et al. 2009; Andersson et al. 2010; Gao et al. 2011).

Notably, besides Frizzled proteins, WNT5a ligand binding to ROR2 has been demonstrated to activate Ca^{2+}/CamKII pathway and is required for axonal pathfinding in mammalian brain development (Logan and Nusse 2004; Li et al. 2009a; Nishita et al. 2010a).

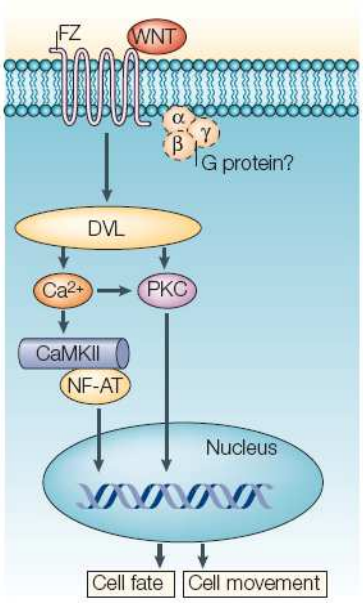

Figure 1.21: WNT/Ca^{2+} signalling. A subset of WNT ligands and Frizzled (FZ) receptors is able to increase intracellular Ca^{2+} levels, leading to subsequent activation of calcium/calmodulin-dependent kinase II (CamKII) and protein kinase C (PKC) downstream of Dishevelled (DVL). The calcium responsive factor NF-AT acts as transcription factor involved in cell fate specifications and cellular movement. NF-AT - nuclear factor of activated T-cells. Figure taken from Ciani and Salinas, 2005.

1.6 WNT signalling components

1.6.1 WNT ligands

The human genome harbours 19 WNT genes, which encode functionally distinct WNT proteins whose expression is spatially and temporally regulated during development (Moon et al. 1997; Logan and Nusse 2004; Mikels and Nusse 2006b). WNT ligands are secreted hydrophobic glycoproteins, which are similar in size (350 - 400 amino acids) and possesses 22 to 24 cysteine residues (Figure 1.22) (Miller 2002; Mikels and Nusse 2006b). WNT proteins bind to the Frizzled family of seven-pass transmembrane proteins and activate intracellular WNT signalling pathways depending on receptor context (Kohn and Moon 2005; Cadigan and Liu 2006).

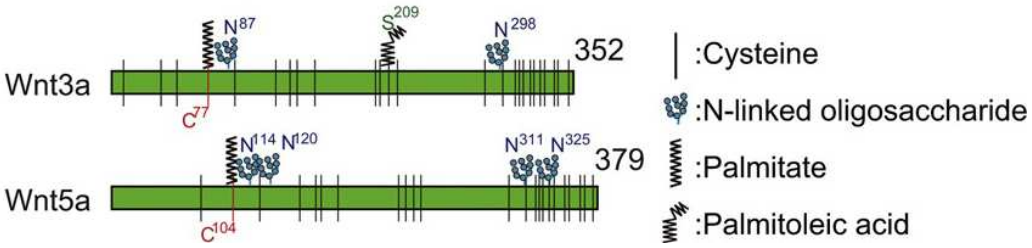

Figure 1.22: WNT ligand structure and post-translational modifications of WNT3a and WNT5a proteins. WNTs are produced from precursor proteins and post translational modified (glycosylation and lipid modification), before being secreted form the cell surface in a matured and active form. WNT proteins are similar in size, rangeing from 320 to 400 amino acids in length, and containing between 22-24 cysteine residues. Figure taken from Kikuchi et al, 2011.

Historically, WNT ligands were subdivided into two functional groups: canonical WNT ligands and non-canonical WNT ligands. Canonical WNTs such as WNT1, WNT3, WNT3a or WNT7a are classified by the ability to induce duplication of the embryonic axis in *Xenopus laevis* embryos or to induce transformation of mammary epithelial cells (Wong et al. 1994; Shimizu et al. 1997), whereas non-canonical WNT ligands have been reported to alter morphogenetic movements or be involved in tumourigenesis through pro-migratory effects as reported for WNT2, WNT4, WNT5a, WNT5b, WNT6, WNT7b or WNT11 (Wong et al. 1994; Du et al. 1995; Shimizu et al. 1997).

WNT3 has been demonstrated to activate canonical and non-canonical WNT signalling and to regulate cell motility through activation of RHO GTPases (Shibamoto et al. 1998; Endo et al. 2005). WNT5 (Slusarski et al. 1997b; Weeraratna et al. 2002; Qian et al. 2007) and WNT11 (Zhou et al. 2007) activate β-catenin independent pathways, modulating embryonic cell movement and polarity (Veeman et al. 2003a).

However, WNT5a has also been observed to signal through the canonical WNT pathway depending on the receptor context (Mikels and Nusse 2006a). In addition, WNT5a is found upregulated in many human tumours and stimulates cell motility and invasiveness of tumour cells (Iozzo et al. 1995; Weeraratna et al. 2002; Kurayoshi et al. 2006; Pukrop et al. 2006; Dissanayake et al. 2007).

1.6.2 Non-WNT ligand modulators of WNT signalling

WNT/β-catenin signaling is modulated at many levels by a number of evolutionarily conserved secreted or transmembrane inhibitors or activators of WNT signalling. With few exceptions, these antagonists and agonists are not pure WNT modulators, but also affect additional signaling pathways, such as TGF-β and FGF signalling (Cruciat and Niehrs 2012).

1.6.2.1 WNT inhibitors

Secreted Frizzled-related proteins (sFRP) were the first WNT antagonists to be identified. These proteins are approximately 300 amino acids in size and contain a signal sequence, a Frizzled-like cysteine-rich domain (CRD), and a small conserved hydrophilic C-terminus harbouring a netrin-related motif (Rattner et al. 1997). sFRPs are able to bind WNT proteins and FZD receptors in the extracellular compartment, which prevents WNT/FZD binding (Wawrzak et al. 2007), similarily to the WNT inhibitory protein (WIF), which can bind WNTs, thereby inhibiting interactions between WNT and WNT receptors (Figure 1.23) (Bovolenta et al. 2008).

Other WNT inhibitors include proteins of the Dickkopf (DKK) (Bafico et al. 2001; Semenov et al. 2001) and the WISE/Sclerostin (SOST) (Li et al. 2005; Semenov et al. 2005) families, which antagonise signalling by binding to LRP5/6 and thus preventing FZD/LRP complex formation.

Mouse Cerberus protein (Cerl-1), in contrast to *Xenopus*, does not bind WNT ligands and thus does not inhibit WNT signalling (Piccolo et al. 1999; Belo et al. 2000). Rather, Cerberus proteins form key regulators of Nodal signalling and play an important role in the establishment of left-right asymmetry in the vertebrate embryo (Zhu et al. 1999; Tavares et al. 2007; Vonica and Brivanlou 2007).

Insulin-like growth factor binding protein 4 (IGFBP-4) has been shown to bind directly to LRP6 and FZD8 through the the C-terminal thyroglobulin domain and thus blocks WNT3a binding (Zhu et al. 2008).

The transmembrane WNT inhibitors Shisa (Yamamoto et al. 2005; Furushima et al. 2007; Pei and Grishin 2012), Waif1 (Kagermeier-Schenk et al. 2011), Adenomatosis polyposis coli down regulated 1 (APCDD1) (Takahashi et al. 2002; O'Shaughnessy et al. 2004), and Tiki1 (Zhang et al. 2012) antagonise WNT signalling by preventing ligand–receptor interactions or WNT receptor maturation.

1.6.2.2 WNT activators

Two WNT ligand unrelated tyes of proteins – Norrin and R-spondins (RSPO), promote WNT signalling by binding to WNT receptors or releasing a WNT-inhibitory step (Kazanskaya et al. 2004; Xu et al. 2004; Kim et al. 2005; de Lau et al. 2012). Norrin binds to FZD4 (but only to that member of the Frizzled family), while RSPO2 interacts with FZD8 and LRP6 (Nam et al. 2006; Wei et al. 2007).

Connective tissue growth factors (CTGF) associate with the extracellular matrix (ECM) and mediate cell adhesion, cell migration and chemotaxis (Hall-Glenn and Lyons 2011; Jun and Lau 2011; Kubota and Takigawa 2011). They have been further implicated to regulate WNT signalling through its ability to bind the LRP6 co-receptor (Mercurio et al. 2004).

The secreted glycoprotein collagen triple helix repeat-containing 1 (CTHRC1) has been demonstrated to promote cell migration (Pyagay et al. 2005) and melanoma cell adhesion and survival (Ip et al. 2011). Recent studies, however, found that CTHRC1 selectively activates the WNT/PCP pathway by stabilising WNT/FZD/ROR2 complex formation (Yamamoto et al. 2008).

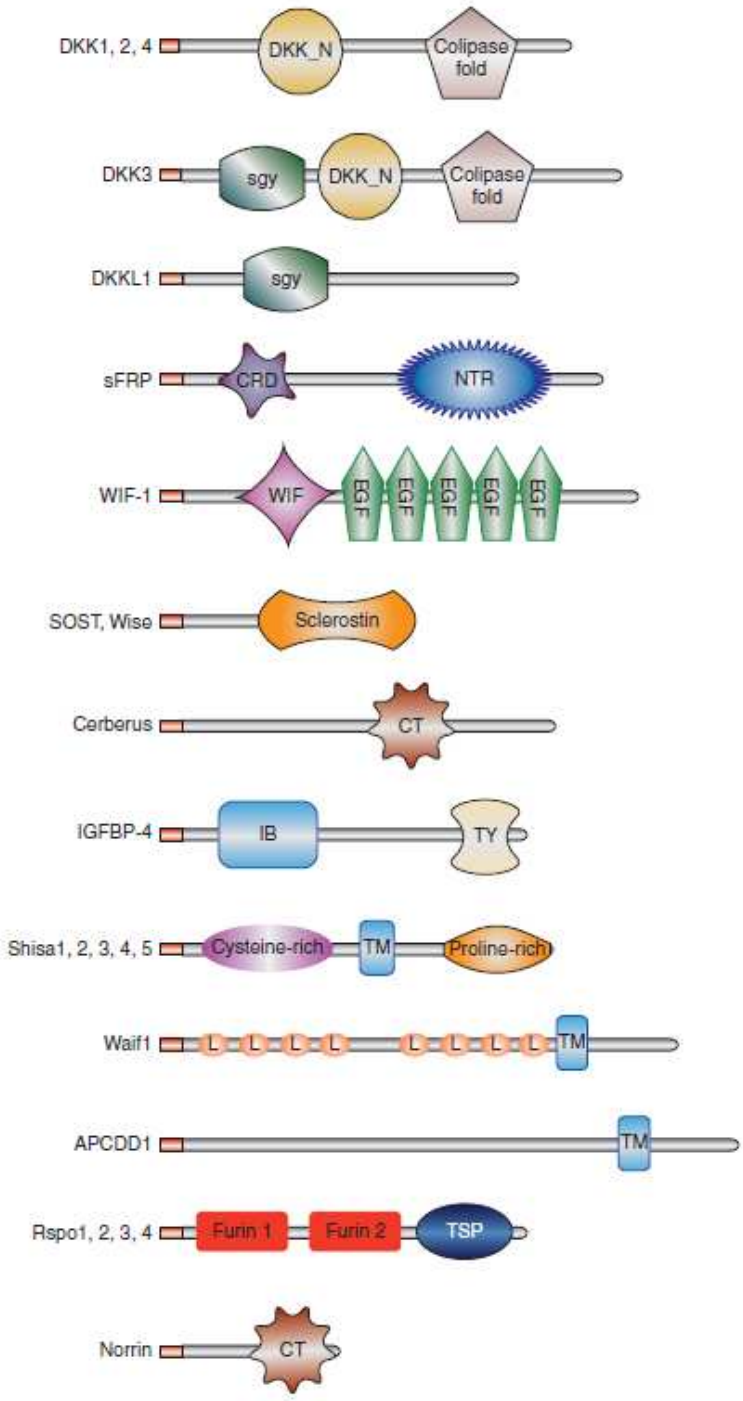

Figure 1.23: Non-WNT ligands modulators. Domain structure of WNT antagonists and agonists. Signal peptides are indicated in red. For more information refer to text. Abbreviations: NTR-Netrin related motif, WIF-WNT-inhibitory factor 1 domain, EGF-epidermal growth factor-like domain, CT-cystine knot-like domain, IB-insulin growth factor binding protein domain, TY-thyroglobulin type-1 domain, TM-transmembrane domain, L-leucine-rich repeats, TSP-thrombospondin type-1 domain. Figure from Cruciat and Niehrs, 2012.

1.6.3 Frizzled receptors

Frizzled (FZD) receptors belong to the seven transmembrane-spanning G-protein-coupled receptor (GPCR) superfamily, and are characterised by a large extracellular N-terminal region containing a cysteine-rich domain, involved in WNT ligand binding (Bhanot et al. 1996; Hsieh et al. 1999; Schulte and Bryja 2007). The intracellular C-terminus interacts with the PDZ domain of DVL proteins through the highly conserved internal KTxxxW motif (Wong et al. 2003). Therefore, Frizzled proteins act as WNT receptors and provide the link between the extracellular WNT ligand and the intracellular components of WNT signalling cascades (Figure 1.24) (Bhanot et al. 1996).

The mammalian FZD subfamily is comprised of 10 members (FZD1 to FZD10), which mediate and modulate different pathway activation and signalling outcome upon binding to various co-receptors and/or other secreted proteins like Norrin, RSPO or CTHRC1 (see section 1.6.2) (Xu et al. 2004; Cadigan and Liu 2006; Nam et al. 2006; Hendrickx and Leyns 2008; Yamamoto et al. 2008; Cruciat and Niehrs 2012).

Like WNT proteins, Frizzled receptors have been grouped historically into two classes: one class is thought to stimulate the β-catenin pathway, whereas the other group is able to stimulate the Ca^{2+} pathway (Kuhl et al. 2000b). However, this understanding has been challenged by observations that Frizzled receptors, for example FZD4 can signal both β-catenin dependently (Ye et al. 2009) and independently (Robitaille et al. 2002; Descamps et al. 2012), based on cell, receptor and ligand context. FZD3 and FZD6 on the other hand have been strongly implicated in PCP signalling, due to observed neural tube closure defects in Fzd3/Fzd6 double deficient mice and defects in hair orientation of inner ear sensory cells (Wang et al. 2006; Stuebner et al. 2010; Wen et al. 2010).

FZD2 has been indicated in β-catenin signalling outcomes and non-canonical context (Ishitani et al. 2003; Li et al. 2008; Verkaar et al. 2009) and has been linked to heart disease (Blankesteijn et al. 1996; Blankesteijn et al. 1997).

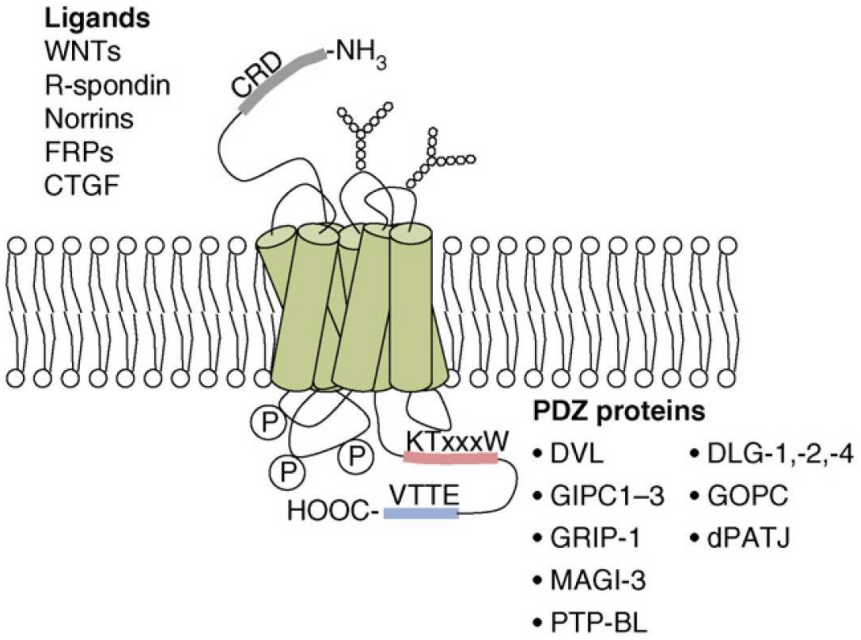

Figure 1.24: Schematic of Frizzled receptor key features and binding proteins and modulators. Frizzled proteins belong to the serpentine receptors composed of a conserved extracellular cysteine rich domain (CRD) involved in WNT ligand binding, a highly divergent linker region, and seven transmembrane spaning regions. The variable intracellular C-terminal domain contains a highly conserved KTxxxW motif important for DVL binding and initiation of WNT signalling, followed by a VTTE PDZ interacting motif. FRPs - Frizzled-Related Proteins, CTGF - Connective Tissue Growth Factor. Figure taken from Schulte et al, 2007.

1.6.4 WNT cell surface receptors

Initiation of WNT signalling depends first and formost on the WNT ligand and bound Frizzled receptor. In the mammalian system, WNTs and FZDs belong to large, multigene families and another layer of complexity is added through various (co)-receptors and cytoplasmic proteins, which determine the signalling outcome (Figure 1.25) (Niehrs 2012; van Amerongen 2012).

One proposed co-receptor for PCP signalling is the receptor tyrosine kinase ROR2 (section 1.6.4.2), which contains an extracellular cysteine rich domain, acting as receptor for WNT ligands (Minami et al. 2010). Other receptor tyrosine kinases, which have been implicated in PCP signalling are RYK (section 1.6.4.4) (Yoshikawa et al. 2003; Li et al. 2009a; Lin et al. 2010; Macheda et al. 2012)

and PTK7 (section 1.6.4.3) (Lu et al. 2004b; Shnitsar and Borchers 2008; Peradziryi et al. 2011).

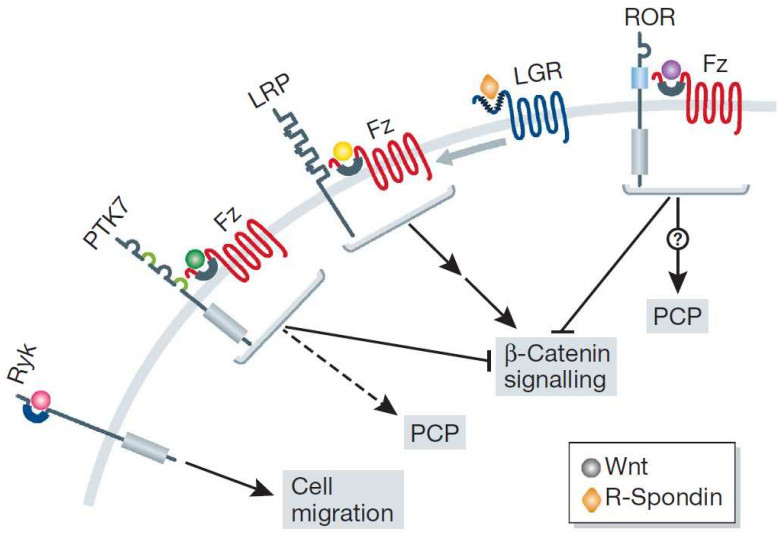

Figure 1.25: Overview of WNT modulating receptors and their effect on downstream WNT signalling. The main WNT ligand receptors are Frizzled (Fz) proteins. However, an expanding number of co-receptors can modulate WNT signalling outcome. For example, PTK7 and ROR transmembrane receptors in conjunction with Frizzled are able to bind to WNT ligands and to modulate β-catenin dependent and β-catenin independent (PCP) pathways. LGR can bind R-spondin, which enhances response to low dose WNT ligands, and has been demonstrated to interact and co-internalise with LDL-receptor related proteins (LRP)/Fz complexes, which are established β-catenin pathway activators. LGR - leucine-rich repeat containing G protein-coupled receptor PTK – Protein Tyrosine Kinase 7, ROR – Receptor tyrosine kinase-like Orphan Receptor, PCP – Planar Cell Polarity. Figure from Vincent and Beckett, 2011.

1.6.4.1 LRP5/6

LDL receptor-related proteins 5&6 (LRP5/6) function as co-receptors for WNT ligand interaction and are required for β-catenin signalling pathway activation (Pinson et al. 2000; Tamai et al. 2000).

They are single-pass transmembrane proteins belonging to the low-density lipoprotein receptor (LDLR)-related protein family. LRP5 and LRP6 are highly homologous and display redundant roles during development (He et al. 2004; Kelly et al. 2004). Structurally, they contain four EGF and three LDLR repeats

within the extracellular domain, and proline-rich motifs in the cytoplasmic part (Figure 1.26) (Brown et al. 1998).

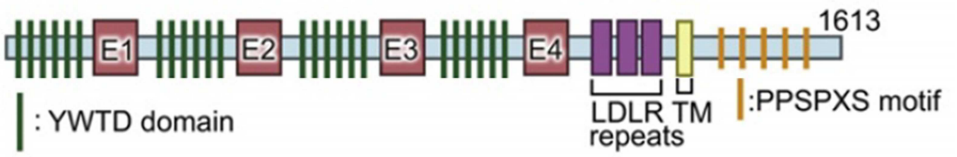

Figure 1.26: Schematic representation of the LRP5/6 receptor domain structure. The extracellular domain of LRP5/6 is about 1400 amino acids (aa) long and contains YWTD domains, EGF-like repeats (E1-E4), and LDL receptor repeats (LDLR), important for WNT ligand binding or interaction with modulating proteins like Sclerostin or Dickkopf. The short 215 aa cytoplasmic C-terminus is comprised of five PPSPXS motifs and juxtaposed casein kinase 1 (CK1) sites. Both serine residues within the PPSPXS motif are phosphorylated after WNT ligand stimulation and are required for β-catenin stabilisation. TM-transmembrane domain. Figure from Kikuchi et al, 2011.

Upon WNT ligand stimulation, LRP6 is phosphorylated at multiple sites including Thr1479, Ser1490, and Thr1493 by kinases such as GSK-3β and CK1, which is required for AXIN recruitment to the plasma membrane facilitating β-catenin accumulation and downstream nuclear signalling (Figure 1.16) (Tamai et al. 2004; Davidson et al. 2005; Zeng et al. 2005).

1.6.4.2 ROR2

The ROR-family of receptor tyrosine kinases (RTKs) (originally identified as RTK-like orphan receptors) are evolutionarily conserved from nematode to human and carry out important roles in regulation of cellular migration, polarity of asymmetric cell divisions, and axonal outgrowth of neurons (Forrester et al. 1999; Oishi et al. 1999; Al-Shawi et al. 2001; Curtin et al. 2003). In vertebrates, ROR-family RTKs contains two structurally related members, ROR1 and ROR2, which are widely expressed during embryogenesis and may play differential roles during development of the nervous system (Oishi et al. 1999; Green et al. 2008).

Ror2 null mice display (similar to Wnt5a knockout mice), PCP and CE defects, manifested as defects in ciliary bundles of cochlear hair cells and shortened anterior-posterior body axis, respectively (Yamaguchi et al. 1999; Seifert and

Mlodzik 2007; Minami et al. 2010). In addition, mouse models revealed that Ror2 mutations display widespread skeletal abnormalities, and are responsible for two classes of genetic skeletal disorders in human, dominant brachydactyly type B and recessive form of Robinow syndrome (Afzal et al. 2000; Oldridge et al. 2000; Schwabe et al. 2000; van Bokhoven et al. 2000).

Both, ROR1 and ROR2, act as receptor or co-receptor for WNT5a that can bind extracellular cysteine-rich domain, initiating intracellular signalling cascades (Oishi et al. 2003; Mikels and Nusse 2006a; Fukuda et al. 2008; Nishita et al. 2010b). However, ROR2 is also able to signal independently of its cytoplasmic domain through its association with Frizzled (at least FZD7) via their respective CRDs (Figure 1.27) (Oishi et al. 2003; Nishita et al. 2010b).

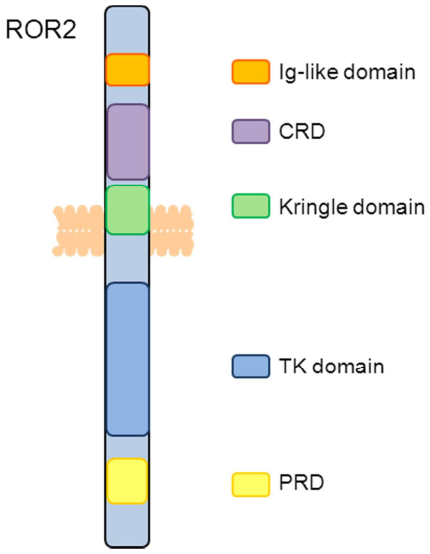

Figure 1.27: Structure of ROR-family receptor tyrosine kinase ROR2. ROR2 is a single spanning transmembrane protein with an extracellular immunoglobuline (Ig) –like domain, WNT ligand binding frizzled like cysteine rich domain (CRD) and a membrane proximal Kringle domain. The latter two are assumed to mediate protein-protein interactions. The intracellular cytoplasmic tyrosine kinase (TK) domain is followed by a serine threonine flanked proline rich domain (PRD).

WNT5a signalling through ROR2 regulates cell polarity, motility and invasiveness via non-canonical WNT signalling pathways (Figure 1.28) (Veeman et al. 2003a; Kohn and Moon 2005; Kikuchi and Yamamoto 2008). In fact, ROR2 has been established to mediate the WNT5a signal both *in vivo* and *in vitro* (Qian et al. 2007; Green et al. 2008; Minami et al. 2010; Gao et al. 2011). In addition,

WNT5a/ROR1 and WNT5a/ROR2 activated WNT signalling cascades are involved in neuronal progenitor cell maintenance as well as neurite extension and synapse formation in the developing nervous system (Endo et al. 2012a). ROR2 also plays a crucial role in canonical WNT signalling inhibition (Torres et al. 1996; Topol et al. 2003; Westfall et al. 2003; Mikels and Nusse 2006a; Li et al. 2008).

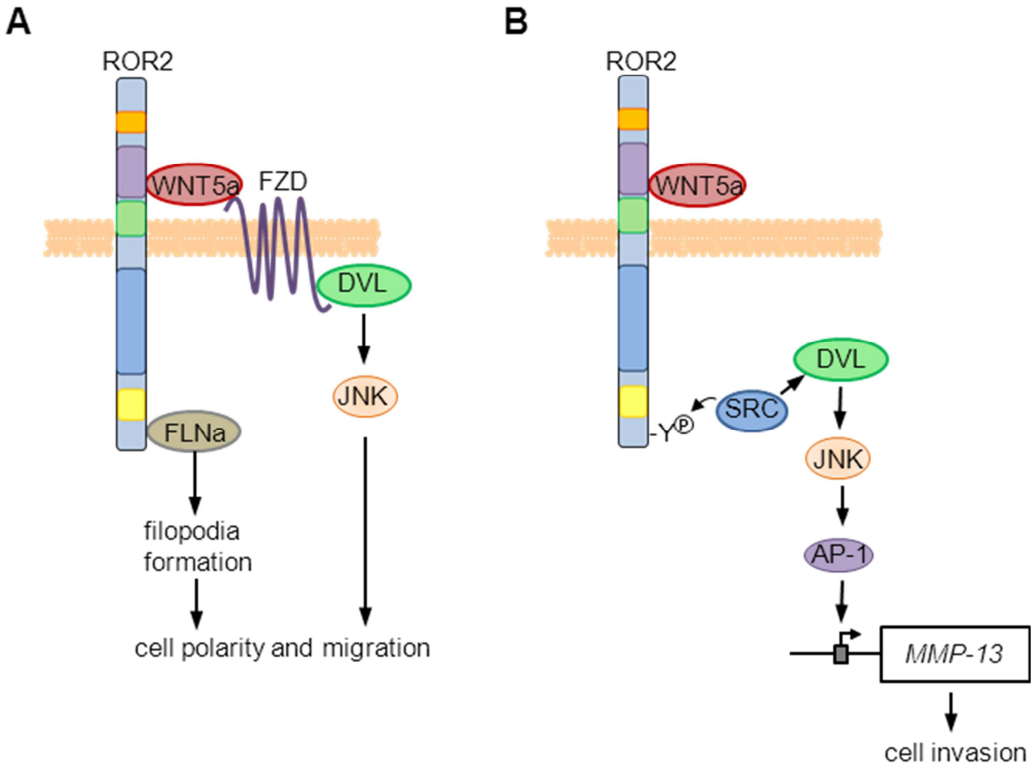

Figure 1.28: ROR2/WNT5a signalling in regulation of cell polarity, migration and invasion. ROR2 acts as a co-receptor in non-canonical WNT signalling and has been implicated in various functions. **(A)** Upon binding of WNT5a to the extracellular frizzled-like cysteine rich domain (CRD), the formed ROR2/Frizzled/WNT5a complex is able to modulate cell polarity and migration through activation of c-Jun N-terminal kinase (JNK) downstream of DVL, and binding of actin binding protein filamin A (FLNa), which associates with the C-terminal proline rich domain of ROR2. **(B)** WNT5 binding to ROR2 leads to recruitment and activation of protein tyrosine kinase c-SRC and results in phosphorylation of the cytoplasmic serine/threonine rich domain of ROR2. This leads in osteosarcoma cells to induced expression of matrix metalloprotease 13 (MMP-13) through activation of c-SRC, DVL, JNK and AP-1 signalling. AP1 - activator protein 1.

ROR2 is required for WNT5a induced polarised cell migration and mediates formation of filopodia through interaction with the actin binding protein filamin A

(FLNa) (Figure 1.28A) (Nishita et al. 2006). Furthermore, polarised cell migration experiments showed that WNT5a stimulated lamellipodium formation and microtubule organizing centre (MTOC) reorientation is mediated through ROR2/FLNa/JNK signalling (Nomachi et al. 2008).

It has been shown that atypical Protein Kinase C (aPKC) associates with DVL, functioning upstream of JNK, suggesting a possible functional link between WNT5a/ROR2/FLNa/JNK and CDC42/PAR/aPKC pathways in polarised cell migration (Schlessinger et al. 2007).

Although the roles of WNT5a in cancers remain controversial, ROR1 and ROR2 have been demonstrated to promote tumour progression (Enomoto et al. 2009; Wright et al. 2009; Ford et al. 2012; Daneshmanesh et al. 2013) (Figure 1.28).

1.6.4.3 PTK7

The transmembrane protein kinase 7 (PTK7) displays extracellular immunoglobulin domains and an intracellular tyrosine kinase homology domain, which is evolutionary conserved but lacks catalytic activity (Mossie et al. 1995; Kroiher et al. 2001). PTK7 functions in cell adhesions, cell migration, cell polarity, proliferation, actin cytoskeleton reorganisation and embryogenesis related apoptosis in order to regulate processes such as epithelial tissue organisation, neural tube closure and neural crest formation as well as axon guidance (Lu et al. 2004b; Toyofuku et al. 2004; Shnitsar and Borchers 2008; Meng et al. 2010).

It has been demonstrated that PTK7 participates in WNT signalling through acting as a co-receptor in both β-catenin dependent and independent WNT signalling cascades, and is involved in the choice of signalling outcome (Shnitsar and Borchers 2008; Wehner et al. 2011; Peradziryi et al. 2012). Despite the lack of any known WNT protein binding domain, PTK7 has been reported to co-immunoprecipitate with WNT3a and WNT8 but not with WNT5a or WNT11 (Peradziryi et al. 2011).

In addition to WNT signalling, PTK7 has been shown to regulate other signalling pathways by functioning as co-receptor with membrane receptors like Plexin A1 and VEGFR1 (Shin et al. 2008; Wagner et al. 2010; Lee et al. 2011).

Furthermore, recent studies showed that PTK7 is a target of matrix metalloproteases (MMP) 14 and ADAM17, leading to proteolytic degradation and extracellular domain shedding, thus resulting in enhanced cell proliferation, migration, and facilitated cancer cell invasion (Golubkov et al. 2010; Na et al. 2012). Originally identified in colon carcinoma cells (Mossie et al. 1995), PTK7 has been further demonstrated to be frequently deregulated in other types of cancer (Easty et al. 1997; Muller-Tidow et al. 2004; Prebet et al. 2010; Gobble et al. 2011).

1.6.4.4 RYK

The transmembrane atypical receptor related tyrosine kinase RYK is required for normal axon guidance and neuronal differentiation during development and involved in WNT signalling (Hovens et al. 1992; Stacker et al. 1993; Fradkin et al. 2010).

RYK functions as a WNT receptor through its WNT protein binding WIF domain and has been demonstrated to regulate convergent extension movements in *Xenopus* embryos through FZD7 and DVL endocytosis (Patthy 2000; Kim et al. 2008). In addition, RYK plays a role in mammalian planar cell polarity signalling, forming a complex with VANGL2 and modulating its stability (Andre et al. 2012; Macheda et al. 2012).

Overall, mammalian RYK is able to mediate both β-catenin dependent and independent signalling pathways downstream of WNT3a, WNT5a and WNT11 (Lu et al. 2004a; Li et al. 2009a; Lin et al. 2010). RYK deficient mice exhibit craniofacial defects associated with perturbed Eph receptor crosstalk (Halford et al. 2000).

1.6.4.5 HSPGs and Syndecans

Heparansulphate proteoglycans (HSPGs) are important for concentrating and stabilising of WNT proteins on the cell surface (Fuerer et al. 2010). Moreover, HSPGs modulate β-catenin independent signalling. For example Glypican 3 (GPC3) binds to WNT5a and enhances WNT5a dependent JNK activity and is required for gastrulation movements in zebrafish (De Cat et al. 2003; Song et al.

2005). GPC4 interacts with WNT11 and enhances WNT stimulated cell migration (Ohkawara et al. 2003). However, recent evidence suggests that GPCs might be also involved in β-catenin dependent signalling (Capurro et al. 2005). It has been suggested that the localisation of GPCs (lipid raft or non-lipid raft micro domains) might be important for selective WNT cascade activation (Sakane et al. 2012).

The syndecan (SDC) protein family also regulates WNT signalling and they have been implicated in β-catenin dependent (Alexander et al. 2000) and independent pathway modulation (Munoz et al. 2006; Ohkawara et al. 2011).

1.6.4.6 Tetraspanins

Tetraspanins are cell surface glycoproteins with four transmembrane domains and are able to form multimeric complexes with other cell surface proteins (Yanez-Mo et al. 2009). Tetraspanin proteins function in many cellular processes including differentiation, adhesion, signal transduction, and play critical roles in the suppression of cancer cell motility and metastasis (Richardson et al. 2011; Rubinstein 2011; Sala-Valdes et al. 2012). The tetraspanin family member TSPAN12 binds to FZD4 and promotes complex formation of FZD4 co-operatively with Norrin, thereby activating the β-catenin signalling cascade (Junge et al. 2009).

1.6.5 Dishevelled proteins

DVL proteins are key components of WNT signalling and interact with more than 50 proteins (Wallingford and Habas 2005; Gao and Chen 2010). They form multi-component signalling complexes and constitute the branching point of WNT signalling cascades (Figure 1.29A) (Gao and Chen 2010). Mammals encode three members of the Dishevelled family, DVL1, DVL2 and DVL3, which all contain the conserved structural features required for downstream WNT signalling (Figure 1.29B).

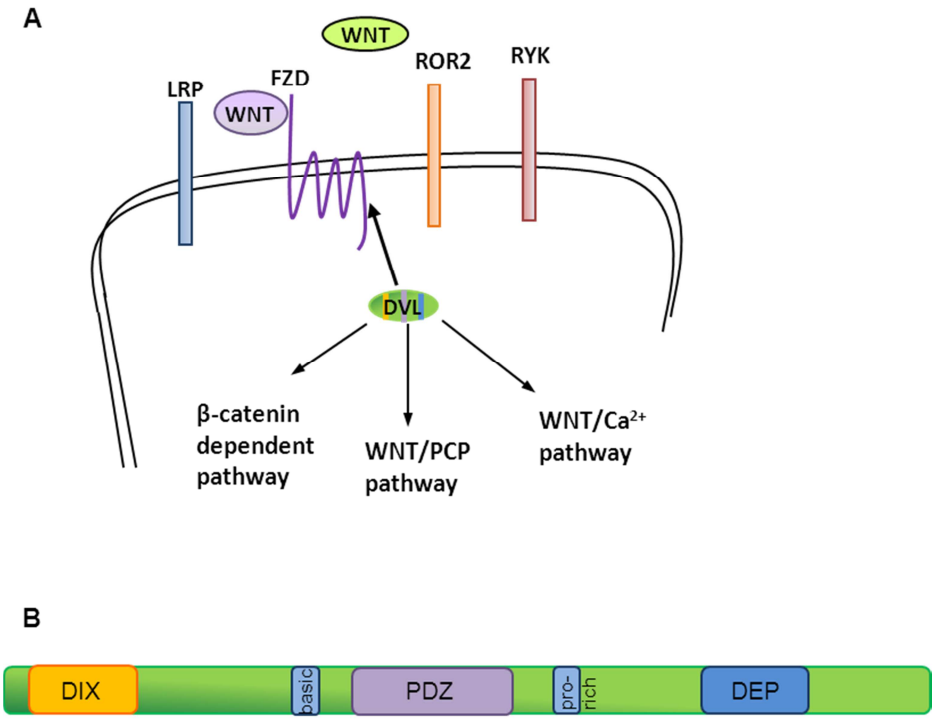

Figure 1.29: DVL proteins form the branching point of WNT signalling pathways. **(A)** WNT ligands bind to Frizzled receptors (FZD), which then recruits DVL to the plasma membrane and depending on receptor context, activates β-catenin (canonical) signalling or β-catenin independent pathways such as WNT/PCP or WNT/Ca^{2+} branches. Refer to section 1.5. **(B)** Conserved structural domains of DVL proteins. The N-terminal DIX (Dishevelled/Axin) domain is followed by a basic and serine/threonine rich region (basic) and a PDZ (PSD-95, DLG1, ZO1) domain, which facilitates interaction with other proteins. The C-terminus habours a proline-rich (pro-rich) region, which is followed by a DEP (Dishevelled, EGL-10, Pleckstrin) domain. Canonical WNT signalling involves the DIX and PDZ domain, whereas for non-canonical WNT signalling the DIX domain is dispensable and the PDZ and DEP domains are required.

During canonical WNT signalling, DVL is required for clustering of Frizzled and LRP6 receptors in order to form polymers for subsequent phosphorylation events of LRP6 (Cong et al. 2004b; Zeng et al. 2005; Bilic et al. 2007). DVL is recruited to Frizzled receptors via its PDZ domain (Wong et al. 2003) and forms polymers at the plasma membrane through its DIX domain, providing a platform for Axin-GSK3β relocation (Cliffe et al. 2003; Schwarz-Romond et al. 2007; Yokoyama et al. 2012).

DVL proteins also associate with actin fibres and cytoplasmic vesicular membranes and mediate endocytosis of the FZD receptor after WNT stimulation

(Capelluto et al. 2002; Chen et al. 2003). Further, DVL has been observed to shuttle from the cytoplasm to the nucleus and to interact with c-JUN and β-catenin (Itoh et al. 2005; Gan et al. 2008).

Upon initiation of non canonical WNT/PCP signalling, DVL associates with DVL associated activator of morphogenesis 1 (DAAM1) through its PDZ domain (Habas et al. 2001; Liu et al. 2008a). In conjunction with WGEF (weak similarity GEF) this complex then stimulates RHO activity and subsequently leads to RHO associated kinase (ROCK) activation, resulting in cytoskeleton remodelling (Figure 1.19) (Habas et al. 2001). In addition, DVL is able to stimulate RAC, which in turn can activate the downstream effector JNK, which regulates polarity, embryonic cell movements (Habas et al. 2003), and dendrite growth (Rosso et al. 2005).

The DIX domain is dispensable for PCP and RHO/RAC activation but is critically required for the β-catenin pathway (Veeman et al. 2003a; Wharton 2003). In contrast, the DEP domain is obligatory for RHO activation and stimulation of JNK activity (Boutros et al. 1998; Li et al. 1999; Habas et al. 2003).

In addition, DVL has been implicated in the modulation of WNT/Ca^{2+} signalling (Sheldahl et al. 2003), aPKC activity in hippocampal neurons (Dollar et al. 2005; Zhang et al. 2007) and is required for mTorc activation by WNT (Mak et al. 2005; Inoki et al. 2006).

WNT stimulation leads to hyper-phosphorylation of DVL, but the mechanism and function remains incompletely understood. Kinases which have been demonstrated to phosphorylate DVLs are Casein kinase 1ε (CK1ε) (Klimowski et al. 2006), CK2 (Wharton 2003) and PAR1 (Elbert et al. 2006).

DVL protein stability is controlled through proteasomal or lysosomal degradation. DVL proteins are targeted for proteasomal degradation through HECT-type ubiquitin ligase NEDL1 (Miyazaki et al. 2004) or KLHL12 (Angers et al. 2006) or mediated through a degradation complex involving PRICKLE1 (Carreira-Barbosa et al. 2003). Lysosomal destabilisation of DVL is mediated by Dapper (Cheyette et al. 2002; Zhang et al. 2006) or through a negative WNT signalling feedback loop (Jung et al. 2009). DVL2 has been reported to be degraded by the autophagy pathway as part of a negative feedback loop of WNT regulation (Gao et al. 2010).

DVL1 null mice are viable and fertile but display social interaction abnormalities (Lijam et al. 1997; Long et al. 2004). In contrast, DVL2 null mice displayed

somite segmentation defects and cardiac outflow tract abnormalities, which is also responsible for perinatal lethality of half of the offspring (Hamblet et al. 2002). DVL3 knockout mice show similar cardiac outflow tract abnormalities as observed for DVL2, but display a mild PCP defect of misoriented stereocilia in the organ of Corti (Etheridge et al. 2008; Wynshaw-Boris 2012).

Individual DVL proteins can rescue knock outs of other DVL genes, suggesting functional redundancy, which is also consistent with overlapping expression patterns (Sussman et al. 1994; Klingensmith et al. 1996; Tsang et al. 1996; Wang et al. 2005; Etheridge et al. 2008). Notably, overexpression of DVL has been reported in certain cancers (Okino et al. 2003; Uematsu et al. 2003).

1.7 VANGL proteins

VANGL proteins are tetra-membrane-spanning proteins, which are highly conserved from fly to human. In flies and worms only one *Vangl* gene can be found, whereas zebrafish, mouse and human contain two VANGL homologues with the exception of frogs, where only a VANGL2 homologue was identified (Torban et al. 2004).

The mammalian VANGL1 and VANGL2 proteins share a 73% total-amino-acid identity if compared to each other, and a 44% (VANGL1) or 50% (VANGL2), similarity to the *Drosophila* homologue *strabismus* (*stbm)*, suggesting that the vertebrate genes evolved by gene duplication from a common ancestor present in flies (Figure 1.30) (Torban et al. 2004).

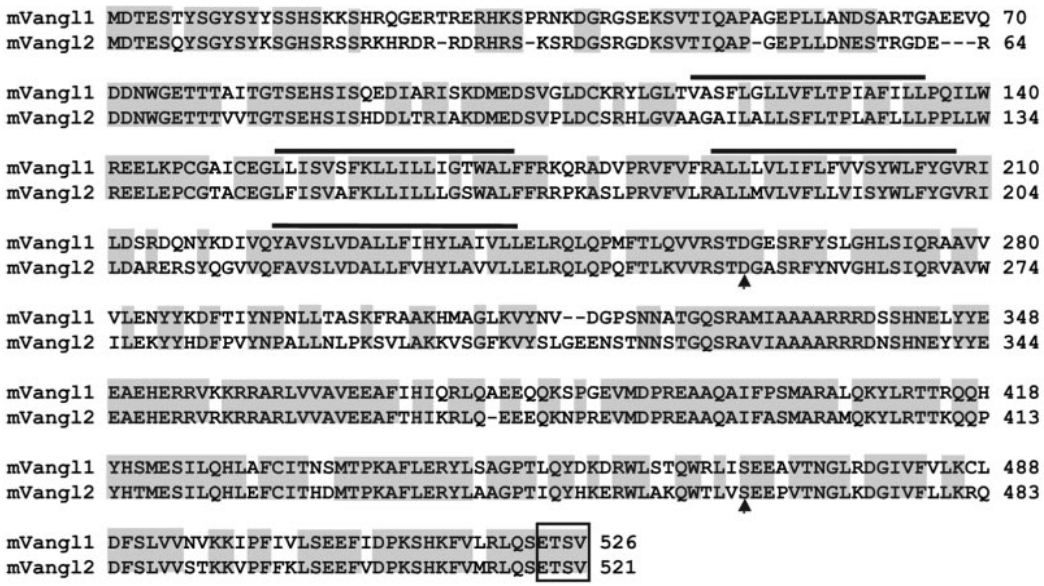

Figure 1.30: VANGL1 and VANGL2 proteins display a high degree of sequence similarity. Alignment of mouse VANGL1 and VANGL2 protein sequences. Identical amino acid (aa) residues of both sequences are highlighted in grey and transmembrane portions are indicated through a black line runnig above the respective amino acids. The C-terminal PDZ-binding motif (ETSV) is indicated by a box and the D255E and S464N mutations causing neural tube defects in *looptail* (*Lp*) mice are indicated by arrowheads. Figure taken from Torban et al, 2004.

Further, both proteins present two solvent accessible extracellular loops and an intracellular amino and carboxy terminus, and share the same C-terminal ESTV

motif, promoting protein interactions with PDZ domain containing proteins (Figure 1.31) (Nourry et al. 2003; Torban et al. 2004).

The presence of a N-terminal cytoplasmic serine/threonine cluster motif is evolutionarily conserved among vertebrate VANGL1 and VANGL2 orthologs and phosphorylation events in this cluster are required for at least VANGL2 activity (Daub et al. 2008; Gao et al. 2011).

Vangl homologues were initially discovered in a study of polarity establishment in the Drosophila eye and termed *strabismus* (Wolff and Rubin 1998). X-irradiation-induced mutations of the *stbm* locus showed disruption of polarity of multiple structures like the orientation of bristles (leg) and hairs (wing) (Figure 1.18b) or affect correct ommatidial rotation (eye) (Figure 1.18f). Studies of Vangl function in vertebrates using Zebrafish and *Xenopus* as model organisms demonstrated a role in mediation of cell movements during gastrulation (Park and Moon 2002).

Van gogh-like (VANGL) proteins play a role in planar cell polarity and convergent extension movements (see section 1.5.2) (Torban et al. 2004; Torban et al. 2008; Torban et al. 2012). Studies in vertebrate systems further identified VANGL proteins to function in unexpected developmental processes such as asymmetric cell division, left-right asymmetry and morphogenesis of different tissues (Torban et al. 2012).

1.7.1 VANGL1

Human *VANGL1*, also termed Strabismus *Drosophila* homologue 2 (STB2), encodes a 524-amino-acid protein, distributed over eight exons. Northern blot analysis detected 4.8- and 6.8-kb transcripts in nearly all human tissues examined (Katoh 2002; Yagyu et al. 2002; Kalabis et al. 2006). VANGL1 proteins localise to various subcellular departments such as cytoplasmic vesicular structures, co-localisation with E-cadherin or at the plasma membrane (see section 5.4) (Kalabis et al. 2006).

Mouse model studies using an inactivating mutation in the *Vangl1* gene showed that heterozygous mutants mice were viable and fertile, whereas homozygous mutants displayed subtle alterations in polarity, displayed by inner hair cells

orientation of the cochlea (Torban et al. 2008). Crosses between *Vangl1* and *Vangl2* heterozygous mice showed profound developmental defects, including severe craniorachischisis, inner ear defects, and cardiac abnormality, suggesting a genetic interaction between *Vangl1* and *Vangl2* (Torban et al. 2008).

In addition, mutational analysis of neural tube defects (NTDs) patients revealed a set of *VANGL1* point mutations across highly conserved amino acids, including the corresponding amino acids affected in the VANGL2 looptail mouse D255E and S464N (Figure 1.30 and Figure 1.31) (Kibar et al. 2007; Kibar et al. 2009). These findings suggests that VANGL proteins play an important role in developmental processes such as co-ordinated cellular migration in convergent extension movements during neurulation.

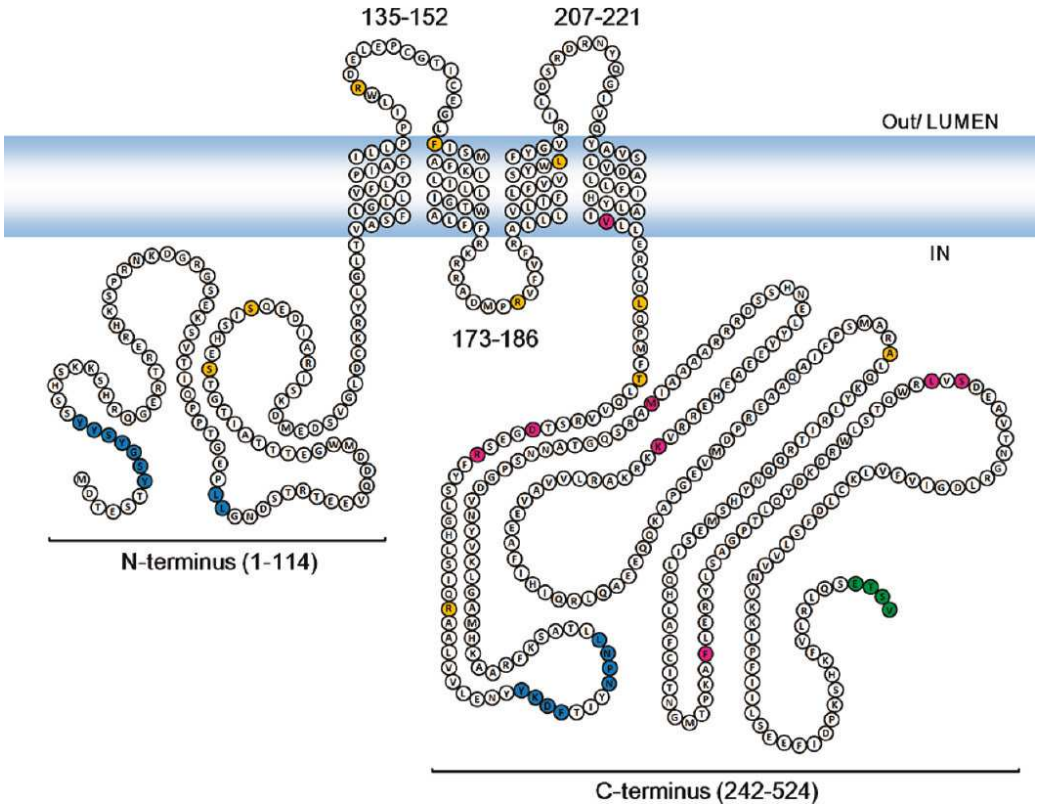

Figure 1.31: Topological model and structural features of VANGL1. This figure illustrates the four transmembrane domains, intracellular and extracellular segments and their respective position in the primary amino acid sequence of VANGL1. Amino acid residues in VANGL1 and VANGL2 associated with neural tube defects in mice and humans are depicted in yellow, whereas loss of function mutations have been demonstrated, are shaded in pink. The PDZ interacting tetrapeptide ETSV is coloured in green. Amino acids highlighted in blue represent consensus tyrosine based and di-leucine motifs associated with protein sorting and membrane targeting. Figure from Iliescu et al, 2011.

Whereas the link of VANGL1 to developmental tube defects is relatively weak (homozygous mice for VANGL1 are normal and fertile), an increasing body of evidence suggests a strong connection between high levels of VANGL1 expression and cancer progression/promotion. Several studies using colorectal cancer cells observed VANGL1 involvement in promotion of migration and invasion processes, while knock down of VANGL1 in various carcinoma cells showed inhibited growth and reduced migration (Yagyu et al. 2002; Lee et al. 2004; Kalabis et al. 2006; Kho et al. 2009; Lee et al. 2009; Ryu et al. 2010).

Expression analysis of gastric tumour samples showed higher VANGL1 levels compared to adjacent normal tissue (Lee et al. 2005). This ties in with the observation that VANGL1 expression in breast cancer cancer patients leads to a poor outcome prognosis, based on the demonstarted relationship between high VANGL1 expression and breast cancer relapse (Anastas et al. 2011).

Taken together, mammalian VANGL1 is involved in neural tube closure during gastrulation and neurolation processes, and modulates cell migration and invasion processes in adult tissues, which can contribute to malignant phenotypes such as abnormal tissue polarity, invasion and metastasis as found in human cancers.

1.7.2 VANGL2

VANGL2 (521 aa) is a well established PCP core protein and interacts with a multitude of WNT and PCP signalling components. Ranging from WNT (co)-receptors, ROR2 (Gao et al. 2011), RYK (Andre et al. 2012; Macheda et al. 2012) and PTK7 (Lu et al. 2004a) (see section 1.6.4), Frizzled receptors (Montcouquiol et al. 2006), DVL2 (Torban et al. 2004; Shafer et al. 2011), SCRIB (Montcouquiol et al. 2003; Montcouquiol et al. 2006), to RHO GTPase RAC1 (Lindqvist et al. 2010). Further, VANGL2 regulates the endocytosis and cell surface level of membrane type-1 matrix metalloproteinase (MMP14 or MT1-MMP) modulation of MMP endocytosis (Williams et al. 2012a; Williams et al. 2012b).

A mouse model termed *looptail* (*Lp*) exhibited independent mutations in the *VANGL2* locus, thus giving VANGL2 the alternative name Loop-tail associated protein (Ltap), displayed typical PCP defects (Kibar et al. 2001a; Kibar et al. 2001b; Torban et al. 2007). *Loop-tail* (*Lp*) mouse model homozygotes die *in*

utero of severe craniorachischisis, display defects in the inner ear cochlea hair orientation, heart outflow tract defects and defects of the musculoskeletal system characterised by fused ribs (Montcouquiol et al. 2003; Phillips et al. 2005; Torban et al. 2008).

VANGL2 point mutations have been identified to contribute to NTDs (Kibar et al. 2011) and several identified mutations are homologous to those found in VANGL1, such as *Lp* specific VANGL2 loss of function mutation S464N and mutant D255E (Kibar et al. 2001a; Kibar et al. 2001b; Guyot et al. 2011). These mutations have been demonstrated to affect plasma membrane targeting and result in ER retention, where protein half-life is reduced and stability affected by increased proteasome dependent degradation (Gravel et al. 2010).

1.8 Cell migration and invasion processes

Cell migration is essential for various cellular activities during the development and maintenance of multicellular organisms. Tissue formation during embryonic development, wound healing and immune responses require the orchestrated movement of cells in particular directions to specific locations. Cell migration involves coordination between protrusion at the anterior end of the cell, construction of new adhesive foci on the substratum, breakdown of old adhesive foci, and retraction of the posterior end of the cell (Ridley 2011). RHO GTPases control all the processes required for spatio-temporal coordination of protrusion, contraction, assembly and disassembly of cell-matrix adhesion, which are required for a moving cell (Ridley 2001b; Ridley 2011).

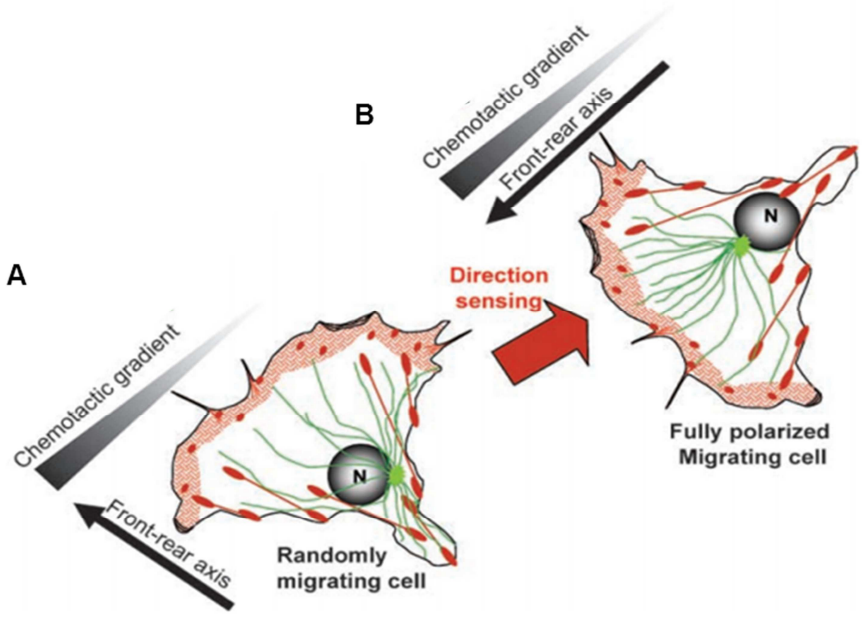

Figure 1.32: Polarity of migrating cells. (A) Application of a chemotactic gradient to a randomly migrating cell initiates direction sensing. Notably, front-rear polarisation is required for migration per se, but is not sufficient for chemotaxis. **(B)** Cell orientation following direction sensing is crucial to promote directed (or oriented) migration, but is not sufficient to drive cell migration. Orientation of the nucleus-centrosome axis is a good indicator of cell orientation during directed migration of most cell types. Actin-driven protrusions (lamellipodia) are shaded in red, microtubules are coloured in dark green and centrosome in light green. Straight red lines represent stress fibers and red patches correspond to focal complexes and focal adhesions. N illustrates the nucleus. Figure from Etienne-Manneville, 2008.

1.8.1 Actin structures and actin-binding protein Filamin A

Actin and myosin II play major roles in cell migration. Actin, a ubiquitous eukaryotic protein, is the major component of the cytoskeleton, controlling cell structure and motility (Herman 1993; Ridley 2001b). Actin exists mainly as a fibrous polymer (F-actin), but in response to cytoskeletal re-organising signals during processes such as cytokinesis, endocytosis, or stress. Cofilin promotes fragmentation and depolymerisation of F-actin, resulting in an increase in the monomeric globular form (G-actin) (Condeelis 2001). The Arp2/3 complex stabilises F-actin fragments and promotes formation of new actin filaments (Condeelis 2001).

Lamellipodia are actin projections on the mobile edge at the front of the cell and form a two-dimensional actin mesh, which pulls the cell forward across a substrate during the process of cell migration (Ridley 2011). Actin microspikes spreading beyond the lamellipodium frontier are termed filopodia (Small et al. 2002). RAC stimulates lamellipodium formation, while Cdc42 promotes filopodium construction (Hall 1998).

Filamin A (FLNa) is a 280-kD actin-crosslinking protein, which regulates re-organisation of the actin cytoskeleton by interacting with integrins, transmembrane receptor complexes, and second messengers (Ohta et al. 2006; Kim and McCulloch 2011; Nakamura et al. 2011). Filamins crosslink actin filaments into orthogonal networks in the cytoplasm and participate in the anchoring of membrane proteins to the actin cytoskeleton (Maestrini et al. 1993; Fox et al. 1998). In addition, cell motility-independent functions of FLNa at cell-cell contacts and adherens junctions affect the development of organs (Feng et al. 2006).

Interestingly, R-RAS (Gawecka et al. 2010; Griffiths et al. 2011) and ROR2 (Nishita et al. 2006; Nomachi et al. 2008) have been demonstrated independently to be interactors of FLNa, and are required for migration processes or endothelial barrier maintenance.

1.8.2 Invadopodial structures and matrix metalloproteases

Invadopodia are cell membrane localised, actin rich protrusions, extending into the extracellular matrix (ECM) where they are able to degrade ECM components (Linder et al. 2011; Murphy and Courtneidge 2011; Ridley 2011; Sibony-Benyamini and Gil-Henn 2012). Invadopodia are therefore thought to be key structures of cell invasion (Linder et al. 2011; Sibony-Benyamini and Gil-Henn 2012).

β1A integrin is a master regulator of invadosome organisation and function, mediated by matrix metalloproteinase MMPs (Destaing et al. 2010). MMPs belong to a family of proteases that target extracellular proteins including other proteases, growth factors, cell surface receptors and adhesion molecules (McCawley and Matrisian 2001). Among MMPs, MMP-2, MMP-3, MMP-7, MMP-9 and MMP-13 have been characterised as important factors for normal tissue remodelling during embryonic development, wound healing, tumour invasion, angiogenesis, carcinogenesis and apoptosis (Nagase et al. 1990; Vu et al. 1998; Sternlicht et al. 1999; Coussens et al. 2002; Kudo et al. 2012). MMPs are synthesised as pro-enzyme and are activated by releasing the inhibitory propeptide domain in order to yield an active, full length protease (Nagase et al. 1990).

Notably, WNT5a-ROR2 signalling confers MMP-13 linked invasive properties assessed by invadopodium formation (Figure 1.28B) (Enomoto et al. 2009). In addition, VANGL2 has been reported to regulate endocytosis and cell-surface availability of MMP14, resulting in proteolytic degradation or remodelling of the extracellular matrix (Cantrell and Jessen 2010; Williams et al. 2012a; Williams et al. 2012b).

1.9 Autophagy

Protein turnover takes place through the ubiquitin mediated proteasome pathway or is lysosome mediated (Ciechanover 2005). Autophagy or autophagocytosis is a key mechanism that clears unnecessary or dysfunctional cellular components through the lysosomal machinery or recycles nutrients during starvation or stress periods, thus maintaining cellular energy levels (Mizushima and Klionsky 2007).

Macroautophagy, the main pathway, generally eradicates damaged cell organelles or unused proteins. This process is tightly regulated through highly conserved genes termed autophagy regulators (ATGs), which are required at several steps along the process and orchestrate for instance the induction, cargo recognition and packaging or vesicle formation (Mizushima et al. 2011). Autophagy is stimulated in response to unfavourable conditions such as nutrient deprivation and is initiated through phagophore formation by class III PI3K, Atg6 (also known as Beclin-1) and ubiquitin-like conjugation reactions (Figure 1.33).

During phagophore nucleation, cytosolic proteins, protein aggregates and organelles are enclosed, and recruitment of ATG proteins such as ATG12, ATG5, ATG16 and covalent lipidated ATG8 together with transmembrane ATG9 facilitate phagophore extension. Upon completion of the double membrane organelle known as an autophagosome vesicle, ATG proteins start to dissociate, and fusion of the autophagosome with a lysosome results in a autolysosome and subsequent degradation of the organells content through acidic lysosomal hydrolases (Figure 1.33) (Yorimitsu and Klionsky 2005; He and Klionsky 2009).

To date, the processed form of microtubule-associated protein 1 light chain 3 (LC3) is the only reliable protein marker associated with completed autophagosomes and phagophores (Mizushima and Yoshimori 2007; Klionsky et al. 2008). LC3 also known as ATG8, is a ubiquitin like protein involved in autophagosome formation (Figure 1.33) (Kabeya et al. 2000). LC3 is initially synthesised as proLC3 (unprocessed form), which is converted into a proteolytical processed form lacking C-terminal amino-acids (LC3-I). Mature LC3 (LC3-II) is achived through modification of LC3-I by phosphatidylethanolamine (PE) conjugation (Kabeya et al. 2000; Klionsky et al. 2007).

Interestingly, a recent study by Gao and colleagues demonstrated negative regulation of WNT signalling through promotion of DVL2 degradation (Gao et al. 2010).

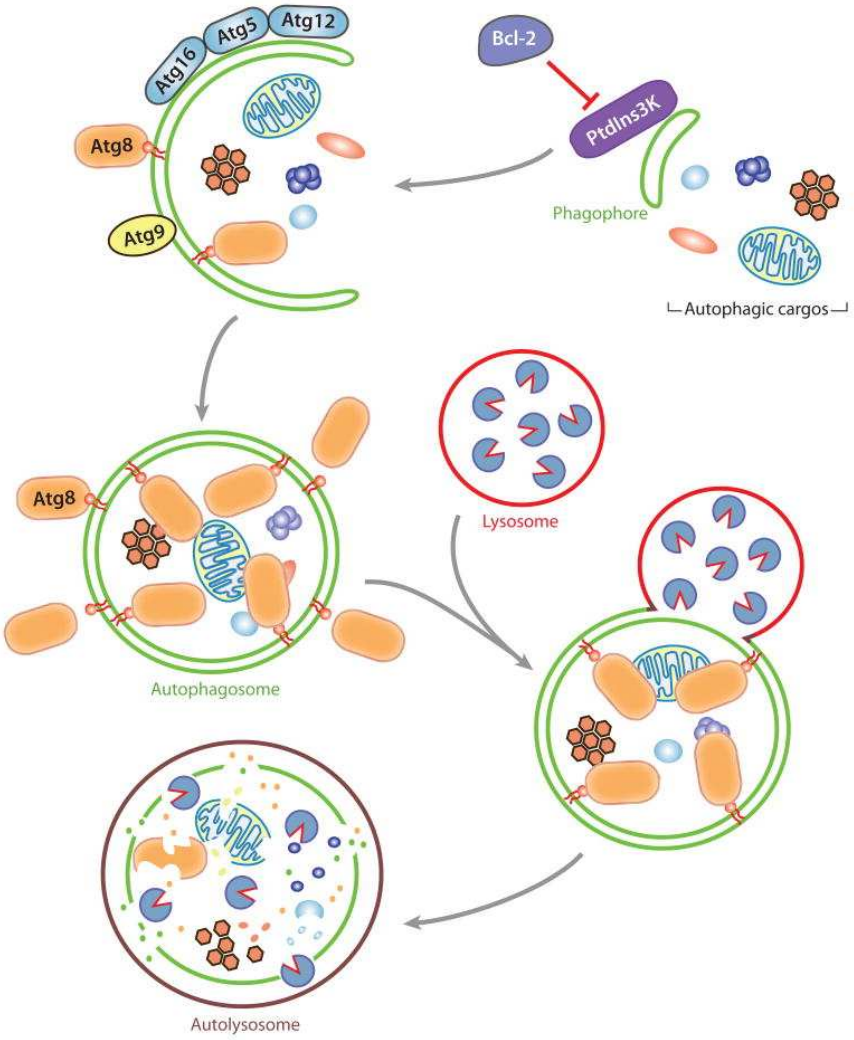

Figure 1.33: Schematic model of the autophagy process. Class III PI3K complex mediates the formation of the phagophore membrane, enwrapping organelles, cytosolic proteins and aggregates. This step could be inhibited through Bcl-2, which binds and inhibits Beclin-1, a component of the PI3K complex. Atg proteins like Atg12, Atg5, Atg16 and phosphatidylethanolamine (PE) conjugated Atg8 are recruited to the forming phagophore, in conjunction with the transmembrane protein Atg9, assisting the phagophore expansion step. Upon completion of vesicle formation, Atg proteins start to dissociate from the now formed autophagosome, enabling autophagosome-lysosome fusion and subsequent cargo degradation through acidic lysosomal hydrolases. Bcl-2 - B-cell lymphoma 2, PI3K - Phosphatidylinositide 3-kinase. Figure from He and Klionsky, 2009.

1.10 Aim of my study and outline of subsequent chapters

RAS proteins mediate important cellular functions such as gene expression, proliferation, differentiation and survival through a wide variety of effector proteins. Despite overlapping regulatory and effector proteins, and similar biochemical and biological features between oncogenic RAS and the closely related R-RAS members, they can also exhibit divergent regulation of signalling and cellular processes. Therefore, a better understanding of the full spectrum of effector pathways regulated by RAS family GTPases is critical to comprehend their many biological functions and their contribution to human disease.

In order to identify novel effector proteins specific to R-RAS members, Dr. Rodriguez-Viciana carried out a non-biased proteomic Tandem Affinity Purification (TAP) approach employing active R-RAS subgroup members as baits. This led to discovery of VANGL1 protein, a component of the WNT/Planar Cell Polarity pathway, as a potential novel effector of R-RAS proteins.

The aim of this thesis project was to validate and characterise the novel R-RAS-interactions, identified by TAP to study how R-RAS members regulate VANGL1 function and how VANGL1 may contribute to the signalling properties of R-RAS. In addition, the possibility was tested that R-RAS GTPases function downstream of WNT ligands in the PCP pathway, co-ordinating the regulation of VANGL proteins in order to control polarity and cell motility.

Cell motility and migration play a paramount role in both normal embryogenesis and the development of diseases such as cancer. Therefore, experiments were carried out to analysis and assess a role of R-RAS and VANGL1 in regulation of cell movement and invasion.

CHAPTER 2

Materials and Methods

2 Materials and Methods

2.1 MATERIALS

2.1.1 Chemical compounds and reagents

Human WNT3a (5036-WN), WNT5a (645-WN) and WNT7a (3008-WN) ligands were purchased from R&D. Murine Wnt3a (315-20) ligand was obtained from Peprotech. The proteasomal inhibitor MG132 (Santa Cruz Biotechnology) was prepared as 10 mM stock solution in Dimethyl sulfoxide (DMSO). Polyethyleneimine (Polysciences Inc) transfection stocks were prepared as 1 mg/mL solution in water and sterile filtered. Polybrene (hexadimethrine bromide), a cationic polymer used to increase the efficiency of retrovirus or lentivirus cell culture infections, was prepared as 5 mg/mL sterile filtered aqueous solution and applied as 5 µg/ml final concentration. Crystal violet dye (Sigma) was prepared as a 0.5% solution in 10% methanol/water mix. Paraformaldehyde (PFA) 4% w/v was dissolved in PBS at 60°C while stirring and subsequently aliquoted and frozen for long term storage. Aliquots were thawed when required and used immediately for fixation purposes. Autophagy reagents 3-methyladenine, Bafilomycin A, and Chloroquine were obtained from Sigma. Hanks balanced salt solution (HBSS) for amino acid starvation was obtained from Invitrogen. For immunoprecipitation experiments, Streptavidin sepharose or Protein A / Protein G sepharose were obtained from GE Healthcare. Non-targeting control siRNA conjugated with Alexa Fluor Red (46-5318, Invitrogen) was used to assess siRNA transfection efficiency.

If not stated otherwise, chemical reagents were obtained from Sigma.

2.1.2 Buffers

Coomassie stain: 0.2% (w/v) Brilliant Blue R (Sigma), 10% acetic acid (BDH), 50% methanol (BDH).

Coomassie destain: 10% acetic acid, 50% methanol.

DNA loading buffer (10x): 0.00125 g/mL Bromophenol Blue, 40% TE, 60 % Glycerol.

Lysis buffer (LB-E): pH 7.4; PBS supplemented with 1% w/v Triton X-100, 1 mM EDTA, 1mM Dithiothreitol (DTT), Protease inhibitor cocktail (Roche) and

Phosphatase inhibitor solution (10mM NaF, 2mM Na_3VO_4, 2 mM $Na_4P_2O_7$, 2 mM β-glycerophosphate).

Lysis buffer (LB-M): pH 7.4; PBS supplemented with 1% w/v Triton X-100, 5 mM $MgCl_2$, 1mM DTT, Protease inhibitor cocktail (Roche) and Phosphatase inhibitor solution (10mM NaF, 2mM Na_3VO_4, 2 mM $Na_4P_2O_7$, 2 mM β-glycerophosphate).

3-(N-morpholino)propanesulfonic acid (MOPS) running buffer: pH 7.7, 50 mM MOPS, 50 mM Tris Base, 0.1% SDS, 1 mM EDTA.

Phosphate buffered saline (PBS) buffer: pH 7.4; 137 mM NaCl, 2.7 mM KCl, 10.1 mM Na_2HPO_4, 1.76 mM KH_2PO_4).

Protein loading buffer (4xLDS): 40% glycerol, 4% lithium dodecyl sulfate (LDS), 4% Ficoll-400, 0.8 M triethanolamine-Cl, pH 7.6, 0.025% phenol red, 0.025% coomassie G250, 2mM EDTA disodium. This buffer was purchased from Invitrogen and supplemented with 0.25 M DTT to achieve reducing capability.

Tween supplemented PBS (PBST): 0.1% Tween in PBS.

Transfer buffer: 10 % (w/v) Methanol, 25 mM Bicine, 25 mM Bis-Tris, 1 mM EDTA.

Tris-Acetate-EDTA buffer (TAE): 40 mM Tris, 20 mM acetic acid, 2.5 mM EDTA.

Tris-EDTA buffer (TE): pH 8, 10 mM Tris, 1 mM EDTA.

2.1.3 Media and growth plates

Luria Bertani (LB) was prepared using 10 g/L Bacto™-Tryptone (BD), 5 g/L Bacto™-yeast extract (BD), 10 g/L NaCl (Sigma), 1 g/L Glucose as a ready to dissolve mix (Sigma). LB selection media contained either 100 µg/mL Ampicillin (Sigma) or 50 µg/mL Kanamycin (Gibco). LB growth plates were prepared as LB media above and supplemented with 15 g/L agar (Sigma) and selection plates were supplemented with appropriate antibiotic post autoclaving.

2.1.4 Antibodies

Table 1: Applied primary antibodies, working dilutions and corresponding suppliers.

antibody	clonal	host	dilution	catalogue number and supplier
AF6	p	rabbit	1:500-1:2000	#A50520, 35/AF6, Trans-duction
pAKT (S473)	p	rabbit	1:1000	9271, Cell Signaling
BRAF	m	mouse	1:2000	sc-5284, F7, Santa Cruz
γ-Tubulin	m	mouse	1:500	Clone GTU-88, T6557, Sigma
CASK	m	mouse	1:1000	sc-13158, C-6, Santa Cruz
DLG1 (SAP97)	m	mouse	1:1000	sc-9961, 2D11, Santa Cruz
DVL-1	m	mouse	1:500	sc-8025, 3F12, Santa Cruz
DVL-2	p	rabbit	1:1000	sc-13974, H-75, Santa Cruz
DVL-2	m	mouse	1:1000	sc-8025, 10B5, Santa Cruz
DVL-3	m	mouse	1:1000	sc-8025, 4D3, Santa Cruz
ERK	p	rabbit	1:2000	9102, Cell Signaling
pERK, (T202/Y204)	p	rabbit	1:2000	9101S Cell Signaling
Flag	m	mouse	1:1000-1:15000	F3165, M2, Sigma
Flag	p	rabbit	1:1000-1:15000	F7425, 0.4mg/mL, Sigma
GM130	m	mouse	1:200	610822, clone 35, BD Transduction laboratories
GST-tag	m	rabbit	1:5000	2625, Cell Signaling
His-tag	m	mouse	1:2000	2366, Cell Signaling
H-RAS	p	rabbit	1:1000	sc-520, C-20, Santa Cruz
JNK1	p	rabbit	1:1000	sc-571, FL, LOT D121, Santa Cruz
pJNK (T183/Y185)	p	rabbit	1:1000	9251, Cell Signaling
LC3B	p	rabbit	1:1250	2775, Cell Signaling

LRP6	m	rabbit	1:1000	2560, Cell Signaling
pLRP6 (Ser1490)	p	rabbit	1:1000	2568, Cell Signaling
Myc	p	rabbit	1:2000	sc-789, A-14, Santa Cruz
PP1	m	mouse	1:1000	sc-7482, E-9, Santa Cruz
RHOA	m	mouse	1:1000	sc-418, 26C4, Santa Cruz
RHOB	p	rabbit	1:1000	sc-180, C-119, Santa Cruz
R-RAS	m	mouse	1:500	sc-81930, YC-16, Santa Cruz
R-RAS	p	rabbit	1:500	sc-523, C-19, Santa Cruz
SCRIB	m	mouse	1:1000	sc-55543, C-6, Santa Cruz
Syntenin-1	m	mouse	1:1000	sc-100336, S-31, Santa Cruz
Tubulin-HRP	p	rabbit	1:5000	PM054-7, MPL
TC21	m	mouse	1:500	Sc-8193, 37-Y, Santa Cruz
TC21	p	rabbit	1:1000	In house generation
VANGL1	m	mouse	1:1000	MAB5476, Clone 497707, R&D systems
VANGL1	p	rabbit	1:15000	In house generation, serum1 and pre-sera

Note: Antibodies are indicated as monoclonal (m) or polyclonal (p) and were prepared in 3% BSA/PBST supplemented with 0.02% NaN_3.

2.1.5 Plasmids

For all cloning and subcloning vector construction, the Invitrogen Gateway® Cloning Technology was employed (www.invitrogen.com/gateway).

This system relies on cloning the gene of interest into an Entry vector (pENTR, see Figure 2.1A), which then can be amplified in bacteria and forms the donation vector for any subsequent subcloning step into various destination vectors by a simple and fast recombination reaction. Destination vectors (for an example refer to mammalian GST-tagged destination vector pDEST27, Figure 2.1B) are available for a wide range of applications and systems (*E. coli*, yeast, insect, or mammalian cell) and thus provide a fast, reliable and convenient method of construct generation.

For interaction studies in mammalian cells, pcDNA™ destination vectors were used, which are designed for constitutive expression in mammalian cell lines

under the Cytomegalovirus (CMV) enhancer-promoter for high-level expression and a Bovine Growth Hormone (BGH) polyadenylation signal and transcription termination sequence for enhanced mRNA stability. Further, a SV40 origin enables episomal replication and simple vector rescue in cell lines expressing the large T antigen such as employed HEK293T cells (Figure 2.1B).

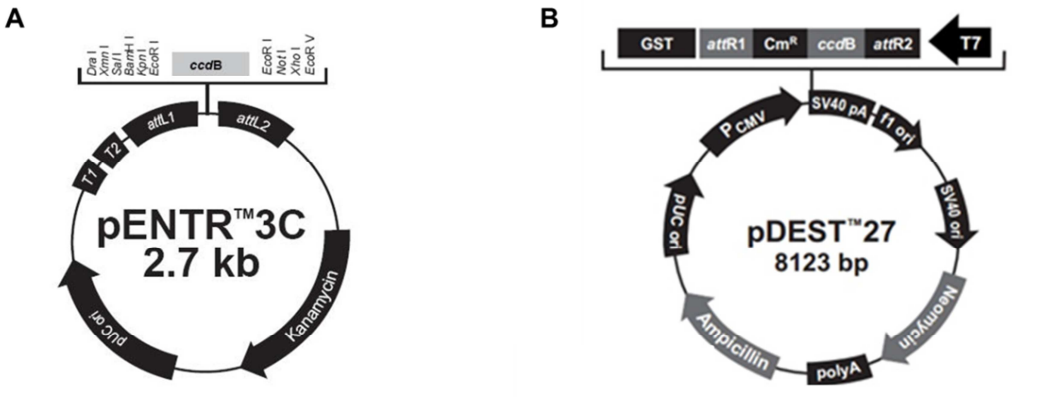

Comments for pENTR™3C
2723 nucleotides

*rrn*B T1 transcription termination sequence: bases 106-149
*rrn*B T2 transcription termination sequence: bases 281-308
*att*L1: bases 358-457 (complementary strand)
*ccd*B gene: bases 618-923
*att*L2: bases 952-1051
Kanamycin resistance gene: bases 1174-1983
pUC origin: bases 2047-2720

Comments for pDEST™27:
8123 nucleotides

CMV promoter: bases 15-608
Glutathione *S*-transferase (GST) tag: bases 635-1303
*att*R1 site: bases 1313-1437
Chloramphenicol resistance gene (Cm^R): bases 1546-2205
*ccd*B gene: bases 2547-2852
*att*R2 site: bases 2893-3017
T7 promoter: bases 3049-3068 (C)
SV40 early polyadenylation signal: bases 3368-3634
f1 intergenic region: bases 3760-4215
SV40 early promoter and origin: bases 4375-4683
Neomycin resistance gene: bases 4742-5536
Synthetic polyadenylation signal: bases 5600-5648
bla promoter: bases 5960-6058
Ampicillin (*bla*) resistance gene: bases 6059-6919
pUC origin: bases 7064-7737
(C) = complementary strand

Figure 2.1: Examples of Gateway cloning vectors. (A) Genes of interest are cloned in pENTR vectors flanked by *att*L1 and *att*L2 sites for site-specific recombination. **(B)** Genes of interest cloned into pENTR vectors can be shuttled to secondary vectors, termed destination vectors, through a fast and efficient recombination reaction using Clonase II enzyme mix. A wide range of vectors is available for expression in various systems. Vector maps were taken from the Gateway manual available at: www.invitrogen.com/gateway.

All pENTR clones were generated by Lucy C. Young, Marta Mũnoz-Alegre or Pablo Rodriguez-Viciana using Image clones or human placental pLIB cDNA library (PT3230.1) (Clontech) as templates for PCR. After cloning, pENTR vectors were sequenced and used for destination vector generation by means of recombination reactions.

Recombination reactions were performed by combining 0.5 µL Entry clone miniprep DNA, 0.2 µL desired Destination vector (100 ng), 1.3 µL 0.2x TE buffer and 0.5 µL 5x Gateway® LR Clonase II Plus enzyme mix (Invitrogen). The reaction volume was well mixed and microcentrifuged to collect at the bottom of the tube. The reaction was incubated at room temperature for at least 60 minutes up to O/N before transforming into bacteria and subsequent DNA isolation as outlined in 2.2.4 and 2.2.5.

2.1.6 Primers

Cloning primers for mutagenesis reactions were generated and obtained from Invitrogen and were delivered lyophilised. Oligos were resuspended with 0.2x TE to yield a stock solution of 100 pmol/µL (100 µM), incubated for 5 min and then vortex thoroughly. Working stocks for Polymerase chain reactions (PCR) were prepared at 10 pmol/µL (10 µM) with 0.2x TE.

2.1.7 RNAi sequences

RNAi duplex oligonucleotides (Stealth RNAi™) were designed and ordered from Invitrogen. Supplied lyophilised primers were reconstituted with Diethylpyrocarbonate (DEPC) treated water to yield a master stock concentration of 100 µM. Working stock concentrations were generated from the master stock at concentrations of 20 µM and 4 µM stock using DEPC-treated water. All employed RNAi duplexes were initially tested for respective protein knock down efficiency. In order to prevent off target effects, dose dependent experiments were carried out to determine minimal siRNA concentrations for efficient knock down, which were observed to be in the range between 2nM to 10nM (data not shown). Furthermore, time course experiments were carried out in order to estimate the longevity of the knock down effect, which lasted up to 7 days in a fast proliferating cell line such as HEK293T (data not shown).

Table 2: Applied siRNA oligo sequences

siRNA	Target sequence
R-RAS-1	5'-GAG AGC AGU ACA UGC GUG CUG GCC A-3'
R-RAS-2	5'-UCG CCA UUA ACG ACC GGC AGA GUU U-3'
TC21-1	5'-CAG UAU AUG AGG ACU GGC GAA GGC U-3'
TC21-2	5'-GGA UCG UGA UGA GUU CCC AAU GAU U-3'
VANGL1-1	5'-AGG CCG AAC AUG AAC GGC GAG UAA A-3'
VANGL1-2	5'-CAA UAU GAC AAG GAC CGC UGG CUC U-3'
VANGL2-1	5'-CGU CUD UGU GCU GCG UGC CCU GCU U-3'
VANGL2-2	5'-UCG UGG UCU CCU ACU GGC UCU UCU A-3'
Scribble-1	5'-GCG UCA GCG UCA UCC AGU UCC UGG A-3'
Scribble-2	5'-GGC CUA CGG GAA CUG UGC AUC CAG A-3'
Shoc2-2	5'-UAC CUU CGC UUU AAU CGU AUA-3'
scramble	5'-UUC UCC GAA CGU GUC ACG UUU-3'

The number post the dash indicates individual siRNA oligos, targeting different regions of the same gene of interest.

In order to assess transfection efficiency of siRNA molecules, an Alexa Fluor® 555-labeled, double-stranded RNA (Invitrogen, BLOCK-iT™ Alexa Fluor® Red Fluorescent Oligo Cat. No. 14750-100) was transfected alongside as control and assessed by fluorescence microscopy for successful delivery 24-48 h post tranfection. Alexa 555 is a duplex with the same length, charge, and configuration as standard siRNA and its sequence is not homologous to any known gene.

2.2 DNA TECHNIQUES

2.2.1 Basic DNA manipulations

2.2.1.1 Cloning approach of VANGL1 truncation constructs

Subcloning tasks were carried out utilising the Invitrogen Gateway® technology with Clonase™ II (Invitrogen) approach (see section 2.1.5.). DNA digestions were performed using New England Biolabs restriction enzymes and the supplied buffers according to the instructions of the manufacturer. Routinely, 0.5 µg of DNA was utilised for diagnostic restrictions, and 1-5 µg of DNA for preparative digests for subsequent use in ligation reactions. DNA restriction digests were usually carried out at 37°C for 2 h according to instructions of the manufacturer. For primer sequences and template plasmids used in this study, refer to Table 3. Chosen bands of DNA were cut out of the gel and purified using QIAquick Gel-extraction kit (Qiagen) according to the instructions of the manufacturer. For ligation reactions 1 µL of T4 ligase (Invitrogen), T4 ligase reaction buffer (Invitrogen), vector and insert DNA were added together to a final reaction volume of 10 µL. The ratio of vector to insert was maintained at 1:3 and ligation was carried out for 1 h to overnight at room temperature. Subsequently, 5 µL of ligation reaction was transformed into chemically competent bacteria (Invitrogen) as described in section 2.2.4.

Table 3: Primer sequences for generation of VANGL1 truncation constructs.

Con-struct	**Size [bp]**	**Forward primer** (5' -> 3') **Reverse primer** (3' -> 5')	**Tm [°C]**
VANGL1-N	343	caccggatccatggataccgaatccacttattc cacgaattcttaggtgaggcccaggtagcgtttgc	59 63
VANGL1-C1	852	caccggatccgagctcaggcagctgcagccca cgcgaattcttaaacggatgtctcagactgta	67 57
VANGL1-C2	426	caccggatccgagctcaggcagctgcagccca cacgaattcttaggctttctgctgctcctcagcc	67 62
VANGL1-C3	426	caccggatccccaggggaggtgatggaccctag cgcgaattcttaaacggatgtctcagactgta	67 57
VANGL1-ΔPDZ-BM	1560	caccggatccatggataccgaatccacttattc cacgaattcttaagactgtaagcgaaggacaaatttg	59 57

Note: For a detailed features and overview about truncated regions refer to Figure 3.8. Annealing temperatures were calculated using Promega online calculation tool, referring to salt adjusted Tm.

Table 4: PCR cycling parameters for VANGL1 truncation constructs

Segment	Cycles	Temperature	Time
1	1	94°C	3 minutes
2	25	94°C (denaturation)	30 seconds
		55°C (annealing)	30 seconds
		72°C (extension)	2 minutes
3	1	72°C	2 minutes
4	1	16°C	∞

Note: The extension time is determined by the length of the expected longest fragment of 1.6 kb (1 kb per minute for extension).

2.2.1.2 Cloning approach of ARHGEF17 truncation constructs

Subcloning and DNA handling techniques were carried out as described above for generation of VANGL1 truncations and respective PCR reactions were carried out using the cycle parameters as outlined in Table 4.

Table 5: Primer sequences for generation of ARHGEF17 truncation constructs.

Con-struct	Size [bp]	**Forward primer** (5′ -> 3′) **Reverse primer** (3′ -> 5′)	Tm [°C]
ARHGEF17-N	1530	caccgaattcatggcccgccgcctgccccgca cacgcggccgctcagtgcttccgcatgtccacctgtg	68 69
ARHGEF17-ΔN	3040	caccgaattcatggccagcaagtgctgcagcaagc cacgcggccgctcacaccctccacaggaggagg	64 69
ARHGEF17-C1	2440	caccgaattcatgggtgtgcggagtgccgaggaggc cacgcggccgctcacaccctccacaggaggagg	67 69
ARHGEF17-ΔC	2120	caccgaattcatggcccgccgcctgccccgca cacgcggccgctcacacacgggcatggcgctccgc	68 72
ARHGEF17-C2	1454	caccgaattcagccacacgcctcacggctcctccg cacgcggccgctcactggtaggcctcagggtcgacact	69 70
ARHGEF17-C3	487	caccgaattcagctccgtgtggctgggcactgag cacgcggccgctcagacgtctacttctgccagctgct	65 68
ARHGEF17-	722	caccgaattcagctccgtgtggctgggcactgag	65

C4		cacgcggccgctcagactgcagccaagaagcggac	69
ARHGEF17-C5	977	caccgaattcagctccgtgtggctgggcactgag agtgtgggaggtgtcctcctccaccaaaac	65 67

Note: annealing temperatures were calculated using Promega online calculation tool, referring to at salt adjusted Tm. (http://www.promega.com/techserv/tools/biomath/calc11.htm)

2.2.2 Plasmid mutagenesis

Generation of VANGL1 point mutations by site directed mutagenesis

A PCR approach was used to introduce VANGL1 point mutations at reported residues associated with neural tube defects and impairment of Dishevelled binding (Kibar et al. 2007) by means of site directed mutagenesis using the Quik change strategy (Stratagene). Extensions of the oligonucleotide primers, containing desired point mutations (Table 6), were generated with the PfuUltra^{TM} high-fidelity polymerase, producing a mutated plasmid (Hemsley et al. 1989). The amplified product was subsequently *Dpn*I treated, which specifically cleaves fully methylated G^{Me6}ATC sequences. As a result, the bacterially generated DNA used as template for amplification was digested and while the unmethylated product of the PCR reaction is left intact. The product of this digestion reaction was used to transform chemically competent *Escherichia coli* (*E.coli)* bacteria and colonies formed on selection plates were sequenced to confirm successful mutations.

PCR reactions were carried out in 50 µL volumes using provided reagents of the Quik Change® II Site-Directed Mutagenesis Kit (Stratagene), according to the instructions of the manufacturer. Conditions for amplification are shown in Table 7, utilised primers are summarised in Table 6 below.

Table 6: Primer sequences for generation of VANGL1 point mutant constructs

Con-struct	**Size [bp]**	**Forward primer** (5' -> 3') **Reverse primer** (3' -> 5')
VANGL1-V239I	1572	ctcttcatccattacctggccatcatcctgctggagctcaggcagctgc gcagctgcctgagctccagcaggatgatggccaggtaatggatgaagag
VANGL1-D259E	1572	gctgcaggtggtccgctccaccgagggcgagtcccgcttctacagcctg caggctgtagaagcgggactcgccctcggtggagcggaccacctgcagc
VANGL1-R274Q	1572	gcctgggacacctgagtatccagcaagcagcattggtggtcctagaaaat attttctaggaccaccaatgctgcttgctggatactcaggtgtcccaggc
VANGL1-M328T	1572	gccactggccagtcccgggccacgattgctgcagctgctcggcgcag ctgcgccgagcagctgcagcaatcgtggcccgggactggccagtggc
VANGL1-S467N	1572	tctctacacagtggaggcttgtcaatgatgaggctgtgactaatggatt aatccattagtcacagcctcatcattgacaagcctccactgtgtagaga

Table 7: PCR cycling parameters for site-directed mutagenesis

Segment	**Cycles**	**Temperature**	**Time**
1	1	95°C	30 seconds
2	18	95°C (denaturation)	30 seconds
		55°C (annealing)	1 minute
		68°C (extension)	11 minutes and 35 sec
3	1	4°C	∞

Note: The extension time was determined by the length of the amplified plasmid (1 kb per minute for extension).

In order to test expression of the generated point and truncation mutants of VANGL1, plasmids were transfected into HEK293T cells and subjected to immunoprecipitation (as described in section 2.5.4). Coomassie staining of a size

separated protein gel displayed similar expression levels of VANGL1 point mutants, except mutant D259E, which was expressed at a significantly lower level. VANGL1-N or C-terminal truncation proteins appeared to be equally expressed whereas VANGL1-C2 or C3 fragments showed severely reduced protein levels (Figure 2.2).

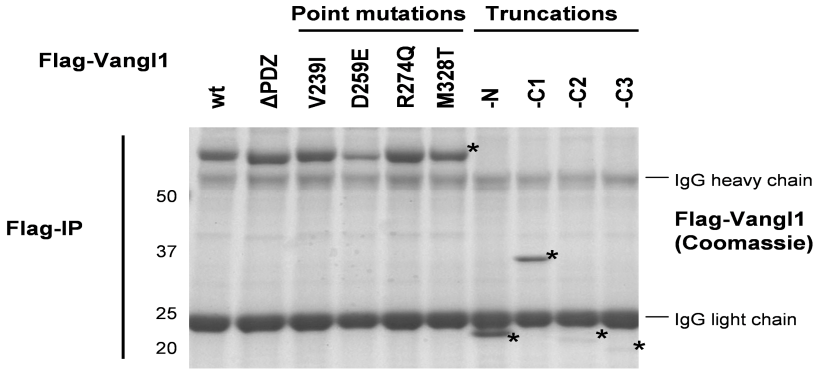

Figure 2.2: Expression analysis of Flag-VANGL1 point mutants and truncation constructs in HEK293T cells. 2ug of Flag-VANGL1 constructs were transfected into HEK293T cells, lysed after 48 hours and subjected to immunoprecipitation using Flag affinity beads. Immunocomplexes were size spearated on SDS-PAGE and Coomassie stained. Asteriks depict respective VANGL1 proteins.

2.2.3 DNA gel electrophoresis

In order to visualise DNA fragments from diagnostic digests or for cloning purposes, 1% or 1.2% agarose gels (Invitrogen) were prepared using 1x TAE buffer and TrackIt™ 1 Kb Plus DNA Ladder (1 µl) (Invitrogen, 0.1 µg/µL,) was run alongside for size estimation.

2.2.4 Transformation of bacteria

Chemically competent *E.coli* DH5α cells (Invitrogen) were gently thawed on ice, 5 µL of prechilled ligation reaction or gateway reaction mix was added to 50 µl aliquots of bacterial cell suspension and then kept on ice for 10 min. Subsequently, bacteria were heat-shocked at 42°C for 45 sec, recovered on ice for another 2 min, combined with 250 µL LB or S.O.C. solution (0.5 % Bacto tryptone, 2 % Bacto yeast extract, 10 mM NaCl, 2.5 mM KCl, 10 mM $MgCl_2$, 10 mM $MgSO_4$, 20 mM glucose) and incubated for one hour at 37°C at 200 rpm.

Bacteria suspensions were spread on LB culture plates supplemented with either 100 µg/mL Ampicillin or 50 µg/mL Kanamycin and incubated overnight at 37°C. Single colonies formed on the plates were picked and grown for extraction of plasmid DNA.

2.2.5 Preparation and purification of plasmid DNA

Bacterial DNA for analytical purposes was isolated from 1.5 mL minipreparation cultures utilizing a QIAprep® mini kit (Qiagen), and for generation of plasmid stocks, 50 mL *E.coli* cultures were extracted using QIAprep® midi kit (Qiagen) according to the instructions of the manufacturer.

2.2.6 DNA sequencing

DNA sequencing was performed by an inhouse service using AB sequencing technology. Supplied ab1 format files were visualised using Finch TV software.

2.3 RNA TECHNIQUES

2.3.1 RNA isolation

Total RNA from SaOS2 cells of equivalents of six well plates were prepared using ISOGEN reagent (Life Sciences). 500 µL ISOGEN was added to a PBS washed well of cells and incubated for 1 min at RT. Next, the ISOGEN solution was collected in an eppendorf tube and after 5 min incubation at RT, 100 µL chloroform added, vigorously shaken for 15 sec and incubated at RT for 2 min. Aqueous phase was separated from organic phase by spinning at 20 000 x *g* for 15 min at 4°C, following transfer of the aqueous phase to a fresh tube. Subsequently, 250 µL isopropanol was added, briefly vortexted and incubated for 10 min at RT. Precipitated RNA was collected as pellet by spinning at 20 000 x *g* for 10 min at 4°C, and the pellet washed with 70% ethanol/water solution, before spinning again at 20 000 x *g* for 5 min at 4°C and subsequent aspiration of ethanol solution. Yielded pellets were air dried at 37°C and dissolved in RNAse free water. Concentration of yielded RNA was determined using a spectrophotometer (Hitachi U-1900).

2.3.2 Semiquantitative PCR

For semi-quantitative reverse-transcription polymerase chain reaction, 0.5 µg of total RNA was used and the polymerase chain reaction was performed using the SuperScript One-Step RT-PCR kit (Invitrogen) according to the instructions of the manufacturer using the primer sequences listed in Table 8. MMP-13 specfic PCR reactions were carried out using following conditions for 40 cycles (Table 9) The amount of 18S rRNA was amplified using the same conditions as outlined for MMP-13 reactions (Table 9) for 25 cycles. The relative amount of MMP-13 was normalised using 18S RNA.

Table 8: Primer sequences for RT-PCR.

Gene	**Primer sequences** (forward/reverse)	**Prod. size**
MMP-13	5'-AAC ATC CAA AAA CGC CAG AC-3' 5'-GGA AGT TCT GGC CAA AAT GA -3'	166 bp
18S rRNA	5'-ATG GCC GTT CTT AGT TGG TG -3' 5'-CGC TGA GCC AGT CAG TGT AG -3'	217 bp

Table 9: RT-PCR cycling conditions

Segment	Cycles	Temperature	Time
1	1	50°C (DNA synthesis)	30 minutes
2	1	94°C (denaturation)	2 minutes
3	25 (18S) 40 (MMP-13)	94°C (denaturation)	15 seconds
		55°C (annealing)	30 seconds
		68°C (extension)	30 seconds
4	1	68°C (final extension)	1 minute
5	1	4°C	∞

2.3.3 Visualisation of RT-PCR products

5 µL of RT-PCR product were combined with 1 µL 10x DNA loading buffer and separated on a 1.8 % agarose/TAE gel (Nacalai). For product size estimation, a broad range DNA ladder (Nacalai) was run alongside.

2.4 MAMMLIAN CELL CULTURE

2.4.1 Cell lines and culture conditions

Immortalised human mammary epithelial cells HMEC, HMLE, 184A1 and MCF10A were cultured in DMEM F12 media (Invitrogen) maintained as described in (Debnath et al. 2003) supplemented with 2mM L-Glutamine (Gibco) in the absence of Penicillin/Streptomycin. Human breast adenocarcinoma MDA-MB-231 and MCF-7, alveolar basal epithelia adenocarcinoma A549, colorectal carcinoma HCT116, embryonic kidney cells 293 (HEK293T), osteosarcoma SaOS2 and U2OS, cervical carcinoma HeLa and mouse parental L cell lines were maintained in DMEM supplemented with 10% fetal bovine serum (FBS) (HyClone). Cells were grown in 150 mm dishes (Falcon) and passaged by washing with PBS and trypsinised by applying 0.05% Trypsin/EDTA (Gibco) solution for 5 up to 20 min. Cell lines were long term stored in FBS supplemented with 10% DMSO and placed in the vapour phase of liquid nitrogen.

2.4.2 Thawing and freezing/long term storage of mammalian cells

Cells were retrieved from liquid nitrogen and thawed in 37°C in a water bath, warm medium added and spun at 400 x *g* for 5 min to pellet cells. The pellet was resuspended in fresh medium and transferred to the appropriate cell culture dish. Medium was replaced the following day.

For long term storage of cell lines, cells were trypsinised and pelleted at 400 x *g* for 4min. Supernatant were aspirated and the pellet resuspended in freezing medium, containing 10% DMSO and 90% FBS. Aliquots of 1ml cell suspension were transferred into cryogenic vials (Corning) and placed in a styrofoam box and kept at -80°C for 24h, before transferred to liquid nitrogen.

2.4.3 Manual cell counting and assessment of viability

For seeding purposes and cell number determination, 10 µL of single cell suspension was applied to a Neubauer haemocytometer (VWR). Cells were counted in four independent areas of the haemocytometer and mean values were determined as cell number per mL. Cell viability was analysed by the Trypan blue dye (Sigma) exclusion method. Equal amounts of cell suspension are mixed with 0.4% trypan blue solution (Sigma), both populations either

positive or negative for dye staining were counted and viability was expressed as percentage of viable (dye negative) cells.

2.4.4 IncuCyte based proliferation or phenotype analysis

Cells were counted manually and seeded in 24 well or 6 well plates at various densities, depending on the cell line and rate of proliferation. They were then placed in the IncuCyte (Essen Instruments) and well density was measured every 2h until cells reached complete confluence. Medium was changed regularly (every 48h) between readings. Readings were analysed using MS Office Excel.

2.4.5 DNA transfection

2.4.5.1 Lipofectamine2000 transfection of plasmid DNA

For overexpression experiments, $1.5x10^6$ HEK293T cells were seeded in six-well dishes 2-4 h prior transfection. For each transfection reaction, 4 µL Lipofectamine2000 (Invitrogen) pre-incubated with 96 µL Opti-MEM for 5 min were mixed with 2.0 µg of plasmid DNA pre-diluted into 100 µL Opti-MEM (Gibco). After 20 min incubation at RT, the transfection solution was then added drop-wise to cells. After 16-24 h, additional 2 mL of full media was added to each well in order to boost growth and cells were harvested the following day.

2.4.5.2 Polyethylenimine transfection of plasmid DNA

For overexpression experiments, $2x10^6$ HEK293T cells were seeded in six-well dishes 2-4 h prior transfection. For each transfection reaction, 2.0 µg of plasmid DNA prediluted into 200 µL Opti-MEM (Gibco) were mixed with 8 µg polyethylenimine (PEI) (as aqueous solution of 1mg/mL). After 30 min incubation at RT the transfection solution was then added drop-wise to cells. After 16-24 h, additional 2 mL of full media was added to each well in order to boost growth and cells were harvested the following day. When performing transfections in 24 wells plates, 0.5 µg DNA constructs and 2ug polyethylenimine were combined in 100 µL Opti-MEM per reaction.

2.4.6 RNAiMAX siRNA transfection

Forward transfection protocols

U2OS cells were plated the day before, at a density of $0.75x10^6$ cells per 24 well in a total volume of 500 µL regular growth media. The next day, 6 pmol RNAi

duplex was diluted in 50 µL serum free OptiMEM®I medium (Gibco), while 1µL of RNAiMAX reagent was diluted with 50 µL serum free OptiMEM®I medium and mixed gently. RNAi duplex and RNAiMAX mixtures were combined and incubated at room temperature for 15 min, before adding the incubated mixture dropwise to wells and mix gently by rocking the plate. The final volume per 24 well came up to 600 µL, which yielded in a final of 10nM RNAi duplex concentration. 16h post transfection, the complete medium was changed and cells were either wound scratched or lysed for knock down efficiency verification 72h post transfection.

Oligonucleotide delivery efficiency into mammalian cells was assessed by transfection of a red-labelled dsRNA oligomer (BLOCK-iT-Alexa), which does not display any homology to any known gene sequences.

Reverse transfection protocols

Reverse transfection protocols were applied for Saos2 invadopodia experiments. Transfection mixes were prepared as above by combining 100uL OPTIMEM/RNAi oligonucleotide solution with a 98 µL OPTIMEM / 2µL RNAiMAX mix, followed by a 15 min of incubation at RT. Transfection mix, media and $2x10^5$ Saos2 cells were combined to yield a 1mL volume prior adding to 6 wells. Media was changed 16h later and cells were manipulated 72h post transfection.

2.4.7 Virus generation

2.4.7.1 Retrovirus

For generation of retrovirus containing supernatants in 60 mm dishes, 5×10^6 cells of the retrovirus producer cell line Phoenix Eco 293 were seeded 4 h before transfection. Cells were lipid-complex transfected using 5µg FBneo plasmids diluted in 250 µL OPTIMEM, which was combined with 10 µL Lipofectamine2000 per 250 µL OPTIMEM, followed by a 20 min incubation period at room temperature. The transfection mix was added drop wise onto cells while rocking gently, leading to final volume of 2.5mL. The next morning, culture media was exchanged with 3 mL regular growth medium and ecotrophic retrovirus supernatants were harvested at 24, 48, 72 hours after this by replacing collected supernatant with 3mL regular growth media. Harvested virus was either frozen

in 1 mL aliquots and stored at -80°C or utilised for immediate subsequent infection of EcoR target cells.

2.4.7.2 Lentivirus

Lentiviral constructs were employed due to its convenient ability to infect most cell types including primary or non-dividing cells, and as an alternative to retroviral transduction approaches in case of lack of required stable EcoR cell lines.

In order to generate lentivirus supernatants for transduction purposes and generation of stable cell lines, 2 x 10^6 HEK293T cells were seeded in 35 mm 6 well plates in a final volume of 1.5 mL. After allowing cells to settle for 4 h, a PEI transfection approach (refer to 2.4.5.2) was carried out in order to deliver all required packaging vectors for virus particle production. Cells were triple transfected with 0.73 µg of the gag-pol expressor plasmid p8.91, 0.43 µg of the VSV-G expressor vector pMDG, and 0.84 µg of either pLEOC (Blasticidin resistance) or pLEX (Puromycin resistance) lentiviral destination vector. Medium was replaced 16 hours later with 1 mL growth medium, and virus harvest was commenced 48h after transfection. Aliquots of 1 mL viral supernatants were supplemented with a final concentration of 5 µg/mL Polybrene in order to increase transduction efficiency and aliquots were either frozen or used fresh for transduction of target cell lines. Virus collection was performed on three consecutive days 48h, 72h and 96h post initial transfection.

In order to transduce mammalian cells with lentiviral particles, cells were seeded into 6-well dishes and allowed to grow overnight to 50% to 70% confluency. Next day, frozen virus stocks in 1 ml aliquots including 5µg/ml Polybrene were thawed at 37°C and then spun for 1 min at 15000 x g rpm at 4°C in order to pellet residual cells in the supernatant. Then, cell medium was replaced by 1ml of the virus/Polybrene solution and plates were gently rocked every 30 min to increase viral transduction efficiency. After 4 hour of incubation, remaining supernatant was removed and replaced with 2ml of growth medium for 24h before adding the appropriate selective agent. The appropriate selection is vector dependent and media was either supplemented with 2.5 µg/mL Puromycin (Sigma) or 5-10 µg/mL Blasticidin (Sigma), until sensitive control populations died under selection pressure. Remaining transduced cell populations were either expanded and used for experiments or frozen for long term storage.

2.4.8 Generation of stable cell lines

2.4.8.1 Generation of stably WNT ligand expressing cell lines and collection of WNT conditioned media

Respective WNT ligand genes were cloned into retroviral FB destination vectors and used for Retrovirus generation. Mouse L cells were subsequently transduced, Geneticin (G418, 500 µg/mL) selected and grown to confluency. WNT ligand conditioned media was collected from 15 cm dishes of control (eGFP) or stable WNT ligand expressing L cells after reaching confluency. Conditioned media was collected every 24 h over the course of three days, centrifuged to remove cell debris and stored at 4°C for up to two months or snap frozen and stored at -80°C for long term storage.

Generated WNT ligand conditioned media was tested for biological activity using ß-catenin dependent transcription Luciferase reporter assay or Dvl2 phosphorylation shift assessed by western blotting.

Dilution of WNT3a CM with regular growth media at 1:2 (50%) or 1:4 (25%) ratios revealed that the biological activity is not compromised compared to undiluted CM (100%) (Figure 2.3A). In fact, the 1:2 (50%) dilution seemed to enhance the biological activity by about 35%, suggesting that at least WNT3a CM might contain other antagonistic factors besides WNT3a, which are able to modulate activation of canonical signalling. Further, a single freeze/thaw (F/T) cycle of WNT3a CM does not significantly affect its biological activity, allowing long term storage of CM at -80°C (Figure 2.3A).

Since I planned to use WNT CM media for various stimulation experiments, which might be sensitive to high FBS concentrations (above 0.25%), I assessed WNT3a ligand activity with conditioned medium containing various FBS concentrations using the β-catenin luciferase readout. Conditions ranged from using serum free, BSA supplemented serum free, 0.25% FBS or regular growth media levels, which demonstrated that WNT3a activity is 3-4 fold less in WNT conditioned media containing low or no FBS. Therefore, we generally produced WNT ligand CM in the presence of 10% FBS (Figure 2.3B).

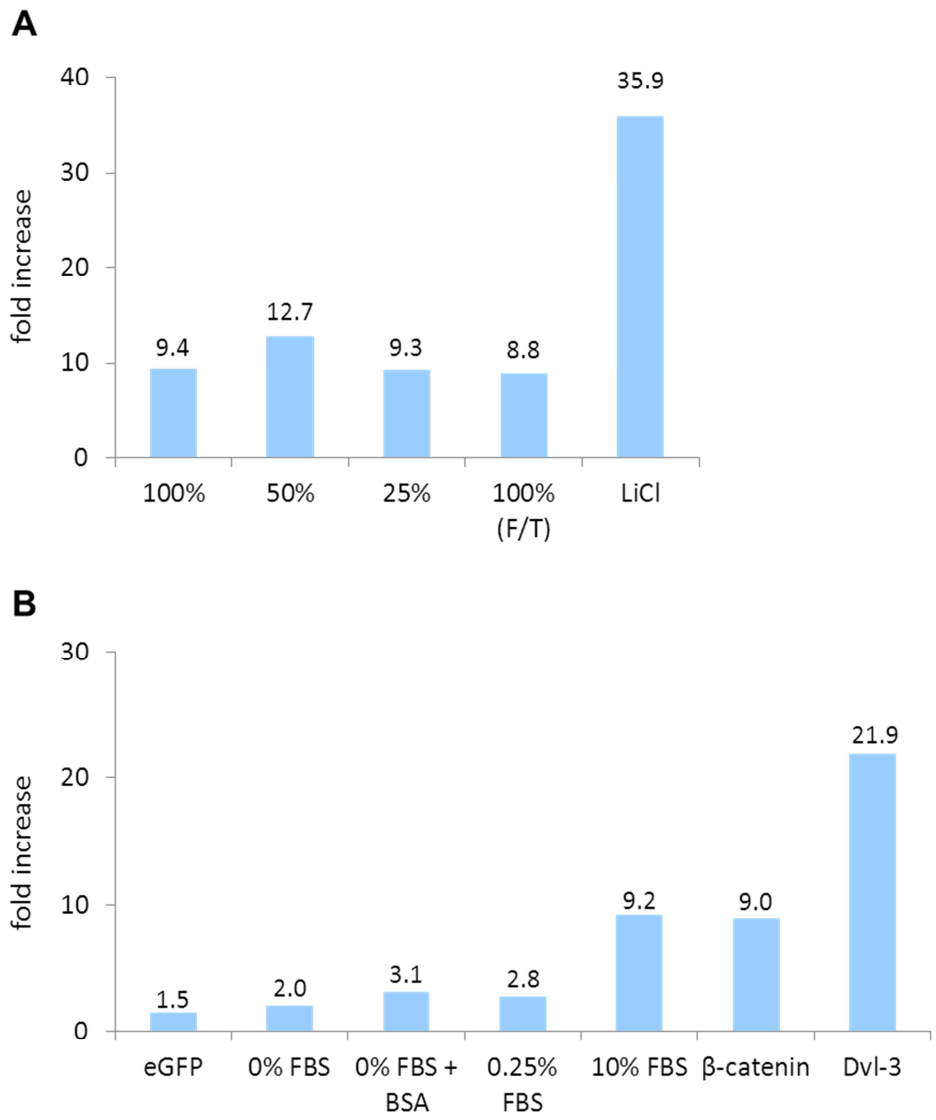

Figure 2.3: Analysis of WNT3a conditioned media biological activity and optimal culture and storage conditions. HEK293T cells were co-transfected with TOPFLASH (firefly luciferase) and renilla luciferase reporter constructs. 24h post transfection, cells were stimulated for 16h with WNT3a conditioned media prior cell harvest. Cell extracts were assayed for firefly and renilla luciferase activities and data obtained were normalised for renilla activity. β-catenin levels were expressed as fold increase across analysed samples using control CM stimulated cells as reference. **(A)** WNT3a conditioned media (CM) either undiluted (100%) or diluted 1:2 (50%) or 1:4 (25%) as indicated were compared to a frozen and thawed (F/T) sample and assessed for biological activity. Treatment with Lithium Chloride (LiCl, 30 mM, 16h) served as positive control. **(B)** In order to examine if FBS concentrations during WNT3a CM generation affect its signalling effectiveness, conditioned media with varied FBS amounts were compared for canonical pathway activation. Expression of β-catenin or DVL3 served as positive canonical stimulation control. eGFP transfection was used as transfection and background control.

2.4.8.2 Generation of stable cells expressing YFP-fusion proteins for localisation studies

In order to analyse subcellular localisation of VANGL or other proteins of interest, YFP-VANGL1, YFP-VANGL2, YFP-Dvl2 and others as outlined on respective figures were subcloned into lentivirus pLEX-YFP (Puromycin selection) destination vectors and viral supernatants generated as described above (refer to 2.4.7.2). Cells were infected and selected as outlined in 2.4.7.2 and seeded on coverslips for immuno-fluorescent analysis (2.7.1.1) or biochemical analysis.

2.5 PROTEIN TECHNIQUES

2.5.1 Preparation of cell extracts and immunoblot analysis

Cells extracts were prepared by washing cells once with ice-cold PBS and adding lysis buffer LB-E or LB-M, while rocking dishes for 5 – 10 min at 4°C. Extracts were collected and centrifuged at 15,000 x *g* for 15 min at 4 °C and normalised according to the Bradford protocol including BSA-standard curve see below (Bradford 1976). 10 µg of protein lysates were generally loaded on 4-20% gradient NuPage SDS–polyacrylamide gels (Invitrogen) and blotted on a polyvinylidene fluoride (PVDF) membrane (Amersham). Membranes were coomassie stained for visualisation of protein content, blocked for 1 h in blocking buffer (5% non-fat dried milk (Sigma)/PBST) and incubated with primary antibody according to Table 1 in 3% BSA/PBST supplemented with 0.02% NaN_3 at 4 °C overnight. Membranes were washed three times with PBST and incubated for 1 h either with donkey anti-rabbit-HRP 1:5000 (Amersham) or sheep anti-mouse-HRP 1:5000 (Amersham), followed by washing three times with PBST and immunodetection was performed by application of a chemiluminescence detection system (Insight Biotechnology) and exposed to medical x-ray film (Fujifilm).

2.5.2 Determination of protein concentractions

Protein contents were determined based on the Bradford protocol (Bradford 1976) employing a BSA standard curve from 10 to 120 µg/mL protein content using a protein assay dye reagent concentrate (Bio-Rad, 500-0006) according to instructions of the manufacturer and measuring absorbance at 595 nm. Unknown protein samples were calculated from BSA readings using a linear regression approach.

2.5.3 Densitometric analysis

Western blot films were scanned at a resolution of 600 dots per inch (dpi) and saved in jpg format at maximum quality. Bands of interest were selected and intensity measured of each individual band as outlined in http://lukemiller.org/index.php/2010/11/analyzing-gels-and-western-blots-with-image-j. Background values were subtracted and densities displayed as fold increase.

2.5.4 GST-pull down and immunoprecipitation experiments

Cell lysates for interaction studies (either IP or pull down experiments) were harvested and centrifuged as described above. GST-proteins were purified using glutathione beads (Amersham), Flag-tagged proteins were immunoprecipitated with Flag-beads (Sigma) using an equivalent of 10 µL packed beads. Lysates were incubated with respective agarose beads for 2 h while rotating at 4°C and subsequently washed 3 times with lysis buffer without protease and phosphatase inhibitors. After completion of washes, beads were drained with a needle (25G, Terumo) and proteins eluded with LDS sample buffer. Interaction were analysed by Westen botting as described above.

2.5.5 Expression and purification of recombinant proteins

Competent *E.coli* strain BL21(DE3) (Invitrogen) were transformed with desired expression constructs. A two ml overnight culture from an individual bacterial colony was used to inoculate 900 mL LB/ampicillin (100 µg/mL) media per construct and incubated at 37°C at 200 rpm until reaching an optical density (OD) value of OD_{600}=0.6. Cultures were induced with 1 mM IPTG (Isopropyl-β-D-Thiogalactopyranoside) and kept shaking for four additional hours. Bacteria were then pelleted at 4500 rpm (JLA-10.500 rotor, 3847 x *g*) at 4 °C for 20 min, and the supernatant was discarded. Pellets were resuspended in 20 mL PBS-E lysis buffer containing 0.5 mg/mL Lysozyme (Sigma), protease inhibitors (tablet, Roche), 5 µg/mL DNase (Sigma) and 5 mM β-Mercaptoethanol on ice. Next, resuspended bacteria were lysed using a sonication approach of 4 rounds at 45 sec each on ice and debris was pelleted by centrifugation at 20000 rpm (JA-25.50 rotor, 32816 x *g*). Fusion proteins were then purified from the yielded lysate with either His, Glutathione, Streptavidin or Flag beads during incubating for 2-4h at 4°C and gentle rotation. After three to four wash steps, proteins were either eluted using the respective elution buffer or sample buffer (LDS).

2.5.6 Generation of GST-RBD beads for RHO/RAS activation assays

Respective GST- Raf, RalGDS or Rhodekin binding domain (RBD) fusion proteins were expressed in *E.coli* and lysed as described above. Lysates were purified using glutathione beads for 2h while gently rotating at 4°C, before collecting beads by centrifugation at 2000 x *g* for 4 min. Supernatant was either discarded or used for a second round of GST-purification. GST-beads were washed for four

times with PBS-0.1% Trition X-100 and once with LB-M/50% Glycerol before storing beads as 1:4 in PBS-M/glycerol (50% Glycerol). An equivalent of 10 uL packed beads were run on a SDS-PAGE gel in order to assess amount of bound protein and purity, and appropriate stimulated lysates were used to test if GST-RBD beads are able to enrich respective GTPases.

2.5.7 RAS and RHO binding domain assays

RAS binding domain (RBD) assays can estimate various endogenous RAS-family protein activities and have been employed to analyse R-RAS and RHO levels in mammalian cells upon various stimulations. In order to monitor levels of activated R-RAS GTPases in cell lysates, I used GST-fusions of the Ras-binding domain (RBD) of the RAS effector RAF1 (residues 2–140) or RALGDS (C-terminal 97 residues), exploiting the fact that RAS family proteins only bind effectors in the GTP-bound state (Brtva et al. 1995; de Rooij and Bos 1997; Franke et al. 1997). Cells were lysed in LB-M lysis buffer, and cleared lysates incubated for 45 min at 4°C with 10 µL packed GST-RBD glutathione sepharose beads (see 2.5.6). Beads were washed three times, and bound proteins were eluted with LDS sample buffer and resolved by SDS-PAGE. Activated H-RAS, R-RAS or TC21 was detected by immunoblotting using respective antibodies (Table 1).

The cellular level of GTP-loaded RHOA and RHOB was determined using a GST fusion protein containing the RHO binding domain of Rhotekin (GST-RBD), corresponding to residues 7-89 of Rhotekin, which specifically precipitates GTP-RHO from cell lysates (Ren and Schwartz 2000; Mezzacappa et al. 2012). Cells were lysed in LB-M lysis buffer, and cleared lysates incubated for 45 min at 4°C with 10 µL packed GST-RBD glutathione sepharose beads (see 2.5.6). Beads were washed three times, and bound proteins were eluted with LDS sample buffer and resolved by SDS-PAGE. Activated RHOA or RHOB was then detected by immunoblotting using respective antibodies (Table 1).

2.5.8 In vitro interaction assays

Spodoptera frugiperda (Sf9) cells were infected with baculoviruses expressing GST-VANGL1 truncations (N and C-terminal) or various ARHGEF17/p164RhoGEF C-terminal truncations (C1-C5). His-R-RAS, His-TC21 and effector proteins were expressed and purified from bacteria as described above (section 2.5.5). In vitro

interactions were carried out by loading purified His-R-RAS or His-TC21 with either GDP or the non-hydrolysable analogue of GTP (GMP-PNP) by incubation for 5 min at 37°C in loading buffer (20 mM Hepes (pH 7.5), 50 mM NaCl, 5 mM EDTA, 5 mg/mL BSA) in a 20-fold molar excess of GDP or GMP-PNP. Reactions were stopped by placing the tubes on ice and adding $MgCl_2$ to a final concentration of 20 mM. 0.5 µg GDP/GMP-PNP loaded R-RAS or TC21 was combined with 15 µL of packed glutathione beads bound to GST-VANGL1 or GST- ARHGEF17/p164RhoGEF (or other effector proteins) in a tube containing 200 µL of PBS, 5 mM $MgCl_2$, 0.1% Triton X-100. After 1-3 h of incubation at 4°C while rotating, GST-beads were washed three times with PBS, 5 mM $MgCl_2$, 0.1% Triton X-100, needle drained and LDS sample buffer added. After separation on 4-12% SDS-PAGE gels, western blots were performed using His antibodies.

2.5.9 TAP-tagged protein transfection and purification for mass spectrometry analysis

For the transient expression approach, eight confluent 15cm dishes (Greiner) of HEK293T cells per condition were seeded at 50% confluence in a volume of 15mL, and transfected 3h post seeding using the PEI approach (2.4.5.2). Per 15 cm dish 10 µg TAP6-VANGL1 plasmid were combined with GST-R-RAS expression plasmids (10 µg), mFzd5 (5ug), ROR2 (5 µg) or empty vector (5-10 µg) to yield a total of 20 µg plasmid DNA, which was combined with 80 µg PEI reagent. The media was exchanged 5 h post transfection with 20 mL growth media and cells were additional boosted with 10 mL media 16 h later. HEK293T cells were harvested 48h after transfection and cells extracts were prepared by washing cells twice with ice-cold PBS and collected in PBS-M lysis buffer (1.6 mL per plate) on ice (2.1.2). Extracts were centrifuged at 20,000 x *g* for 20 min at 4 °C to pellet cellular debris. The soluble fraction was incubated with 250µl packed Streptavidin high performance beads (GE Healthcare, 17-5113-01) per condition for 2 hours at 4°C while rotating gently. Beads were pelleted through centrifugation at 2000 x *g* for 5 min and column washed four times (VWR, gravity flow columns) to remove unbound proteins. Bound proteins were eluted by supplementing 2.5mM biotin in PBS-M wash buffer and shaking beads gently for 10 min prior draining the beads and collecting the eluate. In order to increase eluate protein concentration, proteins were precipitated using a Trichloroacetic acid (TCA) approach. Eluates were supplemented with 2% deoxycholate/PBS (1/100 of total volume) and TCA (1/20 of total volume), vortexed and incubated on ice for 30 min. Precipitated proteins were pelleted by centrifugation at 15000

x *g* at 4°C for 30 min, and supernatants were carefully aspirated before pellets were washed with 500 µl acetone. Pellets were collected again through spinning at 15000 x *g* at 4°C for 5 min and the acetone removed in order to air dry the remaining pellet. Dried pellets were dissolved in 30µl of 2x LDS sample buffer, and left O/N at RT.

2.5.10 Mass spectrometry analysis

LDS samples were resolved on a 4-12% NuPAGE gels (Invitrogen) and stained with SimplyBlueTM SafeStain (Invitrogen) according to the instructions of the manufacturer. Visualised bands were compared to control/background TAP-samples and differential bands were excised with a clean scalpel and proteins were digested in-gel with trypsin as described previously (Rosenfeld et al. 1992) and under http://msf.ucsf.edu/ingel.html.

Mass spectrometry analysis was carried out by Juan A. Oses-Prieto at the Department of Pharmaceutical Chemistry (University of California, San Francisco, California 94143, USA), as described previously (Rodriguez-Viciana et al. 2006).

2.6 CELL BIOLOGICAL TECHNIQUES

2.6.1 Scratch wound migration assays

Cells were seeded in 24 well plates (Imagelock plates distributed by Essen Instruments), grown to confluency and scratch wounded using a woundmaker (Essen Instruments) using 10 µL sterile tips. Wells were washed up to three times with PBS in order to remove debris, and 500 µL media added. Plates were placed in the Essen Instruments IncuCyte device and the wound area including a small area of the bordering monolayer of cells monitored over time. Images were automatically taken over a course of two days with intervals of one to two hours. Scratch induced migration was analysed by tracking the cell repopulation of the wound in percent over a period of time and plotting a graph over time using Essen Instruments provided software IncuCyte version 2010A.

2.6.2 Transwell/Boyden chamber assays

Transwell migration of U2OS was examined by means of 8 µm pore PET membranes of 24-well transwell inserts (BD Biosciences). 72h post siRNA/RNAiMax transfection, U2OS cells were trypsinised and resuspended in serum-containing DMEM at a density of 250,000 cells/mL. 200 µl cell suspension was plated into each insert (upper chamber), which were placed into lower chambers containing 800 µl DMEM/10% FBS. Cells were left to settle on the PET membrane, which required serum presence and after 90 min, media in the top chamber was exchanged with 200 µL serum free media, thus generating a chemoattractant gradient towards the lower chamber. The assay was terminated after 14 h, and non-migrated cells were removed from the upper chamber with a cotton bud and migrated cells were fixed and stained with 0.5% crystal violet/10% Methanol for 15 min. Residual staining solution was rinsed off with water and images taken using a 10x magnification. The number of migrated cells was determined using pictures of five representative fields and normalised as percent of migrated cells using initial seeding densities for calculation.

2.6.3 Cell polarisation assays: GM130 and MTOC assays

To assess polarisation in response to wounding, cells were plated on coverslips and transfected with siRNAs using RNAiMAX lipid complexes as described in section 2.4.6. 72 h post transfection, confluent cell monolayers were wounded

with a sterile pipette tip, wells washed with PBS to remove debris and cells were allowed to migrate for 4h (GM130 experiments) or 60-90 min (γ-tubulin experiments). Cells were fixed, permeabilised and stained as described in section 2.7.1.

2.6.4 Invadopodia assay

Preparation of Alexa Fluor568-gelatin coated coverslips

Prewarmed Alexa Fluor568-gelatin (type A, 300 bloom, Sigma G-1890, prepared by M. Nishita) was mixed with regular gelatin (25 mg/mL) at equal volumes at 37°C until completely melted. For 12 coverslips (18 mm, Matsunami), 75 µL of Alexa Fluor568 was mixed with 75 µL of regular gelatin on a parafilm piece on a heating block until completely dissolved. Coverslips were placed onto the gelatin drop for one sec, excess gelatin removed with an aspirator and the coverslip submerged into ice cold 0.5% Glutaraldehyde/PBS (Nacalai tesque, freshly prepared) solution for 15 min. Next, Glutaraldehyde/PBS was removed and coverslips were washed three times with PBS and subsequently 1mL of 5 mg/mL $NaBH_4$ /PBS (Sigma, S9125-100, freshly prepared) added, following three min incubation at RT. Subsequently, $NaBH_4$ /PBS solution was removed and coverslips washed three times with PBS, before adding 70% ethanol/ddH_2O in order to sterilise coverslips at RT for 15min. After aspiration of the ethanol/ddH_2O mixture, coverslips were washed three times with sterile PBS, and either kept for storage purposes wrapped in aluminium foil at 4°C to avoid bleaching or were used immediately, which required at least 1h quenching with 2 mL culture medium at 37°C. Before cells were seeded onto Alexa Fluor568 treated coverslips, cell culture medium was removed and coverslips were washed two more times with culture medium before seeding of cells.

Experimental process

Saos2 cells were reverse transfected as outlined in section 2.4.6 and 72h later trypsinised and counted in order to plate 3.2 x 10^5 cells per coverslip. Cells were seeded in regular growth media and allowed to attach for 9h. Experiments were terminated at this time point through a single wash with PBS and immediate fixation using 4% PFA (Nacalai) for 10 min. Formation of invadosomes was assesses after actin counterstaining with phalloidin. Thus, fixed coverslips were washed twice with PBS and cells permeabilised for 5 min with 0.2% Triton

X100/PBS. Next, coverslips were washed twice with PBS and blocked for 60min with 2% FBS/PBS at RT before staining with 2% FBS/PBS supplemented with 1:500 Phalloidin-488 (Cambrex, PA-3010) and 1:1000 DAPI (4',6-diamidino-2-phenylindole) (Sigma, 1mg/mL) for 1h. Coverslips were washed three times for 10 min each, before mounting on glass slides (Matsunami) using ProLong Gold antifade mounting media (Invitrogen, P36930). Invadosome formation was quantified by microscope imaging of 30 representative fields per condition at similar cell densities per coverslip at 40x magnification and counting of Alexa Fluor 568 depleted "black spots" indicating ECM degradation.

2.6.5 Luciferase reporter assays for β-catenin level detection

The TCF/LEF reporter assay was employed to monitor the biological activity of WNT ligands through activation of the β-catenin dependent pathway in in cultured cells. WNT ligand binding leads to stabilisation and nuclear translocation of β-catenin, which complexes with TCF/LEF transcription factors, leading to the activation of WNT-responsive genes. The TCF/LEF-responsive luciferase construct encodes the firefly luciferase reporter gene under the control of a minimal CMV promoter and tandem repeats of the TCF/LEF transcriptional response element (TRE) (Korinek et al. 1998; Ishitani et al. 1999). Lithium is a selective inhibitor of the serine/threonine protein kinase GSK-3β at a relatively high concentration (IC_{50} = 2 mM) and has been employed as a positive assay control in all experiments (Klein and Melton 1996; Stambolic et al. 1996).

HEK293T cells were seeded at a density of 3.2 x 10^5 per 24 well, and 4 h later Lipofectamine2000 co-transfected using 75ng of the TOPFLASH reporter construct LEF-Luc (TOPT, firefly luciferase), 2.5 ng control reporter construct *Renilla*-Luciferase, alongside with 100 ng pcDNA3 expression constructs such as the positive controls β-catenin, DVL2 or empty vector in case of ligand treatment. The next morning, cells were boosted with 500 µl of growth medium and 24h post transfection, media was exchanged for WNT ligand conditioned media, recombinant WNT ligands or treated with LiCl acting as an activation control for 16h prior harvest. For luciferase detection, a Dual Dual-Luciferase® Reporter Assay System (Promega) was employed, which is based on a two-step detection method. Cells were passively lysed according to instructions of the manufacturer followed by sequential measurements of firefly (*Photinus pyralis*) and *Renilla* (*Renilla reniformis*) luciferase activities from a single sample. The firefly luciferase reporter is measured first by adding Luciferase Assay Reagent II

(LAR II) and after quantifying the firefly luminescence, this reaction is quenched, and the *Renilla* luciferase reaction is initiated by simultaneously adding Stop & Glo® Reagent to the same reaction tube. Light emissions were detected using a luminometer (Varioscan platereader) and the obtained luciferase values were normalised for variations in transfection efficiency by using the renilla internal control (*Renilla* detection), and are expressed as fold stimulation of firefly luciferase activity.

2.6.6 Autophagy inducing treatments

For starvation purposes and autophagy induction, cells were washed three times with PBS and incubated with HBSS for 6h. Autophagy stimulation and activity was assessed by LC3B-II cleavage. In order to inhibit starvation induced autophagy, cells were treated with HBSS containing 10 mM 3-methyladenine, 25μM Chloroquine or 30nM Bafilomycin A for indicated time points.

2.6.7 Statistical analysis

Data is reported as ±standard errors of the means (SEM) and were examined by one way analysis of variance (ANOVA). Statistical significance was determined at $p<0.05$ for all experiments.

2.7 MICROSCOPY

2.7.1 Preparation and staining procesdure of cells for fluorescent microscopy purposes

2.7.1.1 PFA fixation and permeabilisation for GM130 stainings

Cells were grown and manipulated on coverslips (VWR, 13 mm for 24 wells if not stated otherwise) and washed with PBS once prior to 4% PFA/PBS fixation for 15 min at RT. Subsequently, the PFA/PBS solution was aspirated and washed three times with PBS for 5 min each in order to remove all PFA traces. Cells were permeabilised with 0.1% Triton X-100/PBS for 10 min at RT, washed once with PBS and blocked by incubation with 4% BSA/PBS for 45 – 60 min. Primary antibodies were applied as a dilution in 2% BSA/PBS solution O/N (16h) at 4°C, and coverslips were placed in a hydrated chamber. For polarisation experiments assessing Golgi reorientation, GM130 antibodies were used at 1:200 dilution (Transduction, 610822, clone 35). After completion of the primary antibody incubation period, coverslips were washed three times for 5 min each with 2% BSA/PBS solution, followed by application of the appropriate secondary antibody. For GM130 experiments Goat anti-mouse, Alexa-488 conjugated antibodies (Pierce) diluted 1:200 in 2% BSA/PBS were used and coverslips incubated for 45 min at RT protected from light. In order to counter stain the cellular nucleus, coverslips were immediately treated with Hoechst stain (Sigma H6024) at a concentration of 0.5 µg/mL in 2% BSA/PBS for 10 min and subsequently washed twice for 5 min each with 2% BSA/PBS, followed by one PBS wash for 5 min. Coverslips were desalted by dipping each slide into distilled water, briefly air dried and placed on a glass microscopy slide with a drop of mounting media (Dako S3023). Slides were imaged using a Zeiss AxioImager A1 and images taken of confluent areas or the wound edge.

PFA fixation was usually employed for visualisation of exogenously expressed YFP- or GFP-fusion proteins and associated localisation studies. In several experiments, actin was counterstained using Phalloidin/methanol solution (Sigma, P1951) at a concentration of 0.25 µg/mL carried out simultaneously with the Hoechst nucleus staining step.

2.7.1.2 Methanol based fixation for γ-tubulin staining

Cells were grown and manipulated on coverslips (VWR, 13 mm for 24 wells if not stated otherwise) and washed with PBS once prior to 100% ice cold methanol fixation for 10 min at -20°C, and PBS washed three times, followed by 1 h BSA blocking in 4% BSA/PBS at RT. Immediately after, coverslips were incubated in a hydrated chamber with anti-γ-tubulin primary antibody (Sigma, GTU-88) at a 1:500 dilution in 2%BSA/PBS O/N (16h) at 4°C. After completion of the primary antibody incubation period, coverslips were washed three times for 5 min each with 2% BSA/PBS solution, followed by application of the appropriate secondary antibody. For γ-tubulin MTOC experiments Goat anti-mouse, Alexa-488 conjugated antibodies (Pierce) diluted 1:200 in 2% BSA/PBS were used and coverslips incubated for 45 min at RT protected from light. In order to counter stain the cellular nucleus, coverslips were immediately treated with Hoechst stain (Sigma H6024) at a concentration of 0.5 µg/mL in 2% BSA/PBS for 10 min and subsequently washed twice for 5 min each with 2% BSA/PBS, followed by one PBS wash for 5 min. Coverslips were desalted by dipping each slide into distilled water, briefly air dried and placed on a glass microscopy slide with a drop of mounting media (Dako S3023). Slides were imaged using a Zeiss AxioImager A1 and images taken of confluent areas or the wound edge.

2.7.2 Localisation studies using confocal flourescence microscopy

Fixation protocols were carried out at described above (section), samples were desalted as outlined before and images acquired at 40x, 63x or 100x using either air or oil objectives on a Perkin Elmer spinning disc confocal microscope. Images were processed using Velocity software version 5.4.

CHAPTER 3

Characterisation of VANGL1 as a R-RAS effector

and

ARHGEF17/p164RhoGEF as a TC21 effector

3 Characterisation of VANGL1 as an effector of R-RAS

As outlined in the introduction chapter, R-RAS and H-RAS share many biochemical and biological properties, as well many downstream effectors and regulatory proteins (GEFs and GAPs), including the ability to behave as oncogenes (Buday and Downward 1993; Self et al. 1993; Rey et al. 1994; Spaargaren and Bischoff 1994; Spaargaren et al. 1994; Gotoh et al. 1997; Marte et al. 1997; Ebinu et al. 1998). However, R-RAS appears to have specific functions of its own, including effects on integrin mediated adhesion, being clearly distinct from classical RAS proteins (Zhang et al. 1996; Suzuki et al. 2000; Self et al. 2001; Hansen et al. 2003; Kinbara et al. 2003; Pozzi et al. 2006). How R-RAS regulates integrin activation is not known. A study using partial loss of function effector mutants in combination with pharmacologic inhibitors revealed that no known R-RAS effector could account for the observed effect, suggesting the existence of yet unidentified effector(s) which mediate(s) the effects of R-RAS on integrin activation (Oertli et al. 2000).

Dr Rodriguez-Viciana optimised the Tandem Affinity Purification (TAP) method in order to identify novel RAS family interactors. This methodology has been shown to work efficiently and successfully in identification of the SHOC2-PP1 phosphatase holoenzyme as a specific M-RAS effector (Rodriguez-Viciana et al. 2006). This approach was then employed to identify other novel binding partners of R-RAS GTPases using activated R-RAS and TC21 as baits.

3.1 Identification of potential novel effector of R-RAS and TC21

Dr Rodriguez-Viciana performed three independent TAPs using the constitutively active R-RAS mutant G38V (V38) as bait in three different cell lines: human embryonic kidney (HEK) HEK293, HEK293T, and adeno-carcinomic human alveolar basal epithelial A549 cells. R-RAS co-purified proteins identified by mass spectrometry (MS), which were not detected in control baits are listed in Figure 3.1.

A R-RAS, (HEK293)

	Unique peptides	% Coverage
RRAS	23	79.8
RADIL	55	50.5
VANGL1	24	45.2
CRAF	19	31.6
RAP1GDS1	4	7.9

B R-RAS (HEK293T) EGF stimulation

	Unique peptides	% Coverage
RRAS	37	86.7
RAP1GDS1	10	22.6
VANGL1	3	8

C R-RAS, (A549)

	Unique peptides	% Coverage
RRAS	23	67
RIN1	39	42.7
RAP1GDS1	29	36.1
VANGL1	8	12.6
RIN2	5	6.1
CRAF	1	1.1

Figure 3.1: Tandem affinity purified R-RAS V38 interactors, identified by mass sprectrometry. Cells expressing TAP-tagged R-RAS V38 constructs were lysed, tag-precipitated and co-purified proteins identified by mass spectromery. TAP approaches were perfomed in HEK293 **(A)**, EGF stimulated HEK293T **(B)** or A549 cells **(C)**.

Identification of the well-described R-RAS effectors such as RAF1/CRAF and RINs serve as validation control for this unbiased proteomic approach, indicating that the addition of the TAP tag does not compromise R-RAS function in vivo (Figure 3.1).

In addition to RAP1GDS, a protein that interacts with multiple RAS and RHO family GTPases in a GTP-independent manner (Yamamoto et al. 1990; Mizuno et al. 1991; Hamel et al. 2011), VANGL1 was identified in all three performed purifications (Figure 3.1).

VANGL proteins are highly conserved from fly to humans and the *Drosophila melanogaster* homologue strabismus (stbm) has been described as one of the core components of the WNT/PCP pathway. Therefore, VANGL1 presents an intriguing target due to the potential novel link between RAS signalling and the β-catenin/non canonical WNT pathway.

Employing TC21 G12V as bait in a parallel TAP approach resulted in co-purification of several known RAS family effectors such as CRAF, ARAF, RIN1,

MLLT4/AFADIN/AF6 and the RALGEF RGL2 (Rodriguez-Viciana et al. 2004), again validating the sensitivity of the approach (Figure 3.2). In addition, ARHGEF17/p164RhoGEF, a RHOA activating nucleotide exchange factor (Rumenapp et al. 2002) was identified in A549 cells (Figure 3.2C).

This discovery led to the intriguing hypothesis that R-RAS could act downstream of WNT ligands and modulate VANGL1 function in the WNT/PCP pathway, while TC21 is also able to modulate RHO GTPase activation through ARHGEF17/p164RhoGEF. Recruitment of other factors such as PI3Ks or RALGEFs could then enable the regulation of cell polarity and motility (Figure 3.3).

A

TC21, (HEK293)

	Unique peptides	% Coverage
TC21	28	66.2
RAP1GDS1	36	55.5
RAF1	16	28.9
RADIL	13	13
ARAF	9	17

B

TC21, (HEK293T) EGF stimulation

	Unique peptides	% Coverage
TC21	36	72.1
AFADIN	114	54
RAP1GDS1	21	39
RGL2	10	16.2
SOS1	1	1
GLMN	1	2
SHOC2	1	3.5

C

TC21, (A549)

	Unique peptides	% Coverage
TC21	25	62.7
RIN1	55	63.2
ARHGEF17	9	5.3
KIAA1199	4	3.2
RAF1	3	3.5

Figure 3.2: Tandem affinity purified TC21 V12 interactors, identified by mass spectroscopy. Cells expressing TAP-tagged R-RAS V38 constructs were lysed, tag-precipitated and co-purified proteins identified by mass spectromery. TAP approaches were perfomed in HEK293 **(A)**, EGF stimulated HEK293T **(B)** or A549 cells **(C)**.

To validate VANGL1 and ARHGEF17/p164RhoGEF as novel R-RAS GTPase effectors, characterisation experiments are described in two separate sequential sections. The initial part of this chapter focuses on the VANGL1 and R-RAS interaction (section 3.2), and this is followed by the interaction validation of ARHGEF17/p164RhoGEF as a novel effector of TC21 (section 3.3).

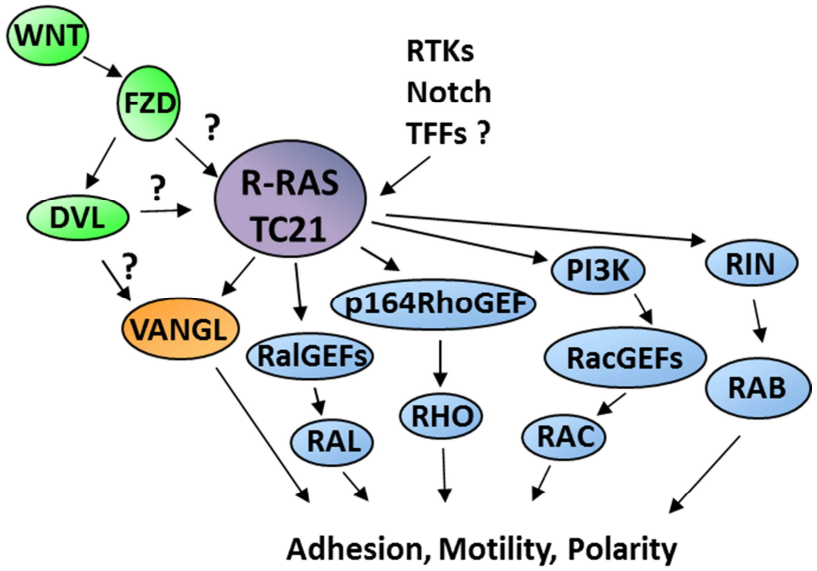

Figure 3.3: Proposed model of how R-RAS GTPases could act downstream of WNT ligands in the non-canonical WNT signalling pathway. R-RAS subgroup members are activated upon binding of WNT ligands (WNT) to Frizzled receptors (FZD) by an unknown mechanism. R-RAS GTPases are able to recruit VANGL1, ARHGEF17/p164RhoGEF as well as other factors such as Phosphatidylinositide 3-kinases (PI3K) or RAL guanine exchange factors (GEFs) in order to modulate cell adhesion, polarity and motility through the activation of RAL and RHO GTPases. R-RAS GTPases could be also activated by Receptor Tyrosine Kinases (RTK), Notch ligands or Trefoil family factors (TFFs). DVL - Dishevelled.

3.2 VANGL1 behaves as an effector of R-RAS subfamily GTPases

3.2.1 R-RAS interacts with VANGL1 in an activation and effector domain dependent manner

TAP experiments identified VANGL1 as a potential R-RAS interacting protein. In order to validate and to characterise this interaction, co-transfection approaches utilising HEK293T were performed, due to the lack of a commercially available endogenous antibody for VANGL1. This system is based on co-transfection of a glutathione S-transferase (GST) tagged bait construct and respective flag-tagged potential interactors. After pull down of GST-proteins with gluthathione beads, binding to the GST-bait is verified by immunoblotting using flag-antibodies. Notably, avoiding antibody based beads for immunoprecipitation has been demonstrated to decrease background and increase signal to noise ratio in co-transfection experiments (Rodriguez-Viciana and McCormick 2006).

To validate VANGL1 as a true R-RAS effector, VANGL1 is required to bind to R-RAS in a GTP-dependent manner, therefore constitutively active mutants of R-RAS (G38V and Q87L, analogous to H-RAS oncogenic mutants G12V and Q61L) were used for binding studies.

Further, RAS effector proteins interact with RAS through a defined small stretch termed the effector domain, only when the RAS is GTP bound and thus active. A point mutation in the effector domain of R-RAS (D64A, equivalent to D38A in H-RAS) leads to disruption of effector protein binding in the activated background (Oertli et al. 2000; Repasky et al. 2004). Therefore, this point mutation was employed to assess RAS effector domain dependent binding of VANGL1. In addition to the initial biochemical interaction studies, further biological assays were carried out in order to address the R-RAS – VANGL1 functional relevance (see section 4.3 and chapter 7).

Co-expression experiments in HEK293T cells showed a strong preferential binding of VANGL1 to R-RAS activating mutants V38 or L87 over R-RAS wild type (wt), whereas no interaction with the effector domain mutants V38 A64 or L87 A64 could be detected, confirming an activation dependent interaction with R-RAS as well effector domain mediated binding (Figure 3.4). This fulfils the requirements of a RAS family effector protein (Repasky et al. 2004). The closely related GTPase RAP2 fails to precipitate VANGL1 and therefore was used as background control (Figure 3.4).

R-RAS L87 showed considerably higher binding than R-RAS V38 and was therefore preferentially employed in all subsequent experiments (Figure 3.4). Preferential interaction with the L87 versus the V38 homologous active mutants have been previously reported for several effectors of RAS Family GTPases (RFGs) and may be related to the fact that the L87 substitution falls within the switch II effector domain (and may thereby have structural effects on effector interactions (Figure 1.10) (McCormick 1992).

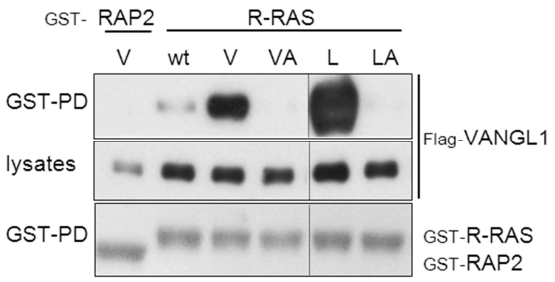

Figure 3.4: VANGL1 interacts with R-RAS activation and effector domain dependent. HEK293T cells were co-transfected with flag-VANGL1 and either GST-RAP2 (negative control) or GST-R-RAS expression plasmids, and GST-pulldowns were probed with flag antibody by western blot. Both constitutively active R-RAS mutants (V38 or L87) and effector domain mutants (V38 A64 or L87 A64) were used to verify activation dependent interaction and effector domain binding. wt- wildtype protein, PD-pull down. Levels of GST baits were determined by staining the western blot membrane with coomassie blue prior to antibody incubation (n=5).

3.2.2 VANGL1 and VANGL2 interact specifically with R-RAS subgroup members

In order to investigate the specificity of the interaction among closely related GTPases, binding of VANGL proteins to a panel of RAS Family GTPases was tested. VANGL1 and VANGL2 interact in an activation-dependent manner with members of the R-RAS subgroup but not with other RAS family members such as oncogenic RAS protein (N-RAS) or RAP proteins (RAP1, RAP2) (Figure 3.5). Notably, under conditions of overexpression of RAS family GTPases (RFGs), the interaction between VANGL1 is restricted to R-RAS subgroup members, highlighting the specificity of interaction.

The levels of expression of TC21 (and RAP1) achieved with our expression plasmids are always consistently lower compared to other RFGs, and therefore the relative amounts of co-immunoprecipitated proteins have to be considered with respect to the levels of baits. With this consideration in mind, VANGL1 can be seen to interact preferentially with R-RAS and TC21 compared to M-RAS (Figure 3.5).

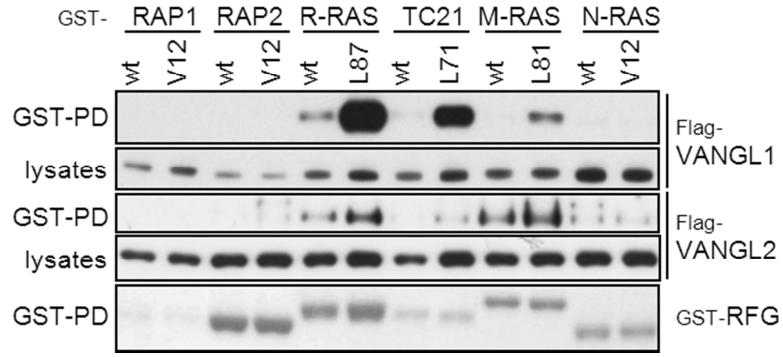

Figure 3.5: R-RAS GTPases interact in an activation-dependent manner with VANGL1 and VANGL2. GST-tagged constructs of wild-type (wt) and activated mutants (V12, L87, L71, L81) of RAS family GTPases (RFG) were expressed in HEK293T cells together with flag-tagged VANGL1 or VANGL2. GST-RFGs were purified with glutathione beads and interacting VANGL proteins detected by western blotting using anti-flag antibodies. PD – pull down. GST-bait levels was visualised by Coomassie blue staining of the western blot membrane prior to antibody incubation (n=3).

Flag-VANGL2 can also be detected to associate with R-RAS subgroup GTPases but with significant lower affinity; much longer exposures had to be carried out during chemoluminescent detection and signal above background was not as high as observed for VANGL1. VANGL2 is known to hetero-dimerise with VANGL1 (Belotti et al. 2012) and therefore at least a certain fraction of the VANGL2 detected level could be indirectly associated through endogenous VANGL1. Furthermore, VANGL1 but not VANGL2 was repeatedly found by mass spectrometry to co-purify with R-RAS (Figure 3.1). Therefore, we decided to focus our studies on VANGL1.

After testing and verification of multiple commercially available VANGL1 immunoglobulins, one antibody was identified to detect immunoprecipitated VANGL1 protein (data not shown), enabling to study the interaction of R-RAS

GTPases with endogenous VANGL1. Due to unavailability of good immunoprecipitating antibodies against R-RAS GTPases coupled to the fact that R-RAS GTPase interaction is strictly GTP dependent, and no potent R-RAS stimulators were known, exogenously expressed activated R-RAS proteins were required to be expressed for effector interaction experiments (Figure 3.6).

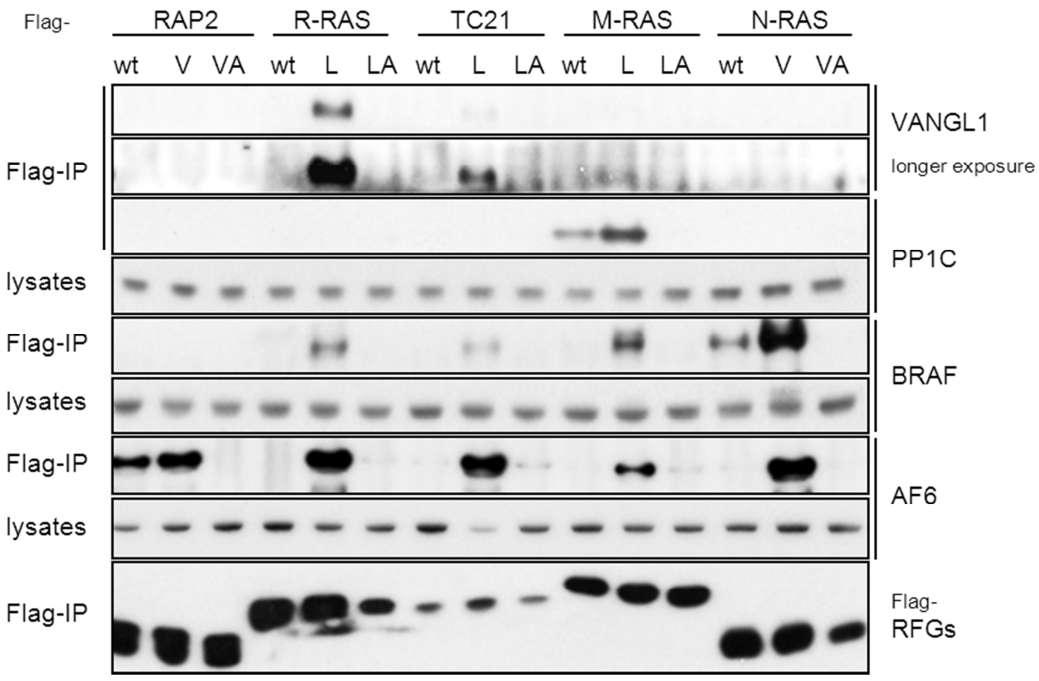

Figure 3.6: Interaction of endogenous VANGL1 and other effectors with RAS family GTPases. Flag-tagged constructs of wild-type (wt), activated mutants (V or L) or respective effector domain mutants (VA or LA) of Ras family GTPases (RFG) were expressed in HEK293T cells. Flag-GTPases were purified 48h after transfection with flag affinity beads and endogenous proteins detected by western blotting using indicated antibodies. IP – Immunoprecipitation, PP1C – protein phosphatase 1C. Applied mutants were the following: RAP2 V12 or V12 A38, R-RAS L87 or L87 A64, TC21 L71 or L71 A48, M-RAS L81 or L81 A48, and N-RAS V12 or V12 A38.

Endogenous VANGL1 immunoprecipitates with activated R-RAS and TC21, and only very faint interaction could be detected with M-RAS (Figure 3.6), consistent with a preferential interaction with these two R-RAS subgroup members observed in previous co-expression experiments (Figure 3.5). It could be confirmed that interaction of endogenous VANGL1 with R-RAS takes place in a strict activation and effector domain dependent manner and no interaction with

closely related GTPases (N-RAS, RAP2) was detected, illustrating VANGL1's binding specificity to R-RAS subgroup members (Figure 3.6).

Probing for other known RFG effector proteins within the same immunoprecipitates, served as internal controls for functionality of each transfected RFG and confirmed differential binding specificities among RFGs (Rodriguez-Viciana et al. 2006). Protein phosphatase 1 (PP1) interacts exclusively with M-RAS, whereas BRAF can bind the R-RAS subgroup but with lower affinity than N-RAS. The junctional multidomain protein AFADIN/AF6 is the more promiscuous effector of this panel, being able to bind to all GTPases tested in this study (Figure 3.6).

It is not uncommon to be able to detect some effector binding to ectopically expressed wild type RAS proteins due to the fact that a small proportion of the total protein (that may vary between RFGs) is expected to be bound to GTP at least in overexpression conditions (Figure 3.6).

3.2.3 Characterisation of VANGL1-R-RAS interaction using R-RAS effector loop mutants and the ΔCAAX truncation

Selective partial loss of function effector domain mutants of H-RAS have been described previously and demonstrated to be a useful tool to dissect signalling by the different Ras effector pathways (Rodriguez-Viciana et al. 1997; Kinashi et al. 2000; Oertli et al. 2000). In order to identify R-RAS mutants that are able to selectively disrupt or retain the ability to interact with VANGL1, and thus could be used as tools to help elucidate the differential contribution of VANGL1 to R-RAS signalling properties, a set of homologous effector mutations to that described for H-RAS were generated (Figure 3.7A). This is based on the fact that the core effector binding domain of R-RAS is identical to those in H-RAS. Further, this study included a CAAX domain deletion (ΔCAAX) construct to test if membrane localisation affects interaction. These constructs were then expressed in HEK293T cells and tested for interaction with VANGL1 or other known effectors (Figure 3.7B and C).

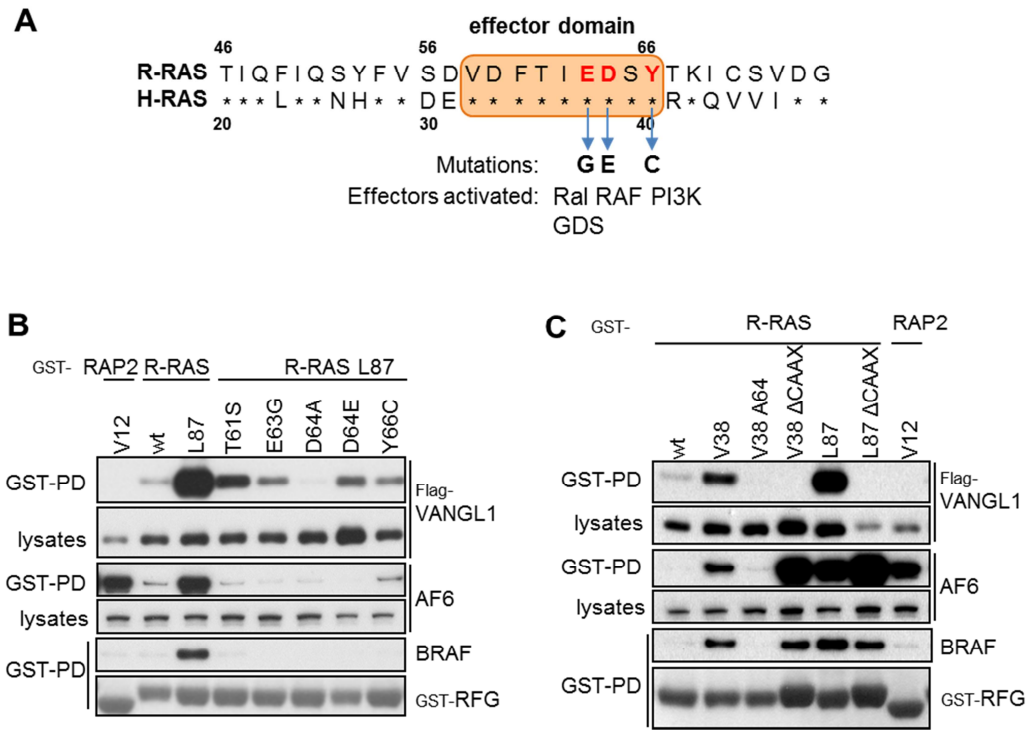

Figure 3.7: R-RAS effector domain mutations do not affect VANGL1 interaction, whereas deletion of the CAAX box completely inhibits VANGL1 binding. **(A)** Partial protein alignment of R-RAS and H-RAS including the effector domain (orange box, R-RAS residues V58-Y66, H-RAS residues V32-Y40). Identical amino acids are marked as asteriks (*) and partial loss-of-function effector mutants are highlighted in red, and repective activated effectors are indicated below. This figure was adapted from Oertli et al. 2000. **(B)** GST-tagged constructs of wild-type (wt) and activated mutants (V12, L87) of RFGs were expressed in HEK293T cells together with flag-tagged VANGL1. GST-GTPases were purified with glutathione beads and interacting proteins detected by western blotting using anti-flag, AF6 or BRAF antibodies. As a negative control for binding served active RAP2 (V12 mutant). **(C)** Deletion of the R-RAS CAAX motif completely disrupts interaction with VANGL1. HEK293T cells were transfected with R-RAS effector domain mutant (A64) or C-terminal CAAX motif (Δ) deletion constructs in both activating backgrounds (V38 and L87). RAP2 V12 served as background binding control. Lysate harvest, purification and detection was carried out as decribed in B.

VANGL1 binds strongly to constitutively active R-RAS L87, but introduction of any of the effector domain point mutation tested led to a significant reduction of interaction. The less well described effector domain T61S, exhibits a slightly milder disruption effect on the VANGL1 binding to R-RAS, whereas the most severe inhibiting effect is observed with the effector domain mutant D64A, which completely abolishes effector interaction and thus is commonly termed defective

mutant (Figure 3.7B). Probing for binding of endogenous R-RAS effectors BRAF and AFADIN/AF6 showed that all employed effector domain mutants completely disrupted binding to R-RAS (Figure 3.7B). Experiments carried out using respective mutants in R-RAS V38 background showed similar results (data not shown).

In summary, all employed effector loop mutants decreased binding to VANGL1 as well as other effectors and therefore, unfortunately, I was not able to identify partial loss of function R-RAS mutants.

Interestingly, deletion of the R-RAS CAAX motif in both activating backgrounds completely disrupts VANGL1 interaction comparable to the level of the defective mutant R-RAS D64A (Figure 3.7C). The CAAX motif is essential for appropriate post translational processing and targeting of RFGs to the plasma membrane (Ahearn et al. 2012), suggesting that membrane localisation of R-RAS is critically required for interaction with VANGL1, which itself is a transmembrane protein.

R-RAS ΔCAAX was still able to interact efficiently with the membrane associated AF6/AFADIN, or with BRAF (Figure 3.7C). In clear contrast to VANGL1, deletion of the CAAX box increased the affinity of the interaction with AF6/AFADIN, while having little effect on BRAF binding (Figure 3.7C).

3.2.4 R-RAS interacts with the C-terminus of VANGL1

RAS effectors interact through a distinct small region termed RAS Binding Domain (RBD). Studies on known RAS effectors such as RAF, PI3K and RALGEFs showed that their respective RBDs share little sequence homology but certain structural similarity. Hence, there is the assumption that a wider array of unidentified RBDs exists, based on the fact that there are also RFG effectors, which do not show any RBD similarity to any of the aforementioned three effector proteins (Matheny et al. 2004; Rodriguez-Viciana et al. 2006).

VANGL1 protein structure prediction revealed four transmembrane domains and a C-terminal tetra-peptide PDZ binding motif. No other domain or motif similarity has been identified. In order to map which part of VANGL1 is binding to R-RAS, one N-terminal (excluding TM region) and various C-terminal VANGL1 truncation mutants were generated (Figure 2.2) and tested in co-expression experiments (Figure 3.8).

The larger C-terminus part was subdivided into two equal pieces based on no apparent notable domain structure (C2 and C3). Also a C-terminal fragment lacking the C-terminal tetra-peptide motif (ETSV), required for PDZ-domain interaction was generated (ΔPDZ-BM) (Figure 3.8A) (Saras and Heldin 1996; Songyang et al. 1997).

Expression of VANGL1 truncation constructs resulted in similar protein levels, except for the shorter C-terminal constructs C2 (Figure 2.2) and C3 (Figure 3.8B), which expressed at considerably lower protein levels.

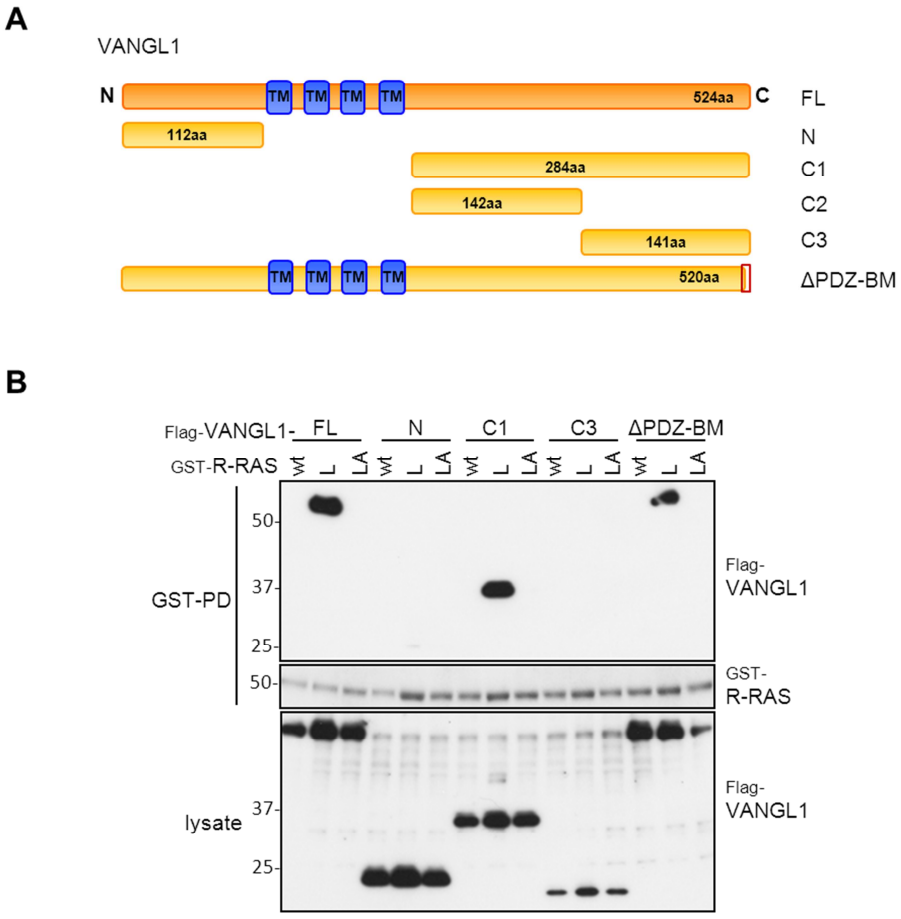

Figure 3.8: VANGL1 interacts with R-RAS through its C-terminus in a PDZ-motif independent fashion. (A) Schematic of VANGL1 protein and generated truncation mutants. TM-transmembrane spanning regions, ΔPDZ-BM, truncation of the PDZ domain interacting tetrapeptide. **(B)** Mapping of the R-RAS interaction region on VANGL1. Flag-VANGL1 or truncations shown in A were co-expressed with GST-R-RAS wild type (wt), activated L87 (L) or effector domain mutant L87 A64 (LA) in HEK293T cells. After 48 h, cells were lysed and immunoprecipitated using glutathione beads. Interactions and levels of expression were visualised by western blot using flag antibody of GST pull downs and lysates, respectively.

Under comparable expression levels of VANGL1 constructs (except C3 truncation), GTP-dependent R-RAS interaction is observed with the full length protein, complete C-terminus (C1) and the ΔPDZ-BM truncation with similar affinity. No interaction of R-RAS L87 could be observed with the VANGL1 N-terminal fragment (Figure 3.8B). This leads to the conclusion that R-RAS interaction with VANGL1 maps to the C-terminus in a PDZ motif independent manner.

Even employing very long exposures, no interaction could be detected with VANGL1-C2 (data not shown) or VANGL1-C3. Therefore, VANGL1-C2 or VANGL1-C3 regions appear insufficient for binding, and the interaction with R-RAS can only be mapped to the C-terminus without further refinement (Figure 3.8B). Similar results were achieved using the activated R-RAS V38 mutant in VANGL1 mapping experiments (data not shown).

3.2.5 R-RAS interaction with VANGL1 is disrupted by the D259E mutant

Point mutants of VANGL1 have been identified in a cohort of neural tube defect patients (Figure 1.31A) (Kibar et al. 2007; Kibar et al. 2009). In order to test whether reported VANGL1 mutations disrupt the interaction with R-RAS, five C-terminal point mutations were generated and included in VANGL1 co-expression interaction studies (Figure 2.2 and Figure 3.9A).

VANGL1 interaction with R-RAS takes place in an activation and effector domain dependent manner with VANGL1 V2391I, R274Q and M328T point mutants at a similar level compared to wild type (wt) or the ΔPDZ-BM truncation. Expression of the D259E mutation construct leads to similar protein levels as the wild type or point mutant M328T, but no interaction with R-RAS could be detected under these conditions. Although longer exposures showed residual interaction, this binding is no longer effector domain dependent and is therefore unspecific. Interestingly, this mutant is homologous to the *looptail* mouse VANGL2 D255E mutant, known to be involved in neural tube defects (Figure 3.9B).

Another analogous point mutation initially identified in the *looptail* mouse, S467N, appears to be defective on short exposures, but expression levels of this protein are considerably lower than other point mutants or wild type VANGL1. On longer exposures, specific binding of VANGL1 S467N to R-RAS L87 could be detected at similar levels than wild type (Figure 3.9B).

Detection of endogenous AFADIN/AF6 served as binding control for transfected RAP2 and R-RAS constructs (Figure 3.9B).

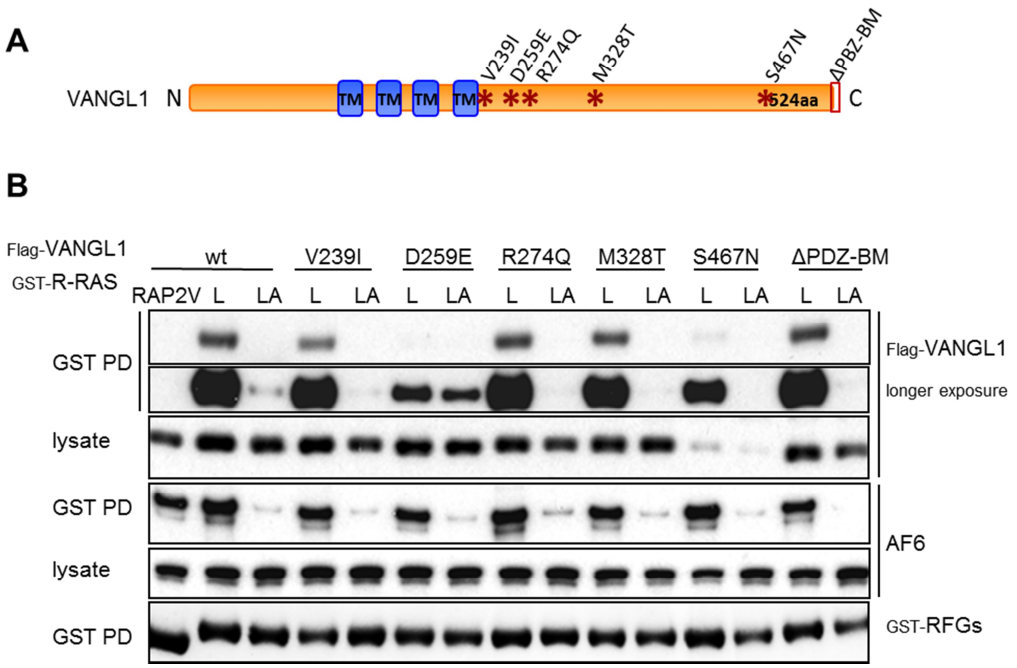

Figure 3.9: VANGL1 point mutations D259E identified in neural tube defect (NTD) patients disrupts binding to R-RAS. (A) Overview of VANGL1 structure and location of employed NTD point mutations. TM-transmembrane domain. **(B)** HEK293T cells were co-transfected with flag-tagged VANGL1 wt or respective point mutants as indicated above with either GST-tagged activated R-RAS (L87) or effector domain mutant (L87 A64). After 48 h, cells were lysed and immunoprecipitated using glutathione beads. Interactions were detected by western blot using flag-antibodies.

3.2.6 R-RAS and VANGL1 interact directly *in vitro*

Identification of VANGL1 as a novel R-RAS interacting protein by TAP or co-immunoprecipitation does not elucidate if this interaction is direct or mediated through other proteins. In order to establish if VANGL1 binds to R-RAS in a direct fashion, an *in-vitro* assay was employed which tests interaction of purified, GDP or GTP loaded R-RAS with purified GST-VANGL1 fusion proteins (Figure 3.10).

Recombinant VANGL1-N and VANGL1-C1 truncations (Figure 3.8A) were expressed as GST-fusion proteins and purified from an insect cell line

(*Spodoptera frugiperda*, SF9) or from bacteria (*E.coli*). As positive control for R-RAS interaction, other known effector proteins, either RBD (CRAF) or fragments containing the RBD (AF6, RASSF5) were expressed in bacteria as GST-fusion proteins and included in the assay. VANGL1 truncations, CRAF, AF6 or RASSF5 purified proteins were then incubated with either a GDP or GMP-PMP (a non-hydrolysable GTP analogue) loaded bacterial purified His-tagged R-RAS. Detection of associated R-RAS was performed by western blotting for the His-tag after extensive washing of glutathione pull-downs.

Included assay controls of established effectors, such as CRAF, AF6 or RASSF5, exhibited the expected pattern of preferred interaction to the GMP-PMP (GTP) bound over GDP-bound R-RAS, indicating direct binding in an activation dependent fashion (Figure 3.10) (Spaargaren et al. 1994).

The C-terminal domain of VANGL1 (VANGL1-C1) also shows a similar level of preferential binding to GMP-PMP bound R-RAS, indicating that VANGL1 interacts directly with R-RAS in the activated conformation. Identical results were obtained when VANGL1 protein was purified from either bacterial or insect cell sources (Figure 3.10).

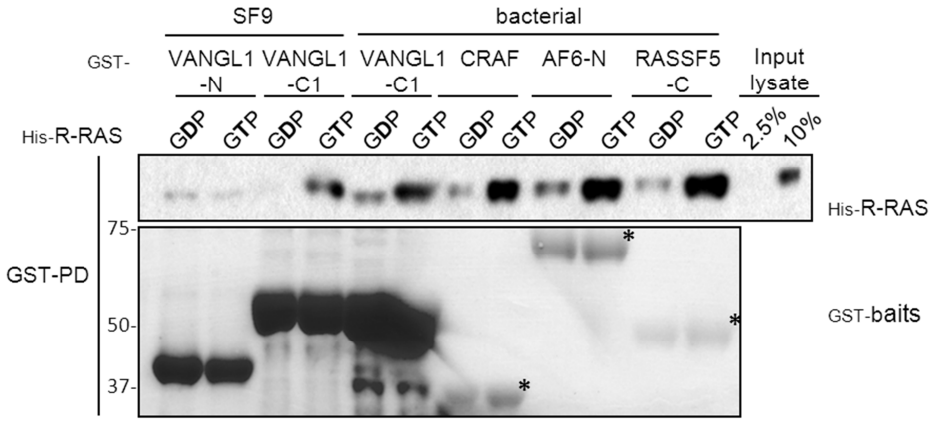

Figure 3.10: R-RAS interacts directly with the cytoplasmic C-terminus of VANGL1. In vitro interaction complex formation between VANGL1 and R-RAS. Bacterial purified His-tagged R-RAS was loaded with either GDP or GMP-PMP (non-hydrolyzable analogue of GTP) and added to immobilized GST-VANGL1 truncations (either N- or C-terminal) purified from bacterial or insect cell origin or well-known indicated effector proteins (indicated by asteriks). After immunoprecipitation and washes, bound R-RAS was detected by western blotting using an His-tag antibody. Indicated amounts of proteins used in this assay (2.5% and 10%) were run alongside to serve as reference.

Very low residual binding of VANGL1 N-terminus (VANGL1-N) at similar levels to the GDP and GTP form of R-RAS was observed, suggesting that this interaction is non-specific, and further confirming previous results that the VANGL1 N-terminus is not involved in R-RAS binding (Figure 3.10).

3.3 ARHGEF17/p164RhoGEF behaves as a TC21 and R-RAS effector

This section will focus on characterisation of ARHGEF17/p164RhoGEF interaction with the R-RAS subgroup members and its ability to act as a RHOA GEF.

3.3.1 ARHGEF17/p164RhoGEF interacts with R-RAS and TC21 in an activation and effector domain dependent manner

Initial binding studies were designed to verify that ARHGEF17/p164RhoGEF interaction with TC21 takes place in an activation dependent and effector domain mediated manner. Binding affinity between two available constitutive activating mutants of TC21 (V13 and L71) and their respective effector domain mutants were carried out. Due to the lack of any commercially available antibodies for ARHGEF17/p164RhoGEF, and failure to successfully generate an antibody against a N-terminal ARHGEF17/p164RhoGEF fragment purified from bacteria, the following binding studies were carried out in a co-expression study as described earlier for VANGL1 (refer to 3.2.1).

ARHGEF17/p164RhoGEF interaction with TC21 was observed with both activating mutants (V13, L71), but no binding could be detected with the effector domain mutation or the wild type protein. Also, despite a lower expression of TC21 L71 and its respective effector domain mutant, it appears that ARHGEF17/p164RhoGEF demonstrates a higher affinity to TC21 L71 over TC21 V13 (Figure 3.11A).

Testing the binding specificity of other R-RAS subgroup members (R-RAS, M-RAS) or closely related RAS family GTPases (N-RAS, RAP1/2) showed that ARHGEF17/p164RhoGEF binds to R-RAS L87 and both TC21 activating mutants but not to any other GTPase tested in this panel. Comparing R-RAS V38 and R-RAS L87 activating GTPases at similar expression levels, p164RhoGEF seems to

only bind to R-RAS L87. No interaction with the third R-RAS member M-RAS could be observed, rendering ARHGEF17/p164RhoGEF interaction specific to TC21 and R-RAS (Figure 3.11B).

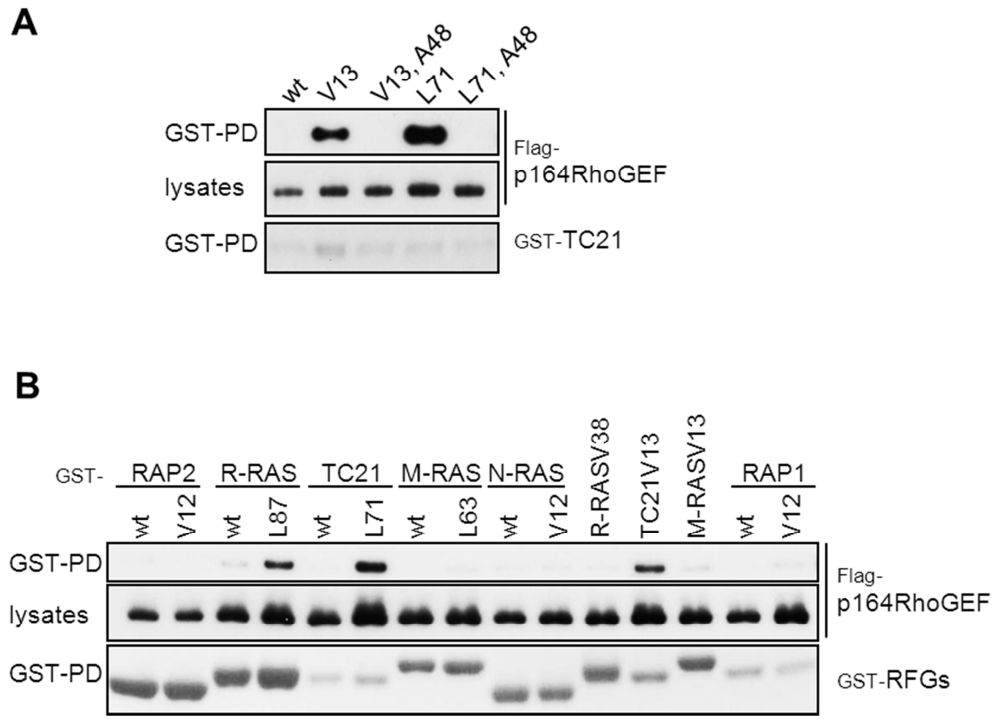

Figure 3.11: ARHGEF17/p164RhoGEF binds specifically to TC21 and R-RAS. (A) HEK293T cells were co-transfected with GST-TC21 and flag-p164RhoGEF expression vectors. GST-TC21 was purified with glutathione beads and interacting proteins detected by western blotting using anti-flag antibodies. **(B)** GST-tagged constructs of wild-type (wt) and activated RFG mutants were expressed in HEK293T cells together with flag-p164RhoGEF. GST-RFGs were purified as described in A. PD - pull down, RFG - Ras Family GTPases. Levels of GST-RFGs were measured by coomassie staining of membrane.

3.3.2 Mapping of p164RhoGEF domains that interact with TC21

RHO GEFs interact with and activate members of the RHO family of small GTPases through Dbl homology (DH) domains. These exchange factors are characterised by the presence of a Dbl domain in tandem with a pleckstrin homology (PH) domain, which interacts with lipids and proteins. Together, these two domains constitute the minimum structural unit necessary for the activity of Dbl family proteins (Zheng 2001; Schmidt and Hall 2002). Interestingly,

p164RhoGEF does not contain any detectable PH motif by conventional domain prediction, but has a WD40 domain, which has been reported for two additional GEFs: GrinchGEF and GEF10 (Rumenapp et al. 2002; Winkler et al. 2005; Mohl et al. 2006).

Therefore, truncation constructs of p164RhoGEF were generated in order to map the TC21 binding region and to test if the WD40 domain is required for interaction. Truncation constructs were designed to cover the N-terminus or C-terminus including or excluding the DH domain. Further, the C-terminal part was shortened to be either WD40 domain excluding, or to contain the WD40 domain only or a truncation thereof (Figure 3.12A).

Binding studies employing all generated truncations showed varied levels of expression, p164RhoGEF-C1 and -C2 being the highest expressed, whereas the shorter C-terminal truncations (p164RhoGEF-C3, -C4 and ΔN) expressed at very low levels (Figure 3.12B).

Full length p164RhoGEF (FL) binds to active TC21, whereas no interaction with the N-terminal fragments p164RhoGEF-N or DH domain containing construct p164RhoGEF-ΔC could be detected. In contrast, a C-terminal fragment lacking the N-terminus (p164RhoGEF-ΔN) exhibited an even higher binding affinity to TC21 than the full length protein, even though it was expressed at greatly reduced levels (Figure 3.12B).

Examining C-terminal truncations excluding the WC40 domain (p164RhoGEF-C2) compared to the DH lacking complete C-terminus (p164RhoGEF-C1) at similar expression levels, the WD40 excluding truncation displayed a significantly reduced interaction with TC21 L71. This indicates that the WD40 domain might not be critically required for binding but has a supporting role (Figure 3.12B).

Taken together these results suggest that TC21 likely interacts predominantly with the region between the DH and WD40 domains although the integrity of the WD domain is likely contributing for a higher affinity interaction.

Notably, flag-p164RhoGEF protein levels in lysates were consistently considerably higher when TC21 L71 was co-expressed suggesting that active TC21 may have an effect on the protein stability of p164RhoGEF (Figure 3.12B).

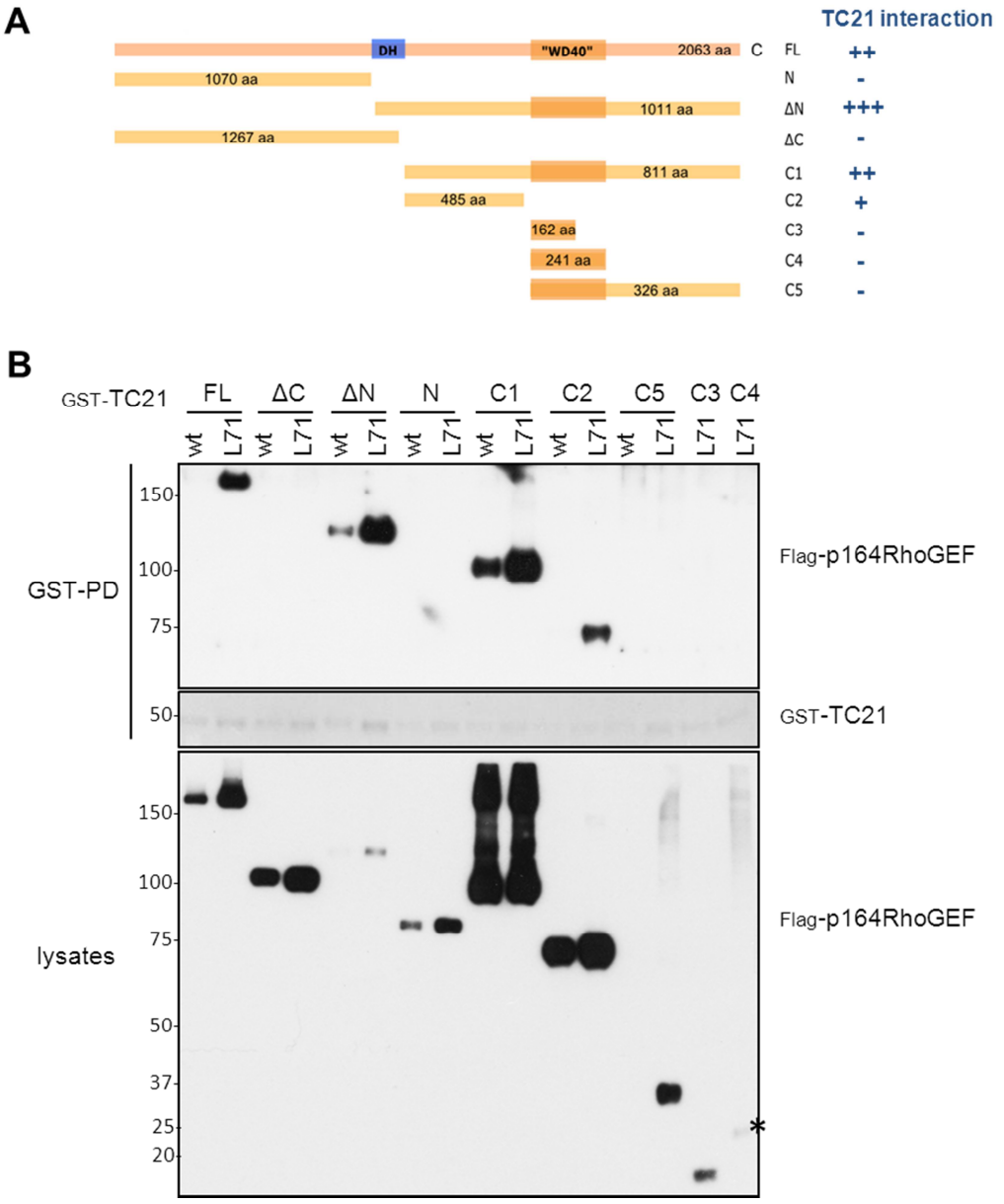

Figure 3.12: Mapping of the p164RhoGEF binding region to TC21. (A) Schematic of p164RhoGEF truncation mutants and summary regarding binding affinity towards activated TC21 (amounts of + indicates binding strength). DH-Dbl-homologous domain. **(B)**. Flag-full length (FL) p164RhoGEF or truncations as illustrated in A were co-transfected with either wild type (wt) or activated GST-TC21 (L71) in HEK293T cells. 48 h post transfection, cells were lysed and purified using glutathione beads. Interactions and protein levels on lysates were detected by western blot using a flag-antibody. Due to its low expression, C4 fragment has been indicted with asteriks.

3.3.3 ARHGEF17/p164RhoGEF and TC21 interact *in vitro*

To establish if ARHGEF17/p164RhoGEF, interacts with TC21 in a direct manner, in vitro binding assays were carried out as described above for R-RAS (see section 3.2.6).

Full length and C-terminal p164RhoGEF fragments were expressed and purified from baculovirus infected Sf9 cells. The N-terminal domain of AF6 containing the two RAS associating (RA) domains was used as a positive control. Full length (FL) and p164RhoGEF-C1 exhibit GTP dependent binding to TC21, comparable to that observed for AF6 (Figure 3.13). In contrast to the results detected in the interaction studies in HEK293T cells, p164RhoGEF-C2 purified from baculovirus was unable to interact with TC21 *in vitro*. We do not know the reasons for this discrepancy but this may be related to differences in protein folding or post-translational modification occurring in mammalian and insect cells. Regardless, the preferential GTP-dependent interaction seen between purified proteins in vitro strongly suggests that ARHGEF17/p164RhoGEF interacts directly with TC21 and thus behaves as a true direct effector (Figure 3.13).

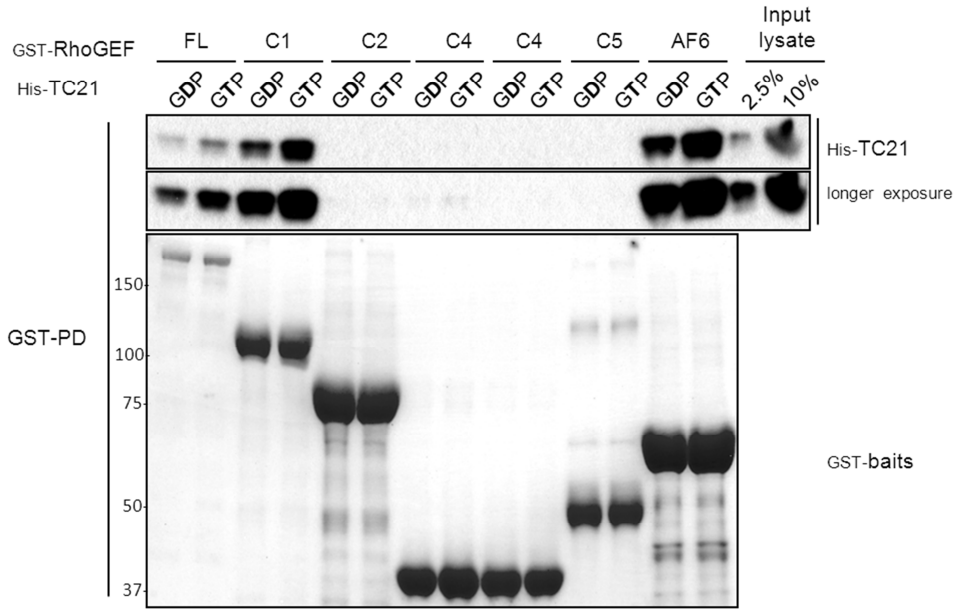

Figure 3.13: *In vitro* interaction between p164RhoGEF and TC21. Bacterial purified His-tagged TC21 was loaded with either GDP or GMP-PMP (GTP) and added to immobilised GST-p164RhoGEF truncations as indicated (Figure 3.12A) purified from Sf9 cells. After extensive washes of glutathione beads, bound TC21 was detected by western blotting using a His-tag antibody. Indicated amounts of proteins used in this assay (2.5% and 10%) were run alongside to serve as reference. AF6 served as a TC21 effector proteins.

3.3.4 ARHGEF17/p164RhoGEF acts as a GEF for RHOA

ARHGEF17/p164RhoGEF has been demonstrated to be a RHOA specific GEF (Rumenapp et al. 2002). In order to confirm that ARHGEF17/p164RhoGEF is able to activate the RHOA, and to establish RHO activation assays to be used in future experiments (see later section 6.3), various GEFs were co-transfected with myc-RHOA and RHOA activation measured using Rhotekin-RBD pull-down assays (Habas and He 2006). ARHGEF19/WGEF, which has been reported to be involved in WNT regulated convergent extension and to act as GEF for RHOA (Tanegashima et al. 2008) was also cloned and used in parallel, as well as the ARHGEF17/p164RhoGEF related proteins ARHGEF10L/GrinchGEF and ARHGEF10/GEF10).

Cells were also stimulated as positive control with serum which is known to trigger activation of RHO GTPases, as well as with EGF, which has been shown to be a much weaker activator (Ridley and Hall 1992). mSOS was included as negative control, since it acts as nucleotide exchange factor for RAS GTPases and RAC (Figure 3.14) (Chardin et al. 1993; Nimnual and Bar-Sagi 2002).

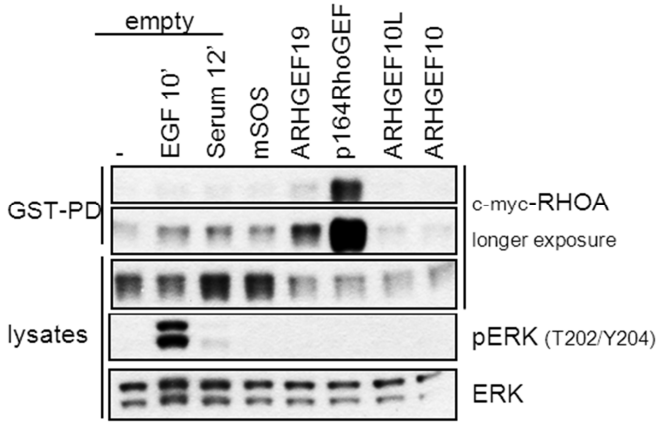

Figure 3.14: p164RhoGEF is an activator of RHOA in HEK293T cells. Empty vector or GEFs (mSOS, ARHGEF19, ARHGEF17/p164RhoGEF, ARHGEF10 and ARHGEF10L) were co-transfected with myc-RHOA. 32h post transfection, cells were serum deprived for 16h and either stimulated with 100 ng/mL EGF or 10% final serum for indicated times, or left untreated (-). The GTP form of RHOA was pulled down (PD) from HEK293T cell lysates using GST-RBD (RHO Binding Domain from Rhotekin). Activated RHOA fraction was detected using myc antibodies.

HEK293T cells stimulated with serum or EGF show a small increase in precipitated activated RHOA over basal level (-). Expression of the RASGEF mSOS elevated activated RHOA levels only slightly over basal levels, whereas the ARHGEF19 exhibited a significant increase. Expression of ARHGEF17/p164RhoGEF on the other hand strongly increased the amount of activated myc-RHOA and therefore represents a very potent RHOA guanine nucleotide exchange factor (Figure 3.14).

3.4 Discussion

3.4.1 VANGL1 functions as an effector of R-RAS subgroup GTPases

Using activating or disrupting mutants of RAS family GTPases, I have shown that VANGL1 demonstrates all the hallmarks required to be a true effector of R-RAS and TC21. VANGL1 binds preferentially to the activated mutants compared to the wild type protein and the interaction is disrupted by mutations in the effector domain. Furthermore, a GTP-dependent interaction can also be observed in vitro binding assays using purified proteins, suggesting that the interaction is direct. This interaction is also very specific for R-RAS subgroup members, as even under conditions of overexpression no binding to any other tested RAS family GTPase could be detected. Taken together, these results indicate that VANGL1 is a direct and specific effector of R-RAS and TC21.

VANGL2 can also be detected in co-transfection studies associating with R-RAS GTPases. However, this interaction is significantly weaker compared to VANGL1. Because VANGL1 and VANGL2 can hetero-dimerise ((Belotti et al. 2012) and our own TAP data), it is possible that the weak association detected with VANGL2 is being mediated through VANGL1, and additional experiments are required to address this possibility. Regardless, it is clear that there are important differences between VANGL1 and VANGL2 function, which need to be further understood (see section 4.2) (Torban et al. 2004; Tissir and Goffinet 2006), and our results suggest VANGL1 is preferentially regulated by R-RAS GTPases.

Notably, R-RAS L87 has higher affinity for VANGL1 (and AF6), but not other effectors such as BRAF, compared to the V38 activating mutant. Both mutants are located within areas important for nucleotide binding, V38 in the so called P-loop, whereas the L87 oncogenic mutant localises within the switch II region, which is also responsible for binding of effector proteins. Hence an amino acid change within the switch II region can modulate both nucleotide and effector binding, which has been previously shown for p120GAP (McCormick 1992).

Both VANGL isoforms bind specifically to R-RAS subgroup GTPases only, and not to other closely related RAS family proteins like RAP2 or N-RAS, despite the fact that R-RAS subgroup members and N-RAS share identical effector domains. It has been suggested that specificity of interaction might be mediated through the sequences flanking the core effector domain, the so called specificity regions (Khosravi-Far et al. 1998). Furthermore, our own data as described above suggests that the switch II region is important for VANGL1 interaction. Therefore, both amino acid differences flanking the effector domain and in the

switch II region may account for this differential interaction with R-RAS GTPases. Consistent with this idea, the switch II loop of R-RAS and TC21 exhibits an identical amino acid pattern, which differs in two amino acids to classical RAS proteins, and shows one residue alteration compared to M-RAS (Figure 3.15).

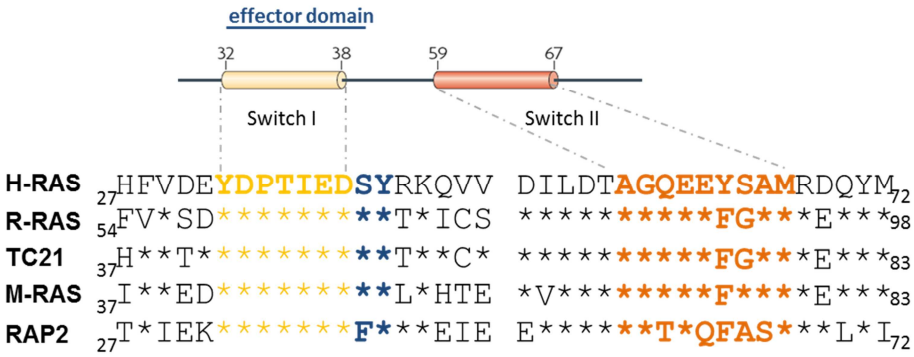

Figure 3.15: Alignment of RAS, RAP2 and R-RAS subgroup members. Indicated GTPases were aligned across switch I and switch II, including flanking regions. Identical amino acids are depicted as asteriks and subscript number specify residue number of respective amino acid position.

VANGL1 has four transmembrane domains and is therefore predicted to be a membrane protein (Iliescu et al. 2011). Localisation studies reported various subcellular distributions including plasma membrane in MDCK cells (Gravel et al. 2010; Iliescu et al. 2011) and ER in COS7 cells (Merte et al. 2011) (see also section 5.4). Notably, VANGL1 interaction with R-RAS requires the membrane targeting CAAX motif, in contrast to other effectors such as the membrane associated AF6 or BRAF, the latter one being only partially affected (Stokoe et al. 1994). Therefore, unlike for other effectors, R-RAS needs to be membrane bound in order to interact with VANGL1.

The domain structure of VANGL1 does not suggest any enzymatic activity; therefore it is likely that R-RAS/TC21 regulates VANGL1 function at least partly by regulating its localisation in some contexts: upon activation, RRAS/TC21 would recruit VANGL1 to specialised signalling platforms at the membrane micro-domains where they reside. Furthermore, R-RAS/TC21 binding could also regulate (stimulate or inhibit) the association of VANGL1 with its interacting partners and thus modulate its signalling properties.

VANGL1 point mutations have been found in sporadic and familial cases of neural tube defects (Kibar et al. 2007; Kibar et al. 2009). These mutants also demonstrated defects in convergent extension in a zebrafish model, strengthening the point of VANGL protein involvement in neural tube closure and migration, and a high degree of functional conservation across vertebrates (Reynolds et al. 2010).

Interaction studies analysing binding of VANGL1 point mutant D259E, identified in human NTDs, demonstrated it to be defective for DVL protein interaction (Kibar et al. 2007). VANGL1 D259E also disrupts binding to R-RAS. This suggests that R-RAS and DVL proteins bind to the same site of VANGL1 and therefore may compete for interaction. In addition, this mutant is located within the first half the C-terminus, which also has been shown to be required for R-RAS-VANGL1 interaction. The VANGL2 homologous point mutant is the conserved Looptail mouse D255E substitution, which has been reported to have a reduced protein half-life, and fails to be shuttled to the plasma membrane (Gravel et al. 2010). Instead, VANGL2 D255E proteins are retained in the ER lumen due to impairment of binding to the transport protein SEC24b (Merte et al. 2011; Wansleeben et al. 2011).

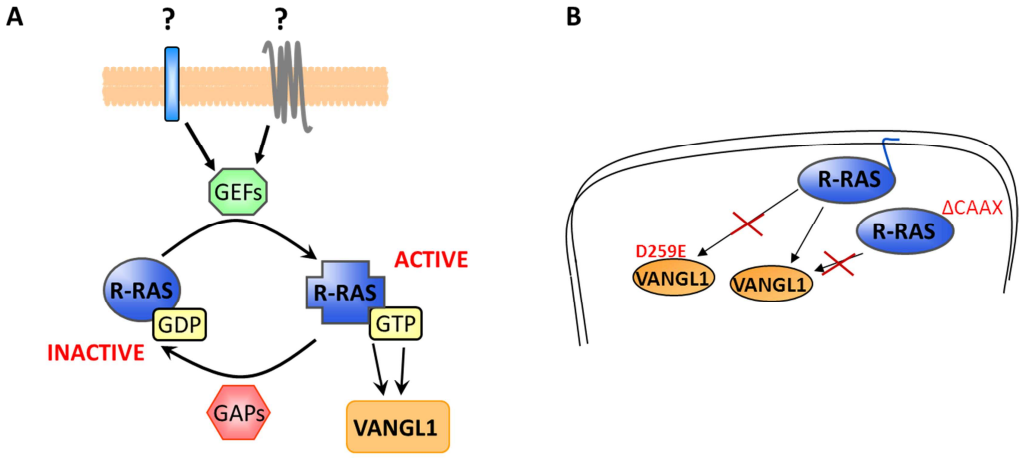

Figure 3.16: R-RAS interaction summary. (A) VANGL1 is a direct and specific effector of the R-RAS subgroup and does not bind to closely related GTPases. **(B)** This interaction is mediated through VANGL1's C-terminus, and R-RAS requires the membrane-targeting CAAX motif for VANGL1 binding. Furthermore, R-RAS-VANGL1 binding is also disrupted through the VANGL1 point mutant D259E, implicated in neural tube defects.

3.4.2 ARHGEF17/p164RhoGEF functions as an effector of R-RAS and TC21

Using constitutively active TC21 in a TAP, we identified various interactors, several of which have been previously published. One hit, identified in A549 cells, was ARHGEF17. This gene encodes for a 164kDa large RhoGEF, thus also known as p164RhoGEF.

Initial validation experiments demonstrated that ARHGEF17/p164RhoGEF binds to both TC21 activated mutants and R-RAS L87 in an activation and effector domain dependent. No interaction with M-RAS, RAP1, RAP2 or N-RAS could be observed.

Interestingly, ARHGEF17/p164RhoGEF does not contain any detectable PH motif, but encompasses a WD40 domain, which in addition has been reported for further two GEFs: GrinchGEF and GEF10 (Rumenapp et al. 2002; Winkler et al. 2005; Mohl et al. 2006). However, a recent publication challenged this finding and descibed that ARHGEF17/p164RhoGEF contains a functional PH domain, which was not detected previously using convential domain prediction software due to an ~70 residue α-helical domain insertion (Mitin et al. 2012). Furthermore, the original paper describing ARHGEF17/p164RhoGEF (Rumenapp et al. 2002) predicted a size of 164 kDa, but annotations by Croix and colleagues descibed ARHGEF17 with an extensive N-terminal domain, resulting in a predicted 222 kDa protein in size (St Croix et al. 2000).

As observed from our experiments, and consistent with literature reports (De Toledo et al. 2000; Rumenapp et al. 2002), ARHGEF17/p164RhoGEF acts as a RHOAGEF. A more detailed study further illuminated that ARHGEF17/p164RhoGEF is able to activate RHOB and RHOC isoforms, but fails to activate RAC or CDC42 (Mitin et al. 2012).

The ARHGEF17/p164RhoGEF N-terminus has been reported to contain a novel actin binding domain, and has been found to be actin stress fibre associated, independently of DH/PH domains (Mitin et al. 2012). Notably, TC21 has been mapped to interact with ARHGEF17/p164RhoGEF C-terminus downstream of the DH domain.

The original paper describing ARHGEF17/p164RhoGEF (Rumenapp et al. 2002) showed a restricted tissue expression in the mouse with predominate expression in the heart. Furthermore, our own TAP data identified ARHGEF17/p164RhoGEF

interacting with TC21 in A549 cells but not HEK293T, consistent with its differential expression in different cell types.

Due to unavailability of commercial antibodies, considerable time and effort was devoted to express and purify from bacteria recombinant fragments of ARHGEF17/p164RhoGEF (and VANGL1) to be used for the generation of polyclonal antibodies. Disappointingly, when the outsourced rabbit serum was received, it could not efficiently recognise or immunoprecipitate even the overexpressed tagged protein for reasons that are not clear. Because of the likely cell type specific expression of ARHGEF17/p164RhoGEF and the unavailability of antibodies to detect its expression, further studies would have been significantly complicated and thus it was decided with my supervisor to focus my PhD studies on VANGL1 and its role as an effector of R-RAS GTPases.

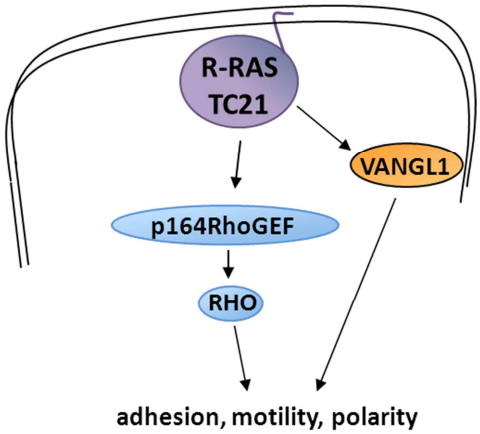

Figure 3.17: TC21 interaction summary. The RhoGEF protein p164RhoGEF binds to R-RAS and TC21 through its C-terminus in an activation and effector domain dependent manner. This leads to the speculation that R-RAS subgroup GTPases could modulate the WNT-PCP member VANGL1 and RHO GTPase activating factors in order to modulate cellular motility, adhesion and polarity.

CHAPTER 4

Identification of VANGL1 interaction partners

4 Identification of VANGL1 interaction partners

4.1 Initial VANGL1 TAP Screen

Initial studies in fruit flies identified the VANGL1 homologue strabismus as a core PCP protein (Wolff and Rubin 1998; Jenny et al. 2003). Despite great advances in the WNT signalling field, very little is known about VANGL1 and its role in PCP in higher vertebrates.

In order to identify in a non-biased approach VANGL1 interacting proteins that may shed light on its function in mammalian cells, we used a proteomic approach by transient expression of TAP-tagged VANGL1 in HEK293T cells.

Three independent TAP purifications were performed by Dr Rodriguez-Viciana and in one case active R-RAS G38V was co-expressed. Proteins identified by mass spectrometry are listed in Figure 4.1. Increased sensitivity was achieved with each purification and the last VANGL1-TAP was performed only with co-expressed R-RAS V38. Therefore no comparison between purifications or the effects of R-RAS on purified interaction could be made. Consequently, further biochemical experiments were employed to investigate if R-RAS has a modulating effect on VANGL1 interacting proteins (see section 4.3).

Several TAP-identified VANGL1 binding proteins confirmed previously reported interactions, known to be involved in polarity such as DVL2, DVL3, SCRIB and DLG1 (Lee et al. 2003; Torban et al. 2004; Torban et al. 2008; Courbard et al. 2009), validating our approach.

In addition to these known interactors, multiple novel interactors were identified, including additional proteins involved in polarity (LIN7C, CASK, CELSR2, LPHN2), several that suggest an role for VANGL1 in vesicle trafficking (YIF1B, Sec24B, RAB3GAP2) (Figure 4.1).

A

VANGL1,(HEK293T)

	Unique peptides	% Coverage
VANGL1	54	66.6
C17orf62	9	40.1
SCRIB	8	5
CSNK2A1	4	14.6
PNN	5	7.1
LIN7C	1	6.1

B

VANGL1,(HEK293T) EGF stimulation

	Unique peptides	% Coverage
VANGL1	45	64.1
SCRIB	7	4.6
C17orf62	3	11.8
YIF1B	1	4.8
LIN7C	1	14.7
DLG1	1	1.3
CSNK2A1	1	4.3
VANGL2	1	1.9
DVL2	1	1.6
DVL3	1	1.7
SYNJ2BP	2	24.8

C

VANGL1, (HEK293T) R-RAS, EGF

	Unique peptides	% Coverage
VANGL1	48	60.9
SCRIB	5	3.1
DLG1	5	5.4
LPHN2	4	4.5
SYNJ2BP	3	26.9
YIF1B	2	19.9
CELSR2	1	0.3
RAB3GAP2	1	0.8
CASK	1	1.7
SEC24B	1	1.2
C17orf62	1	4.3
ESYT1	1	1.1
VANGL2	1	3

Figure 4.1: VANGL1-TAP approach lead to identification of novel interaction partners. TAP-VANGL1 construct was expressed in HEK293T cells, and co-purified proteins identified by mass spectrometry. List of novel VANGL1 interactors categorised by performed TAP experiment are ranked by detected unique peptides, from highest to lowest. **(A)** Initial VANG1 TAP approach. **(B)** Second VANGL1-TAP, which has been EGF stimulated prior to cell lysis. **(C)** Final VANGL1-TAP in which active R-RAS V38 has been co-expressed.

4.2 Validation of VANGL1-TAP hits identified by mass spectrometry

Initial validation of VANGL1 binding proteins focused on polarity proteins for which commercially antibodies were available and hence would allow detection of endogenous proteins. This approach included Disks large homolog 1 (DLG1), Calcium/calmodulin-dependent serine protein kinase 3 (CASK), SCRIB, as well as the WNT signalling components DVL2 and DVL3 (Figure 4.2).

For all interaction studies, flag-VANGL constructs were transfected in HEK293T cells and immunoprecipitations were probed with antibodies against endogenous proteins (Figure 4.2B). It is worth noting that all chosen polarity proteins contain at least one PDZ domain. In order to assess whether VANGL1 PDZ binding motif was mediating the interaction, a VANGL1 mutant lacking the four last amino acids (ΔPDZ-BM) was also employed. In addition, to test for the specificity of PDZ domain interactions, the PDZ domain containing protein AFADIN/AF6, which was not identified by mass spectrometry, was included in my interaction studies.

DLG1, CASK and SCRIB interact with both VANGL1 and VANGL2 and the interaction is dependent on the PDZ-binding motif of VANGL1. Of note, DLG1 and CASK have been reported to interact (Sabio et al. 2005) and therefore could be part of a complex with one mediating the interaction with the other. SCRIB and DLG1 have also been reported to interact in *Drosophila* and mammalian context (Humbert et al. 2008; Li et al. 2009b; Massimi et al. 2012). However, SCRIB was detected in all three TAP purifications, whereas other proteins including DLG1 were only detected in the more sensitive last TAP (Figure 4.1C). Furthermore, a performed TAP with SCRIB as bait detected VANGL but not DLG1 (data not shown). These results suggest that SCRIB and DLG1 are binding independently to VANGL1.

In contrast to DLG1, CASK and SCRIB, DVL proteins interact preferentially with VANGL1 compared to VANGL2. Furthermore, the interaction with DVL proteins appears not to be mediated by their PDZ domains as VANGL1 lacking the PDZ-binding domain can still efficiently interact with DVL3 whereas it is only partially disrupted in the case of DVL2.

The control AF-6 did not show binding to VANGL1 or VANGL2 above background levels, illustrating specificity of VANGL protein interaction with PDZ domain containing proteins (Figure 4.2B).

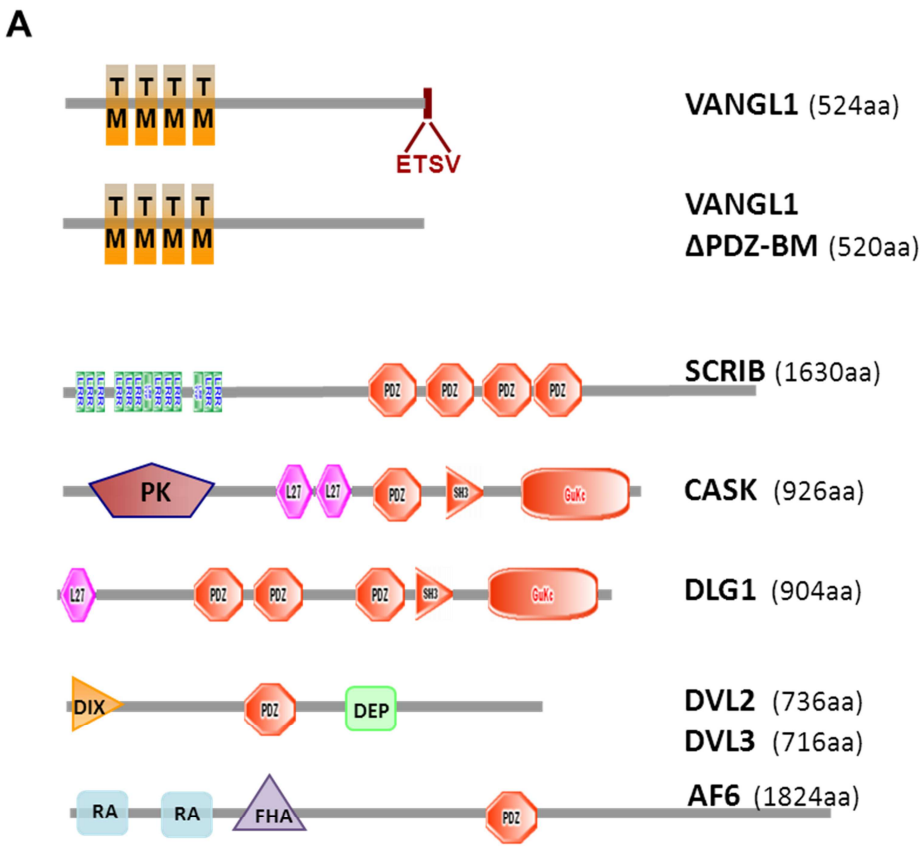
A
TMTMTMTM
ETSV
VANGL1 (524aa)
VANGL1
ΔPDZ-BM (520aa)
SCRIB (1630aa)
PDZ
PK
L27
SH3
GuKc
CASK (926aa)
DLG1 (904aa)
DIX
DEP
DVL2 (736aa)
DVL3 (716aa)
RA
FHA
AF6 (1824aa)

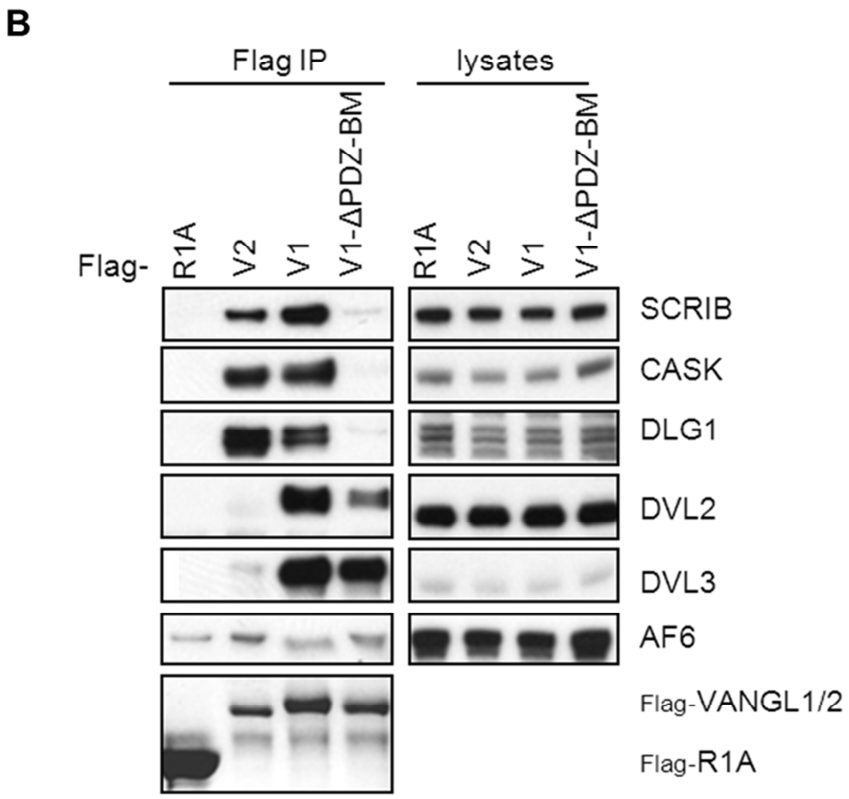
B
Flag IP
lysates
Flag-
R1A
V2
V1
V1-ΔPDZ-BM
SCRIB
CASK
DLG1
DVL2
DVL3
AF6
Flag-VANGL1/2
Flag-R1A

Figure 4.2: Validation of VANGL1 interactions identified by TAP. (A) Overview of protein structure and respective protein domains. VANGL1 (ΔPDZ-BM) lacks the PDZ domain interacting tetra-peptide motif ETSV. Protein sizes are indicated as amino acid (aa) counts. This figure was constructed using the SMART database (http://smart.embl-heidelberg.de). Note that all indicated endogenous proteins possess at least one PDZ domain. Depicted protein domains are abbreviated as follows: TM - Transmembrane, LRR – Leucine Rich Repeat, PDZ - PSD-95-Discs-large-ZO-1, PK - Protein kinase, L27 - Lin-2 and Lin-7, SH3 - SRC Homology 3, GuKc- Guanylate kinase , DIX – Dishevelled and Axin, DEP - Dishevelled, Egl-10 and Pleckstrin, RA - Ras-association, FHA - forkhead-associated. **(B)** VANGL1 interaction with CASK, DLG1 and SCRIB takes place in an strict PDZ-dependent manner, whereas DVL proteins are only partially (DVL2) or mildly affected (DVL3) by the VANGL1 PDZ motif truncation. Flag-VANGL1 (V1), VANGL2 (V2) or control constructs were transfected into HEK293T cells, and flag-proteins were purified using flag affinity beads and interaction with endogenous proteins were detected by western blotting probing for indicated antibodies. The type I regulatory subunit of protein kinase A (R1A) was used as background control.

In summary, relative to the amount of bait expression, which is always lower for VANGL2, the polarity proteins DLG1 and CASK showed higher affinity for VANGL2, whereas SCRIB in turn seems to bind with similar affinity to both VANGL proteins (Figure 4.2B). Overall, it appears that proteins implicated in epithelial cell polarity display a strong dependency on the VANGL1 PDZ-binding motif for interaction.

Several novel VANGL1 binding proteins identified by TAP could not be assessed on endogenous level due to the lack of reliable commercially available antibodies. Therefore, a subset of potential interactors were cloned by PCR and expressed as flag-tagged constructs, in co-transfection studies with GST-VANGL baits as performed before (section 3.3.1).

It is worth noting that many of the proteins identified by TAP contain at least one transmembrane domain, such as CELSR proteins (Figure 4.3A). However, due to their long extracellular domain and resulting cloning issues it was decided to only use the cytoplasmic part for interaction studies. In addition, KAI/CD82 was not identified by TAP but was reported as a VANGL1 interacting protein (Lee et al. 2004). Because of its role in cancer it was considered to be of interest and was also cloned and included in the study (Figure 4.3A) (Lee et al. 2005; Rowe and Jackson 2006; Kho et al. 2009; Lee et al. 2009; Ryu et al. 2010).

Both VANGL proteins demonstrate binding to YIF1B (Figure 4.3B and Figure 4.6B), but it seems that YIF1B has a higher affinity for VANGL2, whereas no interaction could be detected with DVL2, which was used as background control (Figure 4.3B).

Another link for a potential role of VANGL1 in protein trafficking is provided by Synaptojanin 2 binding protein (SYNJ2BP) a widely expressed small 145 aa protein containing a single PDZ domain and a C-terminal transmembrane helix. Initial interaction studies with VANGL1 confirmed a strong specific binding (Figure 4.3B), which is critically PDZ motif dependent and could not be observed for wild type VANGL2, DVL2 or DVL3 (Figure 4.6B).

The uncharacterised *chromosome 17 open reading frame 62* (*C17ORF62*) gene encodes for a 187 amino acid protein, consisting of a single pass N-terminal transmembrane helix. Interaction studies revealed that C17ORF62 exhibits a strong interaction with VANGL1 but not DVL2 or other control proteins (Figure 4.3B).

Nedd4 family proteins are involved in protein trafficking and protein degradation, binding to their targets directly or through the adaptor protein Nedd4 family interacting protein 1 (NDFIP1) (Putz et al. 2008). Interaction studies between VANGL1 and NDFIP1 demonstrated a strong interaction, which is not observed for DVL2 or a control protein (Figure 4.3B).

RAB3GAP1 encodes the catalytic subunit of a RAB GTPase activating protein forming a heterodimer with a non-catalytic subunit (RAB3GAP2), which specifically regulates the activity of the RAB3 subfamily of small G proteins (Diekmann et al. 2011). RAB3 proteins are involved in regulated exocytosis of neurotransmitters and hormones and are required for normal eye and brain development (Lledo et al. 1994; Corbeel and Freson 2008; Fukuda 2008; Stenmark 2009).

Binding studies using both RAB3GAP subunits individually revealed that only the catalytic protein (RAB3GAP1), but not RAB3GAP2 binds to VANGL1 (Figure 4.3B and data not shown). Interestingly, RAB3GAP2 and not RAB3GAP1 has been observed to bind to DVL2 (data not shown).

Due to its large extracellular protein structure, only the complete cytoplasmic regions starting immediately after the 7TM region of CELSR1 and CELSR2 proteins were cloned and used for interaction studies. Interestingly, binding of VANGL1 to CELSR cytoplasmic truncations was only observed with the

cytoplasmic fraction of CELSR2, whereas CELSR1 failed to interact with VANGL1 (Figure 4.3B), despite the fact that expression of the CELSR1 construct yielded much higher protein levels than CELSR2 (data not shown).

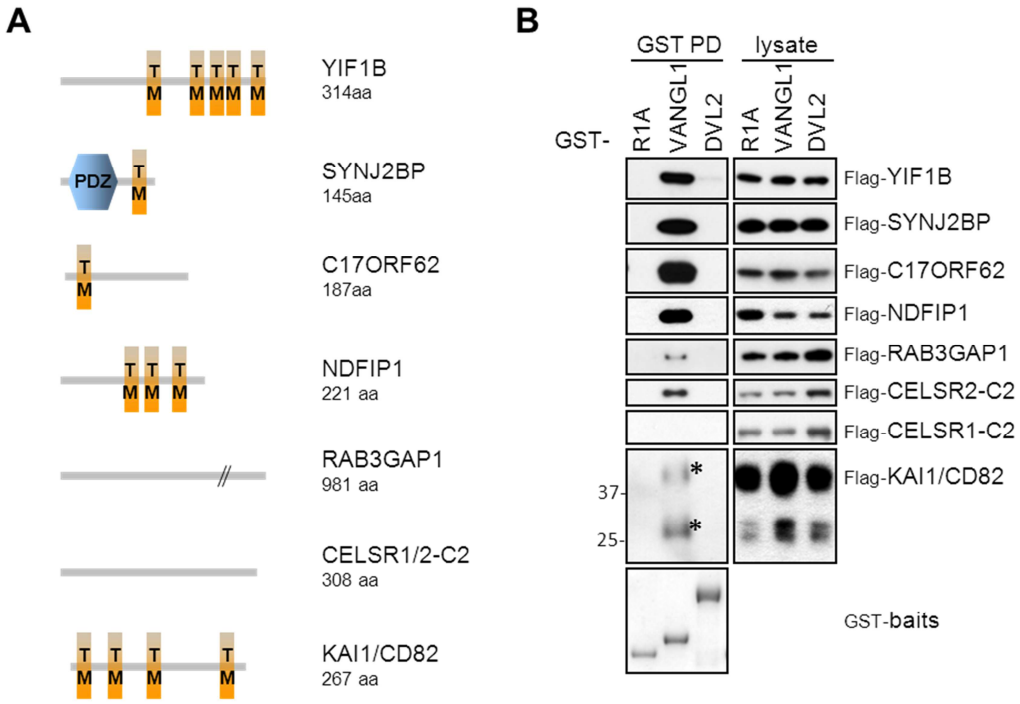

Figure 4.3: Validation of TAP-identifed VANGL1 interacting proteins. **(A)** Schematic of validated proteins depicting structural features such as transmembrane regions (TM) or PDZ domains. Protein sizes are indicated in amino acids (aa). **(B)** GST-tagged constructs of wild-type VANGL1, DVL2, or R1A serving as control, were co-expressed with potential flag-tagged VANGL1 interactors in HEK293T cells. Cells were harvested 48h post transfection and subjected to purification using glutathione beads. Interactions were detected using flag-antibodies. Protein appreviations and functions are detailed in the text. Note that CELSR1 and CELSR2 are membane proteins with a long extracellular domain, but for technical reasons, this study only employed the respective cytoplasmic C-termini. KAI1/CD82, a heavily glycosylated protein, has been reported to migrate at different molecular sizes at around 27kDa and 45 kDa depicted by asterisks (Wang et al. 2012).

The membrane glycoprotein Kangai1 (KAI1) also termed Cluster of Differentiation 82 (CD82) is a member of the tetraspanin transmembrane superfamily (TM4SF) (Yanez-Mo et al. 2009; Wang et al. 2011). VANGL1 was identified to interact with the C-terminus of KAI1/CD82, and thus enables to

modulate VANGL1 function through this binding and therefore might act as a negative regulator of cell motility (Zhang et al. 2003; Lee et al. 2004; Rowe and Jackson 2006).

Carried out interaction studies in HEK293T cells exogenously expressing VANGL1 and KAI1/CD82 confirmed reported binding, whereas no interaction to the control protein or DVL2 was detected (Figure 4.3B). KAI1/CD82 is a heavily glycosylated protein and post translational modification studies confirmed various KAI1 moieties, which could be distinguished on SDS-PAGE (Wang et al. 2012). Notably, VANGL1 binds to both KAI1/CD82 forms, but it seems that there is a preference for the faster migrating form of KAI1/CD82 (lower band Figure 4.3B), taking overall expression levels in consideration.

Interaction studies showed that VANGL2 and VANGL1 bind each other due to the ability of these proteins to form heterodimers and therefore were not included in this interaction study (Belotti et al. 2012).

Validation of LIN7C as VANGL1 binding partner was tested in overexpression approaches or by endogenous binding assays. However, I was unable to observe convincing binding of LIN7C to either VANGL1 or VANGL2, therefore detection of LIN7C in VANGL1-TAP screens could be a case of indirect co-purification due to binding as a complex member. For example, CASK and Lin7C form a complex to target the epidermal growth factor receptor basolaterally in C. elegans (Kaech et al. 1998; Doerks et al. 2000). Also, DLG1 forms a complex with LIN7 members (A or C) and MPP-7, modulating stability and localisation of DLG1 to cell-cell junctions (Bohl et al. 2007).

The VANGL1-TAP hit ubiquitin fusion degradation 1-like (UFD1L) protein is an essential component of the ubiquitin-dependent proteolytic pathway and is able to delay cell cycle progression in response to ER stress (Chen et al. 2011). Mutations in this gene have been associated with cardiac and craniofacial defects (Yamagishi et al. 1999). However, interaction studies were not able to confirm binding of UFD1L to VANGL1 (data not shown).

In conclusion, VANGL1-TAP approaches led to the identification of multiple novel VANGL1 interacting proteins, displaying a wide range of structural and functional properties, but with a enrichment in PDZ domain or transmembrane domain containing proteins. Therefore, VANGL1 seems to be involved in various cellular functions ranging form cellular polarity establishment to vesicular trafficking.

4.2.1 Effect of VANGL1 point mutations found in NTC patients on interaction with SCRIB and DVL3

Screening of neural tube defect patients revealed a set of VANGL1 point mutations across highly conserved amino acids, of which mutant D259E lost the ability to interact with R-RAS (Figure 3.9). Therefore it was intriguing to test if this particular mutation influences VANGL1 binding to other interaction partners (Kibar et al. 2007; Kibar et al. 2009; Bartsch et al. 2012). Thus, a panel of flag-tagged VANGL1 point mutants including the ΔPDZ binding motif truncation were expressed in HEK293T cells and tested for endogenous SCRIB or DVL3 binding (Figure 4.4).

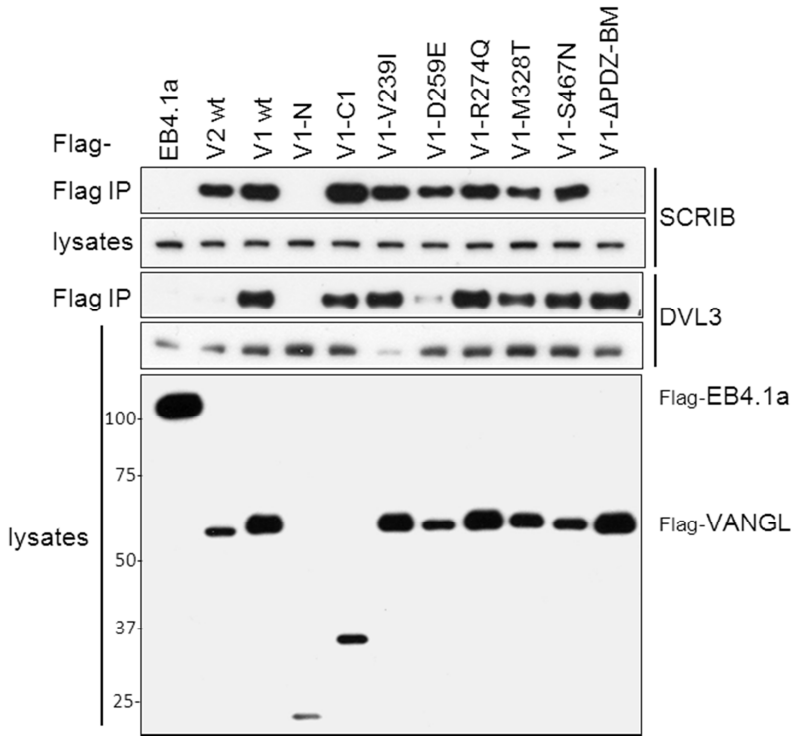

Figure 4.4: VANGL1 D259E mutant disrupts binding to DVL3 but not SCRIB. VANGL1 interacts with SCRIB via its C-terminus in an PDZ-dependent manner, but none of the employed NTD mutants show disruption of binding. On the other hand, DVL3 binds to VANGL1 C-terminus in a PDZ independent manner and is disrupted by the D259E mutant. Flag-tagged constructs of wild-type VANGL1 (V1) or VANGL2 (V2), VANGL1- N or C-terminal fragments or point mutants as indicated were expressed in HEK293T cells. Flag-constructs were purified with flag affinity beads 48 hours later. Detection of endogenous SCRIB or DVL3 was performed by western blotting using respective endogenous antibodies. Employed extracellular soluable binding protein (EB4.1a) served as control protein. NTD - neural tube defects.

None of the tested point mutants of VANGL1 (Figure 3.9) interferes with SCRIB binding, consistent with the possibility that the interaction is exclusively mediated by the PDZ-binding motif of VANGL1 to a PDZ of SCRIB (Figure 4.4).

Among the reported mutations identified in neural tube defect patients, only VANGL1-D259E severely impairs binding to DVL3 but not SCRIB, suggesting that this mutation disrupts selective protein interactions (Figure 4.4). Notably, this point mutation is identical to the one observed to disrupt R-RAS binding specificity (Figure 3.9).

4.3 Modulation of VANGL1 interactions by R-RAS

4.3.1 VANGL proteins or R-RAS GTPases do not modulate canonical WNT signalling

Initial experiments in zebrafish demonstrated that the VANGL homologue *trilobite* (*tri*) is able to antagonise canonical WNT signalling, while promoting c-JUN phosphorylation (Park and Moon 2002). In conjunction with the observation that VANGL2/tri interacts with DVL/dsh, these findings suggest that VANGL1 might be able to modulate the PCP pathway downstream of WNT ligands and Frizzled activation through its interaction with DVL (Park and Moon 2002). Particularly, since it has been observed that activation of either the canonical or PCP pathway seems to be exclusive within a given cell (Vincent and Beckett 2011). Therefore, it was intriguing to test whether R-RAS or VANGL proteins have a modulating effect on WNT canonical signalling, analysing β-catenin activity using a β-catenin/TCF-mediated transactivation luciferase assay.

To assess a potential effect of VANGL1 or R-RAS on WNT signal modulation in a mammalian context, exogenous expression of VANGL or R-RAS GTPases in combination with β-catenin firefly luciferase and renilla control reporter constructs were transfected into HEK293T cells.

Overexpression of VANGL1 or VANGL2 did not alter β-catenin reporter activity compared to the GFP transfection control or unstimulated cells. Similarly, no effect of activated R-RAS or TC21 was observed (Figure 4.5). Thus, under these conditions tested, VANGL or R-RAS GTPases do not affect basal β-catenin levels.

However, stimulation of the canonical pathway could be detected by transfection of DVL2 or DVL3 constructs, which were able to increase reporter activity by more than 15-fold (Figure 4.5). As positive control in this assay served expression of a non-degradable N-terminal β-catenin truncation (ΔN-β-cat), which prevents its phosphorylation and thus impairs proteasome targeting, leading to stimulation of reporter activity by approximately 350-fold (Yost et al. 1996; Amit et al. 2002).

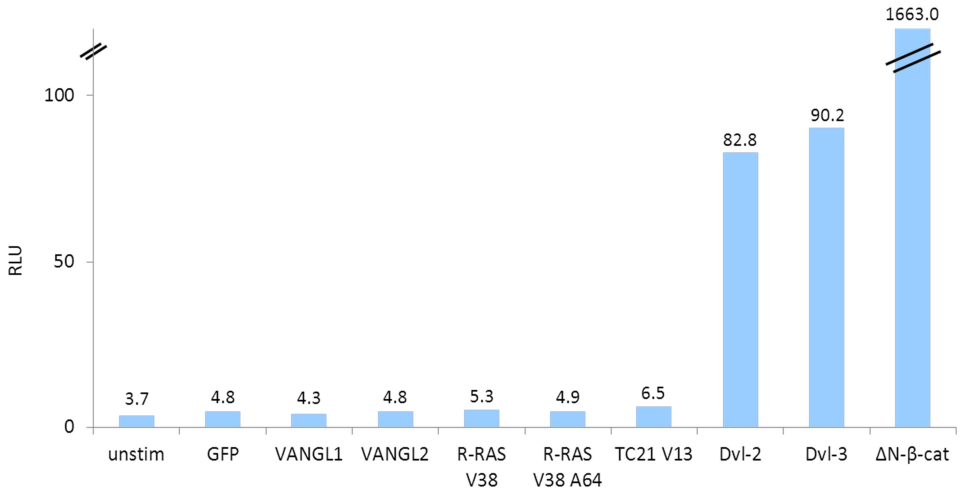

Figure 4.5: Expression of VANGL proteins or activated R-RAS/TC21 do not alter β-catenin reporter activity. HEK293T cells were co-transfected with the TCF-4 luciferase (firefly) (TOPFLASH) reporter construct and a Renilla vector, together with indicated plasmids. Cell extracts were harvested and analysed 40h post transfection for firefly and renilla luciferase activities. Data obtained were normalised for Renilla activity. RLU – relative luciferase units. GFP transfection sample served as transfection control. Expression of transfected plasmids were confirmed by western blotting.

4.3.2 Active R-RAS modulates a subset of VANGL1 binding partners

As noted before, VANGL1 does not display catalytic activity and therefore it is likely that R-RAS governs VANGL1 function by regulating either localisation to specialised signalling platforms and/or modulation of its interactions within these signalling platforms.

In order to test the possibility of an R-RAS modulation effect on VANGL1 interacting proteins, co-transfection studies were performed in which the ability of flag-VANGL1 to interact with endogenous proteins in the presence of activated R-RAS L87 or the defective mutant L87-A64 was assessed.

Interestingly co-expression of active R-RAS decreased the interaction with SCRIB, CASK, DLG1 and DVL2, whereas it has no effect on the interaction of VANGL1 with SYNTENIN-1 (Figure 4.6A), a VANGL1 interacting protein identified in a subsequent TAP experiment (section 4.5).

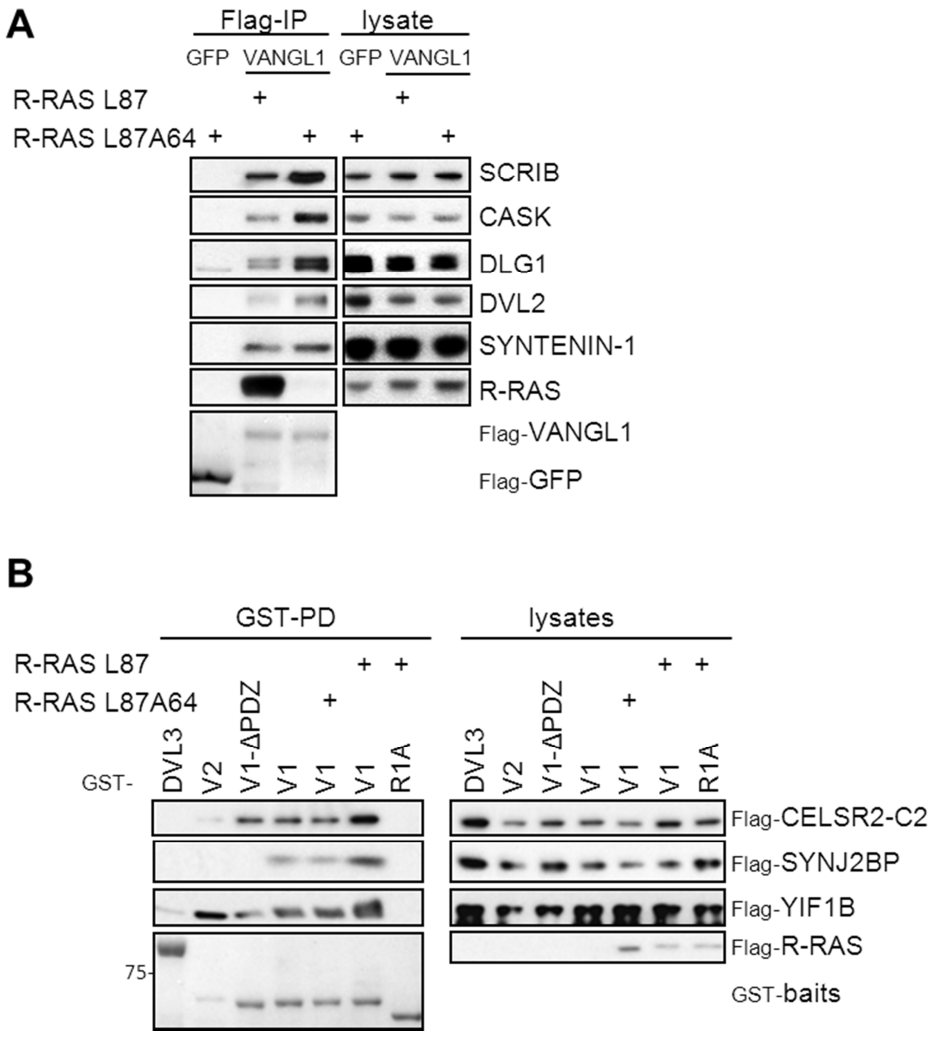

Figure 4.6: R-RAS modulates a subset of endogenous VANGL1 binding partners involved in cell polarity and WNT signalling. (A) In order to test R-RAS specific modulation of VANGL1 binding partners, flag-VANGL1 was co-tranfected with either GST-R-RAS L87 or GST-R-RAS L87 A64, and lysates were purified 48h post transfection using flag beads. Binding of endogenous VANGL1 interactors were detected using the respective antibodies as indicated above. As background binding control served flag-GFP. **(B)** Activated R-RAS modulates VANGL1 interaction with the cytoplasmic portion of CELSR2-C2, SYNJ2BP and YIF1B. Due to the lack of endogenous antibodies for both proteins, flag-R-RAS L87 or L87 A64 was co-expressed with flag-YIF1B, flag-SYNJ2BP or flag-CELSR-C2 in addition with GST-tagged DVL3, VANGL2 (V2), VANGL1 (V1) or respective PDZ binding motif mutant (ΔPDZ). As background binding control served R1A. Cells were harvested 48 h later and subjected to gluthathion purification and were probed for binding proteins using a flag antibody.

Due to the unavailability of antibodies to detect the endogenous proteins, the effect of R-RAS on the interaction with ER and Golgi localised YIF1B and SYNJ2BP, as well the cytoplasmic domain of CELSR2 (CELSR2-C2) was tested in co-transfections assays with tagged constructs. In contrast to the inhibitory effect of R-RAS on the interaction of VANGL1 with polarity proteins shown in Figure 4.6A, expression of active R-RAS had a modest stimulatory effect on the interaction of VANGL1 with CELSR2-C2, YIF1B and SYNJ2BP (Figure 4.6B).

4.4 WNT ligand and Frizzled effects on VANGL1 interactions

The ability of activated R-RAS to differentially modulate distinct subsets of VANGL1 binding partners suggested a model that R-RAS upon activation by WNT ligands could regulate VANGL1 function in polarity/PCP.

The next sections will describe the characterisation of ligands and cellular systems that was performed in order to be able to assess the role of R-RAS and VANGL1 in polarity downstream of WNT ligands in mammalian cells.

To investigate VANGL1's physiological role(s) and a potential modulation of these by R-RAS, a cellular based system was required in order to investigate VANGL1 biological function downstream of WNT signalling, focussing on PCP activation.

Initial studies of the PCP pathway were carried out in fruit flies and pathway activation read-outs assessed included alignment of wing hairs, hexagonal packing of wing epithelial cells, or the orientation of photoreceptors in the eye (Mlodzik 2002; Zallen 2007). In zebrafish or *Xenopus* models, DVL membrane recruitment or developmental defects such as convergent extension is used to assess PCP activation or disruption (Tada and Kai 2009). In higher vertebrates, cochlea stereocilia orientation of the neurosensory hair cells is a commonly used in-vivo assessment (Lewis and Davies 2002; Wallingford 2012).

Because our lab does not have direct access to any of these developmental systems, my studies focused on identifying biochemical and cell based assays of WNT ligand stimulation in a panel of mammalian cell lines.

A commonly applied read out of WNT ligand stimulation in mammalian cells is to observe an upward mobility shift of phosphorylated DVL when analysed by SDS-PAGE (Gonzalez-Sancho et al. 2004; Bryja et al. 2007b). However, since this technique is not able to distinguish between canonical versus PCP activation, this is a straight forward but limited approach (Gonzalez-Sancho et al. 2004; Angers

and Moon 2009). Other biochemical assays are assessment of JNK phosphorylation at residues T183/Y185 or activation of the heterodimeric transcription factor activator protein-1 (AP-1), which might be cell type specific (Boutros et al. 1998; Cheyette et al. 2002; Yamanaka et al. 2002; Pukrop et al. 2006; Nomachi et al. 2008; Nishita et al. 2010b).

In order to test above mentioned methods, the next step was to obtain or generate WNT ligands and to find a readout that demonstrated biological activity in the particular cell type.

4.4.1 WNT ligand generation and assessment

For a long time, research studies using WNT ligands were mostly hampered by the fact that these lipid-modified, hydrophobic secreted proteins are hard to isolate and purify. At the time of these studies, WNT3a, WNT5a, WNT7a ligands had just become commercially available. In order to address the possibility that other WNT ligands might be preferentially involved in the regulation of R-RAS and/or VANGL1, it was decided to generate our own panel of WNT ligands independently. This approach required stable transduction of WNT ligand constructs into mouse L cells and collection of resulting conditioned media, which then can be used for subsequent cell based assays (2.4.8.1) (Shibamoto et al. 1998).

Initial experiments were performed with commercial WNT ligands that were subsequently compared with our own generated ligands. Commercially available WNT3a, WNT5a and WNT7a ligands were tested using a β-catenin based luciferase reporter assay, and employing lithium chloride (LiCl) as positive control due to inhibition of GSK3β function and thus leading β-catenin accumulation (Klein and Melton 1996).

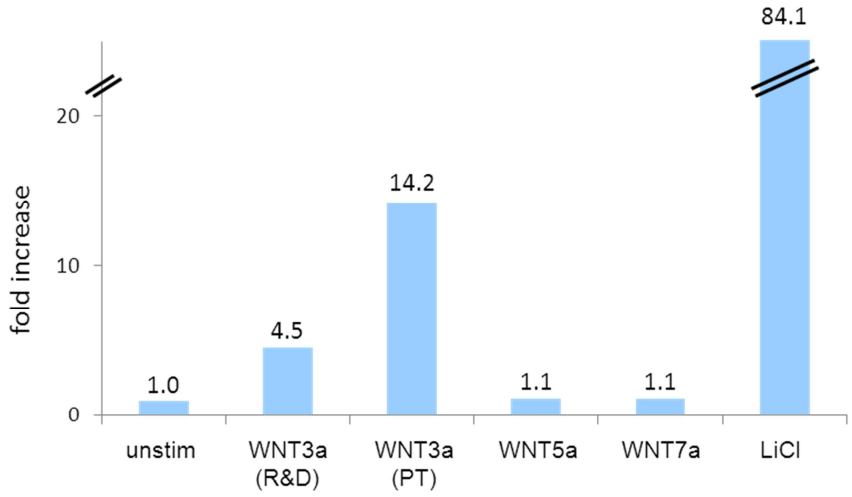

Figure 4.7: Recombinant WNT3a, but not WNT5a or WNT7a is able to stimulate canonical β-catenin signalling. HEK293T cells were co-transfected with TOPFLASH and Renilla luciferase reporter constructs. 24h post transfection, cells were stimulated for 13h with recombinant WNT ligands WNT3a (R&D, 300 ng/mL), WNT3a (Peprotech (PT), 300 ng/mL), WNT5a (500 ng/mL) or WNT7a (1 µg/mL) prior cell harvest. Treatment with lithium chloride (LiCl, 30 mM, 13h) served as positive control. Cell extracts were assayed for firefly and renilla luciferase activities and data obtained were normalised for renilla activity. Reporter construct levels (Firefly luciferase) were expressed as fold increase across analysed samples using unstimulated cells (unstim) as reference.

WNT3a (R&D source) ligand treatment resulted in elevated β-catenin levels by about 4.5 fold, whereas WNT3 ligand obtained from Peprotech (PT) at the same concentration proved more potent by increasing intracellular β-catenin levels by over 14-fold compared to untreated cells (Figure 4.7).

Samples stimulated with recombinant WNT5a or WNT7a ligand failed to show a significant elevation of β-catenin levels, indicating that these ligands do not activate β-catenin dependent signalling in this context and thus biological activity cannot be tested with this method (Figure 4.7).

4.4.2 Assessment of WNT ligand responsiveness in a panel of cell lines

Upon WNT ligand interaction with Frizzled receptors, DVL proteins are recruited to the membrane and are regulated through phosphorylation events (Schulte et al. 2005; Bryja et al. 2007b; Bernatik et al. 2011). Hence, activation of WNT

signalling could be assessed by analysis of DVL hyper-phosphorylation in gel shift assays (Figure 4.8 and Figure 4.9) (Bryja et al. 2007b).

The ability of cells to activate WNT signalling cascades depends on the available WNT ligands, expression of cognate receptors and co-receptors (Gordon and Nusse 2006; Green et al. 2008; Kikuchi et al. 2009; Sato et al. 2010; Niehrs 2012). In order to identify a suitable cellular system for subsequent experiments in this study, a panel of tumour cell lines were chosen from breast (MCF-7, MDA-MB-231), lung (A549), colon (HCT-116), bone (SaOS2) or neuroblast origin (IMR32, SY5YSH), as well non-transformed immortalised cell lines of mammary epithelial origin and investigated for response to WNT ligands 3a, 5a and 7a (Figure 4.8).

Notably, all investigated cancerous cell lines employed in the panel showed a response to WNT5a conditioned media after two hours of treatment, demonstrated by a slower migrating form of DVL2 (Figure 4.8A upper part). Stimulation of the same cell line panel with WNT3a conditioned media showed responsiveness, with the exception of MDA-MB-231 cells, displayed by a phosphorylation induced shift of DVL2. However, WNT7a conditioned media did not seem to stimulate any of the tumour derived cell lines (Figure 4.8A upper section).

However, even though all tested tumour cell lines respond to WNT3a and WNT5a CM, there are cell line dependent preferences. For example HCT-116 and SaOS2 cells show a similar DVL2 phosphorylation shift in response to WNT3a and WNT5a CM, A549 cells react more strongly to WNT3a, whereas MDA-MB-231 cells respond very strongly to WNT5a as judged by DVL2 phosphorylation shift (Figure 4.8).

In contrast, treatment of four different immortalised non-tumorigenic mammary epithelia cell lines with WNT3a, WNT5a or WNT7a conditioned media failed in all four tested cell lines to induce a DVL2 phosphorylation shift (Figure 4.8A lower part).

In order to assess if generated WNT conditioned media performs similar to recombinant commercially available purified WNT ligands, SaOS2, HCT116 and MDA-MB-231 were treated either with WNT3a, WNT5a, WNT7a CM or corresponding recombinant ligands under similar conditions and lysates were analysed for DVL2 phosphorylation shift (Figure 4.8A upper part and B). Overall, CM and recombinant ligands yielded the same DVL2 migration pattern, except

for MDA-MB-231 cells, which showed a strong response to recombinant WNT3a ligand, which was not observed for WNT3a CM. This could be due to lower ligand concentration in WNT3a CM.

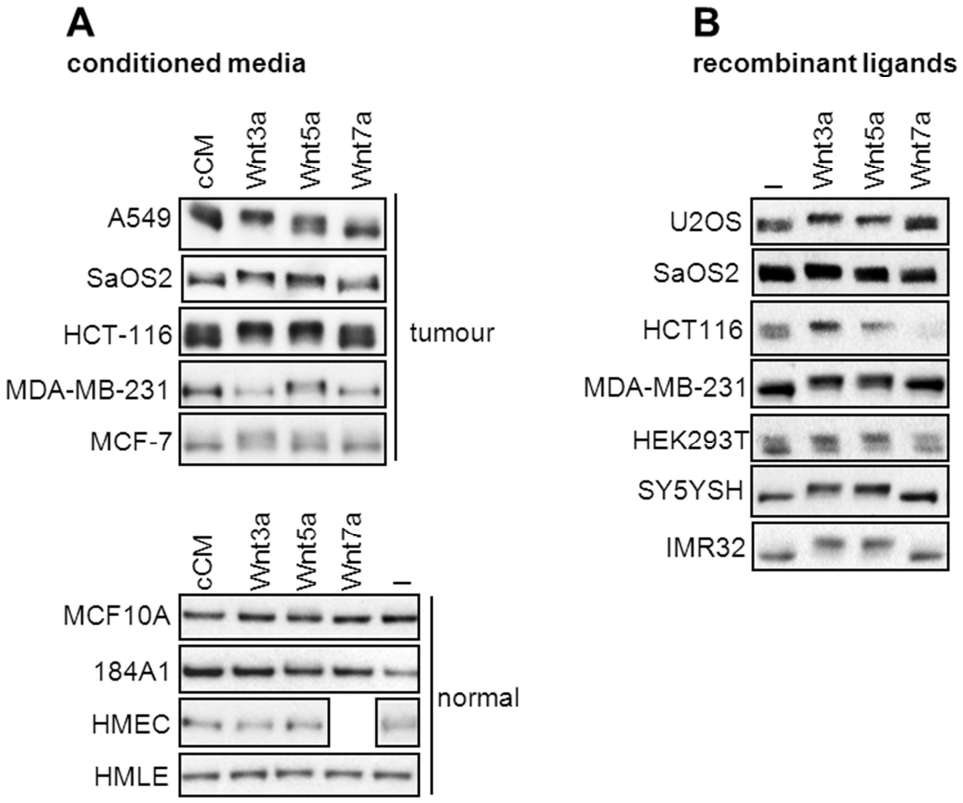

Figure 4.8: WNT ligands differentially stimulate DVL2 phosphorylation in tumour derived cell lines but have no effect on non-transformed breast cell lines. Assessment of WNT responsiveness in a panel of cell lines. Cancerous and non-tumourigenic cell lines were chosen in order to test responsiveness to selected WNT ligands and analysed by DVL2 migration on SDS-polyacrylamide gels. **(A)** A549 (lung adenocarcinoma), SaOS2 (osteosarcoma), HCT-116 (colorectal carcinoma), MCF7 and MDA-MB-231 (breast adenocarcinoma), or non-tumorigenic mammary epithelia cell lines MCF10A, 184A1, HMEC and HMLE cell lines (normal) were grown to confluency, regular growth media aspirated and replaced with either control (cCM), indicated WNT ligand conditioned media or left untreated (-). Cells were lysed after 2 hours and analysed by Western blot for endogenous DVL2 protein shift. **(B)** U2OS (osteosarcoma), HEK293T (embryonic kidney), SY5YSH and IMR32 (human neuroblastoma) cell lines were grown to confluency and treated with recombinant WNT3a (225 ng/mL), WNT5a (225 ng/mL) or WNT7a (550 ng/mL) for 2h or left untreated (-). Cells were harvested and probed for endogenous DVL2. Recombinant and conditioned media induced a similar DVL2 phosphorylation shift when compared to SaOS2, HCT-116 or MDA-MB-231 cells under both stimulation conditions (A versus B).

Assessment of WNT ligand responsiveness of neuroblastoma derived SY5YSH or IMR32 cells displayed a strong DVL2 phosphorylation shift if stimulated with recombinant WNT3a or WNT5a, but not if treated with WNT7a ligand. Notably, HEK293T cells have a high basal level of phosphorylated DVL2 (Figure 4.8B).

4.4.3 Frizzled expression alters sensitivity towards WNT ligands

WNT ligands bind to Frizzled receptors in order to activate downstream signalling cascades. Since there are 19 different WNT ligands and 10 Frizzled receptors known in mice and humans, it is difficult to find appropriate ligand-receptor combinations for *in vitro* studies. Therefore, we first tested if overexpression of Frizzled receptors could stimulate WNT signalling or enable cells to selectively respond to specific WNT ligands. Based on reports in the literature of their involvement in non-canonical WNT signalling (Wang et al. 2006; De Marco et al. 2012), FZD5 and FZD6 were cloned and stably expressed by lentiviral transduction in HMEC and MDA-MB-231 cells. For technical reasons, a human FZD5 construct could not be cloned. Alignment of human FZD5 and mouse Frizzled5 (mFzd5) indicted a 97% amino acid identity and was therefore used as alternative in all corresponding experiments.

The effect of mFzd5/FZD6 expression in HMEC cells, which were unresponsive to various WNT ligand conditioned media (Figure 4.8A lower part and Figure 4.9A) was assessed by DVL2 phosphorylation induced shift by immunoblotting.

Expression of either mFzd5 or FZD6 in HMEC cells resulted in a slight increase of endogenous DVL2 phosphorylation, compared to vector control cells (Figure 4.9A, lanes 5, 9 and 1, respectively). Interestingly, stimulation of mFzd5 cells with WNT3A or WNT5A CM resulted in a clear phospho-shift of DVL2. In contrast, expression of FZD6 did not lead to increased responsiveness towards WNT3a or WNT5a CM, indicating that FZD6 might not bind to WNT3a or WNT5a ligands in this cellular context (Figure 4.9A).

In contrast, expression of mFzd5 or FZD6 in MDA-MB-231 cells led to a higher constitutive level of hyper-phosphorylated DVL2, which could not be further stimulated by WNT3A or WNT5A ligands (Figure 4.9B).

Therefore, overexpression of the mFzd5 receptor provides a great tool to stimulate formerly unresponsive HMEC cells with WNT ligands and this system is utilised in a later section.

Because R-RAS GTPases could possibly function downstream of only selected Frizzled receptors that could be expressed or function together with co-receptors in a cell-type specific manner, we decided to employ and expand the aforementioned overexpression approach of Frizzled receptors. Out of the eight remaining Frizzled members available in a mammalian system, we achieved to clone further FZD2, FZD3, FZD4, and FZD7 by PCR from cDNA clones ordered from Open Biosystems.

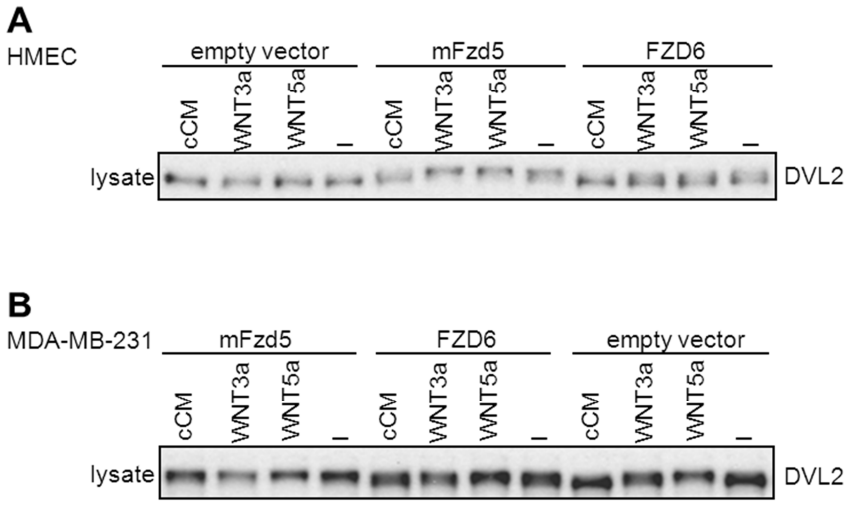

Figure 4.9: HMECs expressing mFzd5 gain responsiveness to WNT3a and WNT5a ligands. Human mammary epithelial cells (HMECs) or breast adenocarcinoma cells (MDA-MB-231) were transduced using lentiviral vectors encoding mFrizzled5 (mFzd5-mouse homologue), Frizzled6 (FZD6) or empty vector, serving as control. **(A)** Responsiveness of HMECs towards WNT ligand 3a and 5a was assessed by DVL2 gel shift post treatment with either control conditioned media (cCM), indicated WNT ligand conditioned media or cells that were left untreated in regular growth conditions (-). Treatment of indicated CMs were performed for 2h. Activation by WNT ligands was assessed by immunoblotting for phosphorylation shift of endogenous DVL2 protein. **(B)** Assessment of MDA-MB-231 cells response to WNT5a or WNT3a conditioned media in stably expressing mFzd5 or FZD6 cells. Treatments were carried out as described for A.

Expression of mFzd5 but not FZD6 in HMEC resulted in a slight increase of basal DVL2 phosphorylation, which was further stimulated by WNT3a and WNT5a, indicating that mFzd5 exogenous expression renders these cells responsive to these ligands. On the other hand, expression of both mFzd5 and FZD6 in MDA-MB-231 cells, resulted in a maximal DVL2 shift that cannot be further stimulated

(Figure 4.9). This suggests that expression of at least a subset of Frizzled receptors is able to induce a DVL2 phosphorylation-shift, suggesting that expression of Frizzled receptors alone can stimulate downstream signalling without WNT ligand interaction. Therefore, taking advantage of this tool, we used the cloned panel of Frizzled receptors including FZD2 and mFzd5, which have been suggested to carry a role in non-canonical signalling (Sato et al. 2010; Yu et al. 2012). Further, this also enabled us to test which Frizzled and/or ROR2 combination could be useful for further experiments.

4.4.4 FZDs and ROR2 specifically stimulate VANGL1 interaction with DVL2

Expression of ROR2 in HEK293T cells strongly increases the amount of DVL2 co-immunoprecipitating with VANGL1 compared to the empty vector sample (Figure 4.10A). Similarly, expression of mFZD5, FZD2, FZD4 and FZD7, but not FZD3 or FZD6, stimulated VANGL1 binding to DVL2, suggesting that the ability to modulate the VANGL1-DVL interaction is specific to a subset of FZD receptors (Figure 4.10A). Furthermore, under conditions where exogenous expression of ROR2 or Frizzled proteins stimulates the interaction of VANGL1 with DVL2, no effect was seen on the interaction of VANGL1 with SCRIB, CASK or DLG1 suggesting that a subset of Frizzled receptors or ROR2 specifically modulate VANGL1 interaction with DVL proteins (Figure 4.10A).

It has been reported that ROR2 can act as co-receptor for Frizzled proteins prompting the question if ROR2 and Frizzled could further stimulate the VANGL1-DVL2 interaction in a cooperative manner (Nishita et al. 2010b) (Figure 4.10B). Hence, the same panel of Frizzled proteins were co-expressed in the presence or absence of ROR2 and flag-VANGL1 constructs, and lysates were flag-VANGL1 immunoprecipitated and probed for endogenous DVL2 interaction (Figure 4.10C).

Co-expression of ROR2 and FZD2 is able to further increase bound DVL2 to VANGL1 compared to ROR2 expression alone. This cooperative effect was also observed with a FZD4, mFzd5 or FZD7 - ROR2 combination, but not in case of Frizzled receptor FZD3 or FZD6 (Figure 4.10C).

Furthermore, two mutations of mFzd5 were included in this study, the point mutation W530G and a deletion of the C-terminal PDZ binding motif (Figure 4.10C).

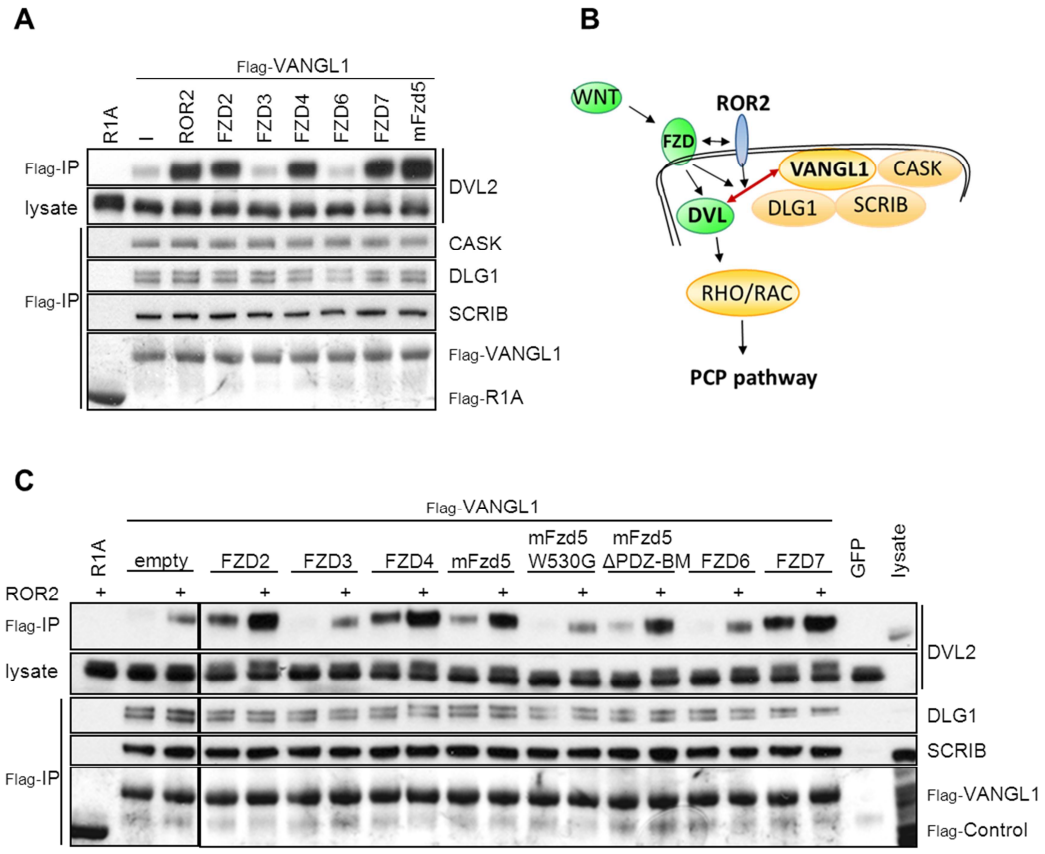

Figure 4.10: FZDs and ROR2 cooperate to stimulate VANGL1-DVL2 interaction. **(A)** HEK293T cells were transfected with indicated Frizzled (FZD) and ROR2 constructs together with flag-VANGL1. Two days after transfection, cells were harvested, immunoprecipitated using flag-sepharose beads and probed for endogenous DVL2, CASK, DLG1 and SCRIB. **(B)** Schematic of WNT signalling pathway (incomplete illustration), focused on the PCP branch and our observations of ROR2 and FZD overexpression. **(C)** Co-expression of Frizzled and ROR2 cooperate to increase VANGL1-interacton with DVL2 but not other proteins. Flag-VANGL1 was co-transfected with a panel of FZD receptors in the absence or presence (+) of ROR2. Cell harvest, immunoprecipitation and detection was carried out as in A. Flag-tagged Protein Kinase A regulatory subunit type 1 (R1A) and GFP constructs were expressed for assessment of background binding. Note that part C of this figure represents one gel, where the vertical line indicates omitted lanes.

The highly conserved cytosolic KTxxxW motif of Frizzled receptors interacts with the PDZ domain of DVL proteins and is required for Frizzled-induced translocation of DVL to the plasma membrane and DVL phosphorylation (Umbhauer et al. 2000). The mFzd5 W530G point mutation localises to this motif and has been demonstrated to disrupt the receptors' association with DVL (Umbhauer et al. 2000; Cong et al. 2004b). Deletion of the PDZ binding motif in

mFzd5 (mFzd5-ΔPDZ-BM) interferes with binding of a multitude of PDZ domain containing proteins, but not with DVL, as binding takes place through the conserved KTxxxW motif (Figure 1.24) (Cong et al. 2004b; Wawrzak et al. 2009).

mFZD5-W530G expression fails to enhance VANGL1-DVL2 interaction, whereas deletion of the ΔPDZ-BM has no effect on the ability of mFzd5 to stimulate the VANGL1-DVL2 interaction. This suggests that DVL2 needs to be recruited to the membrane through its interaction with mFzd5 in order to interact with VANGL1 with increased affinity (Figure 4.10C).

It has been reported that DVL2 is phosphorylated at the plasma membrane through CK1 (Cong et al. 2004a; Bryja et al. 2007a; Bryja et al. 2007b). Consistently, endogenous DVL2 immunoprecipitations with VANGL1 displayed a slower migration pattern compared to the detected respective lysate band, suggesting that VANGL1 might bind to a specific modified moiety of DVL2 (Figure 4.10C, compare immunoprecipitated lanes to lysate lane on the right hand side).

4.4.5 TC21 can co-immunoprecipitate with ROR2 or VANGL1 in the presence of specific FZD receptors

As demonstrated earlier, a subset of Frizzled proteins are able to stimulate DVL2 binding to VANGL1, which is further enhanced if ROR2 is co-expressed (Figure 4.10C). This suggests that this particular subset of Frizzled proteins and/or ROR2 is able to activate intracellular non-canonical WNT signalling pathways.

Based on our results we hypothesised that certain WNT ligands, acting through their specific receptors, may activate R-RAS GTPases in the context of non-canonical WNT signalling. The ROR2 tyrosine kinase in particular is an attractive candidate to mediate this effect, as other RTKs are well known to activate RAS family GTPases.

In order to study a possible association of R-RAS GTPases with ROR2, a C-terminal flag-tagged ROR2 construct was transiently expressed in HEK293T cells in combination with FZD proteins and the associations of endogenous TC21 was analysed by western blot after flag immunoprecipitations. Remarkably, co-expression of FZD2 stimulates the interaction of ROR2 with endogenous TC21, whereas FZD4 and mFZD5 only have a marginal effect. Therefore, in some contexts, ROR2 can associate with TC21 (Figure 4.11).

For technical reasons it was difficult to perform similar experiments in other cell types such as HMEC and MDA-MB-231 cells as transient transfection efficiency is much lower than HEK293T cells. Unfortunately, the cell lines stably expressing ROR2 were generated using an untagged ROR2 construct therefore precluding analogous HEK293T cell experiments.

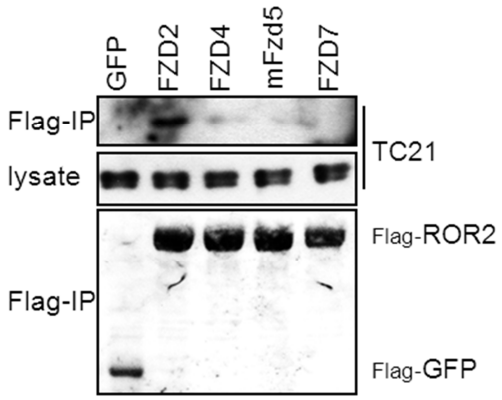

Figure 4.11: ROR2 co-expressed with FZD2 is able to immunoprecipitate endogenous TC21 in HEK293T cells. C-terminal flag-tagged ROR2 was co-transfected with FZD2, FZD4, mFzd5 and FZD7, and cell lysates were harvested 48 h post transfection and purified using flag-sepharose beads. Immunoprecipitates were probed for endogenous TC21 protein using a specific antibody.

However, in MDA-MB-231 and HMEC cells stably expressing flag-tagged VANGL1 in the context of mFZD5 stable exogenous expression, VANGL1 is able to co-purify endogenous TC21 but not R-RAS (Figure 4.12). Since VANGL1 is a strict GTP dependent interactor of R-RAS GTPases, this suggests that mFzd5 expression in this cellular context may be able to selectively activate TC21.

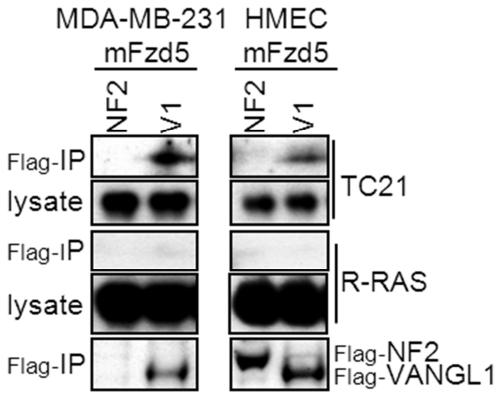

Figure 4.12: VANGL1 is able to immunoprecipitate endogenous TC21 but not R-RAS in two breast cell lines stably expressing mFzd5. MDA-MB-231 or HMEC cells were transduced using a lentiviral mFzd5 construct and selected, before a second round of lentiviral infection with either flag-VANGL1 (V1) or Flag-NF2 was performed. Cells were lysed and flag immunoprecipitates probed for endogenous R-RAS or TC21.

4.4.6 WNT5a modulates VANGL1 interaction with DVL but not SCRIB, CASK or DLG1

HMEC cells stably expressing mFzd5 become responsive to WNT5a as shown in Figure 4.9A, and provided an attractive cellular system to study the effects of WNT5a stimulation. Therefore, tagged VANGL1 or VANGL2 were stably introduced into HMEC mFzd5 cells and the resulting cell lines were subsequently used to study the effect of WNT5a on VANGL interactions with endogenous proteins (Figure 4.13).

Treatment of HMEC mFzd5 cells with WNT5a conditioned media for two hours stimulated binding of VANGL1 to DVL1 and DVL3 compared to control media. Similar results could be observed for VANGL2, albeit levels are much lower (Figure 4.13). Probing for additional endogenous VANGL1/2 interactors, using the same immunoprecipitated samples, did not display WNT5a mediated modulation effects for CASK or DLG1 proteins (Figure 4.13).

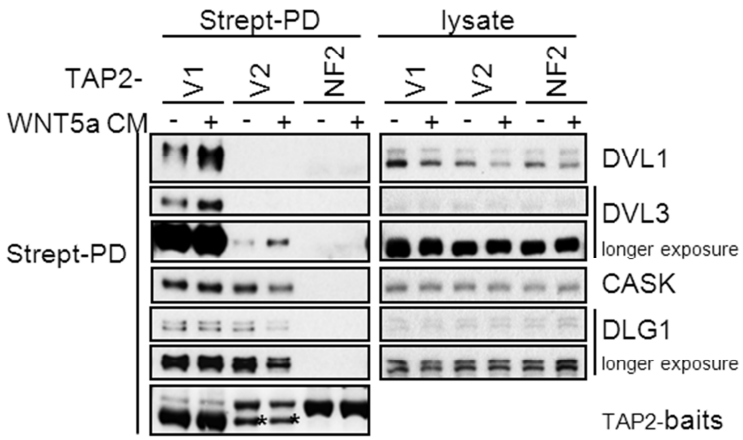

Figure 4.13: WNT5a stimulation of HMEC mFzd5 cells leads to modulation of VANGL1 and VANGL2 interaction with DVL proteins, but not CASK or DLG1. HMEC cells stably expressing mFzd5 were transduced by lentivirus encoding TAP2-VANGL1 (V1), TAP2-VANGL2 (V2) or TAP2-NF2 as a control. Cells were grown to confluence and stimulated for 2h with WNT5a conditioned media (+) or control conditioned media (-), lysed and subjected to streptavidin pull downs. Binding of endogenous VANGL interaction partners was analysed by western blot using indicated antibodies. The TAP2 tag harbours a calmodulin binding peptide (CBP) and a streptavidine binding peptide (SBP) tag. VANGL2 baits after pull down are indicated by asteriks.

As observed before, CASK and DLG1 bind to both VANGL proteins with a preference for VANGL2, considering lower bait levels for VANGL2. In contrast, DVL proteins appear to selectively interact with VANGL1 as compared to VANGL2 (Figure 4.2B and Figure 4.13).

It is known that ligand induced RTK stimulation results in rapid intracellular downstream signalling within seconds to minutes after ligand binding. Therefore, it was interesting to determine in what time frame this occurs. Thus, I transiently expressed TAP6-tagged VANGL1 into HEK293T cells and treated cells with WNT5a conditioned media in a time course dependent manner over four hours (Figure 4.14).

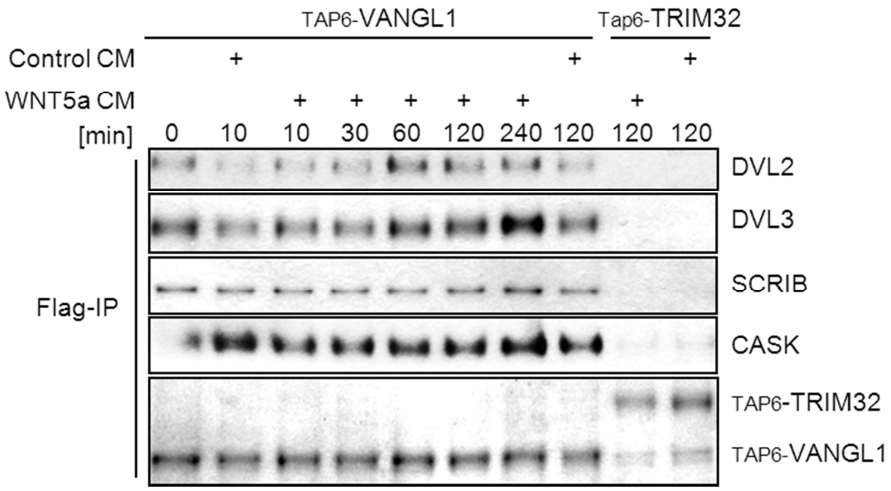

Figure 4.14: WNT5a treatment enhances binding of DVL2 and DVL3 to VANGL1 after 60 min, but SCRIB or CASK interactors are not modulated. HEK293T cells were transfected with TAP6-VANGL1 or TAP6-control constructs. 44h after transfection, cells were stimulated either with conditioned WNT5a media (WNT5a CM) at time points indicated above or control media (Control CM) for either 10 or 120 min. Cells were harvested and immunoprecipitated using flag-sepharose beads and probed with the indicated endogenous antibodies. TAP6 contains a large tag cassette, harbouring an EE-tag, streptavidine binding peptide, histidine-tag and flag-tags.

Stimulation of HEK293T cells with WNT5a conditioned media resulted in enhanced DVL2 and DVL1 binding to VANGL1, which could be observed from 60 min after WNT5a application and was sustained for four hours (Figure 4.14). In contrast, no effect on the interaction with SCRIB or CASK is seen at any time point. Therefore, WNT5a selectively stimulates the association of VANGL1 with DVL2, which takes place in a delayed manner.

Taken together, these experiments showed that either WNT5a or Frizzled proteins in cooperation with ROR2 are able to stimulate VANGL1-DVL2 interaction. This binding is specific for DVL proteins, preferentially interacting with VANGL1 over VANGL2.

WNT5a mediated enhanced VANGL1-DVL2 stimulation displays a response delay of approximately 60 min that may correlate with potential phosphorylation of DVL2, possibly by CK1. Furthermore, TC21 could be immunoprecipitated with ROR2 if FZD2 was co-expressed. Likewise, TC21 could be detected to precipitate with VANGL1 if mFzd5 was stably expressed, indicating that TC21 could be activated but in a Frizzled and ROR2 context dependent manner.

4.5 Proteomic analysis of VANGL1 interaction and their modulation by R-RAS, mFZD5 and ROR2

ROR2 and mFzd5 both selectively stimulate VANGL1 interactions with DVL proteins and when expressed together cooperate to enhance this interaction (Figure 4.10). On the other hand, active R-RAS appears to negatively regulate several VANGL1 interactions (Figure 4.6).

In order to shed more light on the VANGL1 interactome and study in an unbiased approach how these interactions may be modulated *in vivo*, an additional proteomic study was performed. TAP-tagged VANGL1 was affinity purified from cells co-expressing either mFzd5, ROR2, a combination thereof, activated (L87) or dominant negative R-RAS (N43) (Figure 4.15).

This purification achieved high sensitivity and in addition to proteins already detected in previous TAPs, multiple potential novel VANGL1 interactors were identified. Furthermore, many of the proteins appear to be modulated in one or more of the conditions tested, as suggested by this semi-quantitative approach. A summary of the mass spectrometry results is shown in Figure 4.15.

Co-expression of R-RAS L87 led to the identification by mass spectrometry of fewer peptides for DVL proteins, SCRIB and DLG1, suggesting that active R-RAS decreases these interactions with VANGL1. This is consistent with the results obtained previously (Figure 4.6) and independently suggests that R-RAS, upon activation, is likely to modulate the VANGL1 interactome.

The mass spectrometry results for this experiment were received towards the end of my PhD study and therefore I was unable to perform further validation and follow up experiments.

A

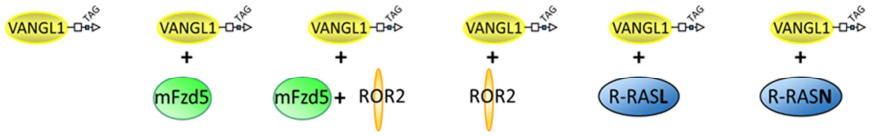

B

	empty		mFZD5		mFZD5+ROR2		ROR2		RRAS L87		RRAS N43	
ID	Unique peptides	Peptide Count	Unique peptides	Peptide Count	Unique peptides	Peptide Count	Unique peptides	Peptide Count	Unique peptides	Peptide Count	Unique peptides	Peptide Count
VANGL1	57	611	61	613	57	518	59	596	54	549	59	609
VANGL2	14	19	15	17	14	19	16	19	8	11	12	16
NKTR	13	16	6	9	7	12	4	4			1	2
DVL2	12	13	7	7	8	9	14	16	3	3	7	9
DVL3	4	4			5	6	4	4			2	2
SCRIB	11	11	7	8	11	11	10	10			12	12
ZC3H18	12	16	9	11	6	10	4	5	1	1		
UBE2O	7	7	7	10	7	7	5	5			5	5
PTPN3	3	3	4	4	11	11	6	6			9	9
DLG1	2	2	2	2	2	2	6	6	1	1	5	5
SDCBP	4	4	3	3	4	4					1	1
FGF2	4	5	4	4	3	3	4	5			2	3
KIAA0913	3	3	1	1	3	3	2	3			1	2
CSNK2A2	8	8	8	9	9	10	12	12	2	2	7	7
SYNJ2BP	8	15	7	10	11	15	6	13	8	15	6	13
C17orf62	6	11	4	7	6	11	7	13	7	12	6	13
SYNGR2	4	4	3	3	6	8	4	4	5	5	4	4
SYNGR3	1	1	1	1			1	1	1	1	1	1
DCAF5	10	10	6	6	7	9	9	11	2	2	6	8
TFRC					3	3			2	2		
EIF3M			4	4	3	3						
PRICKLE3			3	3	4	5					3	3
LIN7C			2	2	2	2	2	2				
CANX					3	3						
EVI5L					2	2						
RNF213					4	4						
ABTB2					2	2	1	1				
PTPN9			1	3			1	5				
ASPM	2	2	3	3	9	9	3	3	3	3	7	7
RAB10					2	3			3	4		
RAB8A					1	2			1	2	2	
RAB13							1	1	1	1	3	
RAB21									1	1		

Figure 4.15: Summary of proteins identified by mass spectrometry in VANGL1 affinity purifications. (A) VANGL1 protein complexes were isolated from HEK293T cells expressing a flag-tagged VANGL1 construct alone or in combination with mFzd5, ROR2, a combination of mFzd5 and ROR2, activated R-RAS L87 (R-RasL) or the dominant negative analogue R-RAS N43 (R-RasN) as indicated in the illustration. **(B)** Cell lysates were harvested 48h after transfection and subjected to flag-sepharose purification. Purified proteins were precipitated and separated by SDS-PAGE, gel bands cut, trypsinised and analysed by tandem mass spectrometry. Proteins are ranked by percent coverage and are colored blue or coral if the interaction with VANGL1 was decreased or increased respectively, as judged by the number of peptides identified.

4.6 Discussion

4.6.1 Identification and characterisation of VANGL1 interacting proteins

Using TAP as an unbiased proteomic approach, multiple VANGL1 interacting proteins have been identified. Some of them such as DVL/Dsh, Scrib and Dlg1 had been previously identified as interacting with the VANGL homologue in *Drosophila*, and confirm a role in cell polarity (Park and Moon 2002; Lee et al. 2003; Bellaiche et al. 2004; Courbard et al. 2009).

VANGL1 contains a PDZ domain binding motif at its C-terminus, allowing interaction with PDZ domain containing proteins. PDZ proteins are found from bacteria to vertebrates and are involved in various cellular functions including cell polarity (Ponting 1997; Subbaiah et al. 2011). Notably, a subset of PDZ containing VANGL1 interactors, such as SCRIB, DLG1 and CASK, which are involved in polarity and migration have been demonstrated to be strictly dependent on the VANGL1-PDZ binding motif for interaction.

SCRIB, one of the identified VANGL1 interactors, has been reported in mammalian cells to associate with the PIX/GIT complex that regulates RAC/CDC42 and ARF GTPases (Audebert et al. 2004; Frank and Hansen 2008) and be involved in cell polarity during epithelial migration through regulation of RHO GTPase recruitment to the leading edge (Dow et al. 2007), and to mediate neural migration and CE (Qin et al. 2005a; Wada et al. 2005). SCRIB's role in PCP is further strengthened by the observation that SCRIB mouse mutants have neural tube closure defects (Murdoch et al. 2003) and display hair cell polarity defects in the inner ear (Montcouquiol et al. 2003).

SCRIB is a cytosolic protein but can localise to the plasma membrane, e.g. sites of cell-cell contact in epithelial cells and leading edge in migrating cells, nonetheless how SCRIB translocation to the membrane is regulated is not clear. A recent report has confirmed that SCRIB forms a complex with VANGL1 and further showed that VANGL1 co-localises with SCRIB at the leading edge in migrating cells (Anastas et al. 2011). Therefore, SCRIB interaction with VANGL1, a membrane protein, may provide a mechanism to recruit SCRIB to the membrane. Based on our results, we propose that activation of R-RAS GTPases by extracellular signals would recruit the VANGL1-SCRIB complex to sites of activation at specialised membrane micro-domains and thus be a mechanism to spatially coordinate polarity with other signalling pathways regulated by R-RAS GTPases.

DLG1 has been shown to interact with VANGL1 in a PDZ binding motif dependent manner. Consistent with earlier findings in *Drosohila*, Dlg and Stbm form a complex which is important in plasma membrane formation (Lee et al. 2003). It has been suggested that this complex is required to recruit membrane-associated proteins and lipids from internal membranes to sites of new plasma membrane formation (Lee et al. 2003).

Notably, DLG1 null mice suffer from skeletal defects throughout the embryo and characteristic PCP defects such as open neural tube and misorientation of cochlear hair cell stereociliary bundles, consistent with the possibility that at least in mice, DLG1 functions with SCRIB in planar cell polarity (Rivera et al. 2013).

CASK, has been originally described to be localised at neuronal synapses (Zheng et al. 2011) and to act as a scaffold for proteins involved in synaptic junctions, vesicle exocytosis and ion channel trafficking (Butz et al. 1998; Setou et al. 2000; Leonoudakis et al. 2004). In addition, CASK has been shown to interact with DLG1 (Sabio et al. 2005) and it remains to be determined if both bind independently to VANGL1 or as a complex with each other.

Unlike other PDZ domain containing proteins like SCRIB, DLG1 and CASK, VANGL1 interaction with DVL2 is not exclusively mediated through the VANGL1 PDZ-binding motif, which is in line with observations of the corresponding *Drosophila* homologue (Park and Moon 2002). Remarkably, R-RAS interaction is specific to VANGL1 and so is the DVL interaction. Furthermore, R-RAS and DVL3 binding to VANGL1 is disrupted by the point mutant D259E, suggesting that both proteins could be competing for the same binding site. This is further confirmed by observations that active R-RAS modulates VANGL1-DVL binding, suggesting a common 'axis' of VANGL1 function.

DVL proteins are major signalling hubs, which interact with a multitude of proteins, and mediate canonical and non-canonical WNT signalling (Boutros and Mlodzik 1999; Gao and Chen 2010; Wynshaw-Boris 2012) for example WNT5a induced migration through activation of RHOA or RAC in breast cancer cells (Zhu et al. 2012; Zhu et al. 2013). Therefore, VANGL1 interaction with all three DVL proteins highlights its potential role in downstream WNT signal mediation, which will be discussed later in this section.

The observation that VANGL1 is able to bind to the intracellular domain of CELSR2 but not CELSR1, which was also the only CELSR isoform detected in

VANGL1-TAP experiments, indicates C-terminus mediated functional differences across CELSR proteins. Indeed, CELSR1 is a major player in PCP and is directly linked to cochlear stereocilia bundle misorientation and neural tube closure defects (Curtin et al. 2003; Devenport and Fuchs 2008; Robinson et al. 2011). CELSR2 and CELSR3 regulate less direct PCP processes such as ciliogenesis, maintenance of dendrites, neuronal migration and axon guidance (Shima et al. 2002; Tissir et al. 2005; Wada et al. 2006; Shima et al. 2007; Tissir et al. 2010), implicating that VANGL1 might not be directly involved in neurulation and related CE (Torban et al. 2008; Antic et al. 2010; Song et al. 2010), but rather in PCP directed processes associated with ciliogenesis and neuronal development and maintenance.

Due to technical reasons, interaction studies were carried out with the intracellular C-terminus of CELSR1 and CELSR2, but it cannot be ruled out that the large ectodomain could be also involved in VANGL1 binding in order to establish PCP across a plane of cells. It has been reported for the *Drosophila* homologue of VANGL proteins, that stbm interacts with Frizzled proteins through their respective extracellular domains (Wu and Mlodzik 2008) and thus VANGL1-CELSR protein interaction could also take place through extracellular domain association.

The adhesion-GPCR Latrophilin 2 (LPHN2) was detected in the VANGL1-TAP co-expressing activated R-RAS (Figure 4.1C). This is particular interesting since LPHN2 is structurally related to CELSR proteins and plays an essential role in the establishment of tissue polarity and thus could constitute a novel PCP pathway mediator (Langenhan et al. 2009). Unfortunately, several cloning attempts of the full length protein or truncation constructs led to very low or undetectable expression levels, rendering interaction approaches unfruitful.

Multiple other novel VANGL1 - interacting proteins identified by TAP are involved in vesicle trafficking and imply additional roles for VANGL1 function. For example YIF1B interacts with the transport GTPases Ypt1p, Ypt31p and Sec4p, and loss of YIF1 function results in a block of ER-to-Golgi protein transport and vesicle accumulation, suggesting a vital role in vesicle docking and fusion (Matern et al. 2000). YIF1B localisation to ER or Golgi membranes suggests that VANGL1 might interact with YIF1B on its way to the plasma membrane as shown for Sec24B and VANGL2 transport (Wendeler et al. 2007; Merte et al. 2011; Wansleeben et al. 2011). Another possibility is that VANGL1 could also localise to ER or Golgi membranes, consistent with what is observed for its subcellular localisation pattern (see section 5.4.

NDFIP1 is found associated with the exosome, Golgi or vesicles. It forms an adaptor for Nedd4 family proteins in order to bind respective target proteins for subsequent ubiquitination. Interestingly, NEDDL family proteins have been demonstrated to negatively regulate WNT signalling through DVL2 ubiquitination (Wei et al. 2012; Ding et al. 2013). Thus, it would be interesting to determine if VANGL1 could act as a modulator for DVL2 directed ubiquitination or might be a target of NEDD4 proteins itself.

Endocytosis of WNT ligand-receptor complexes is required for WNT signalling regulation, which is achieved through clathrin or caveolin mediated endocytosis (Sorkin and von Zastrow 2009; Traub 2009; Lajoie and Nabi 2010). Clathrin mediated internalisation has been shown to regulate β-catenin dependent (Chen et al. 2001; Blitzer and Nusse 2006) and independent pathways (Sato et al. 2010; Ohkawara et al. 2011; Sakane et al. 2012). SYNJ2BP a putative growth-promoting factor implicated in breast tumourigenesis and tumour development (Li et al. 2009c), has been shown to be involved in clathrin-mediated endocytosis and recycling (Matsuzaki et al. 2002; Verstreken et al. 2003). VANGL1 interaction with SYNJ2BP, which takes place in a PDZ-dependent manner, suggests a regulatory function for VANGL1 in vesicle formation and trafficking.

RAB proteins control intracellular trafficking (Chua et al. 2010; Mizuno-Yamasaki et al. 2012) and have been shown to regulate WNT signalling (Lee et al. 2007; Zhu et al. 2013). VANGL1 interacts specifically with the catalytic subunit of a RAB3GAP (RAB3GAP1), whereas DVL2 binds to the non-catalytic subunit (RAB3GAP2). Therefore it could be speculated that RAB3GAP2 could be associated with DVL2 and upon binding of VANGL1 to DVL2, the catalytic subunit is recruited to this complex and is now able to modulate RAB protein activity in vesicle trafficking processes.

C17ORF62 still remains mostly uncharacterised besides the MS detected C-terminal serine/tyrosine phosphorylation cluster (at position S159, S168, S170, S173, S175, S176, S178, S187 and Y124) (http://www.phosphosite.org). Initial co-localisation studies found C17ORF62 associated with the Golgi complex and it has been proposed that this protein could be involved in cell death induction (Deng et al. 2011). However, more studies will be required to shed light into C17ORF62 function and its relation to VANGL1.

Sec24b has been recently demonstrated to be part of the endoplasmic reticulum to Golgi complex transport machinery, important for VANGL2 transport and thus

has not been the focus of our efforts (Merte et al. 2011; Wansleeben et al. 2011).

Although some of the proteins tested in this study bind to both VANGL1 and VANGL2 isoforms (SCRIB, DLG1, CASK, YIF1B, CELSR2-C2, RAP3GAP1, SYNTENIN-1), others show differential interaction affinities and suggest different functions for the two VANGL proteins (DVL proteins, SYNJ2BP).

4.6.2 Frizzled expression leads to enhanced VANGL1-DVL2 interaction

Immunoprecipitation experiments demonstrated that TC21 associates with ROR2 in HEK293T cells co-expressing FZD2. Furthermore, employing HMEC and MDA-MB-231 cells expressing stably mFzd5, endogenous TC21 but not R-RAS co-immunoprecipitates with VANGL1. This is despite the fact that R-RAS protein levels could be readily detected in lysates of these cells. This suggests that depending on the receptor/co-receptor combination and cellular context different R-RAS GTPases might be differentially regulated.

R-RAS and TC21 seem to be regulated by the same set of GEFs and GAPs, whereas M-RAS showed a regulation pattern more similar to classical RAS proteins (Ohba et al. 2000), suggesting that R-RAS and TC21 are likely to be co-activated by extracellular signals. On the other hand, TC21 has been shown to constitutively interact with the T-cell and B-cell antigen receptors (TCR and BCR, respectively) through a direct interaction with a signalling sequence known as the Immunoreceptor Tyrosine-based Activation Motif or ITAM, which is present in the CD3 signalling subunits of the TCR and the Igα and β subunits of the BCR (Alarcon and Martinez-Martin 2011). This fact highlights the possibility that there might be additional mechanisms to achieve differential regulation of R-RAS GTPases. It remains to be determined if in some contexts TC21 may interact directly with ROR2 by a mechanism similar to that shown for the ITAMs of the TCR and BCR.

However, in section 6.2 I will provide evidence that R-RAS can also be activated by ROR2 expression or WNT5a stimulation, and thus both TC21 and R-RAS GTPases seem to play a role in non-canonical WNT signalling.

DVL proteins interact with a multitude of proteins and serve as a key signalling components downstream of Frizzled receptors, regulating WNT/β-catenin and non-canonical WNT pathways (Wharton 2003; Wallingford and Habas 2005; Malbon and Wang 2006; Gao and Chen 2010). WNT-induced activation of DVL is

visible as a electrophoretic mobility shift of all three DVL isoforms (Gonzalez-Sancho et al. 2004; Bryja et al. 2007a; Bryja et al. 2007b), and leads to activation of DVL downstream of WNT ligands (Peters et al. 1999; Sakanaka et al. 1999; Kishida et al. 2001; Cong et al. 2004a; Foldynova-Trantirkova et al. 2010).

VANGL1 interacts with all three DVL proteins. Deletion of the PDZ-binding motif in VANGL1 displays only a modest effect on interaction reduction, whereas the point mutation D259E, which is found in patients with NTDs, disrupts the interaction. This suggests that a membrane proximal region, which remains to be further mapped, interacts with a region of DVL other than the PDZ.

Interestingly the interaction of VANGL1 with DVLs, but not with other proteins such as SCRIB, DLG1 and CASK (whose interactions are mediated via PDZ domains) is stimulated by a subset of FZD proteins as well as by ROR2. The underlying mechanism by which FZD and/or ROR2 achieve this stimulatory effect remains to be identified but may be related to DVL hyper-phosphorylation (see below).

Based on the observation that the DVL bound to VANGL1 appears to migrate more slowly and that WNT stimulation of the DVL-VANGL1 interaction follows a delayed time course that correlates with DVL phosphorylation, it is tempting to speculate that the interaction of DVL with VANGL1 is stimulated by DVL phosphorylation. Therefore, DVL phosphorylation (by casein kinase or other kinases) may be at least part of the mechanism regulating this interaction. Future experiments should address this possibility.

ROR2 contains WNT-binding domains in its extracellular region and could therefore bind WNTs directly (Green et al. 2008; Angers and Moon 2009). Further, ROR2 could also function as a co-receptor operating in combination with FZDs. It has been proposed that one mechanism by which WNTs can trigger canonical versus non-canonical signalling is through a differential use of co-receptors in combination with FZD receptors (Sato et al. 2010; Niehrs 2012).

Genetic interactions between ROR2 and WNT5a were suggested by observations that mice with inactivation of the gene encoding Ror2 showed striking similarities to $Wnt5a^{-/-}$ mice, including perinatal lethality, dwarfism, facial abnormalities, and limb shortening (Green et al. 2008). Of note, $Ror2^{-/-}$ embryos also exhibited defects in the orientation of the sensory hair cells in the inner ear, a hallmark of WNT planar polarity pathway aberrations observed in $Wnt5a^{-/-}$, $Fzd3^{-/-}$, and

Fzd6$^{-/-}$ mice (Wang et al. 2006; Qian et al. 2007; Yamamoto et al. 2008). In addition, ROR2 was shown to be involved in the effects of WNT5a in some cellular and developmental processes, such as polarised cell migration and convergent extension movements (He et al. 2008; Nomachi et al. 2008; Enomoto et al. 2009; Laird et al. 2011).

FZDs recruit DVL to the plasma membrane by a still poorly understood mechanism. FZD proteins contain a C-terminal PDZ binding motif required for recruitment of PDZ proteins (Wawrzak et al. 2009), as well as an additional KTxxxW motif which is required for DVL translocation to the membrane and subsequent phosphorylation (Rothbacher et al. 2000; Umbhauer et al. 2000; Axelrod 2001; Cong et al. 2004b). Our studies demonstrated that deletion of the PDZ binding motif of mFzd5 has no effect on the stimulated VANGL1-DVL2 binding, whereas a mutation in its KTxxxW motif (W530G) abolishes the enhanced interaction. Therefore, the ability of mFzd5 to stimulate the VANGL1-DVL2 interaction correlates with its ability to translocate to the membrane and phosphorylate DVL2 and further suggests that DVL translocation and phosphorylation could be one mechanism of recruitment of VANGL1 (and its associated interactome) to sites of activation by WNT ligands.

Of the tested panel of Frizzled receptors, FZD2, FZD4, mFzd5 and FZD7 stimulate the VANGL1-DVL2 interaction, whereas FZD3 and FZD6 did not display a detectable interaction enhancement. Interestingly, FZD3 and FZD6 form a distinct phylogenetic branch of Frizzled proteins (Huang and Klein 2004), and have been demonstrated to be required with VANGL2, CELSR1 and PRICKLE2 for inner ear stereociliary bundle orientation (Montcouquiol et al. 2006; Montcouquiol et al. 2008).

As mentioned earlier, DVL interacts preferentially with VANGL1 compared to VANGL2, and VANGL1 interacts with CELSR2 but not CELSR1. Taken together, these observations suggest the possibility that a subset of FZD receptors, possibly in combination with different CELSR co-receptors, may use different VANGL isoforms to regulate various aspects of non-canonical signalling.

Notably, VANGL2 has been reported to form a WNT5a dependent complex with ROR2, which leads to VANGL2 phosphorylation and PCP induced limb elongation (Gao et al. 2011). It remains to be established if VANGL1 can also associate with ROR2, although in a preliminary experiment I was able to detect endogenous VANGL1 co-immunoprecipitating with ROR2 only in the presence of mFzd5 (data not shown).

Several observations strongly suggest that DVL phosphorylation correlates with the ability to interact with VANGL1. First, DVL2 that co-immunoprecipitates with VANGL1 appears to migrate more slowly on SDS-PAGE compared to lysates. Second, WNT stimulation of the DVL2-VANGL1 interaction follows a delayed time course that correlates with DVL phosphorylation. Third, co-expression of certain Frizzled receptors with ROR2 cooperates to enhance the VANGL1-DVL interaction and this correlates with enhanced DVL phosphorylation shift. Therefore, DVL phosphorylation may be at least part of the mechanism regulating the interaction with VANGL1. Future experiments should further address this possibility.

DVL proteins display a variety of post translational modification sites (Wu et al. 2012) and are phosphorylated by at least three kinases CK1 (Klimowski et al. 2006; Bryja et al. 2007b; Corbit et al. 2008), CK2 (Wharton 2003) and PAR1 (Sun et al. 2001; Elbert et al. 2006), whereas protein phosphatase 2A (PP2A) has been shown to negatively regulate DVL activity (Yokoyama and Malbon 2007).

CK1δ/ε have been identified as the relevant kinases hyper-phosphorylating DVL in response to WNT5a, whereas WNT3a stimulation leads to β-catenin stabilisation which was not reliant on hyper-phosphorylated DVL2 (Bryja et al. 2007a; Bryja et al. 2007b). However, activation of DVL mediated β-catenin related downstream signalling appears in less than 10–15 min, whereas the earliest formation of hyper-phosphorylated DVL is detected after 30 min (Gonzalez-Sancho et al. 2004; Bryja et al. 2007b; Witte et al. 2010) and seems to be stable for at least 12 h (Bryja et al. 2007a). Additionaly, CK1 induced hyper-phosphorylation of DVL2 can result in the inactivation of β-catenin signalling (Bernatik et al. 2011).

The role of DVL phosphorylation in WNT signalling remains obscure. Based on these and our observations, a model emerges where DVL phosphorylation may be a mechanism for the separate temporal control of β-catenin dependent and independent WNT signalling. According to this model, the phosphorylation of DVL that occurs at later time points of WNT stimulation and that correlates with increased interaction with VANGL1, may shift WNT signalling from the β-catenin pathway to the PCP pathway.

Expression of active R-RAS leads to a modest decrease in the ability of VANGL1 to interact with DVL2, CASK, DLG1, and SCRIB. This has been seen in co-transfection-western blot experiments and was independently confirmed by mass spectrometry. The decreased binding of VANGL1 with DVL in the presence of R-

RAS is consistent with the observation that mutation D259E in VANGL1 disrupts the interaction with both R-RAS and DVL3. This suggests that both R-RAS and DVL bind to the same region of VANGL1 and may therefore compete for its interaction.

Furthermore, the proteomic study identified other proteins both negatively and positively modulated by R-RAS. While these additional results remain to be validated, our observations clearly suggest that R-RAS has the ability to regulate VANGL1 interaction with a subset of its partners.

We propose a model where upon activation by extracellular signals, R-RAS GTPases will recruit VANGL1 (and its associated proteins) to sites of activation. This will not only lead to the localisation of VANGL1 complexes at spatially distinct micro-domains at the plasma membrane but also to a selective 'rearrangement' of the interacting partners within the complex to give rise to VANGL1 complexes with specialised signalling properties.

The observation that WNT stimulation can lead to both the activation of R-RAS GTPases and its association with VANGL1 on one hand and to the association of VANGL1 with DVL on the other hand, with both interactions potentially being mutually exclusive may seem counter-intuitive. However, the spatial-temporal dynamics have to be considered. R-RAS proteins are activated within minutes of WNT stimulation; whereas the WNT induced increase in the interaction of VANGL1 with DVL is first detected after 60 minutes and therefore clearly displays a delayed response that may correlate with DVL phosphorylation. This will be more clearly outlined and discussed in a subsequent chapter (see section 6.2) and the final discussion (see section 8.1).

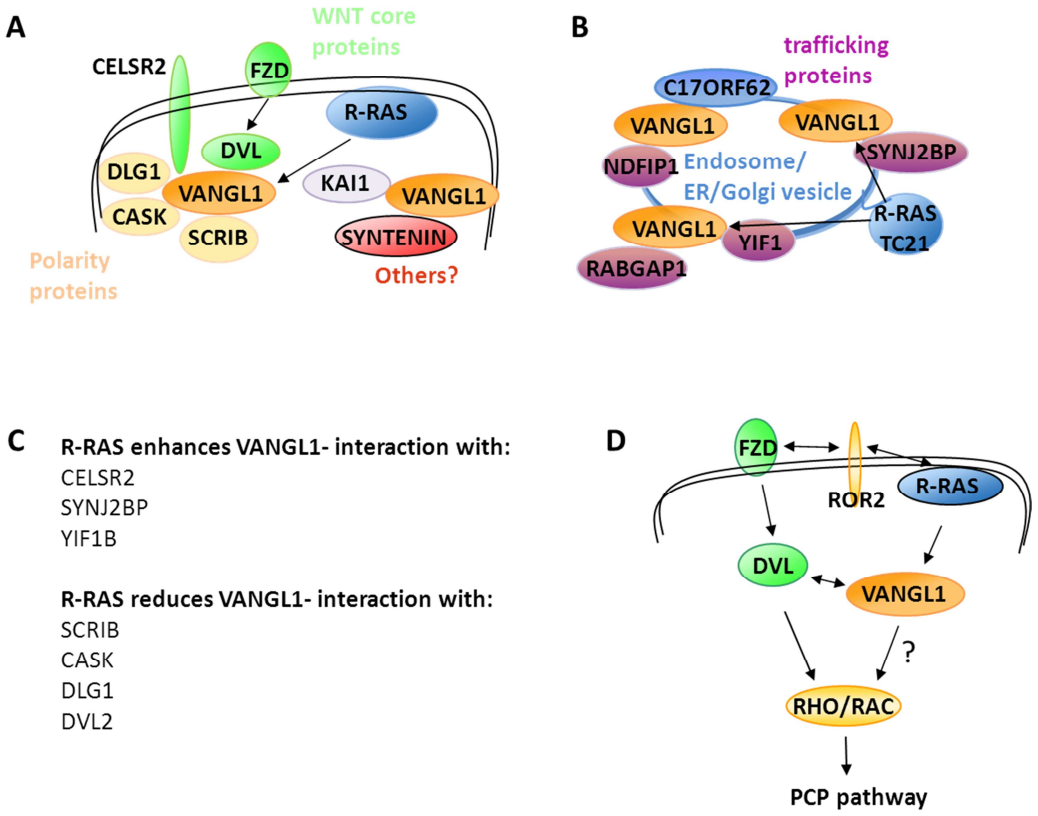

Figure 4.16: Overview of VANGL1 binding partners and R-RAS dependent modulation of respective interactions. (A) VANGL1 interacts through its PDZ motif with polarity proteins like DLG, CASK, SCRIB or the WNT core proteins DVL or CELSR2. In addition, further interaction studies showed that VANGL1 binds to the Tetraspanin KAI1 or the Syndecan-binding protein SYNTENIN. **(B)** Other novel VANGL1 interactors are implicated in vesicle trafficking such as YIF1 (ER-GOLGI transport), RAB3GAP (intracellular trafficking), SYNJ2BP (clathrin-mediated endocytosis) or endosome associated (NDFIP1). **(C)** Overview of R-RAS modulating effect on identified VANGL1 binding partners. **(D)** Biochemical studies presented that R-RAS subgroup members (at least TC21) are found associated with ROR2, suggesting that R-RAS GTPases act downstream of WNT inducing stimuli, leading to enhanced DVL-VANGL1 interaction and further to RHO GTPase modulation and PCP pathway activation.

CHAPTER 5

R-RAS GTPases inhibit VANGL1 mediated PRICKLE degradation

5 R-RAS GTPases inhibit VANGL1 induced PRICKLE degradation

5.1 VANGL1 interacts with PRICKLE1 and stimulates its destabilisation

Strabismus and Prickle have been shown to form a functional complex in *Drosophila* that is proximal to the distally localised Frizzled-Dishevelled complex, and this asymmetric distribution is required for tissue polarity patterning (Bastock et al. 2003; Jenny et al. 2003; Rawls and Wolff 2003).

Due to unavailability of commercial antibodies against human PRICKLE proteins at the time, human PRICKLE1 and PRICKLE2 were cloned by PCR. Vertebrate PRICKLE1 consists of an N-terminal Prickle, Espinas and Testin (PET) domain and three zinc binding LIN-11, Isl1 and MEC-3 (LIM) motifs. To test if these domains are required for VANGL1 binding and to map the interaction, two truncation constructs were further generated; PRICKLE1-N contains the PET and LIM domains, whereas the larger PRICKLE-C truncation construct contains the remaining part of the protein without any known domains (Figure 5.1A).

Initial interaction studies in HEK293T cells using co-transfection showed that human VANGL1 binding maps to the C-terminal region of PRICKLE1 (Figure 5.1B).

Both VANGL1 and VANGL2 are able to interact with PRICKLE1 (Figure 5.1C). In the course of these studies it became apparent that co-expression of VANGL proteins leads to a strong reduction of transfected PRICKLE1 protein levels on lysates. This effect is more prominent with VANGL1 but differences in the levels of expression achieved between the two VANGL proteins have to be taken into consideration (Figure 5.1C). Under conditions were PRICKLE1 is destabilised by VANGL proteins, simultaneous binding experiments for VANGL1 interacting proteins such as the PCP core protein DVL1 displayed the expected binding, but did not exhibit any modulation effect on PRICKLE1 protein levels, indicating that the decreased PRICKLE1 protein level is specific for VANGL co-expression (Figure 5.1C).

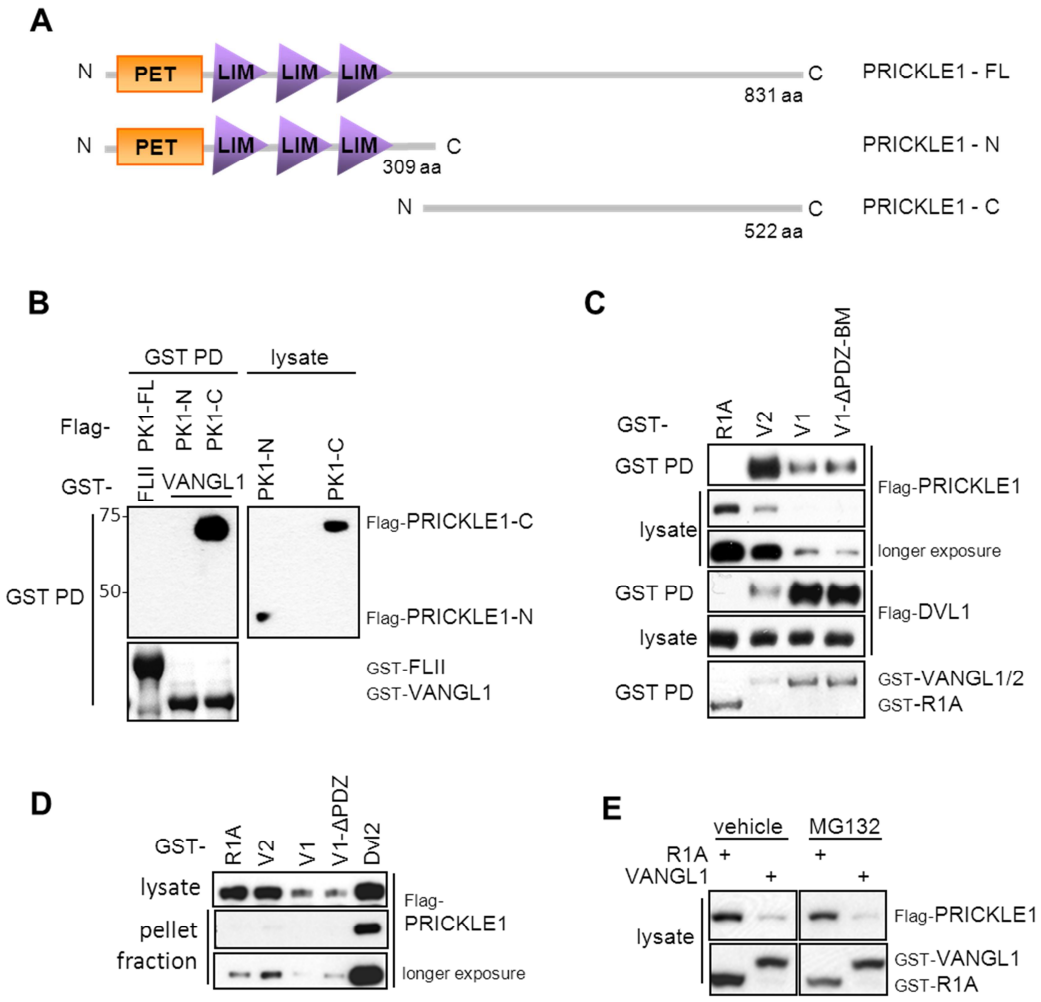

Figure 5.1: VANGL1 and VANGL2 interact with and destabilise PRICKLE1. **(A)** Diagram of PRICKLE1 structure and generated constructs. PRICKLE1 is an 831 amino acid (aa) protein, containing a N-terminal PET domain followed by three LIM zinc binding motives. FL-full length, PK-N or PK-C refer to respective N- or C-terminal truncations. **(B)** PRICKLE1 binds to VANGL1 through its C-terminus. GST-tagged VANGL1 or control expression plasmids (FLII) were co-transfected with flag-PRICKLE1 (PK1-FL), or respective N- (PK1-N) or C-terminal (PK1-C) truncations. GST-baits were purified with glutathione beads and flag-PRICKLE1 detected by western blotting using anti-flag antibodies. **(C)** PRICKLE1 binds to VANGL1 (V1) and VANGL2 (V2), independently of the PDZ-binding motif. Flag-PRICKLE1 levels (but not flag-DVL1) are reduced upon co-expression of VANGL1/2. GST-VANGL2 or GST-VANGL1 full length proteins, VANGL1-PDZ binding motif truncation mutant (ΔPDZ-BM), or R1A control protein were co-transfected with flag-PRICKLE1 into HEK293T cells. Proteins were purified and detected as described for B. **(D)** PRICKLE1 protein levels are negatively affected by VANGL1 in both soluble and insoluble lysate fractions. GST-tagged constructs as in C including GST-tagged DVL2 were co-transfected with flag-PRICKLE1 constructs in HEK293T cells and lysed two days later. Expression levels of flag-PRICKLE1 were assessed in the soluble fraction (lysate) and the

guanidinium chloride resolubilised pellet (pellet fraction). Total levels of ectopic PRICKLE1 were detected with flag-antibodies. **(E)** Treatment with proteasome inhibitor MG132 does not counteract VANGL1-induced PRICKLE1 degradation. HEK293T cells were double transfected with GST-VANGL1 or control protein (R1A) and flag-PRICKLE1 as indicated. 42h after transfection, cells were either treated with the proteasomal inhibitor MG132 or vehicle control (DMSO) at a concentration of 10 μM for 4.5 h. Cells were subsequently lysed and analysed by western blot, probing with either flag- or GST-antibodies.

In order to confirm that PRICKLE1 protein levels are reduced and not associated with insoluble structures during the generation of lysates, insoluble lysate fractions were subjected to guanidinium chloride solubilisation and analysed by western blot for PRICKLE1 levels. Indeed, the pellet fraction showed the same relative reduced amounts of flag-PRICKLE1 in VANGL1 expressing cells, as observed for the soluble fractions (Figure 5.1D, compare lysates versus reconstituted lysates).

These results suggest that VANGL proteins interact strongly with PRICKLE1, since even under conditions where expression levels were hardly detectable in whole cell lysates, PRICKLE1 could be readily detected in flag-VANGL co-immunoprecipitates. Furthermore, these observations also imply that VANGL proteins may lead to the degradation of PRICKLE1 proteins.

To test this possibility, similar experiments were performed in the presence of the proteasomal inhibitor MG132 which is known to interfere with the 26S proteasome function and consequently would allow stabilisation of proteins otherwise targeted for proteasomal degradation (Tawa et al. 1997). Treatment of cells with 10μM MG132 did not prevent reduced levels of PRICKLE1 induced upon VANGL1 expression (Figure 5.1E). Additional experiments employing higher concentrations of MG132 or longer treatment periods also failed to yield increased PRICKLE1 levels (data not shown). This suggests that VANGL1 may decrease PRICKLE1 levels by a mechanism other than ubiquitin mediated proteasome degradation.

5.2 R-RAS GTPases inhibit VANGL1 induced PRICKLE1/2 protein destabilisation

I next addressed if R-RAS interaction with VANGL1 is able to regulate VANGL1 binding to PRICKLE1 and/or regulate PRICKLE1 protein stability. Activated R-RAS L87 does not alter interaction between VANGL1 and PRICKLE1 taking VANGL1 bait levels in consideration (Figure 5.2A), but significantly prevents the destabilisation effect of PRICKLE1 protein exerted by VANGL1 (Figure 5.2B).

I also compared the effect of other R-RAS subgroup members on the degradation of both PRICKLE1 and PRICKLE2. Expression of all three R-RAS members can partially rescue the VANGL1 induced PRICKLE1/2 destabilisation in a manner dependent on an intact effector domain (Figure 5.2C). This effect is specific to R-RAS subgroup GTPases as the RAP2 member of the RAS family did not display a stabilisation effect. Surprisingly, the ability to prevent PRICKLE1/2 destabilisation does not correlate with the binding affinity to VANGL1; TC21 and M-RAS do not show as strong an interaction with VANGL1 as observed for R-RAS (Figure 3.5) but can however prevent the VANGL1 induced PRICKLE1/2 destabilisation more efficiently than R-RAS (Figure 5.2C).

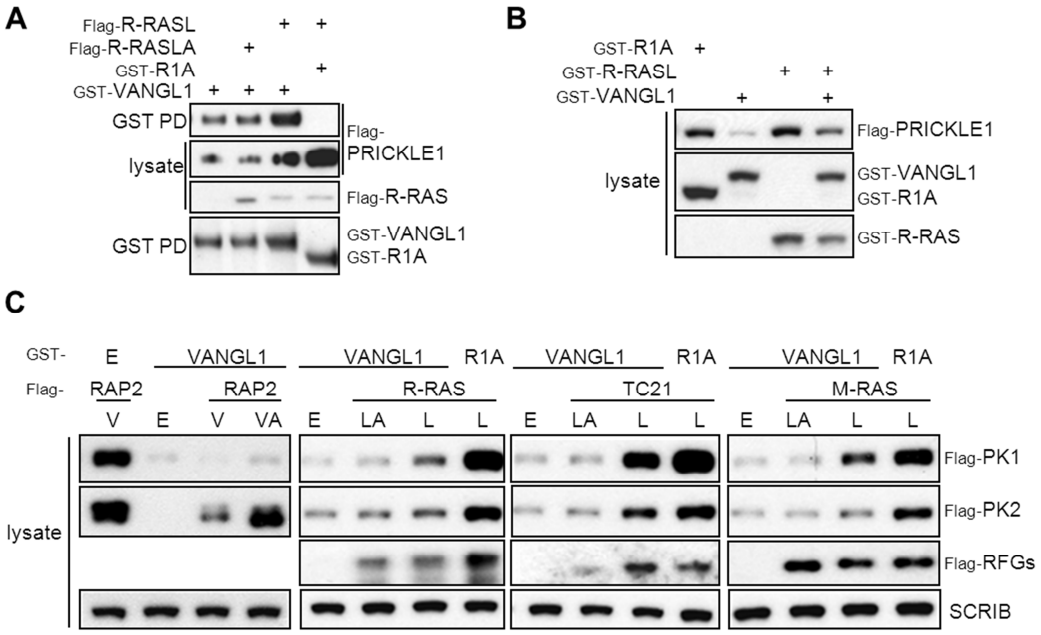

Figure 5.2: R-RAS subgroup GTPases are able to rescue VANGL1 induced destabilisation of PRICKLE1 and PRICKLE2. (A) Activated R-RAS L87 does not modulate VANGL1 and PRICKLE1 interaction. HEK293T cells were triple transfected with GST-VANGL1 or control contstruct (R1A), GST-R-RAS active mutant L87 (R-RASL) or respective defective mutant L87 64A (R-RASLA) and flag-PRICKLE1, as indicated. 48h after transfection, cells were lysed and GST proteins precipitated using glutathione sepharose beads. Interactions were analysed by western blot, probing with flag- or GST-antibodies. **(B)** R-RAS L87 partially rescues VANGL1-induced PRICKLE1 decay. HEK293T cells were triple transfected with GST-VANGL1 or control (R1A) contstructs, GST-R-RAS active mutant L87 (R-RASL) and flag-PRICKLE1, as outlined. 48h after transfection, cells were lysed and analysed by western blot, probing with flag- or GST-antibodies. **(C)** R-RAS subgroup members TC21 and M-Ras (but not the closely related GTPase RAP2) rescue VANGL1-induced PRICKLE1/2 destabilisation more efficiently than R-RAS. HEK293T cells were triple transfected with GST-VANGL1 or R1A, flag-PRICKLE1 or flag-PRICKLE2, and flag-RAP2 or flag-R-RAS subgroup GTPases using respective consitutive active (V or L), effector domain mutant (VA or LA) or empty vector (E). 48h post transfection, cells were subjected to lysis and analysed by western blot by probing with a flag antibody. Blotting of endogenous SCRIB protein served as loading control. Employed GTPase mutations are as followed: Rap2 V (V12), Rap2 VA (V12 A38), R-RAS L (L87), R-RAS LA (L87 A64), TC21 L (L71), TC21 LA (L71 A48), M-Ras (L81), M-Ras LA (L81 A48). RFG – Ras Family GTPases.

5.3 VANGL1 localises to vesicle like structures upon autophagy induction

Inhibition of proteasome-mediated degradation utilising the MG132 inhibitor could not prevent the decrease in PRICKLE1/2 levels, observed upon VANGL1 co-expression, suggesting alternative mechanisms of degradation.

Another mechanism for the degradation and recycling of cellular components is lysosome-mediated autophagy. Autophagy is a highly conserved self-digestion process to promote cell survival in response to nutrient starvation and other metabolic stresses (He and Klionsky 2009). During the autophagic process, portions of cytoplasm are first surrounded by a single-membrane structure and these autophagic vacuoles or autophagosomes then fuse with pre-existing lysosomes to form autolysosomes. Autophagic dysfunction is associated with cancer, neurodegeneration, microbial infection and ageing (Kundu and Thompson 2008).

Consistent with a role of autophagy in the PCP pathway, DVL2 has been reported to be regulated through autophagy mediated degradation (Gao et al. 2010). Therefore, experiments were conducted in order to test if VANGL1 expression leads to PRICKLE1 protein destabilisation through the lysosome mediated pathway.

Expression of YFP-VANGL1 or YFP-PRICKLE1 fusion proteins in HMEC cells allows monitoring their respective subcellular localisation in presence or absence of autophagy stimulants. In untreated cells, YFP-VANGL1 displays diverse localisation patterns with staining of various subcellular compartments including plasma membrane, vesicle-like structures and perinuclear rings (Figure 5.3A and B, Figure 5.4D).

Notably, YFP-PRICKLE1 displays similar membrane (Figure 5.4A) and vesicle-like structures (Figure 5.3C and D, Figure 5.4A-C), suggesting that VANGL1 and PRICKLE1 localise to overlapping compartments such as vesicle-like structures, indicative of potential autophagosomes.

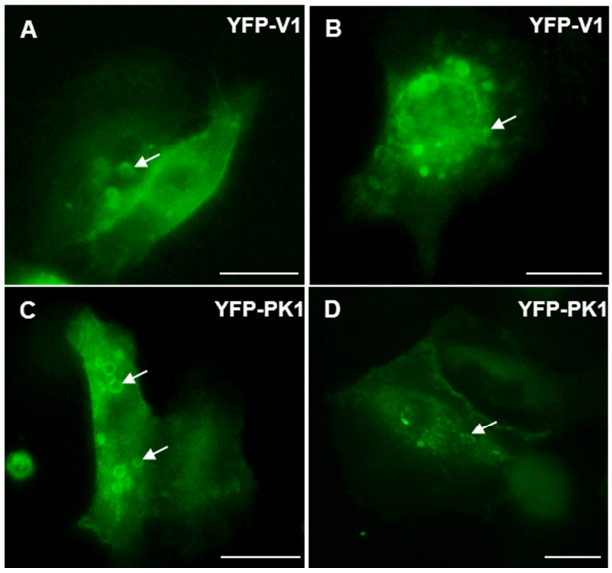

Figure 5.3: VANGL1 and PRICKLE1 localise to ring-like structures suggestive of autophagosomes. HMEC stably expressing YFP-VANGL1 (V1) or YFP-PRICKLE1 (PK1) constructs, were seeded in six well plates and used for live cell imaging purposes. Cells were maintained in full growth media and images represent a snap shot of an acquired video using a Zeiss CellObserver life cell imaging microscope at 40x magnification, scale bar represents 20 µm. Selected ring-like structures are indicated with arrows.

Further studies of YFP-VANGL1 and YFP-PRICKLE1 cellular localisation at higher resolution confirmed life cell imaging results. Ectopic expression of YFP-VANGL1 displayed dot-like structures and perinuclear-ring staining (Figure 5.4D, arrows). Similarly, YFP-PRICKLE1 expression exhibited membrane localisation (Figure 5.4A) or vesicle/dot-like staining (Figure 5.4B and C), suggesting that a subset of YFP-PRICKLE1 expressing cells are able to form vesicle-like structures, whereas others display a more diffuse localisation pattern (Figure 5.4A-C).

In order to assess if VANGL1 and/or PRICKLE proteins localise to autophagosomes, cells were treated with Chloroquine (CQ). CQ is a weak base that accumulates in acidic vesicles, leading to an increase pH and thus causes lysosomal dysfunction (Fedorko 1967). This in turn leads to a blockage of autophagosome fusion with lysosomes and therefore prevents cargo degradation, resulting in an accumulation of autophagosomes which appear as characteristic dot like structures (Figure 5.5).

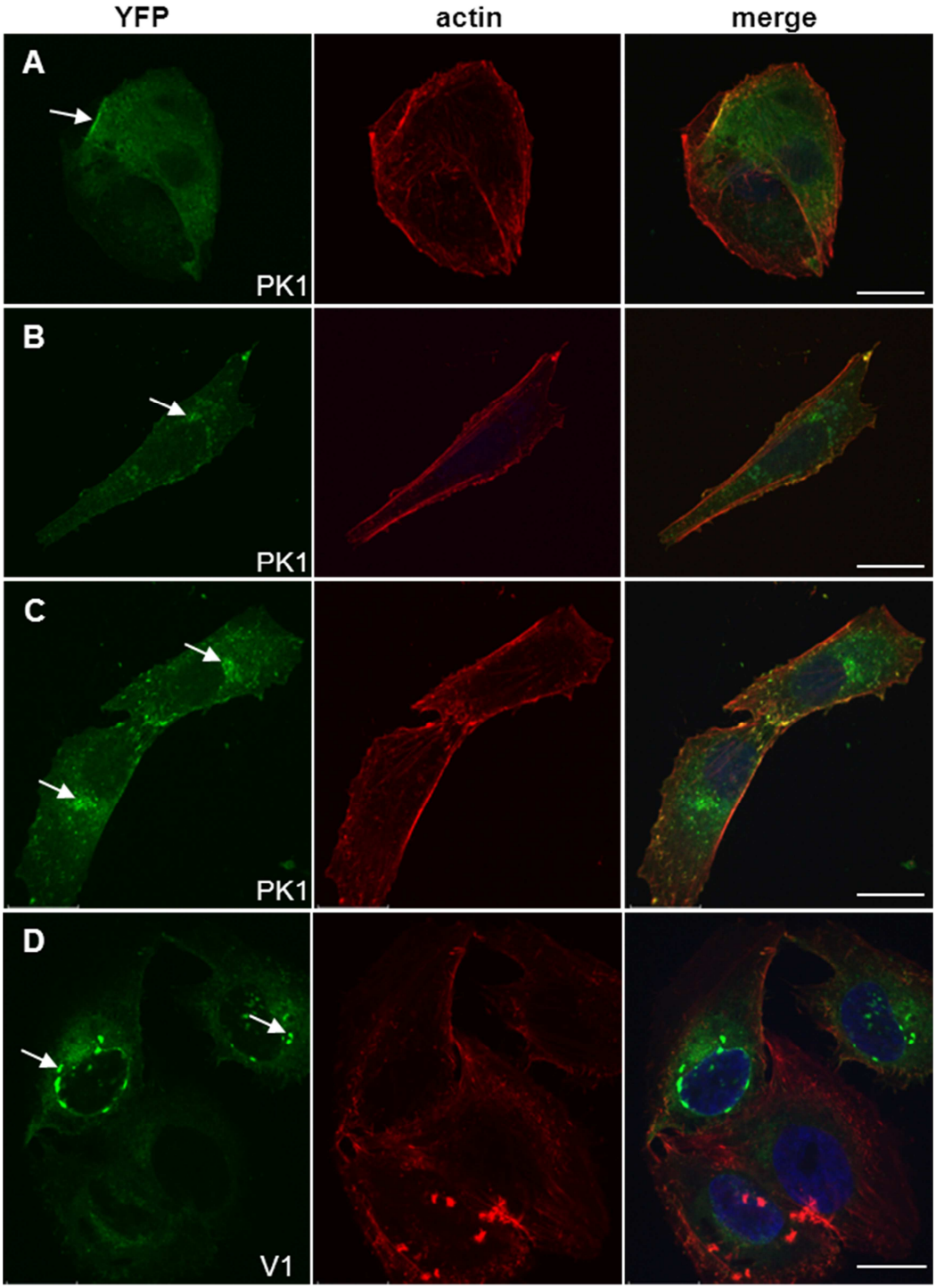

Figure 5.4: YFP-PRICKLE1 and YFP-VANGL1 exhibit similar subcellular localisation. SaOS2 cells were stably transduced with YFP-PRICKLE1 (PK1) or YFP-VANGL1 (V1) constructs, and seeded on coverslips and stained for F-actin (red) or the cell nucleus (blue). Images were aquired using a spinning disc confocal microscope and a cross section is displayed. YFP-PRICKLE1 displays membrane and vesicle-like structures similar to YFP-VANGL1 stainings. Bar represents 19 µm.

Figure 5.5: Treatment with Chloroquine (CQ) causes acumulation of VANGL1 and VANGL2 but not PRICKLE1 or DVL2 in autophagosome-like structures. HMEC cells stably expressing YFP-VANGL1 (V1), YFP-VANGL2 (V2), YFP-PRICKLE1 (PK1) or YFP-DVL2 were treated with 25 μM CQ or DMSO vehicle control for 4h. Cells were fixed, counterstained with Hoechst to stain nuclei (blue) and imaged at 20x magnification. Bar represents 40 μm. YFP - Yellow fluorescent protein.

DVL2 has been reported to be regulated both through proteasomal (Wei et al. 2012) and autophagy processes (Gao et al. 2010), and therefore was included as a control (Figure 5.5 lowest panel). YFP-DVL2 resulted in a cytoplasmic or punctuate staining, which has been previously reported (Schwarz-Romond et al. 2005), and this localisation pattern was not changed upon CQ treatment (Figure 5.5).

In contrast, CQ treatment resulted in a strong accumulation of both YFP-VANGL1 and YFP-VANGL2 in dot-like structures that might represent autophagosomes. Surprisingly however, YFP-PRICKLE1 localisation did not change upon CQ treatment (Figure 5.5).

In summary, YFP-VANGL1/2 but not PRICKLE1, DVL2 or SCRIB (data not shown) accumulate in endodome-like structures upon CQ treatment suggesting that VANGL proteins may be degraded through the lysosome-autophagy route.

In order to test if this possibility, the autophagosome marker microtubule-associated protein 1 light chain 3 (LC3) was chosen for detection of endogenous LC3B either for co-localisation studies with VANGL1/PRICKLE1 upon autophagy induction, or as read out to monitor autophagy-induced LC3B lipidation assessed by western blot, since the amount of phosphatidylethanolamine modified LC3 correlates well with the number of formed autophagosomes and therefore serves as a good indicator of autophagosome formation (Kabeya et al. 2000). The latter approach was further combined with other autophagy inhibiting drugs such as Bafilomycin (Yamamoto et al. 1998; Sarkar et al. 2007) or 3-Methyladenine (Seglen and Gordon 1982; Wu et al. 2010).

Because the PRICKLE1 degradation experiments were not entirely conclusive and critically were relying on exogenously expressed transfected protein, it was decided to put PRICKLE1 studies on hold, until we could detect the endogenous protein and validate the observed effects with the overexpressed tagged protein on endogenous PRICKLE1.

In order to generate an antibody against PRICKLE1, fragments of different lengths of PRICKLE1 N- and C-terminal regions were cloned into bacterial expression vectors. An N-terminal fragment, resulting in highest expression of recombinant protein, was purified and shipped to Thermo Scientific for rabbit immunisation. To our great disappointment, after arrival of the generated antibody and several company-caused delays, the provided anti-sera failed to recognise any specific protein bands on lysates and failed to immunoprecipitate exogenous flag-PRICKLE1 (data not shown). This setback, in combination with my focus on other areas of the project and time constrain issues meant that no further work was carried out in this area. Future studies should help elucidate the mechanism of VANGL-mediated degradation of PRICKLE1 as well as the potential role of VANGL proteins in autophagy.

5.4 VANGL1 subcellular localisation studies

R-RAS GTPases have been reported to be membrane associated and to localise to various subcellular localisations such as plasma membrane, Golgi, ER and endosomes (Ohba et al. 2000; Takaya et al. 2007). VANGL1, being a tetraspanin protein has been reported to be mostly plasma membrane associated (Kalabis et al. 2006; Gravel et al. 2010; Anastas et al. 2011; Iliescu et al. 2011).

In order to study the intracellular localisation of VANGL1 and assess the possibility that its localisation might be regulated by interaction with R-RAS GTPases, ROR2 or WNT ligands, YFP fusion proteins of R-RAS GTPases and VANGL proteins were ectopically expressed in multiple cell types and its localisation studied in both live and fixed cells.

During the course of localisation studies using stably expression of YFP-fusion proteins it became apparent that VANGL1 displays very diverse localisation in different cell types (Figure 5.4D, Figure 5.6A-D and Figure 5.6).

In HMLE mammary epithelial cells, YFP-VANGL1 localises at the plasma membrane, at areas of cell-cell contact in some cells (Figure 5.6A), whereas in other cells it localised in vesicle/ring like structures as well as in an area surrounding the nucleus giving a characteristic perinuclear staining (see arrows in Figure 5.6 B,C and Figure 5.7A, F).

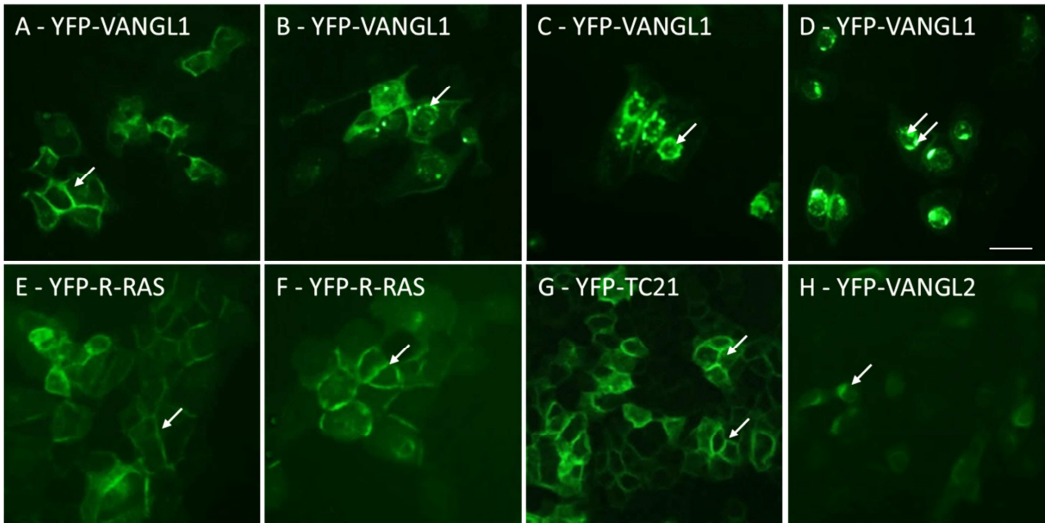

Figure 5.6: VANGL1 localises to various subcellular compartments, whereas R-RAS or TC21 are mostly found membrane associated. HMLE cells were stably transduced with lentivirus encoding YFP-VANGL1, YFP-VANGL2, YFP-R-RAS wt or YFP-TC21 wt fusion proteins as indicated. YFP - yellow fluorescent protein, wt - wild type. Pictures were aquired with a Zeiss fluorescent micoscope at 20x magnification amd the scale bar represents 50 µm.

VANGL1 observed subcellular localisations varied depending by cell type, cell density and also likely during phases of cell cycle as suggested by characteristic mitotic localisations observed in live cell imaging studies (data not shown). Even within a field of cells of the same cell type, different localisation patterns could often be detected. These observations strongly suggest that VANGL1 can localise to multiple membrane sub-compartments within the cell, and this localisation seems to be dynamically regulated.

In contrast, expression of YFP-VANGL2 in various cell lines exhibited a staining pattern (Figure 5.6 and Figure 5.7), which is clearly different from VANGL1, highlighting potential functional differences.

YFP-VANGL2 expression resulted in ER-type staining with little plasma membrane localisation in osteosarcoma (SaOS2) and thyroid-carcinoma cells (8505C) (Figure 5.7). Notably, breast cancer cells MDA-MB-231 displayed additionally vesicle-like structures, which seem to be similar for YFP-VANGL1 and YFP-VANGL2 expression (Figure 5.7H and I, respectively).

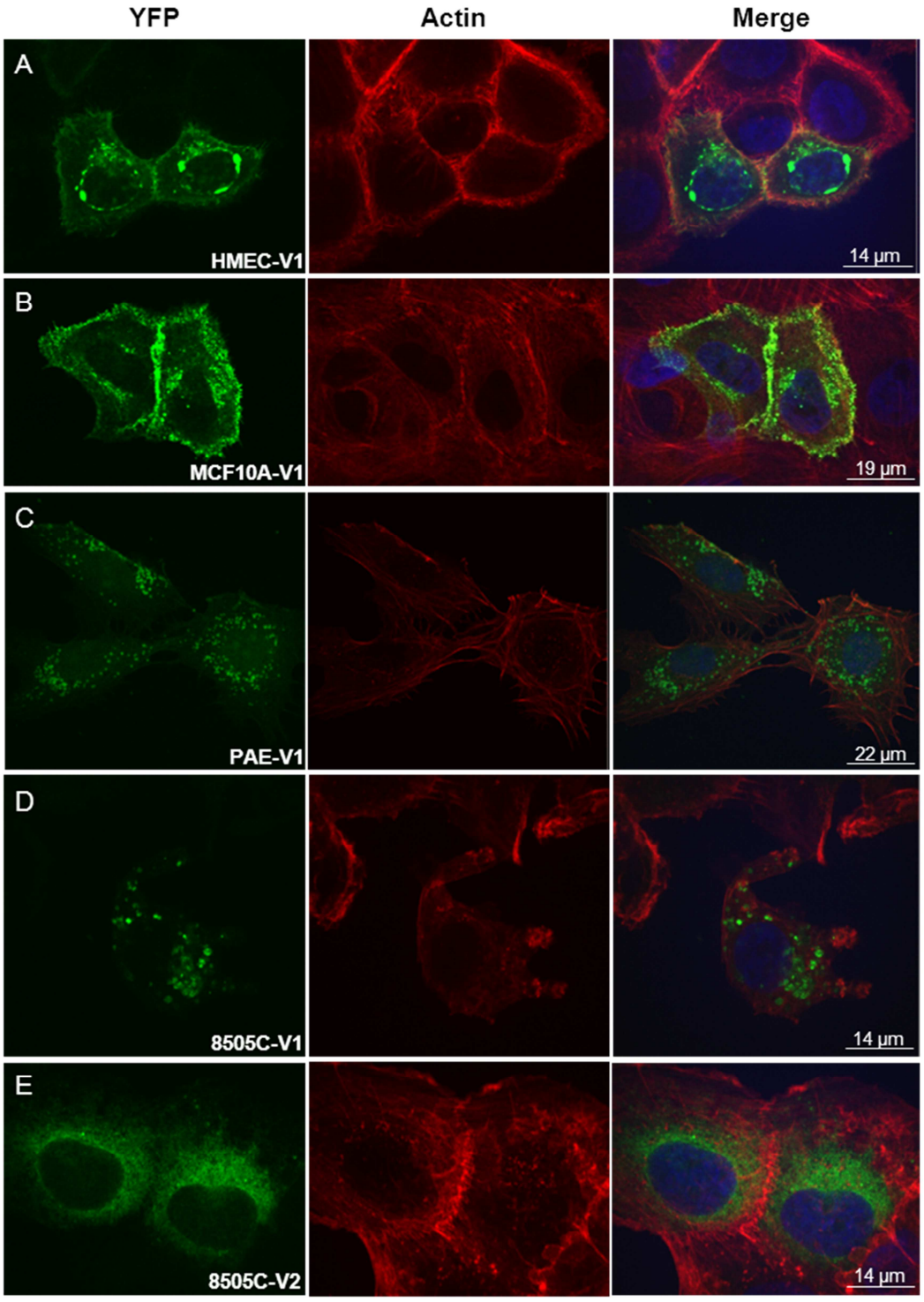
YFP
Actin
Merge
A
HMEC-V1
14 µm
B
MCF10A-V1
19 µm
C
PAE-V1
22 µm
D
8505C-V1
14 µm
E
8505C-V2
14 µm

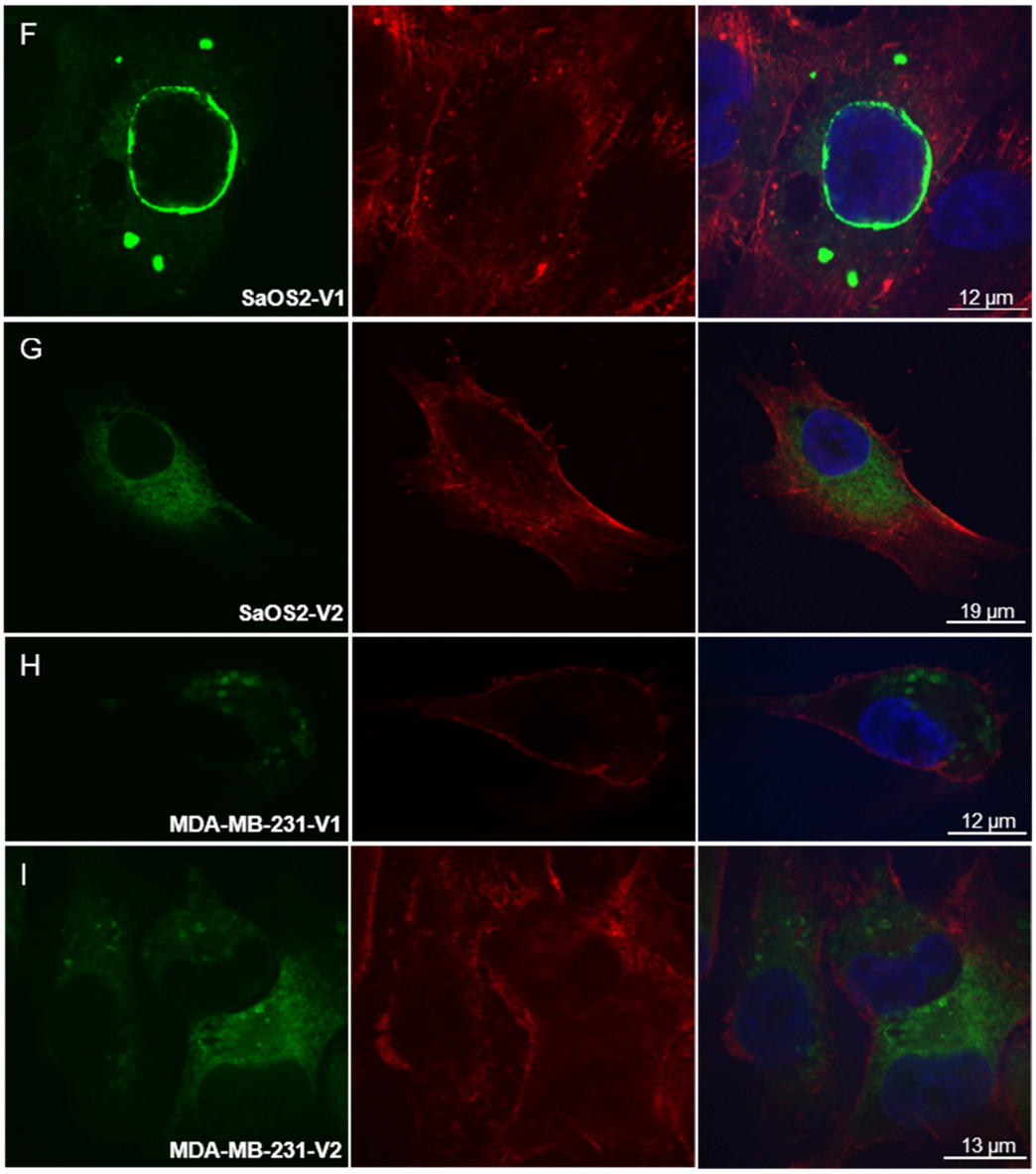

Figure 5.7: Localisation of YFP-VANGL1 and YFP-VANGL2 in different cell lines. Indicated cell lines stably transduced with either lentiviral or retroviral YFP-VANGL1 (V1) or YFP-VANGL2 (V2) constructs were seeded and fixed on coverslips for confocal image acquisition. Cells were counterstained for the cell nucleus (blue) and actin (red). Images were aquired using a spinning disc confocal microscope and a cross section displayed. YFP-VANGL1 displays various subcellular localisations such as membrane, vesicle-like structures or perinuclear staining. YFP-VANGL2 displays rather a Golgi/ER and vesicle staining pattern. Bar size in µm is indicated in individual images.

Initial localisation studies showed that YFP-R-RAS and TC21 are predominantly localised at the plasma membrane (Figure 5.6E-G). Therefore, CFP-R-RAS or CFP-TC21 constructs were generated in order to co-express them with YFP-VANGL1-R-RAS for co-localisation studies. However, because of technical issues, I was not able to get these experiments to work.

I also performed live cell imaging studies on YFP-VANGL1 cells to assess the dynamic localisation of the protein in different contexts (e.g. growing cells, cells stimulated with WNT ligands and cells induced to polarise in scratch/ wound closure assays). Mainly due to technical issues associated with lack of sensitivity I was unable to observe any changes on VANGL1 localisation in these studies. In order to increase sensitivity, time course treatments of WNT5a stimulation were performed in YFP-VANGL1 cells and fixed cells analysed by confocal microscopy. However, no effects were observed in preliminary experiments and studies on the regulation of VANGL1 localisation were stopped.

5.5 Discussion:

PRICKLE1 is involved in PCP signalling and has been demonstrated to be a key intermediate for gastrulation cell movements in *Drosophila* (Gubb et al. 1999) *Xenopus* (Takeuchi et al. 2003) and zebrafish (Carreira-Barbosa et al. 2003; Takeuchi et al. 2003; Veeman et al. 2003b). Furthermore, mouse knock out models of Prickle1 resulted in embryonic lethality (E5.5-6.5), whereas down regulation causes severe morphogenetic defects in CE. Prickle2 phenotypes appear less severe, while a combination of Prickle1 and Prickle2 loss demonstrates a synergetic effect on CE defects (Veeman et al. 2003b).

In this chapter, I presented evidence that VANGL proteins strongly interact with PRICKLE1/2. Surprisingly, overexpression of VANGL1/2 leads to a strong reduction of PRICKLE1/2 protein levels, which can be partially rescued by active R-RAS subgroup GTPases without affecting VANGL1-PRICKLE1 interaction.

It has been reported that that PRICKLE1 protein levels can be targeted for proteasomal degradation by SMURF1/2 ubiquitin ligases (Narimatsu et al. 2009). SMURF ubiquitin ligases regulate signalling, cell polarity and motility; and mice mutants for Smurf1 and Smurf2 display PCP defects in the cochlea and CE defects that include a failure to close the neural tube (Narimatsu et al. 2009). According to the proposed model, WNT5a stimulation leads to activation of DVL2 by phosphorylation and subsequent recruitment of SMURF1/2, which then targets PRICKLE1 for ubiquitin-mediated degradation (Narimatsu et al. 2009).

Besides proteasome mediated regulation of WNT signalling, autophagy regulation has been implicated to negatively impact WNT signalling through DVL2 degradation (Gao et al. 2010). Another link between PCP and autophagy stems from the protein activating molecule Beclin-regulated autophagy (AMBRA), which upon functional inactivation, displays impaired autophagy (Fimia et al. 2007). In addition, homozygosity of Ambra1 mutation causes embryonic lethality and embryos exhibit PCP typical neural tube defects or spina bifida characteristics (Cecconi et al. 2007; Fimia et al. 2007).

In endothelial cells, PCP signalling is required for cell growth, polarity, and migration (Masckauchan et al. 2006; Cheng et al. 2008). Silencing of either DVL2 or PRICKLE1 suppressed endothelial cell proliferation, highlighting the function of a DVL2-PRICKLE complex (Cirone et al. 2008). However, it also has been reported that PRICKLE1 acts as negative regulator of DVL/Dsh (Carreira-Barbosa et al. 2003; Veeman et al. 2003b; Fujimura et al. 2009) and facilitates a

proteasome mediated degradation of DVL3 through its two destruction box motifs, essential for E3 ligase activity (Chan et al. 2006).

Knockdown of PRICKLE1 causes reduced axonal and dendritic extension in hippocampal neurons, thus implicating a function for PRICKLE in axonal-dendritic development (Liu et al. 2013). Notably, studies in *C.elegans,* which contains only one Vangl isoform, demonstrated that Vangl co-operates with Prickle1 to negatively regulate neurite formation (Sanchez-Alvarez et al. 2011).

Misshapen-like kinase (MINK1), a Ste20 group kinase, has been described to be important for clustering of VANGL1 within PRICKLE1 plasma membrane puncta. Further, MINK induced phosphorylation of PRICKLE1 at a conserved threonine residue (T370) regulates RAB5 mediated endosomal trafficking of PRICKLE1, which is important for localised plasma membrane accumulation and function (Daulat et al. 2012). Further, PRICKLE1 has been reported to be a farnesylation target, implying that this post translational modification can target cytoplasmic PRICKLE1 to (plasma) membrane subcellular localisations (Maurer-Stroh et al. 2007).

A role for VANGL in regulating PRICKLE levels is in agreement with localisation studies of VANGL/stbm and Prickle in *Drosophila* pupal wings, illustrating that in the absence of VANGL/stbm, Prickle protein levels were found to be increased within the cytosol and at the apicolateral cell cortex (Bastock et al. 2003; Jenny et al. 2003).

PET/LIM domains have been reported to be important for PRICKLE function in zebrafish gastrulation (Takeuchi et al. 2003). Interestingly, VANGL1 binds to the C-terminal part of PRICKLE1, lacking both PET and LIM domains, but still harbour both destruction box motifs implicated in DVL degradation (Chan et al. 2006).

Asymmetrical localisation of VANGL and PRICKLE1 is a hallmark of PCP in *Drosophila* and this interaction seems to be conserved from fly to humans (Jenny et al. 2003; Sanchez-Alvarez et al. 2011; Daulat et al. 2012). VANGL induced PRICKLE degradation could therefore be a mechanism to ensure the proteins are asymmetrically localised. Interestingly, PRICKLE1 has been reported to stimulate proteasomal degradation of DVL, another VANGL1 interacting protein (Chan et al. 2006). Therefore a complex regulatory interplay emerges between VANGL1, PRICKLE and DVL at the level of protein degradation where VANGL1, by regulating PRICKLE stability, may indirectly control DVL levels. Critically, R-RAS GTPases are able to modulate this regulatory interplay, potentially by recruiting

VANGL1 to specialised membrane domains and away from the pool of PRICKLE proteins.

The mechanism of VANGL1/2 induced PRICKLE1/2 degradation remains to be determined as preliminary experiments suggested that this degradation is not proteasome mediated. Furthermore, localisation studies suggested a potential role for VANGL proteins in autophagy. Treatment with chloroquine resulted in a dramatic accumulation of YFP-VANGL1 and YFP-VANGL2 in autophagosome-like structures. However, due to technical and time constraining issues, I was not able expand on these studies. Future experiments need to be performed in order to elucidate the mechanism of VANGL-mediated degradation of PRICKLE1/2 as well as the potential role of VANGL proteins in autophagy.

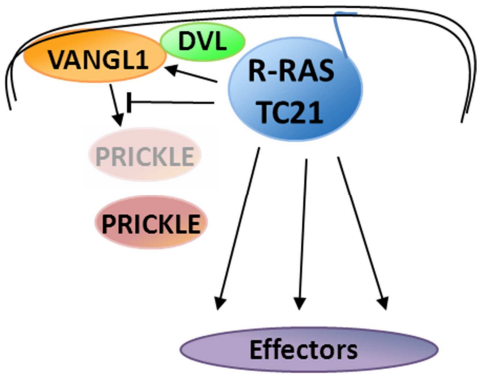

Figure 5.8: Chapter summary. VANGL1 interacts with PRICKLE1 and PRICKLE2 through its C-terminus. However, exogenous expression of VANGL1 results in PRICKLE protein destabilisation through a not fully understood mechanism, whereas other PCP core components such as DVL are not affected. Expression of activated R-RAS subgroup members like R-RAS, TC21 and M-RAS are able, at least partially, to rescue this effect.

CHAPTER 6

Effect of WNT ligands and Frizzled proteins on R-RAS and RHO activation

6 Effect of WNT ligands and Frizzled receptors on R-RAS and RHO activation

Our working model aims to test if R-RAS GTPases act downstream of WNT ligands and Frizzled receptors, resulting in modulation of VANGL1 function. In order to assess R-RAS activity, RAS binding domain (RBD) assays were optimised and performed with the intention to assess R-RAS activity upon WNT stimulation. The receptor tyrosine kinase ROR2 was an attractive candidate to mediate R-RAS activation due to its WNT5a binding and signalling capabilities (Oishi et al. 2003; Mikels and Nusse 2006a; Nishita et al. 2010b), and the potential link through the common interactor filaminA (Nishita et al. 2006; Nomachi et al. 2008; Gawecka et al. 2010; Griffiths et al. 2011). Furthermore, VANGL2 has been demonstrated to be phosphorylated by ROR2 in a WNT5a dependent manner (Gao et al. 2011). And lastly, due to our observations, which detected the R-RAS member TC21 in ROR2 immunoprecipitations (Figure 4.11), indicating that ROR2, VANGL2 and R-RAS GTPase TC21 could form a complex. Therefore, WNT ligands will be tested in ROR2 contexts for R-RAS GTPase member activation.

6.1 Establishment of RAS binding domain assays

In order to monitor and assess R-RAS activation levels upon WNT stimulation in cell lysates, glutathione S-transferase (GST)-fused RAS binding domains (RBDs) from downstream effectors such as RAF1 and RALGDS were employed (Brtva et al. 1995; de Rooij and Bos 1997; Franke et al. 1997; Castro et al. 2005; Rodriguez-Viciana and McCormick 2006). These effector domains preferentially interact with GTP-bound RAS and act as activation specific probes, since affinity for GDP is three orders of magnitude lower (Herrmann et al. 1995). Thus, glutathione beads enable the selective purification from lysates and subsequent quantification of active RAS proteins by immunoblotting.

Several reports suggest that R-RAS subgroup GTPases have considerably lower affinity in their ability to interact with RAF1 compared to classical RAS proteins, whereas they interact as strongly as classical RAS proteins with RALGEFs (Figure 3.6) (Rodriguez-Viciana et al. 1994; Huff et al. 1997; Marte et al. 1997). However, these experiments assessed the interaction with the full length protein and it is known that the interaction with the isolated RBD may not accurately

reflect the affinity of the interaction with the full length protein (Rodriguez-Viciana and McCormick 2006).

In order to determine which RBD was more effective in capturing activated R-RAS GTPases, GST fusion proteins immobilised on glutathione beads of either the RAF1 RBD (residues 2–140) or RALGDS RBD (C-terminal 97 residues) were incubated with equal amounts of the same lysate of cells transfected with tagged GTPases. In order to evaluate the specificity of the interaction, activating and effector domain mutants were compared to the respective wild type protein (Figure 6.1A). After incubation, precipitated amounts of flag-tagged GTPases were detected by immunoblotting using flag antibodies.

Both GST-RBD beads exhibited a strong increase in precipitated protein if the constitutive active mutant was expressed, compared to wild type protein. Moreover, GTPase effector domain mutants (A38 or equivalent) did not show any significant interaction, demonstrating that the interaction is specific and activation and effector domain dependent. Detection of lower levels of wild type RAS GTPases can be explained by the fact that under conditions of overexpression a significant amount of wild type protein may be GTP-bound (Figure 6.1A).

Overall, both GST-RBDs performed similarly in their ability to selectively precipitate active tagged N-RAS, and the three R-RAS family members R-RAS, TC21 and M-RAS, although the RAF1 RBD beads displayed more sensitivity and were therefore used in all subsequent studies (Figure 6.1A).

In order to measure the ability of our RAF1 beads to detect activation of endogenous GTPases, HEK293T cells were stimulated with EGF, a strong stimulator of classical RAS proteins and the MAPK pathway (Figure 6.1B) (Buday and Downward 1993; Zheng et al. 1994).

Over a time course ranging from 0 to 20 min, samples were taken, incubated with GST-RAF1 RBD protein and precipitated using glutathione sepharose beads. Immunoblotting for H-RAS illustrated a characteristic activation pattern, which peaked around 2 min by over 20 fold compared to basal levels and started to decline within 5 min after stimulation and dropped to 8-fold over basal level within 20 min after stimulation (Figure 6.1B and C). This illustrates that detection of endogenous levels of RAS activation with our RBD beads is possible and specific.

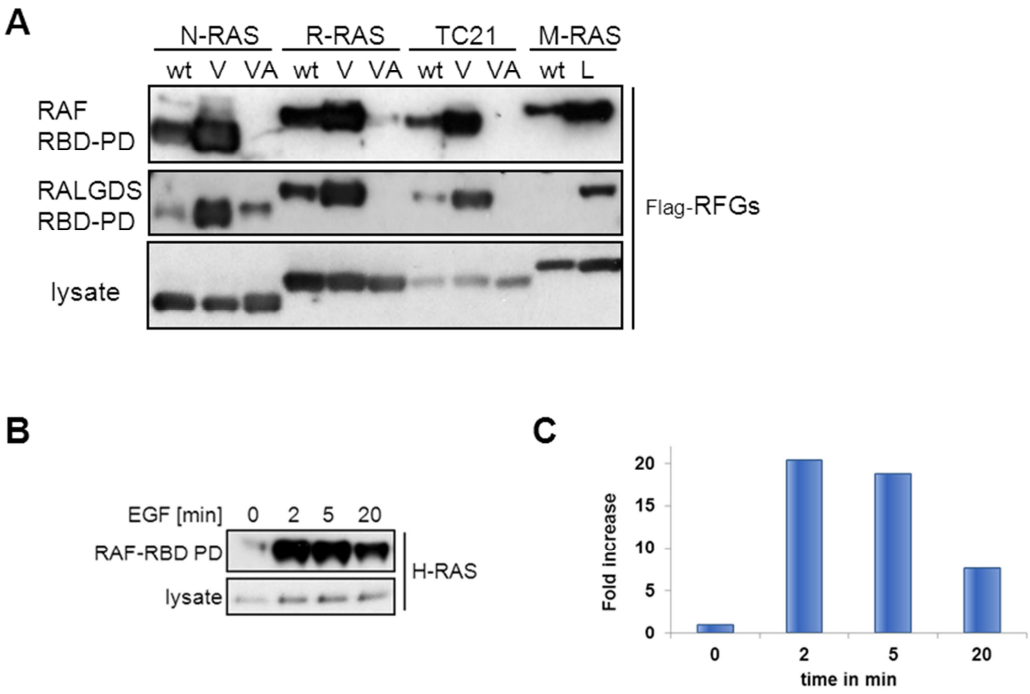

Figure 6.1: RAF1 or RALGDS RAS binding domain (RBD) constructs are able to precipitate activated RAS and R-RAS. (A) HEK293T cells were transfected with indicated flag-tagged wild type (wt), activated mutant (V or L) or respective effector domain mutant (VA) GTPases constructs. 32h post transfection, cells were serum starved for 16h and then subjected to cell lysis and GST-RBD pull down. GTP loaded RAS Family GTPases (RFGs) were detected by western blotting using a flag antibody. **(B)** Activation of endogenous H-RAS by epidermal growth factor (EGF). HEK293T cells were grown to confluency and serum deprived for 16h prior stimulation with 100ng/mL EGF for 2, 5 or 20 min as indicated. Cells lysates were incubated with GST-RBD beads and bound endogenous H-RAS detected with a the respective antibody. **(C)** Densitometry analysis of B. Western blot images of B were scanned and analysed using ImageJ software. The fold increase was normalised to basal activation levels of H-RAS in the untreated condition. Employed mutants: N-RAS V12 (A38), R-RAS V38 (A64), TC21 V13 (A48) and M-RAS L63 (A48).

Next, we tested if R-RAS or TC21 could be activated in this context using serum deprived HEK293T or HeLa cell lines stimulated with EGF. Immunoprobing of RAF1 RBD precipitates confirmed EGF dependent H-RAS activation (Figure 6.2A). However, under the same conditions, activation of R-RAS or TC21 activation could not be detected. Probing for phosphorylated ERK1/2 levels, the target of the MAPK signalling pathway downstream of RAS, served as EGF stimulation control (Minden et al. 1994; Yang et al. 2013).

Time course experiments performed in HEK293T (data not shown) or HeLa cells, confirmed the previous observation that EGF is a potent activator of H-RAS but fails to activate R-RAS or TC21 GTPases (Figure 6.2B). As shown earlier (Figure 6.1C), EGF stimulation of H-RAS exhibits a short lived activation pattern, which starts to decline after 2-3 minutes, which was consistently observed (Figure 6.2B). To exclude cell context dependent phenomena, this experiment was further carried out in U2OS and HMLE cells, with similar results (data not shown).

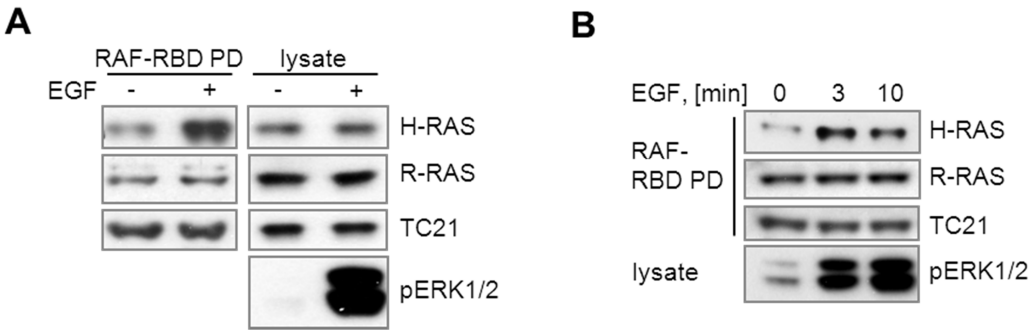

Figure 6.2: EGF activates H-RAS not R-RAS or TC21 in HEK293T or HeLa cells. (A) HEK293T cells were grown to confluency and serum deprived for 16h, stimulated with 50 ng/mL EGF for 5 min and subsequently lysed. Cleared cell lysates were incubated with GST-RAF1 RBD protein and precipitated using glutathione sepharose beads. Endogenous purified RAS GTPases were detected using respective antibodies. **(B)** Confluently grown HeLa cells were serum deprived for 14h prior EGF stimulation (50ng/mL) for 3 or 10 min or left untreated. Cells were subsequently lysed and purified as outlined in A. Endogenous RAS GTPases were detected using indicated antibodies. As control for sucessful EGF activation served ERK phosphorylation levels.

RAS and R-RAS GTPases are activated by overlapping GEFs, but also exhibit different biological functions (see section 1.2.1 and Figure 1.5). In order to identify GEFs that selectively activate R-RAS proteins, and thus could serve as control in order to detect activation of wild type R-RAS GTPases in our RBD assay, as well as confirm previous studies of RASGEF specificity against R-RAS GTPases (Mitin et al. 2006), a panel of myristoylated RAS family GEFs was tested in co-transfection experiments.

N-terminal N-myristoylation is a lipid anchor modification that targets proteins to membrane locations (Levental et al. 2010; Martin et al. 2011). The enzyme N-

myristoyltransferase (NMT) recognises the sequence motif (MGSSKSKPK) of appropriate substrate proteins at the N terminus, and covalently attaches the myristoyl group to the α-amino group of an N-terminal amino acid of a nascent polypeptide (Martin et al. 2011). Thus, employed GEF constructs containing a myristoylation (myr) sequence are constitutively targeted to the cell membrane, even in the absence of an upstream activating signal, and therefore are able to constitutively activate their target RAS GTPases.

Expressing myristoylated RASGEFs alongside flag-tagged wild type R-RAS in HEK293T cells resulted in a strong activation of R-RAS through RASGRF2, RASGRP1, RASGRP3 and RASGRP4. RASGRP2, despite having the highest levels of expression in lysates, showed a weaker activating ability. In contrast, mSOS and RAPGEF5, a RAP1 GEF that was used as a negative control, do not exhibit any effect on R-RAS activation compared to basal levels (empty vector) (Figure 6.3).

TC21 displays a similar GEF activation pattern as observed for R-RAS, but additionally demonstrates a mild activity increase over basal by mSOS (Figure 6.3).

M-RAS activation is stimulated by the same set of GEFs as observed for TC21 but mSOS can lead to a stronger activation, whereas RASGRP2 only marginally activates M-RAS (Figure 6.3).

N-RAS, the representative classical RAS GTPase in the panel, is potently activated by mSOS and also by RASGRF2, RASGRP1, RASGRP3 and RASGRP4, but not by RASGRP2 or RAPGEF5. RASGRF1 does not display activity against any of the tested GTPases but the levels of expression achieved were relatively low so no conclusions can be drawn regarding its activity (Figure 6.3).

In summary, mSOS preferentially activates N-RAS and more weakly M-RAS, but has little or no effect on TC21 and R-RAS, respectively. RASGRF2, RASGRP1, RASGRP3 and RASGRP4 work equally well on all the GTPases tested, whereas RASGRP2 has weaker activity that, however, appears to be specific for R-RAS and TC21 (Figure 6.3).

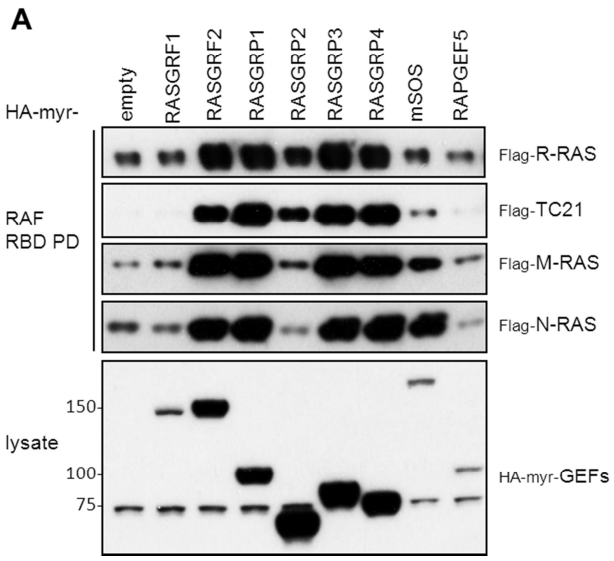

B

myr-GEF	activation of	exp level
RASGRF1	-	+
RASGRF2	all tested	++
RASGRP1	all tested	++
RASGRP2	R, T	+++
RASGRP3	all tested	+++
RASGRP4	all tested	+++
mSOS	(T), M, N	+
RAPGEF5	-	+

Figure 6.3: Characterisation of RAS family GEF activity towards RAS and R-RAS GTPases. **(A)** HEK293T cells were transfected with various myristoylated (myr) guanine exchange factors (GEF) or empty vector alongside with flag-tagged R-RAS, TC21, M-RAS or N-RAS. 32h post transfection, cells were serum deprived for 16 h and subsequently lysed. Cell lysates were incubated with GST-RAF1 RBD fusion proteins immobilised on glutathione beads and RAS family GTPases were detected by immunoblotting with a flag antibody. **(B)** Summary of myr-GEF stimulating activity towards individual GTPases. R - R-RAS, T – TC21, M – M-RAS, N – N-RAS. RasGRF - Ras-specific guanine nucleotide-releasing factor, RasGRP - RAS guanyl nucleotide-releasing protein, mSOS – mouse Son of Sevenless.

6.2 WNT ligands activate R-RAS

In order to test if WNT ligands are able to stimulate R-RAS GTPase activity, various cell types were treated with recombinant WNT5a, and lysates subjected to the GST-RAF1 RBD pull down assay approach.

There are 19 WNT genes in the human genome but my studies will focus on those that have been previously reported to activate the PCP pathway and/or affect cell motility, such as WNT5a and WNT7a, (Heisenberg et al. 2000; Veeman et al. 2003a; Ulrich et al. 2005; Kikuchi and Yamamoto 2008).

WNT5a is known to activate PCP signalling through VANGL2 and to regulate cell migration processes (Qian et al. 2007; Gao et al. 2011). In addition, WNT5a is

up-regulated in many human tumours and stimulates cell motility and invasiveness of tumour cells (Iozzo et al. 1995; Lejeune et al. 1995; Weeraratna et al. 2002; Kurayoshi et al. 2006; Pukrop et al. 2006). Therefore, WNT5a provided an excellent candidate as potential R-RAS GTPase activator.

However, WNT5a will initiate the PCP pathway by binding to specific FZD receptor and/or co-receptor combinations and these are likely differentially expressed in a cell type dependent manner. Similarly, R-RAS GEFs (or other factors) that could potentially mediate WNT5a activation of R-RAS GTPases may also be expressed in a cell type dependent manner. Because we could not control for these variables, R-RAS RBD assays were performed in different cell types and in different contexts in an attempt to find a suitable experimental system.

Initial WNT5a stimulation experiments were carried out in stable HMLE mFzd5 cells, which exhibit WNT5a ligand sensitivity upon mFzd5 expression (see 4.4.3). In order to determine the activation period of R-RAS downstream of WNT5a, time course experiments were carried out, covering the first 15 min after WNT5a treatment. This approach demonstrated WNT5a dependent R-RAS activation that peaks at around 3 minutes post treatment, and rapidly declines to basal levels within 6 min after stimulation (Figure 6.4).

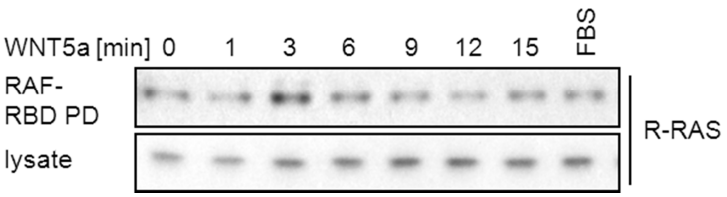

Figure 6.4: WNT5a stimulation leads to sharp and short lived R-RAS activation peak around 3 min after treatment. Stable HMLE mFzd5 cells were grown to confluency and further nutrient deprived for 14h by supplementing basal media with only 5% of regular growth additives. HMLE cells were WNT5a stimulated at indictated times of a period from 0 to 15 min at a concentration of 150 ng/mL or with 10% FBS final concentration for 5min. Cells were immediately harvested and subjected to GST-RAF1-RBD pull down assays. R-RAS ativity was detected by western blot for endogenous R-RAS.

To test if the R-RAS signal could be increased, cell lines were stably transduced with retroviral flag-tagged R-RAS wild type constructs, selected and expanded for subsequent stimulation experiments. WNT5a addition again leads to a sharp and transient increase in R-RAS activity within three minutes, which returns to basal levels five minutes post stimulation (Figure 6.5). Similar results have been observed with WNT5a time courses carried out in HCT116 cells (data not shown and Figure 6.7B).

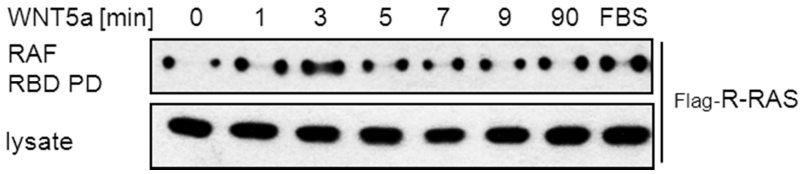

Figure 6.5: WNT5a stimulation leads to transient activation of flag-R-RAS in U2OS cells. U2OS cells stably expressing wild-type flag-R-RAS were serum deprived for period of 18h before recombinant WNT5a (100 ng/mL) stimulation for indicated time points between 0 and 90 min or treated with 10% FBS final concentration for 7 min. Cells were harvested and subjected to RAF1 RBD pull-down assays. Flag-R-RAS was detected using flag-tag specific antibody.

ROR2 has been demonstrated to function as (co)-receptor for WNT5a (Oishi et al. 2003; Mikels and Nusse 2006a; Nishita et al. 2006), leading to the question if ROR2 expression is able to enhance WNT5a responsiveness. Therefore, time course experiments were set up covering the first 6 or 8 min after WNT5a stimulation in U2OS cells stably expressing ROR2 compared to parental control cells. Parental U2OS cells responded to recombinant WNT5a ligand as observed before, resulting in a fast and sharp peak at around three minutes post WNT5a ligand application, which rapidly declined to basal levels within six minutes after stimulation (Figure 6.6 A, left panel). However, stable introduction of ROR2 exhibits accelerated response to WNT5a treatment which can now be detected after one minute, and in addition is sustained for longer time points (Figure 6.6, A, right panel).

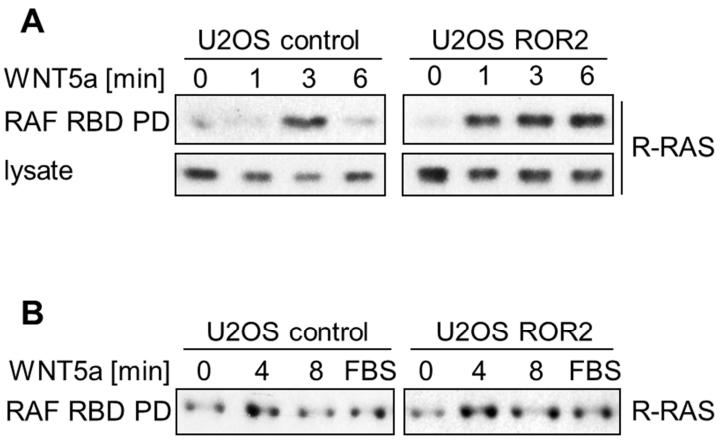

Figure 6.6: ROR2 expression leads to sustained R-RAS activation in U2OS cells. U2OS cells stably expressing ROR2 were grown to confluency and starved for 16h. Cells were treated with recombinant WNT5a (150ng/mL) for either 1, 3, or 6 min or left untreated, and were subsequently lysed. Cleared cell lysates were subjected to GST-RAF1 RBD pulldown assays and endogenous R-RAS detected by western blot using the respective antibody. **(B)** Independent replicate of the experiment described in A. WNT5a ligand treatment times were performed for 4 or 8 min, and a control treatment using 10% fetal bovine serum (FBS) for 8 min was included.

Repetitions of U2OS based experiments resulted in similar WNT5a induced R-RAS activation pattern, demonstrating a short lived peak at around 4 minutes, which rapidly decreased to basal levels within the next 4 min (Figure 6.6B). Although, the effect of ROR2 expression in the time course used, in this independent experiment, was not as striking as observed previously, significant R-RAS activation is still detected 8 minutes after stimulation in U2O2- ROR2 expressing cells compared to parental U2OS (Figure 6.6B) No effect could be observed when activation of endogenous TC21 was measured (data not shown).

As mentioned earlier, WNT5a and WNT7a have been implicated in PCP activation and thus I tested if WNT7a is able to stimulate R-RAS activity in a similar manner to WNT5a. Indeed, WNT7a is able to activate flag-tagged R-RAS to similar extents than WNT5a in HEK293T cells. Notably, stimulation with both WNT ligands results in phosphorylation of JNK, a downstream target of WNT5a induced PCP signalling although this effect in JNK phosphorylation was not consistently reproduced (Figure 6.7A).

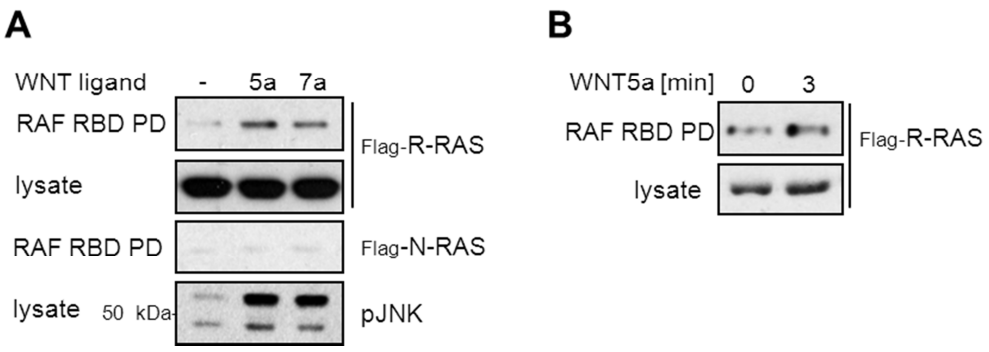

Figure 6.7: WNT5a and WNT7a are able to activate R-RAS in different cellular contexts. **(A)** HEK293T cells transiently expressing flag-R-RAS were grown to confluency, serum deprived for 16h and either stimulated for 3 min with WNT5a (120ng/mL), WNT7a (250 ng/mL) or left untreated (-). Cells were subsequently harvested and subjected to GST-RAF1 RBD pulldown assays. Activity of flag-tagged R-RAS or control GTPase N-RAS was detected by immunoblotting with a flag antibody, lysates we tested for c-Jun N-terminal kinase (pJNK) phosphorylation. **(B)** HCT116 cells stably expressing flag-R-RAS wild type were serum starved for 18h and recombinant WNT5a (150 ng/mL) stimulated for 3 min or left untreated. RBD assay was performed and R-RAS activity determined as decribed in A.

In summary, recombinant WNT5a and WNT7a ligands are able to induce a transient activation of R-RAS, which can be enhanced and prolonged when ROR2 is overexpressed.

6.3 R-RAS and TC21 is required for WNT5a dependent activation of RHOA and RHOB

PCP signalling events lead to activation of RHO GTPases such as RHO or RAC, which are involved in cytoskeletal rearrangements and regulating cell morphology (Kikuchi et al. 2007; Schlessinger et al. 2009; Tada and Kai 2009), critical for vertebrate gastrulation movements (Keller 2002; Wallingford et al. 2002; Veeman et al. 2003a).

R-RAS can regulate RHO family GTPases in a cell type-dependent manner. In NIH3T3 fibroblasts and 32D myeloid cells, R-RAS stimulates RAC activity (Holly et al. 2005; Goldfinger et al. 2006), whereas in MCF10A and T47D epithelial cells R-RAS stimulates RHO but not RAC (Jeong et al. 2005; Wozniak et al. 2005). R-

RAS stimulation of RAC may be mediated by PI3Ks, as R-RAS GTPases are strong activators of PI3K and several RACGEFs are activated in a PI3K-dependent manner (Rodriguez-Viciana et al. 2004; Hawkins et al. 2006). On the other hand, how R-RAS activates RHO is not known.

To assess RHO activation, pull-down assays using GST-fusion proteins using the RHO-binding domain of Rhotekin that specifically bind RHO family members were employed (Habas and He 2006; Mezzacappa et al. 2012). This activation-specific probe functions analogous to RAS RBD constructs and was used to test the possibility that R-RAS GTPases regulate the activation of RHO GTPases downstream of WNT ligand stimulation. GST-Rhotekin RBD functionality and specificity had already been tested in earlier experiments as part of the studies on ARHGEF17/p164RhoGEF (Figure 3.14).

As mentioned above R-RAS has been reported to stimulate RHO in a cell type dependent manner. This could be due to the differential expression of different RHOGEFs in different cell types, only some of which may be regulated by R-RAS and/or the WNT/PCP pathway. Because the RHOGEFs used by R-RAS or the WNT/PCP pathway are not known, several cell types were screened for RHO activation in different contexts.

Initially, I tested the panel of available Frizzled receptors in the absence or presence of ectopically expressed ROR2 for their ability to activate RHOA in co-transfection experiments in HEK293T cells. ROR2 expression by itself in HEK293T is a strong RHO activator, achieving similar levels of active RHOA as FBS stimulation (for 15 min) which was used as a positive control (Figure 6.8).

Overexpression of FZD2, FZD4, mFzd5 and FZD7 also stimulated RHOA activation compared to empty vector control with FZD4 exhibiting the largest effect. Interestingly, co-expression of ROR2 with FZD2 (but not other FZDs) leads to a synergistic activation of RHOA. Treatment of mFzd5/ROR2 expressing cells with recombinant WNT5a ligand only had a marginal effect compared to unstimulated mFzd5/ROR2 samples (Figure 6.8).

In summary, ROR2 and Frizzled proteins can elevate RHOA activity to different degrees and in some cases can cooperate to stimulate RHO activity, highlighting a key role for ROR2 in the regulation of the RHO pathway.

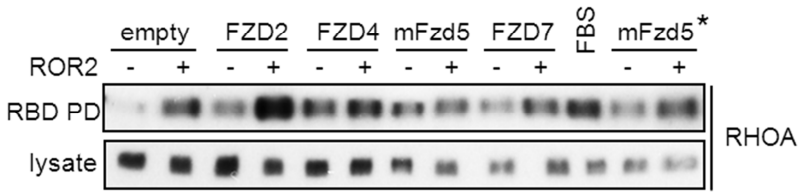

Figure 6.8: ROR2 and Frizzled receptors stimulate RHOA activation. HEK293T cells were transiently transfected with FZD2, FZD4, mFzd5 or FZD7 in combination with empty vector (-) or ROR2. 36 hour later, cells were serum starved for 16h and harvested. Cell lysates were incubated with GST-Rhotekin RBD beads and associated GTP-loaded endogenous RHOA detected using a RHOA antibody. mFzd5 was transfected in duplicate (with or without ROR2), and one set was stimulated with 100 ng/mL recombinant WNT5a for 10 min prior to lysis, indicated with an asterisk (*).

Next, employing the synergistic FZD2/ROR2 combination, I wanted to test whether WNT5a or WNT7a ligands could further enhance RHOA signalling in this context (Figure 6.9).

As observed before (Figure 6.8) ROR2 expression by itself results in enhanced RHOA precipitation, which is not further enhanced by WNT5a or WNT7a stimulation. Expression of FZD2 also elevates RHOA activity, which is further increased when ROR2 is co-expressed. But WNT5a or WNT7a treatment was not able to further enhance RHOA activation in this experiment (Figure 6.9A). However, there appears to be some variability within experiments with regards to the effect of WNT addition, as in an independent experiment using the same cell line and conditions, both WNT5a and WNT7a were able increase activation of RHOA in ROR2 expressing cells (Figure 6.9B).

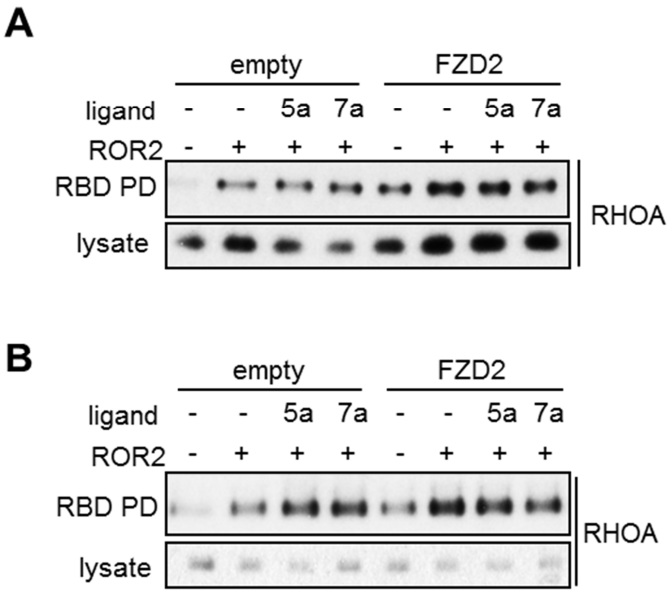

Figure 6.9: Expression of ROR2 in combination with FZD2 stimulates RHOA activity. (A) HEK293T cells were transiently transfected with empty vector or FZD2, in with the presence or absence of ROR2. 46h post transfection, cells were stimulated with recombinant WNT5a (125 ng/mL) or WNT7a (250 ng/mL) for 10 min or left untreated (-). Lysates were subjected to GST-Rhotekin RBD pull down assays and bound RHOA detected with the respective antibody. **(B)** Independent replicate of the same experiment as described in A.

As demonstrated above, WNT5a can lead to the activation of both R-RAS and RHO GTPases. On the other hand, active R-RAS has been previously shown to lead to the activation of RHOA in MCF10A and T47D epithelial cells (Jeong et al. 2005; Wozniak et al. 2005).

In order to assess the possibility that R-RAS GTPases may mediate RHO activation by WNT ligands, the effect of inhibition of R-RAS GTPases by RNAi on the ability of WNT ligands to active RHO proteins was tested. In order to avoid the possibility of redundancy between R-RAS GTPases, both R-RAS and TC21 were inhibited simultaneously by co-transfecting independent siRNA oligos in HMEC mFzd5 cells, which display responsiveness to WNT5a (Figure 4.9A). A time course of WNT5a stimulation was performed over 120 min and RHO RBD pull down assays performed.

In contrast to previous results in HEK293T cells where RHOA but not RHOB was activated by WNT ligands and FZD receptors (Figure 6.9), in HMEC-mFzd5 cells, WNT5a led to a sharp and transient increase in RHOB activation that peaked at 5

min and returned to below basal levels 15 min after WNT5a addition (Figure 6.10). It is noteworthy that this time course of RHOB activation is reminiscent of the early and transient activation of R-RAS (with a sharp peak at 3-4 min) observed before (Figure 6.4 to 6.7).

Probing the same pull downs for RHOA, showed that RHOA activation followed a somewhat different time course, with a weaker activation detected by 5 min of WNT5a addition that was sustained over 30 min and returned to basal levels by 60 min.

Strikingly, depletion of both R-RAS and TC21 resulted in a strong inhibition of RHOA and RHOB activation by WNT5a. In contrast, RHO activation by FBS, which was used as a positive control, was not affected by R-RAS/TC21 depletion (Figure 6.10). Therefore R-RAS GTPases selectively function downstream of WNT5a to mediate the activation of RHO GTPases.

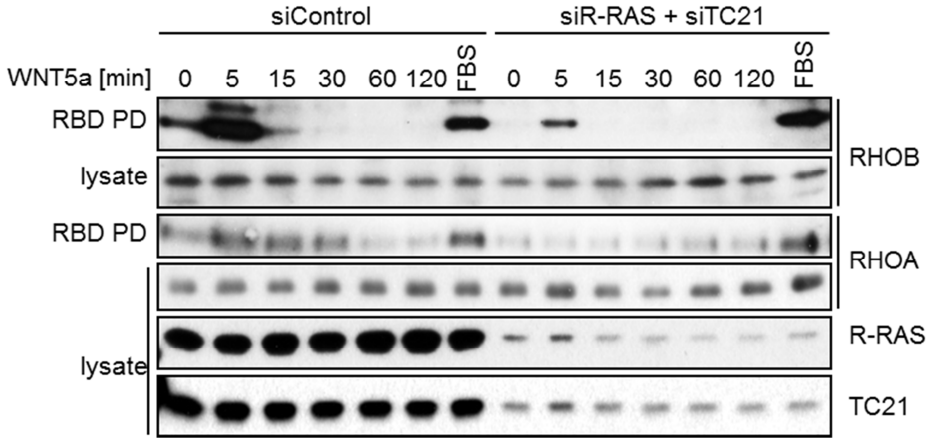

Figure 6.10: R-RAS and TC21 depletion inhibits RHOA and RHOB activation by WNT5a but not FBS. HMEC mFZD5 cells were transfected with either control siRNA or a combination of R-RAS and TC21 siRNAs at a final concentration of 10nM. Cells were serum starved 62 h post transfection for 16h, and recombinant WNT5a (125ng/mL) added for the indicated times. 10% FBS addition for 15 min served as a positive control of RHO activation. Lysates were subjected to GST-RBD pulldowns and endogenous RHOA and RHOB detected by immunoblotting using respective antibodies.

6.4 Discussion

In this chapter I was able to show that WNT ligands alone or in combination with the receptor tyrosine kinase ROR2 are able to activate R-RAS in a specific and short lived manner. Furthermore, R-RAS and TC21 seem to be required in WNT5a mediated RHOA/RHOB activation. These findings demonstrate a novel link between R-RAS and WNT signalling networks.

The PCP pathway has been demonstrated in *Drosophila* to genetically interact with the EGFR and Notch pathways (Brown and Freeman 2003; Gaengel and Mlodzik 2003; Strutt and Strutt 2003). Interestingly, to date, the only R-RAS activator described to stimulate R-RAS activity is the intracellular Notch fragment (Hodkinson et al. 2007). Whereas well established growth factors such as EGF, known to activate classical RAS proteins, fail to stimulate R-RAS activity.

Other potential candidates thought to be able to activate R-RAS, which were not be tested in this thesis, are the migration regulators Trefoil Factors (TFFs) (Taupin and Podolsky 2003), which have been demonstrated to act upstream of VANGL1 (Kalabis et al. 2006). TFFs are known to synergise with the EGFR pathway (Taupin and Podolsky 2003) and it is likely that directed migration is regulated through cross-talk between multiple signalling pathways.

One of the main types of membrane receptors that activate RAS GTPases are RTKs, which led to the appealing hypothesis that the tyrosine kinase ROR2 could be functioning as a potential R-RAS activator. Our findings support this possibility and suggest R-RAS interaction with VANGL1 could be modulated by WNT ligands downstream of ROR2.

Studies showed that ROR2 can act as receptor for WNT5a through its extracellular cysteine-rich domain and WNT5a mediated activation resulted in ROR2 dependent phosphorylation of VANGL2 (Gao et al. 2011).

WNT5a can lead to the activation of R-RAS in multiple cell lines with a characteristic activation pattern displaying a short lived burst of activation 3-4 minutes after WNT5a treatment. Stable expression of ROR2 in U2OS cells exhibited an accelerated as well prolonged WNT5a mediated R-RAS stimulation, compared to parental cells. This is the first time that WNT ligands have been demonstrated to stimulate the activity of RAS family GTPases and confirm our model that R-RAS GTPases can function downstream of WNT ligands in the regulation of VANGL1 function.

I have been unable to detect activation of endogenous TC21 but this could be due to the lower sensitivity of the TC21 antibody, which may be below the threshold of detection achieved in our RBD assays. Notably however, TC21 (but not R-RAS) can be detected in association with ROR2 in some contexts.

How WNT signalling components are able to activate R-RAS GTPases remains to be determined. Regulation by GEFs or GAPs is a likely mechanism of R-RAS activation. Although GEF activation is the most direct and common mechanism for RAS protein activation (Quilliam et al. 2002), inhibition of GAPs by extracellular stimuli also occurs. For example, p120GAP inhibition after stimulation of T cells with phorbol ester or TCR engagement (Downward et al. 1990), Ca^{2+} regulation of the RASGAP, CAPRI (Lockyer et al. 2001), PI3-kinase/AKT mediated regulation of the RHEB GAP, TSC2 (Castro et al. 2003) or regulation of RAPGAP1 by G protein coupled receptors (Jordan et al. 1999). Another example is CK1ε, regulating gastrulation movements through induced phosphorylation of the RAPGAP SIPA1L1 (signal induced proliferation associated protein 1 like 1), which in turn leads to reduced protein stability and thus results in higher RAP1 activity (Tsai et al. 2007).

Despite the fact that the mechanism by which WNT5a activates R-RAS remains to be determined, members of the RASGRP and RASGRF family of RAS family GEFs are likely candidates for R-RAS activation. RASGRPs possess a pair of atypical EF hands that may bind Ca^{2+} *in vivo* and contain a DAG-binding C1 domain (Buday and Downward 2008; Stone 2011). A rise in the intracellular concentration of Ca^{2+} and DAG are therefore possible mechanisms that could lead to activation of R-RAS GTPases. Furthermore, accumulating evidence links Ca^{2+} signalling to WNT/PCP pathway, although the molecular links are not well understood (refer to section 1.5.2 and 1.5.3) (De 2011; Stone 2011; Niehrs 2012).

Interestingly, in prostate PC3 cells, WNT5a addition lead to a sharp and transient peak of Ca^{2+} release starting at around three min after stimulation, which subsided within six min after WNT5a treatment (Wang et al. 2010). This stimulation pattern is strikingly reminiscent of the time course of activation observed for R-RAS in our studies. Future experiments will aim to determine the link between Ca^{2+} signalling, R-RAS activation and the PCP pathway.

There are multiple reports linking the WNT/PCP pathway to activation of RHO GTPases but the molecular mechanisms remains unclear. There are likely to be multiple mechanisms operating in a cell type and context dependent manner. For

example, our data shows that WNT5a can activate RHOA but not RHOB in some cells such as 293T whereas in others such as HMEC it activates RHOB more strongly that RHOA. Strikingly, in at least some context and cell types, R-RAS GTPases play a critical contribution to RHO activation downstream of WNT ligands as simultaneous knock-down of both R-RAS and TC21 in HMEC-mFZD5 cells strongly inhibits RHOA and RHOB activation by WNT5a. Although the mechanism by which R-RAS/TC21 regulate RHO activity remains to be determined, based on our finding that ARHGEF17/p164RhoGEF functions as an effector of TC21 (see section 3.3), this RHOGEF is an excellent candidate to mediate this effect. Future studies should address this exciting possibility.

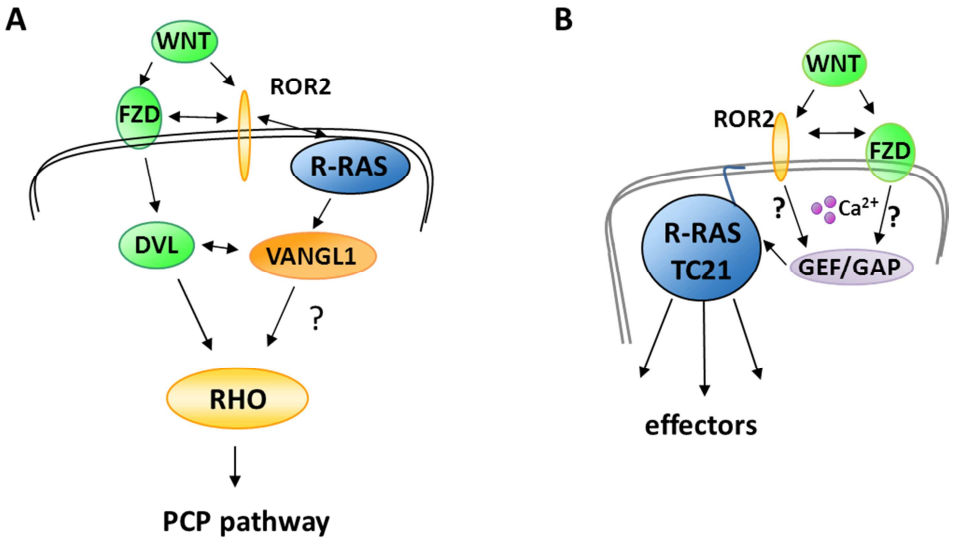

Figure 6.11: Chapter summary. (A) It has been demostrated that WNT ligands are able to activate R-RAS, and the R-RAS subgroup member TC21 has been shown to be ROR2 associated. In addition, enhanced expression of a subset of FZD proteins lead to enhanced VANGL1-DVL2 interaction, sugesting that WNT signalling, R-RAS activation and VANGL1 recruitment are co-ordinated processes required for PCP pathway activation. **(B)** A potential mechanism of WNT signalling induced R-RAS GTPase activation could be mediated through WNT stimulated intracellular Ca^{2+} accumulation, which in turn binds to RASGRP family members, and thus leads to R-RAS activation and subsequent effector interaction.

CHAPTER 7

Role of VANGL1 and R-RAS in polarised migration

7 Role of VANGL1 and R-RAS in polarised migration

In both developmental models and in cultured mammalian cells, the PCP/WNT signalling pathway has been implicated in cell migration (Vladar et al. 2009; Endo et al. 2012b). VANGL1 has been demonstrated to affect cell migration and invasion in colorectal cancer cells (Lee et al. 2004; Lee et al. 2005), and VANGL2 has been implicated in WNT5a mediated migration and invasion (Phillips et al. 2005; Cantrell and Jessen 2010; Lindqvist et al. 2010; Kibar et al. 2011; Shafer et al. 2011; Williams et al. 2012a). Therefore, I aimed to establish biological assays in order to investigate if VANGL1 and R-RAS GTPases are involved WNT ligand mediated cellular migration processes.

Cell migration is a complex process which is orchestrated through extensive transient signalling networks (Vicente-Manzanares et al. 2005; Ridley 2011). In general, cells start to polarise and protrude in the direction of migration before modulating adhesion, following translocation of the cell body by retraction of the rear (Ridley et al. 2003). In order to establish an experimental system to study VANGL1 and R-RAS function in this process in a mammalian context, two frequently used assays of directed or polarised migration were considered; the scratch/wound closure assay and the transwell migration assay.

Wound scratch or wound healing assays have been widely employed to study migration as well as the establishment of cell polarity during directed locomotion (Nobes and Hall 1999; Etienne-Manneville and Hall 2001; Etienne-Manneville and Hall 2003). Wound induction within a compact monolayer provides a directional cue (or mechanotactic signal), which enables a cell to define a distinct front and rear (Valster et al. 2005; Etienne-Manneville 2006; Liang et al. 2007). This results in a strong actin polymerisation at the leading edge and creates protrusive structures such as filopodia or lamellipodia, while the nucleus is positioned in the centre of the cell and the centrosome reorients toward the direction of migration, serving as a microtubule-organizing centre and elongating microtubules to fill in protrusions (Ridley 2011).

The Boyden chamber approach, also termed transwell assay, monitors cell migration towards a chemoattractant cue. This is achieved through two chambers separated by a microporous membrane, in which cells are seeded in the upper chamber and migrate towards chemotactic agents applied in the lower chamber (Chen 2005; Falasca et al. 2011). This method further allows

investigating signal pathway activation based on specific extracellular matrix components, which are coated onto the porous membrane.

7.1 VANGL1 and R-RAS are required for migration

Wound healing assays rely on a compact and dense monolayer of cells which is wounded with a pipette tip and repopulation and closure of the wound is monitored over time. No specific chemoattractants are required, since the wound scratch generates a strong directional migratory response, and cells migrate perpendicular into the generated wound space. Depending on the cell line used, cells can either break free and individually infiltrate the wound area, or remain intact as a cell sheet (Figure 7.1B to E).

Initial experiments were carried out in order to establish suitable cell lines for wounding and closure analysis (Figure 7.1A). For read out purposes, we aimed to identify cell lines, which upon wound induction form a polarised leading edge, display protrusive features and preferentially migrate as sheet, rather than single cells.

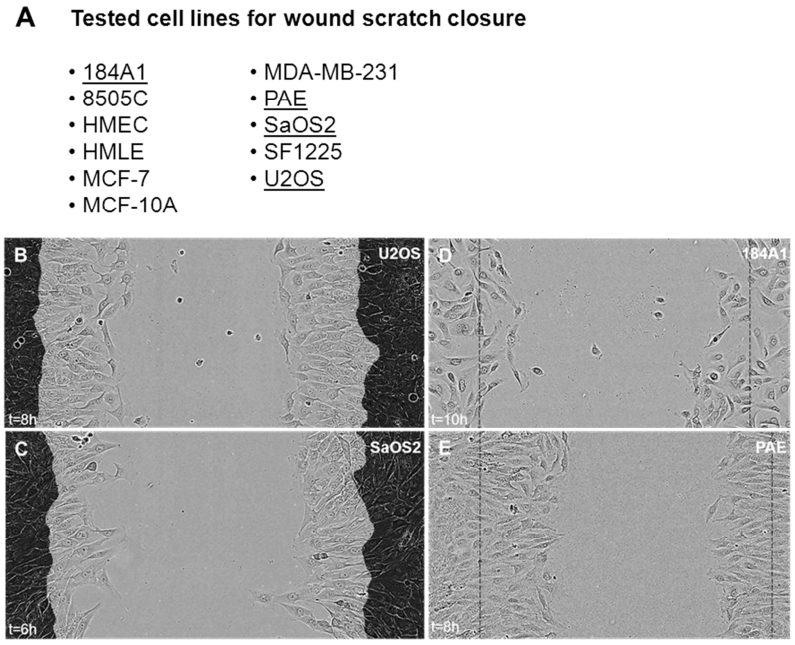

Figure 7.1: Establishment of wound scratch assays. Cells lines listed in A were seeded in 24 wells and upon reaching confluency, scratched and wound closure monitored over time. Created wound at t=0 is indicated as light grey area (B and C) or by a dotted line (D and E). The time point of wound closure assessment has been displayed as in hours post wounding.

The osteosarcoma U2OS cell line exhibited all the desired features (Figure 7.1A) and has been demonstrated to be a good system to study WNT5a mediated signalling processes (Liu et al. 2007; Liu et al. 2008b; Enomoto et al. 2009; Yamagata et al. 2012). Therefore, initial scratch wound experiments focused on investigating the effect of loss of VANGL proteins or R-RAS GTPases on migratory behaviour in U2OS cells. R-RAS GTPases or VANGL proteins were depleted using an RNAi approach. 72h post transfection, confluent monolayers were wounded with a tip, generating approximately 800µm wounds in width (Figure 7.2C and D). Within 24h, cells usually repopulated the wound, through sheet-like migration into the wound space (Figure 7.2C).

Cell lysates were assessed for siRNA mediated knock down efficiency by immunoblotting. Overall, VANGL1, R-RAS and TC21 siRNA transfected samples exhibited significant reduction of respective protein levels (Figure 7.2A).

Depletion of VANGL1, R-RAS or TC21 protein levels resulted in migration defects, exhibited as delayed wound closure (Figure 7.2 B and C). The strongest effect was observed in VANGL1 deficient conditions, that lead to a very strong block in migration, observable as early as 2h post wounding (Figure 7.2B, purple). Knock down of VANGL2 also inhibited migration, although not as strongly as VANGL1 (Figure 7.3B) and double knock down of VANGL1 and VANGL2 did not display an additional effect (data not shown).

R-RAS and TC21 knock down both resulted in slightly delayed wound closure compared to control cells (Figure 7.2B red, green, black). Notably, double knock down samples of R-RAS/TC21 displayed a slightly stronger inhibitory effect (Figure 7.2B, blue). However, this might be related to lower TC21 protein levels in R-RAS/TC21 double knock down samples (Figure 7.2A).

Multiple siRNA oligomer sequences targeting the same gene were employed and tested for efficiency and required concentration (data not shown). Analysis of different VANGL1 RNAi oligomers confirmed the robust negative effect on migration, supported by the observation that VANGL1 protein expression correlates well with a less severe migration defect observed with a second less efficient VANGL1 oligomer (oligo2), compared to oligo 1 (Figure 7.3B and C).

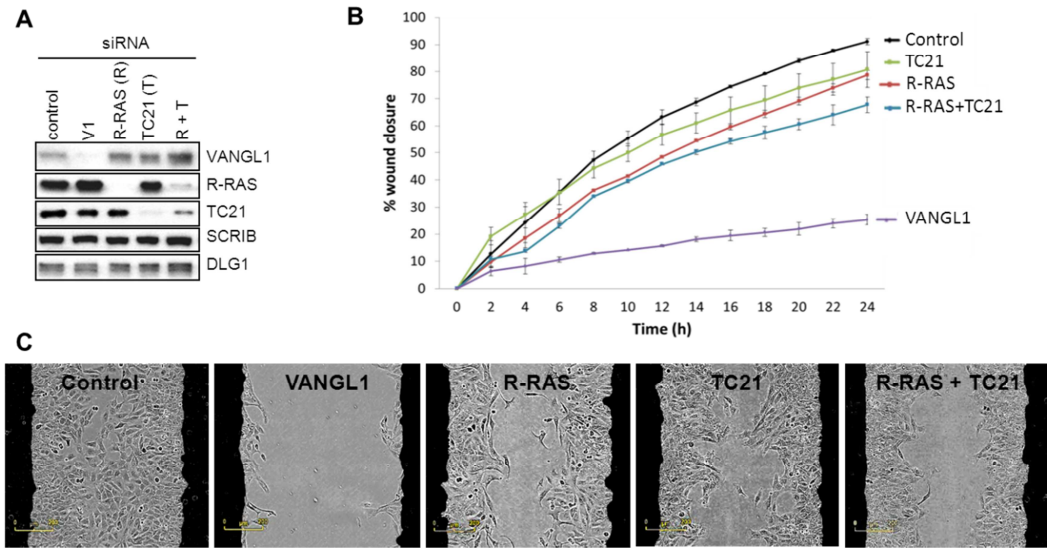

Figure 7.2: VANGL1 and R-RAS/TC21 are required for wound closure. U2OS cells were transfected with siRNA oligomer targeting VANGL1 (V1), R-RAS or TC21 individually or in combination as indicated at final concentration of 10 nM each. 72h post transfection, cells were either harvested or scratched. **(A)** In order to assess knock down levels, cells were lysed and targeted endogenous protein levels detected by immunoblotting, using indicated antibodies. Detection of SCRIB or DLG1 served as loading control. **(B)** Quantification of induced wound closure over a 24h period, assessed through wound repopulation in percent (wound density). Data were obtained using a IncuCyte imaging device (Essen Instruments) and plotted using Excel software (Microsoft) and represent the mean relative wound density ± S.D. of two independent experiments. **(C)** Confluent U2OS monolayers were wounded with a pipette tip and allowed to migrate for 24 h in the presence of 10% serum. Images were aquired periodically every 2h using a imaging IncuCyte (Essen Instruments) device. Dark grey areas represent the wound at the time point of wounding (t=0), whereas light grey regions display the wound area and highlight migrated cells after 14h. Yellow bar represents 200 µm. As control served a non-targeting Alexa-fluorophore labeled siRNA.

Although R-RAS and TC21 knock down exhibited only mild effects on the rate of wound closure compared to VANGL1 knock down conditions, this effect was more apparent at earlier time points (Figure 7.2B) consistent with the possibility that R-RAS/TC21 may be preferentially involved in the initial polarisation associated with migration towards the wound. An enlarged phase contrast field of U2OS cells during wound closure 4 h post scratching, depicts cell migration and protrusion and further illustrates this point, as combinational knock down of R-RAS and TC21 demonstrates a decreased amount of cell protrusion and migration into the wound (Figure 7.4A, right panel and arrow).

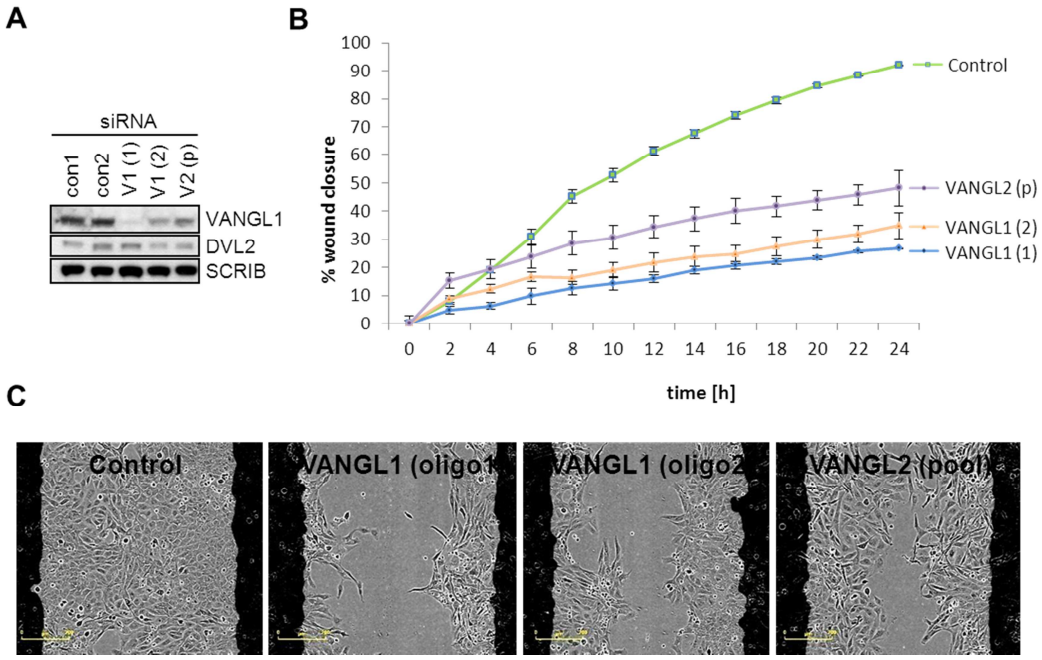

Figure 7.3: VANGL1 knock down leads to a more severe migration defect than VANGL2. Assessment of two individual VANGL1 siRNA oligomers (oligo 1 (1) and oligo (2)) and VANGL2 (pooled oligmers (p)) on wound closure (10 nM final concentration each). Confluent U2OS monolayers were wounded with a pipette tip and allowed to migrate for 24 h in the presence of 10% serum. **(A)** Immunoblotting of cell lysates to assess knock down efficency, as control served scramble (con1) or a non-targeting sequence Alexa-fluorophore (con2). **(B)** Quantification of induced wound closure over a 24 h period, assessed through wound repopulation in percent (wound density). Data were obtained using a IncuCyte imaging device (Essen Instruments) and plotted using Excel software and represent the mean relative wound density ± S.D. of two independent experiments. **(C)** Representative images of the repopulated wound. Dark grey areas represent the wound at the time point of wounding (t=0), whereas light grey regions illustrate the wound area and highlight migrated cells after 14h.

VANGL1 knock down cells fail to extend protrusions towards the wound (Figure 7.4A middle panel), highlighting a key role for VANGL1 in this type of polarised migration.

Immunostaining of the actin skeleton (red) and the Golgi marker protein (GM130, green) revealed that control U2OS cells displayed clear lamellipodial protrusions towards the wound, exhibiting an extensive and elongated actin polymerisation (Figure 7.4B, left image, red staining) as well as Golgi localisation (green) anterior of the nucleus towards the wound, which marks the first important step prior to actin polymerisation.

In comparison, lamellipodial protrusions are clearly shorter and compact in VANGL1 and R-RAS/TC21 knock down cells and lack the extensive actin polymerisation towards the wound detected in control cells (Figure 7.4B, middle and right panel).

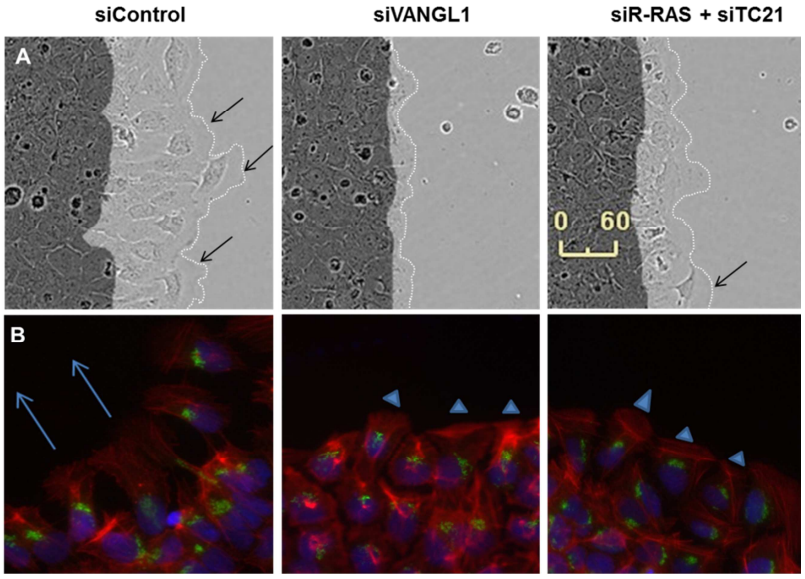

Figure 7.4: Loss of VANGL1 or R-RAS/TC21 inhibits membrane protrusion and migration in scratch/wound closure assays that is particularly apparent at early time points. U2OS cells were siRNA transfected and grown to confluency within 72h. Cells were wounded with a plastic pipette tip and either monitored for wound closure over time or immunostained for actin polymerisation and Golgi orientation. **(A)** siRNA mediated downregulation of VANGL1 or R-RAS and TC21 severely disrupts cell migration into the wound. The untouched cell monolayer at time of scratching is coloured in dark grey, whereas newly migrated cells are highlighted in light grey and the outmost cell border is emphasised with a white, dotted line for better visualisation. Control siRNA transfected U2OS cells displayed fan-like lamellipodia structures at the leading edge. Phase contrast images taken 4h after wound induction exhibit strong negative effect on wound closure in siRNA VANGL1 treated cells and a milder but clear effect in the siRNA R-RAS and TC21 sample, compared to non-targeting scrambled siRNA control (siControl). Arrows depict lamellipodia protrusions into the wound. **(B)** Actin stainings of cells as in A shows inhibition of membrane protrusions and lamellipodial extension at the leading edge by VANGL1 or RRas/TC21 siRNAs. red - phalloidin, green-Golgi marker GM130, blue – nucleus stain by Hoechst. Arrows depict areas of actin polymerisation and the direction of wound triggered cell migration, which displays severely condensed and short lamellipodia formation (illustrated by arrow shapes) in VANGL1 or R-RAS/TC21 knock down cells. Yellow bar represents 60 µm.

Previous experiments were performed in the presence of 10% FBS. In order to study a selective role of R-RAS GTPases in the migratory response specifically stimulated by the WNT/PCP pathway, the ability of WNT ligands to stimulate migration in the scratch assay was initially tested in this assay.

Unfortunately, using conditioned medium for an extensive panel of the WNT ligands generated (section 2.4.8.1) no additional effect over control conditioned medium was observed. Similarly, when purified WNT5a and WNT7a were used at different concentrations on serum starved cells, no stimulation on migration could be detected. These negative results precluded further studies using this experimental system.

As an alternative assay to study polarised migration, the transwell assay was also employed. Small interfering RNA transfected U2OS cells were seeded in the upper chamber maintained in serum free media, while the lower chamber was filled with regular growth media containing 10% FBS, generating a serum gradient due to distinct pores within the membrane and thus providing a chemotactic migration cue. Assay quantification was performed based on percent of cell population travelled through the membrane towards the lower chamber, normalised by initial cell seeding density.

Both knock down conditions, VANGL1 and R-RAS/TC21, displayed a lower number of membrane passed cells, compared to the control transfected sample (Figure 7.5). VANGL1 deficient cells showed a strong migratory reduction of about 5 fold, whereas the R-RAS/TC21 combination resulted in milder decrease of migrated cells. These results display a similar pattern as observed with wound scratch closure assays, where VANGL1 knock-down resulted in a much stronger inhibitory effect compared to R-RAS/TC21 depletion (Figure 7.2).

In order to study a selective role of R-RAS GTPases in cellular migration specifically stimulated by the WNT/PCP pathway; experiments were set up using the transwell assay approach to test the ability of WNT ligands to stimulate migration.

Unfortunately, addition of different WNT ligands at different concentrations in the absence of serum did not show a robust effect on migratory behaviour, in U2OS or other cell lines tested.

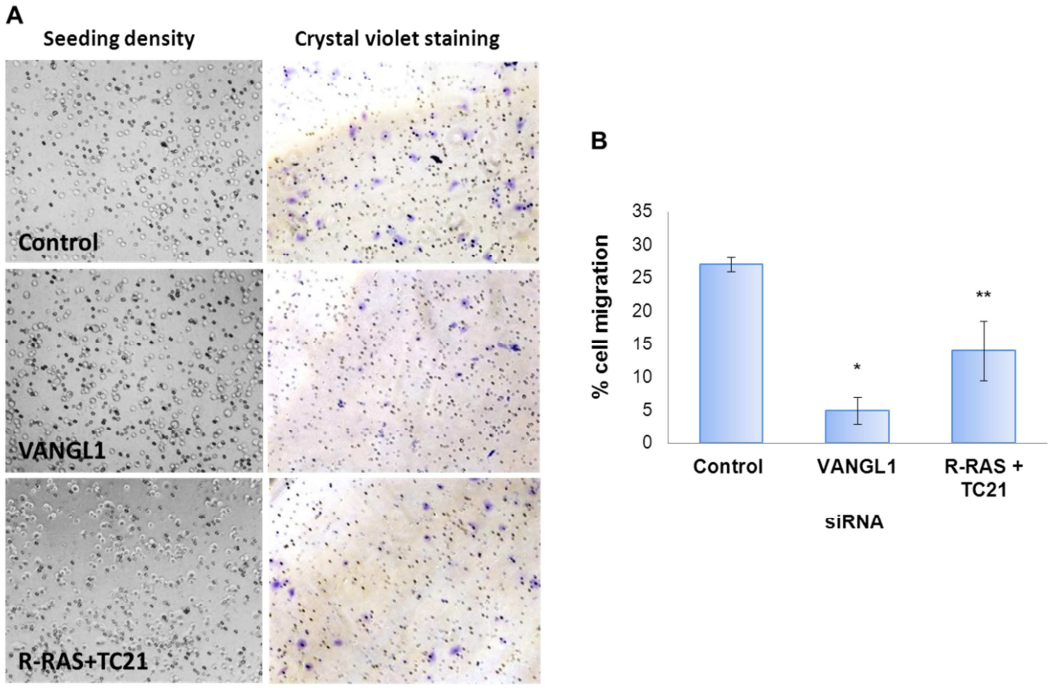

Figure 7.5: VANGL1 or R-RAS/TC21 are required for transwell migration. Migration of siRNA treated U2OS cells (either scramble (control), VANGL1 or combination of R-RAS and TC21), 72h post transfection, towards 10% FBS growth medium was assessed in a Boyden chamber assay using 24 well PET inserts of 8 µm pore size. **(A)** 50000 cells were seeded in the top part of a 24 well transwell insert and after attachment, media was exchanged to serum free media. Left hand panel pictures were taken 30 min after cell seeding in order to correct for potential discrepencies in cell numbers. After 14h of incubation, the assay was terminated by removing non migrated cells on the top of the tranwell membrane, and subsequent staining of migrated cells on the membrane facing the lower chamber by crystal violet dye (right hand side panel). **(B)** Quantification of chemotactic migration was performed by counting representative fields of cells at 10x magnification, normalised by initial seeding densities and plotting the numbers of total migrated cells in percent for each condition. Data represent the mean ± standard error of the mean (SEM) from 3 independent experiments. (*$p<0.001$, **$p<0.05$).

7.2 VANGL1 and R-RAS are required for scratch induced polarisation

In order to further explore the possibility that VANGL1 and R-RAS function in the context of the WNT/PCP pathway activation in order to control initial cell polarisation which take place at the onset of migration, Golgi and MTOC re-orientation at a scratch-induced wound were analysed.

U2OS cell based experiments were carried out in order to assess VANGL1 or R-RAS/TC21 polarisation effects on Golgi orientation. Golgi structures within a cell can be detected by immunostaining for a Golgi marker such as the cis-Golgi protein GM130 (Nakamura et al. 1995).

In order to analyse and quantify Golgi immunostained samples, set criteria for scoring parameters were determined, demanding that a cell is considered polarised if the entire Golgi staining localises within a 120° angle towards the wound edge (Figure 7.6A). A representative scored image is presented in Figure 7.6B. A time course assessing Golgi re-orientation after wound scratch, comparing scramble control with VANGL1 knock down cells showed that VANGL1 deficient cells exhibited delayed Golgi re-orientation. These differences in orientation were most apparent at 4h after wounding and thus this time point was used for subsequent experiments (Figure 7.6C).

Knock-down of R-RAS, or TC21 had a similar inhibitory effect with 20-25% of cells showing an oriented Golgi compared to ~40% of cells in scramble controls. Simultaneous knock-down of R-RAS and TC21 had no further effect (Figure 7.6D). Knock-down of VANGL1 caused the biggest disruption, with only ~15% cells showing wound oriented Golgi (Figure 7.6D).

Another way of determining wound cell orientation is MTOC staining using γ-tubulin detection (Stearns et al. 1991; Etienne-Manneville 2006). Due to the fact that the centrosome structure, which serves as MTOC towards the direction of migration, is a very distinct and confined structure, I applied more stringent scoring parameters. In order to be counted as correct polarised, MTOC staining has to be localised within a 90° angle towards the wound (Figure 7.7A), which is demonstrated on a representative image in Figure 7.7B.

Time course experiments were performed to determine the most suitable point for cell fixation and MTOC assessment over the course of 7h post wounding.

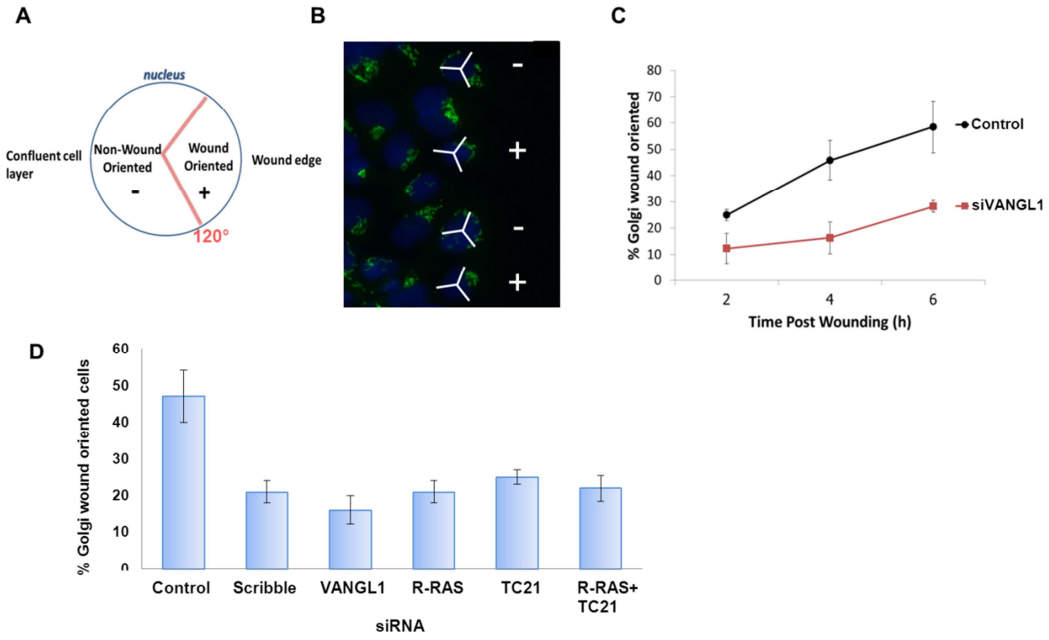

Figure 7.6: VANGL1, SCRIB or R-RAS GTPases delay Golgi wound orientation. U2OS cells were transfected with indicated siRNAs and grown to confluency. 72h post transfection, cells were wounded and allowed to migrate for the indicated times. **(A)** Scoring schematic. Correctly oriented cells (+) were counted when GM130 Golgi staining (green) localised within the 120° wound oriented wedge. If GM130 Golgi staining localised partly or completely outside the 120° criteria, cells were quantified as non oriented (-). Cells were counted across multiple representative images per sample and more then 100 cells per conditon were assessed for analysis. **(B)** Example of a representative scored GM130 image. Nuclei are stained with Hoechst dye (blue) and immunostained for the Golgi marker GM130 (green). **(C)** Time course experiment to determine the most appropriate time point for fixation of cells after wound scratch, comparing control transfected versus VANGL1 siRNA treated cells. Cells were scratched and fixed either 2, 4 or 6 h after wounding and subsequently immunostained for visualisation of the nucleus (blue) and the Golgi (green). **(D)** Quantification of Golgi orientation towards the wound 4 h post scratching were performed from immunostained samples using multiple images per condition, aquired with a Zeiss microscope and analysed applying criteria as described in A.

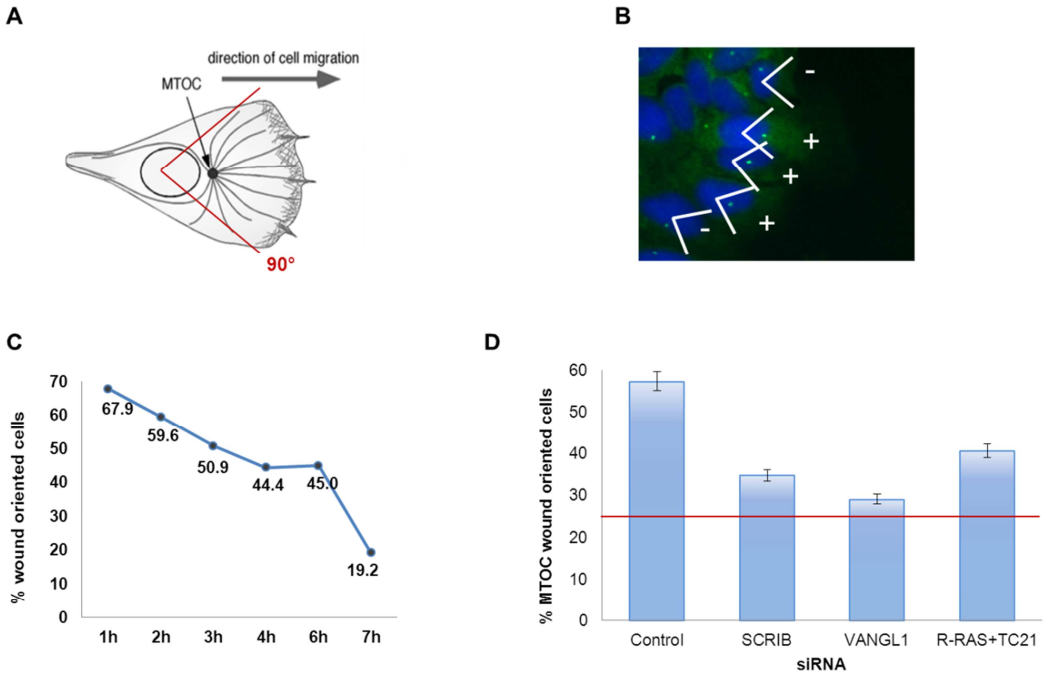

Figure 7.7: Loss of VANGL1 or R-RAS/TC21 disrupts MTOC polarisation towards a wound. U2OS cells were seeded on coverslips, transfected with siRNA targeting either SCRIB, VANGL1 or R-RAS and TC21 protein level expression at a final concentration of 10 nM. Cells were grown to confluency and wounded 72h post transfection. **(A)** Scoring schematic. Correctly oriented cells (+) were counted when the distinctive γ-tubulin stain (MTOC, microtubule organisation centre) located within a 90° wound oriented wedge. If more than one MTOC stain was visible, the respective cell was not considered for analysis. Individual samples were imaged across multiple fields along scratch induced wound, and more then 100 cells per sample were analysed and counted for quantification. **(B)** Example of a scored γ-tubulin image. Cells were nucleus counterstained with Hoechst (blue) dye and immunostained using the MTOC marker γ-tubulin (green). Note that the weak resiual staining of the cell body by γ-tubulin was utilised to assess the cell positioning towards the wound. **(C)** Time course experiment to determine the most suitable time point for fixation of cells after wound scratch induction. Cells were wound scratched and fixed either 1, 2, 3, 4, 6 or 7 h after wound scratch generation. Cells were immunostained for visualisation of the nucleus (Hoechst) and MTOC (γ-tubulin), and wound orientation quantified as described in B. **(D)** Quantification of wound scratch cell orientation using siRNA U2OS transfected samples, 90 min post wounding. Samples were immunostained for the nucleus and MTOC location and various images were recorded using a Zeiss fluorescent microscope. Wound cell orientation was quantified using criteria as described in A. Red line marks 25%, which indicates the expected percentage of a non polarised random cell population.

MTOC wound orientation appears to take place in a rapid fashion, showing the highest orientation within one hour post wounding, with a decline during the next hours (Figure 7.7C). Thus, experiments assessing MTOC orientation towards the wound were harvested between one and two hours post wounding.

Analysis and quantification of MTOC orientation experiments confirmed Golgi orientation results (Figure 7.6), demonstrating that SCRIB, VANGL1 or R-RAS/TC21 knock down negatively affects cellular polarisation. In addition, VANGL1 deficient cells demonstrated in both orientation assays the highest defects with only 29% correctly aligned cells, while SCRIB or R-RAS/TC21 siRNA treated cells displayed 35% or 41%, respectively (Figure 7.7D). These results indicate that VANGL1 and R-RAS/TC21 are required for initial migration processes such as correct polarisation towards as wound, consistent with our observation that a lack of VANGL1 or R-RAS/TC21 results in delayed wound closure.

Interestingly, immunoblotting for endogenous VANGL1 protein in SCRIB deficient conditions revealed a gel-shift, compared to control transfected samples (Figure 7.8). It is known that VANGL2 phosphorylation occurs at the N-terminus in a WNT5a mediated fashion through ROR2 (Gao et al. 2011). Since VANGL1 and VANGL2 share the same N-terminal serine/threonine cluster, and VANGL1 is reported to be N-terminal phosphorylated (Kalabis et al. 2006; Daub et al. 2008), this gel-shift suggests potential protein phosphorylation if SCRIB is absent (Figure 7.8). SCRIB has been implicated in the regulation of directed cell movements and interacts with VANGL1 (Dow et al. 2007; Anastas et al. 2011), and thus this evidence implies a potential SCRIB dependent post-translational VANGL1 regulatory mechanism.

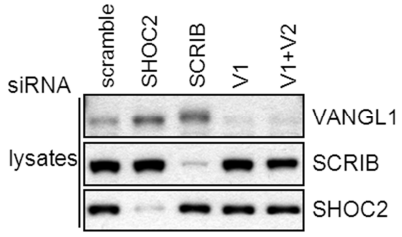

Figure 7.8: Downregulation of SCRIB levels leads to VANGL1 gel migration shift. U2OS cells were siRNA transfected as indicated above and harvested 72h later. Cell lysates were immunoblotted for endogenous proteins with indiacted antibodies. Knock down of SCRIB induced a gel-shift of VANGL1 (V1) protein, which was absent in scramble or SHOC2 transfections, which interacts with SCRIB but not with VANGL1 and thus served as control protein. V2-VANGL2.

7.3 VANGL1 depletion leads to increased invadosome formation

Recent studies have implicated VANGL2 in the regulation of endocytosis and cell-surface availability of membane-type-1 matrix metalloprotease (MMP-14), and in formation or stability of invadopodia (Cantrell and Jessen 2010; Williams et al. 2012a; Williams et al. 2012b).

Regulation of MMPs and remodelling of ECM has been demonstrated to be required for non-canonical WNT signalling and vertebrate gastrulation movements (Coyle et al. 2008). This triggered the question if VANGL1 migratory and invasive properties are mediated through similar signalling events as reported for VANGL2.

To test if a R-RAS and VANGL1 are required for invasiveness, the human osteosarcoma cell line SaOS2 was employed for invadopodium formation studies, since this cell line shows invasive properties *in vitro* and metastasis in mouse models (Dass et al. 2006; Guo et al. 2008).

The invadopodium formation assay relies on a fluorophore labelled matrix and detection of potential extracellular matrix degradation through invadopodium formation (Figure 7.9A) (Artym et al. 2009). In order to assess if VANGL1 and R-RAS/TC21 exhibit an effect on ECM degradation, siRNA transfected SaOS2 cells, which showed a significant down regulation of VANGL1, or R-RAS/TC21 (Figure 7.9B), were seeded on Alexa568 fluorophore labelled gelatin coverslips. After 9h of incubation, coverslips were harvested and analysed for ECM degradation, apparent through loss of staining and thus resulting in black spots (Figure 7.9C).

Quantification of ECM degradation ability was carried out by counting generated spots across fields of cells, resulting in a spots per field read out. Control SaOS2 cells lead to an average of six generated spots per field, whereas down regulation of VANGL1 shows a significant reduction by more than 80% in generated spots. R-RAS/TC21 knock down samples also display a reduced spot number of almost 50% (Figure 7.9D).

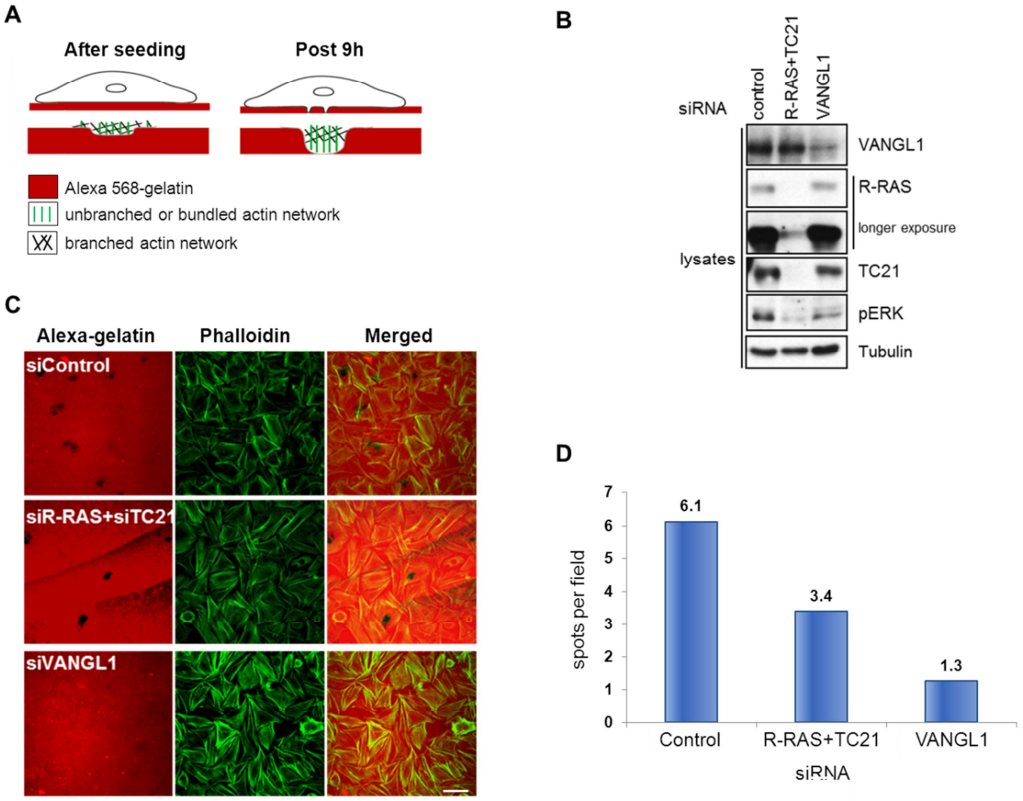

Figure 7.9: VANGL1 or R-RAS/TC21 knock down reduces invadosome formation. **(A)** Schematic of experimental setup and time line. SaOS2 cells were transfected with VANGL1, R-RAS and TC21 or scramble control siRNAs, and 72h later seeded at the same density on Alexa568-gelatin coated coverslips prepared as outlined in section 2.6.4. Cells were allowed to attach and to spread for 9h, during which time cells start to degrade the Alexa-gelatin layer through formed invadosomes, resulting in formation of dark spots within the red matrix layer. After the 9h incubation on Alexa coverslips, cells were fixed and subsequently prepared for immunofluorescence. **(B)** Western blot analysis for endogenous protein levels 81h post transfection using indicated antibodies. As loading control served tubulin. **(C)** Representative immunofluorecent image of scramble (control), R-RAS and TC21 or VANGL1 siRNA treated cell populations on coverslips and induced matrix degradation spots (black). Actin cytoskeleton was counterstained using Phalloidin (green) in order to assess if cell populations across conditions were comparable and equally disributed. Scale bar represents 45 µm. **(D)** Quantification was performed by counting yielded dark spots per field of cells (30 fields per condition) at a comparable density per condition.

Due to reports that WNT5a/ROR2 signalling leads to MMP-13 (collagenase-3) expression (Yamagata et al. 2012), and further observations that MMP-13 has been implicated directly and indirectly to promote tumour angiogenesis (Kudo et

al. 2012), MMP-13 mRNA quantification experiments were carried out using the SaOS2 cell model. In this context, ROR2 knock down has been demonstrated to negatively affect MMP-13 levels (Enomoto et al. 2009) and thus was employed as positive control (Figure 7.10).

Preliminary experiments showed consistently that loss of VANGL1 leads to decreased MMP-13 mRNA level (Figure 7.10), indicating that VANGL1 might be able to modulate migration and invasion properties through ECM remodelling. In contrast, R-RAS or TC21 by itself or in combination did not affect MMP-13 expression levels (Figure 7.10A and B), suggesting MMP-13 expression is modulated through a VANGL1 dependent mechanism, which is independent of R-RAS or TC21.

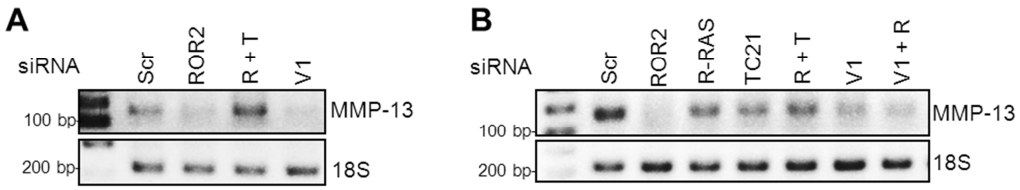

Figure 7.10: MMP-13 expression is regulated through VANGL1 but not R-RAS or TC21. (A) SaOS2 cells were siRNA transfected using ROR2, either R-RAS and TC21 single or in combination (R+T) or VANGL1 (V1) and harvested 72h later for RNA extraction and were subjected to semi-quantitative RT-PCR. Amounts of yielded MMP-13 DNA was compared to 18S, serving as input control. **(B)** Independent replicate of experiment as described in A, examing a larger panel of siRNA conditions. As control served a non-targeting scramble (scr) control.

Taken together, VANGL1 and R-RAS/TC21 have been demonstrated to be required for cellular migration and are likely involved in initial polarisation processes through a yet undetermined mechanism. In addition, VANGL1 seems to be necessary for MMP-13 expression, required for remodelling of ECM and thus migration and invasion processes.

7.4 Discussion

PCP signalling in vertebrates plays a vital role in convergent extension and gastrulation movements (Bisgrove and Yost 2006; Fliegauf et al. 2007; Zallen 2007; Tada and Kai 2009) through activation of RHO GTPases and regulation of the formation and polarisation of actine rich membrane protrusions (Roszko et al. 2009).

To study VANGL1 and R-RAS function in cell migration, wound closure and transwell (Boyden chamber) assays were chosen (Etienne-Manneville 2006; Dow et al. 2007) to assess migration and polarisation properties of VANGL1 or R-RAS GTPases deficient cell lines. Following wounding or migration stimulation by serum gradient, cells at the edge of the wound polarise the nucleus, actin cytoskeleton and microtubule organising centre/Golgi network in the axis of migration, a process known to involve RHO GTPases (Hall 2005; Ridley 2011).

Inhibition of either VANGL1 or R-RAS/TC21 expression with two different siRNA oligos disrupted the scratch induced re-orientation of the Golgi and the centrosome towards the wound, membrane protrusion at the leading edge and inhibited directed migration when measured in transwell and scratch/wound closure assays. The wound closure delay upon VANGL1 and to a milder degree of R-RAS/TC21 was particularly apparent at early time points suggesting a possible role of VANGL1 and R-RAS/TC21 in the initial scratch-induced polarisation. Taken together these results strongly suggest that VANGL1 and R-RAS/TC21 play an important role in polarised migration. This is consistent with previous reported data using colorectal cancer cell lines, demonstrating that VANGL1 is critically required for migration and invasion (Lee et al. 2004; Kho et al. 2009; Lee et al. 2009).

As outlined earlier, VANGL1 interacts with SCRIB, a protein with a well-established role in polarity and migration (Qin et al. 2005b; Osmani et al. 2006; Dow et al. 2007; Nola et al. 2008; Michaelis et al. 2013). Therefore, we hypothesised that R-RAS may be involved in recruiting the VANGL1-SCRIB complex to the membrane and thereby exert a role in polarised migration. In support of this idea, SCRIB is found associated at the leading edge with VANGL1 (Anastas et al. 2011). In addition, it was noticed that knock down of R-RAS/TC21 resulted in significantly shorter and compacter lamellipodial protrusions. Consistent with observations that R-RAS is found associated to sites of lamellipodia (Fernandez-Borja 2012).

In mammalian cells, SCRIB associates with the PIX/GIT complex that regulates RAC/CDC42 and ARF GTPases (Audebert et al. 2004; Frank and Hansen 2008), which has been implicated in the control of polarity associated with directed cell migration (Qin et al. 2005b; Osmani et al. 2006; Dow et al. 2007; Michaelis et al. 2013).

Upon depletion of SCRIB, VANGL1 exhibits an altered, retarded gel migration shift. Since VANGL2 has been described to be phosphorylated (Gao et al. 2011) and both VANGL proteins share a N-terminal serine/threonine cluster, it is tempting to speculate that VANGL1 is phosphorylated by a kinase whose activity is normally inhibited by SCRIB. The identity of this kinase and the regulatory mechanisms involved remain to be determined.

Notably, VANGL2 has been reported to affect cell adhesion and the cytoskeleton by recruiting RAC1 and targeting its activity in the cell to adherens junctions (Lindqvist et al. 2010).

Using melanoma cell lines in a WNT5a/CXCL12-mediated cell migration model, it was observed that WNT5a promotes cell polarity in a manner that requires a chemokine CXCL12 gradient (Witze et al. 2008). CXCL12 signals through the CXCR4 receptor and has been shown to promote cell invasion (Murakami et al. 2002; Bartolome et al. 2004). Based on experiments carried out by Witze and colleagues, in combination with our observation that initial polarisation seems to be strongly affected rather than migration, this suggests that the WNT/PCP pathway is regulating polarisation and not migration.

Classical RAS proteins are activated in response to a wide variety of extracellular signals and function as master regulators of cell proliferation. We propose that R-RAS GTPases may function in a similar manner as master regulators of cell migration.

VANGL2 has been implicated to modulate invasive properties through MMP regulation (Cantrell and Jessen 2010; Williams et al. 2012a). Utilising the invasive osteosarcoma cell line SaOS2, which has been established to show a ROR2 dependent MMP-13 expression (Enomoto et al. 2009; Yamagata et al. 2012), it could be demonstrated that VANGL1 is required for ECM degradation and MMP-13 expression.

MMP-13 facilitates local invasion (Milner and Cawston 2005) through its ability to degrade fibrillar collagen (Uitto et al. 1998) and a wide variety of ECM components (Ashworth et al. 1999; Tardif et al. 2004). MMP-13 has been

reported to be overexpressed in a variety of tumours (Freije et al. 1994; Pendas et al. 2000; Elnemr et al. 2003; Culhaci et al. 2004; Corte et al. 2005; Luukkaa et al. 2006) and has been correlated with tumour invasion, metastasis and poor prognosis in patients (Johansson et al. 1997; Pendas et al. 2000; Krecicki et al. 2003; Roeb et al. 2004; Luukkaa et al. 2006). Expression studies in tumour cells showed that MMP-13 is predominantly found in the tumour invasive front and to a lower extent in stromal fibroblasts, surrounding tumour cells (Johansson et al. 1997; Ashworth et al. 1999).

WNT5a has been demonstrated to promote cell migration and invasion in osteosarcoma cells or prostate carcinoma cells (Enomoto et al. 2009; Yamamoto et al. 2010). In fact, constitutively active WNT5a/ROR2 is required for *MMP-13* expression and invasive properties of osteosarcoma SaOS2 cells. It has been established that for WNT5a/ROR2 dependent *MMP-13* expression, SRC-family protein tyrosine kinases (SFKs), DVL and RAC are required, mediated through c-JUN and ATF2 transcription factors, which are recruited to the AP-1 promotor site of *MMP-13* (Enomoto et al. 2009; Yamagata et al. 2012). Notably, DVL2 and RAC1 but not DVL3 are required for MMP-13 expression in SaOS2. In contrast, studies carried out in U2OS cells reported that DVL3 and RAC1, but not DVL2 are required for *MMP-13* expression (Yamagata et al. 2012), illustrating the presence of distinct signalling machineries in order to lead to MMP-13 expression in osteosarcoma cell lines.

SiRNA mediated knock down of VANGL1 consistently showed a strong decrease of gelatin degraded areas (spots) indicating that VANGL1 is required for ECM degrading activities. This observation correlated well with a reduced level of *MMP-13* expression in VANGL1 deficient cells.

These findings are consistent with literature reports stating that ectopic VANGL1 promoted cell adhesion to fibronectin, and invasion of ECM, while loss of VANGL1 protein decreased adhesion and invasiveness (Lee et al. 2004). In addition, ectopically expressed VANGL1 increased tumour growth rates in mice and metastasis formation, whereas anti-sense VANGL1 mice exhibited a reduced tumour volume and no metastasis formation (Lee et al. 2004).

MMP-13 was identified as a common up-regulated gene by cancer invasion-related factors (Kudo et al. 2012). MMP-13 has been shown to mildly promoted tumour invasion, and to be involved in tumour angiogenesis. Furthermore, MMP-13 promoted capillary tube formation was mediated by activation of FAK and

ERK. Based on findings by Kudo and colleagues it was suggest that MMP-13 may directly and indirectly promote tumour angiogenesis (Kudo et al. 2012).

MMP-14 is required for cell polarity and CE and exhibits a genetic interaction with the WNT co-receptor GLYPICAN4 (Coyle et al. 2008). Studies investigating a potential connection between PCP mediated cell migration and MMP-dependent ECM remodelling, showed that VANGL2 regulates MMP-14 cell surface expression, MMP-2 activation and invasion through an ECM barrier (Cantrell and Jessen 2010). A subsequent study then revealed that VANGL2 directly regulates cell surface levels of MMP-14 by controlling its trafficking to and from the plasma membrane (Williams et al. 2012a). Moreover, VANGL2 dependent MMP-14 endocytosis requires focal adhesion kinase phosphorylation at Y397 (Williams et al. 2012a). In summary, these findings suggest that VANGL2 mediated MMP-14 trafficking might be coordinated with integrin function and the formation of cell matrix adhesions.

Therefore, experiments are required in order to test if VANGL1 mediated MMP-13 modulation might be regulated in a similar manner as discussed for VANGL2-MMP-14. Due to time constraints, I was not able to investigate if VANGL1 is also able to modulate MMP-14 localisation as observed for VANGL2.

CHAPTER 8

Final Discussion and Summary

8 Final Discussion and Summary

8.1 Conclusions and and proposed model

To date, it is still poorly understood how signalling specificity is achieved among the closely related GTPases of the RAS subfamily. It has been suggested that individual GTPases have overlapping but specific blueprints of effector interactions, and that their signalling and biological properties should be considered in the context of the full spectrum of their many effector interactions (Rodriguez-Viciana et al. 2004). A further degree of complexity is illustrated by the observation that RAS family GTPases can cross-talk with each other and co-operate in the activation of the same effector pathway (Rodriguez-Viciana et al. 2006).

Employing a proteomic approach in order to identify novel effectors of R-RAS and TC21 led to the discovery of VANGL1 and ARHGEF17/p164RhoGEF, respectively. Initial validation experiments demonstrated that ARHGEF17/p164RhoGEF binds to both TC21 activated mutants and R-RAS L87 in an activation and effector domain dependent manner. No interaction with M-RAS, RAP1, RAP2 or N-RAS could be observed. Furthermore, I mapped the TC21-ARHGEF17/p164RhoGEF interaction region to the ARHGEF C-terminus downstream of the DH domain, and this interaction is direct as it can be observed in in vitro interaction assays with recombinant proteins. Employing RHO-RBD assays, I could confirm that ARHGEF17/p164RhoGEF acts as GEF for RHOA.

Using activating or disrupting mutants of RAS family GTPases, I have shown that VANGL1 has all the hallmarks of a bona fide effector of R-RAS and TC21. The interaction is very specific for R-RAS subgroup members and VANGL1 does not exhibit binding to other closely related RAS proteins such as N-RAS or RAP2. VANGL1 binds preferentially to the activated mutants compared to the wild type protein and the interaction is disrupted by mutations in the effector domain. Furthermore, a GTP-dependent interaction can also be observed *in vitro* binding assays using purified proteins, suggesting that the interaction is direct. Taken together, these results indicate that VANGL1 is a direct and specific effector of R-RAS and TC21.

VANGL1 is a membrane protein with four transmembrane domains (Iliescu et al. 2011). Interaction studies employing CAAX domain truncations showed that in

contrast to other effectors such as AF6 or BRAF, R-RAS need to be membrane associated in order to interact with VANGL1.

Interaction studies analysing binding of VANGL1 point mutants identified in human NTDs, demonstrated a defective DVL interaction with VANGL1 D259E (Kibar et al. 2007). VANGL1 D259E also disrupts interaction with R-RAS. This suggests that R-RAS and DVL proteins bind to the same region in the VANGL1 C-terminus and therefore may compete for interaction. Notably, even though the VANGL1 D259E mutation disrupted R-RAS and DVL3 binding, it did not affect the interaction with other proteins such as SCRIB, thus indicating that R-RAS and DVL bind to a different region than SCRIB and potentially linking R-RAS and DVL to the pathogenesis of NTDs.

VANGL1 has no enzymatic domains or known function and it is likely to function as a scaffold-type protein by interaction with other proteins. In this model R-RAS/TC21 could regulate VANGL1 function at least partly by regulating its localisation in some contexts: upon activation, RRAS/TC21 would recruit VANGL1 to specialised signalling platforms at the membrane micro-domains where they reside. Furthermore, R-RAS/TC21 binding could also regulate the association of VANGL1 with its interacting partners and thereby modulate its signalling properties.

In order to shed more light into VANGL1 function and interaction partners, we performed the tandem affinity method using VANGL1 as bait. This approach resulted in the identification of various VANGL1 binding partners, including several involved in polarity and vesicular trafficking. Although some of the proteins tested in this study bind to both VANGL1 and VANGL2 isoforms (SCRIB, DLG1, CASK, YIF1B, CELSR2-C2, RAP3GAP1, SYNTENIN-1), others show different interaction affinities and suggest different functions for the two VANGL proteins (e.g. DVL proteins and SYNJ2BP preferentially interact with VANGL1, as does R-RAS and TC21) (Figure 8.1).

In order to test the hypothesis that R-RAS modulates VANGL1 interactor binding, pull down experiments in the presence of activated or effector domain R-RAS mutants were carried out. These studies revealed that indeed R-RAS is able to either inhibit the interaction of VANGL1 with polarity proteins such as DVL, SCRIB, DLG and CASK whereas it can stimulate VANGL1 interaction with the PCP member CELSR2 or membrane trafficking proteins such as YIF1B or SYNJ2BP.

Although R-RAS has no effect on the VANGL1-PRICKLE1 interaction, R-RAS GTPases partially inhibit the VANGL1 induced destabilisation of PRICKLE1/2 protein levels, which occurs by a mechanism that remains to be determined. Taken together, these observations suggest that R-RAS regulates VANGL1 function by direct recruitment and spatial localization and/or modulation of its interactome.

We propose a model where upon activation by extracellular signals, R-RAS GTPases will recruit VANGL1 (and its associated proteins) to sites of activation. This will not only lead to the localisation of VANGL1 complexes at spatially distinct micro/nano-domains at the plasma membrane but also to a selective 'rearrangement' of the interacting partners within the complex to give rise to VANGL1 complexes with specialised signalling properties. Furthermore, it will provide a mechanism to spatially coordinate VANGL1 function with other signalling pathways regulated by R-RAS GTPases that jointly contribute to regulate polarity.

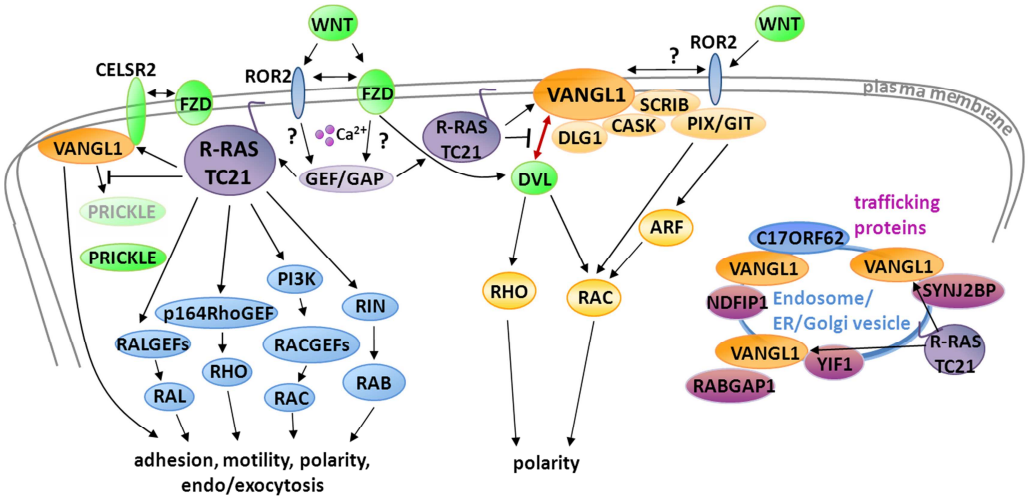

Figure 8.1: R-RAS-VANGL1 signalling model. See text for details.

DVL proteins form major signalling hubs, which interact with a multitude of proteins, and mediate canonical and non-canonical WNT signalling (Boutros and Mlodzik 1999; Gao and Chen 2010; Wynshaw-Boris 2012). VANGL1 interaction with all three DVL proteins highlights its role downstream of WNT signalling.

Remarkably, R-RAS interaction is specific to VANGL1 and so is the DVL interaction. Furthermore, R-RAS and DVL3 binding to VANGL1 is disrupted by the point mutant D259E, suggesting that both proteins could be competing for the same binding site. This is further confirmed by observations that active R-RAS modulates VANGL1-DVL binding, suggesting a common 'axis' of VANGL1 function.

CELSR proteins are membrane adhesion proteins with key roles in PCP that remain to be fully understood. CELSR1 is directly linked to cochlear stereocilia bundle misorientation and neural tube closure defects (Curtin et al. 2003; Devenport and Fuchs 2008; Robinson et al. 2011). CELSR2 and CELSR3 regulate other PCP processes such as ciliogenesis, maintenance of dendrites, neuronal migration and axon guidance (Shima et al. 2002; Tissir et al. 2005; Wada et al. 2006; Shima et al. 2007; Tissir et al. 2010). VANGL1 is able to bind to the intracellular domain of CELSR2 but not CELSR1, which was also the only CELSR isoform detected in VANGL1-TAP experiments. This finding is consistent with the possibility that VANGL1 might not be directly involved in neurolation and related CE (CELSR1 dependent functions) (Torban et al. 2008; Antic et al. 2010; Song et al. 2010), but rather in PCP directed processes associated with ciliogenesis and neuronal development and migration (CELSR2 dependent processes).

Multiple other novel VANGL1 - interacting proteins identified by TAP (NDFIP1, SYNJ2BP, YIF1B, RAB3GAP) are involved in vesicle/membrane trafficking, and imply additional roles for VANGL1 function that remains to be further studied.

VANGL1 might interact with these proteins as part of its regulated transport to the plasma membrane as shown for Sec24B and VANGL2 transport (Wendeler et al. 2007; Merte et al. 2011; Wansleeben et al. 2011). Another possibility is that VANGL1 could have specific functions within other endomembrane compartments such as ER, Golgi or endosomes where others and myself have shown that VANGL1 can also localise. Whether R-RAS can modulate VANGL1 function at these endomembrane compartments remains to be determined, but R-RAS as well as other RAS family proteins, in addition to residing primarily at the plasma membrane, have also been shown to localise at ER, Golgi and endosomes (Chiu et al. 2002; Bivona and Philips 2003) (Conklin et al. 2010; Sandri et al. 2012).

In order to test the idea that WNT signalling modulates VANGL1 interaction with endogenous binding partners was assessed in the presence of a panel of FZD proteins and or ROR2. Interestingly stimulation of interaction of VANGL1 with DVLs, but not with other proteins such as SCRIB, DLG1 and CASK (whose

interactions are mediated via PDZ domains) is enhanced by a subset of FZD proteins as well as by ROR2. The underlying mechanism by which FZD and/or ROR2 achieve this stimulatory effect remains to be identified but may be related to DVL hyper-phosphorylation.

FZDs recruit DVL to the plasma membrane by a still poorly understood mechanism. FZD proteins contain a C-terminal PDZ binding motif required for recruitment of PDZ proteins (Wawrzak et al. 2009), as well as an additional KTxxxW motif which is required for DVL translocation to the membrane and subsequent phosphorylation (Rothbacher et al. 2000; Umbhauer et al. 2000; Axelrod 2001; Cong et al. 2004b). The ability of mFzd5 to stimulate the VANGL1-DVL2 interaction is abrogated in the mFzd5 KTxxxW motif W530G mutant and thus correlates with the ability of mFZD5 to initiate DVL2 translocation to the plasma membrane for subsequent phosphorylation events. This further suggests that DVL translocation and phosphorylation could be an additional mechanism of recruitment of VANGL1 to sites of activation by WNT ligands and of spatiotemporal control of VANGL1 function.

The role of DVL phosphorylation in WNT signalling remains still incompletely understood, but a model has been proposed where DVL phosphorylation may be a mechanism for the separate temporal control of β-catenin dependent and independent WNT signalling. The interaction of DVL with VANGL1 correlates with the phosphorylation of DVL that occurs at later time points of WNT stimulation.

The observation that WNT stimulation can lead to both the activation of R-RAS GTPases and its association with VANGL1 on one hand and to the association of VANGL1 with DVL on the other hand, with both interactions potentially being mutually exclusive may seem counter-intuitive. However, the spatial-temporal dynamics have to be considered. R-RAS proteins are activated within minutes of WNT treatment, whereas the WNT induced increase in the interaction of VANGL1 with DVL is first detected after 60 minutes and therefore clearly displays a delayed response that may correlate with DVL phosphorylation.

Of the tested panel of Frizzled receptors, FZD2, FZD4, mFzd5 and FZD7 stimulate the VANGL1-DVL2 interaction, whereas FZD3 and FZD6 did not display a detectable interaction enhancement. Interestingly, FZD3 and FZD6 form a distinct phylogenetic branch of Frizzled proteins (Huang and Klein 2004), and have been demonstrated to be required with VANGL2, CELSR1 and PRICKLE2 for inner ear stereociliary bundle orientation (Montcouquiol et al. 2006; Montcouquiol et al. 2008).

As mentioned earlier, DVL interacts preferentially with VANGL1 compared to VANGL2, and VANGL1 interacts with CELSR2 but not CELSR1. Taken together, these observations suggest the possibility that a subset of FZD receptors, possibly in combination with different CELSR co-receptors, may use different VANGL isoforms to regulate various aspects of non-canonical signalling.

In order to assess if WNT ligands or the tyrosine kinase ROR2 could be functioning as a potential R-RAS activators, RAS RBD assays were performed. Our findings demonstrated that WNT5a leads to the activation of R-RAS in multiple cell lines with a characteristic stimulation pattern displaying a short lived burst of activation 3-4 minutes after WNT5a treatment. Stable expression of ROR2 in U2OS cells exhibited an accelerated as well prolonged WNT5a mediated R-RAS stimulation, compared to parental cells. This is the first time that WNT ligands have been demonstrated to stimulate the activity of RAS family GTPases and confirm our model that R-RAS GTPases can function downstream of WNT ligands in the regulation of VANGL1 function.

Despite the fact that the mechanism by which WNT5a activates R-RAS remains to be determined, Ca^{2+} dependent mechanisms provide a compelling possibility. RASGRPs are the only known GEFs for R-RAS regulated by Ca^{2+} *in vivo.* Furthermore, GAPs such as CAPRI and RASAL are also regulated by Ca^{2+}. Therefore, a rise in the intracellular concentration of $Ca^{2+,}$ could account for the very transient activation of R-RAS observed by joint regulation of GEFs and GAPs.

Multiple reports link Ca^{2+} signalling to WNT/PCP pathway, although the molecular links are still not well understood (De 2011; Stone 2011; Niehrs 2012). A compelling possibility is that Ca^{2+} dependent activation of R-RAS GTPases may be the missing link between Ca^{2+} signalling and the PCP pathway. Further experiments need to be performed to test this hypothesis. Additionally, how WNT ligands regulate Ca^{2+} signalling remains to be determined.

There are multiple reports linking the WNT/PCP pathway to activation of RHO GPTases but the molecular mechanisms remains unclear. There are likely to be multiple mechanisms operating in a cell type and context dependent manner. Strikingly, R-RAS GTPases play a critical contribution to RHO activation downstream of WNT ligands as simultaneous knock-down of both R-RAS and TC21 in HMEC-mFZD5 cells strongly inhibits RHOA and RHOB activation by WNT5a. Although the mechanism by which R-RAS/TC21 regulate RHO activity remains to be determined, based on our finding that ARHGEF17/p164RhoGEF

functions as an effector of TC21, this RHOGEF is an excellent candidate to mediate this effect. Future studies should address this exciting possibility.

Our results strongly suggest that VANGL1 and R-RAS/TC21 play an important role in polarised migration. This is consistent with previous reported data using colorectal cancers cell lines, demonstrating that VANGL1 is critically required for migration and invasion (Lee et al. 2004; Kho et al. 2009; Lee et al. 2009).

As outlined earlier, VANGL1 interacts with SCRIB, a protein with a well-established role in polarity and migration (Qin et al. 2005b; Osmani et al. 2006; Dow et al. 2007; Nola et al. 2008; Michaelis et al. 2013). SCRIB associates with the PIX/GIT complex that regulates RAC/CDC42 and ARF GTPases (Audebert et al. 2004; Frank and Hansen 2008). Therefore, we hypothesised that R-RAS may be involved in recruiting the VANGL1-SCRIB complex to the membrane and thereby help coordinate other members of the RAS superfamily of GTPases to help coordinate polarization associated with migration.

In addition, VANGL1 seems to promote also R-RAS independent functions such as ECM degrading activities (Lee et al. 2004) and MMP-13 expression regulation.

In conclusion, the discovery of WNT/ROR2 mediated activation of R-RAS GTPases in combination with the identification of VANGL1 and ARHGRF/p164RhoGEF as novel effectors of R-RAS GTPases provide an exciting new link between the R-RAS subgroup and the WNT/PCP pathway. Perturbations in this pathway contribute to the pathogenesis of several diseases including NTDs and to the invasiveness of cancer cells. Identifying and characterising additional components in this pathway will hopefully lead to the identification of new genes involved in disease aetiology as well as reveal novel targets for drug discovery and therapeutic intervention.

CHAPTER 9

References

9 References

Aberle, H., Bauer, A., Stappert, J., Kispert, A., and Kemler, R. 1997. beta-catenin is a target for the ubiquitin-proteasome pathway. *The EMBO journal* **16**(13): 3797-3804.

Ada-Nguema, A.S., Xenias, H., Hofman, J.M., Wiggins, C.H., Sheetz, M.P., and Keely, P.J. 2006. The small GTPase R-Ras regulates organization of actin and drives membrane protrusions through the activity of PLCepsilon. *J Cell Sci* **119**(Pt 7): 1307-1319.

Adler, P.N. 2002. Planar signaling and morphogenesis in Drosophila. *Developmental cell* **2**(5): 525-535.

Adler, P.N., Krasnow, R.E., and Liu, J. 1997. Tissue polarity points from cells that have higher Frizzled levels towards cells that have lower Frizzled levels. *Current biology : CB* **7**(12): 940-949.

Afzal, A.R., Rajab, A., Fenske, C.D., Oldridge, M., Elanko, N., Ternes-Pereira, E., Tuysuz, B., Murday, V.A., Patton, M.A., Wilkie, A.O., and Jeffery, S. 2000. Recessive Robinow syndrome, allelic to dominant brachydactyly type B, is caused by mutation of ROR2. *Nat Genet* **25**(4): 419-422.

Ahearn, I.M., Haigis, K., Bar-Sagi, D., and Philips, M.R. 2012. Regulating the regulator: post-translational modification of RAS. *Nat Rev Mol Cell Biol* **13**(1): 39-51.

Ahearn, I.M., Tsai, F.D., Court, H., Zhou, M., Jennings, B.C., Ahmed, M., Fehrenbacher, N., Linder, M.E., and Philips, M.R. 2011. FKBP12 binds to acylated H-ras and promotes depalmitoylation. *Molecular cell* **41**(2): 173-185.

Al-Shawi, R., Ashton, S.V., Underwood, C., and Simons, J.P. 2001. Expression of the Ror1 and Ror2 receptor tyrosine kinase genes during mouse development. *Dev Genes Evol* **211**(4): 161-171.

Alarcon, B. and Martinez-Martin, N. 2011. RRas2, RhoG and T-cell phagocytosis. *Small GTPases* **3**(2): 97-101.

Alexander, C.M., Reichsman, F., Hinkes, M.T., Lincecum, J., Becker, K.A., Cumberledge, S., and Bernfield, M. 2000. Syndecan-1 is required for Wnt-1-induced mammary tumorigenesis in mice. *Nat Genet* **25**(3): 329-332.

Amit, S., Hatzubai, A., Birman, Y., Andersen, J.S., Ben-Shushan, E., Mann, M., Ben-Neriah, Y., and Alkalay, I. 2002. Axin-mediated CKI phosphorylation of beta-catenin at Ser 45: a molecular switch for the Wnt pathway. *Genes Dev* **16**(9): 1066-1076.

Anastas, J.N., Biechele, T.L., Robitaille, M., Muster, J., Allison, K.H., Angers, S., and Moon, R.T. 2011. A protein complex of SCRIB, NOS1AP and VANGL1 regulates cell polarity and migration, and is associated with breast cancer progression. *Oncogene* **31**(32): 3696-3708.

Andersson, E.R., Bryjova, L., Biris, K., Yamaguchi, T.P., Arenas, E., and Bryja, V. 2010. Genetic interaction between Lrp6 and Wnt5a during mouse development. *Dev Dyn* **239**(1): 237-245.

Andre, P., Wang, Q., Wang, N., Gao, B., Schilit, A., Halford, M.M., Stacker, S.A., Zhang, X., and Yang, Y. 2012. The Wnt coreceptor Ryk regulates Wnt/planar cell polarity by modulating the degradation of the core planar cell polarity component Vangl2. *J Biol Chem* **287**(53): 44518-44525.

Angers, S. and Moon, R.T. 2009. Proximal events in Wnt signal transduction. *Nat Rev Mol Cell Biol* **10**(7): 468-477.

Angers, S., Thorpe, C.J., Biechele, T.L., Goldenberg, S.J., Zheng, N., MacCoss, M.J., and Moon, R.T. 2006. The KLHL12-Cullin-3 ubiquitin ligase negatively regulates the Wnt-beta-catenin pathway by targeting Dishevelled for degradation. *Nat Cell Biol* **8**(4): 348-357.

Ansley, S.J., Badano, J.L., Blacque, O.E., Hill, J., Hoskins, B.E., Leitch, C.C., Kim, J.C., Ross, A.J., Eichers, E.R., Teslovich, T.M., Mah, A.K., Johnsen, R.C., Cavender, J.C., Lewis, R.A., Leroux, M.R., Beales, P.L., and Katsanis, N. 2003. Basal body dysfunction is a likely cause of pleiotropic Bardet-Biedl syndrome. *Nature* **425**(6958): 628-633.

Antic, D., Stubbs, J.L., Suyama, K., Kintner, C., Scott, M.P., and Axelrod, J.D. 2010. Planar cell polarity enables posterior localization of nodal cilia and left-right axis determination during mouse and Xenopus embryogenesis. *PLoS One* **5**(2): e8999.

Apolloni, A., Prior, I.A., Lindsay, M., Parton, R.G., and Hancock, J.F. 2000. H-ras but not K-ras traffics to the plasma membrane through the exocytic pathway. *Molecular and cellular biology* **20**(7): 2475-2487.

Arora, S., Matta, A., Shukla, N.K., Deo, S.V., and Ralhan, R. 2005. Identification of differentially expressed genes in oral squamous cell carcinoma. *Mol Carcinog* **42**(2): 97-108.

Artym, V.V., Yamada, K.M., and Mueller, S.C. 2009. ECM degradation assays for analyzing local cell invasion. *Methods Mol Biol* **522**: 211-219.

Ashworth, J.L., Murphy, G., Rock, M.J., Sherratt, M.J., Shapiro, S.D., Shuttleworth, C.A., and Kielty, C.M. 1999. Fibrillin degradation by matrix metalloproteinases: implications for connective tissue remodelling. *Biochem J* **340 (Pt 1)**: 171-181.

Audebert, S., Navarro, C., Nourry, C., Chasserot-Golaz, S., Lecine, P., Bellaiche, Y., Dupont, J.L., Premont, R.T., Sempere, C., Strub, J.M., Van Dorsselaer, A., Vitale, N., and Borg, J.P. 2004. Mammalian Scribble forms a tight complex with the betaPIX exchange factor. *Curr Biol* **14**(11): 987-995.

Axelrod, J.D. 2001. Unipolar membrane association of Dishevelled mediates Frizzled planar cell polarity signaling. *Genes Dev* **15**(10): 1182-1187.

Bafico, A., Liu, G., Yaniv, A., Gazit, A., and Aaronson, S.A. 2001. Novel mechanism of Wnt signalling inhibition mediated by Dickkopf-1 interaction with LRP6/Arrow. *Nat Cell Biol* **3**(7): 683-686.

Baines, A.T., Xu, D., and Der, C.J. 2011. Inhibition of Ras for cancer treatment: the search continues. *Future Med Chem* **3**(14): 1787-1808.

Ballester, R., Furth, M.E., and Rosen, O.M. 1987. Phorbol ester- and protein kinase C-mediated phosphorylation of the cellular Kirsten ras gene product. *The Journal of biological chemistry* **262**(6): 2688-2695.

Barbacid, M. 1987. ras genes. *Annu Rev Biochem* **56**: 779-827.

Barker, K.T. and Crompton, M.R. 1998. Ras-related TC21 is activated by mutation in a breast cancer cell line, but infrequently in breast carcinomas in vivo. *Br J Cancer* **78**(3): 296-300.

Barry, S.T. and Critchley, D.R. 1994. The RhoA-dependent assembly of focal adhesions in Swiss 3T3 cells is associated with increased tyrosine phosphorylation and the recruitment of both pp125FAK and protein kinase C-delta to focal adhesions. *J Cell Sci* **107 (Pt 7)**: 2033-2045.

Bartolome, R.A., Galvez, B.G., Longo, N., Baleux, F., Van Muijen, G.N., Sanchez-Mateos, P., Arroyo, A.G., and Teixido, J. 2004. Stromal cell-derived factor-1alpha promotes melanoma cell invasion across basement membranes involving stimulation of membrane-type 1 matrix metalloproteinase and Rho GTPase activities. *Cancer research* **64**(7): 2534-2543.

Bartsch, O., Kirmes, I., Thiede, A., Lechno, S., Gocan, H., Florian, I.S., Haaf, T., Zechner, U., Sabova, L., and Horn, F. 2012. Novel VANGL1 Gene Mutations in 144 Slovakian, Romanian and German Patients with Neural Tube Defects. *Mol Syndromol* **3**(2): 76-81.

Bastock, R., Strutt, H., and Strutt, D. 2003. Strabismus is asymmetrically localised and binds to Prickle and Dishevelled during Drosophila planar polarity patterning. *Development* **130**(13): 3007-3014.

Beales, P.L., Elcioglu, N., Woolf, A.S., Parker, D., and Flinter, F.A. 1999. New criteria for improved diagnosis of Bardet-Biedl syndrome: results of a population survey. *J Med Genet* **36**(6): 437-446.

Bellaiche, Y., Beaudoin-Massiani, O., Stuttem, I., and Schweisguth, F. 2004. The planar cell polarity protein Strabismus promotes Pins anterior localization during asymmetric division of sensory organ precursor cells in Drosophila. *Development* **131**(2): 469-478.

Bellaiche, Y., Gho, M., Kaltschmidt, J.A., Brand, A.H., and Schweisguth, F. 2001. Frizzled regulates localization of cell-fate determinants and mitotic spindle rotation during asymmetric cell division. *Nat Cell Biol* **3**(1): 50-57.

Belo, J.A., Bachiller, D., Agius, E., Kemp, C., Borges, A.C., Marques, S., Piccolo, S., and De Robertis, E.M. 2000. Cerberus-like is a secreted BMP and nodal antagonist not essential for mouse development. *Genesis* **26**(4): 265-270.

Belotti, E., Puvirajesinghe, T.M., Audebert, S., Baudelet, E., Camoin, L., Pierres, M., Lasvaux, L., Ferracci, G., Montcouquiol, M., and Borg, J.P. 2012. Molecular characterisation of endogenous Vangl2/Vangl1 heteromeric protein complexes. *PLoS One* **7**(9): e46213.

Bernards, A. 2003. GAPs galore! A survey of putative Ras superfamily GTPase activating proteins in man and Drosophila. *Biochim Biophys Acta* **1603**(2): 47-82.

Bernards, A. and Settleman, J. 2004. GAP control: regulating the regulators of small GTPases. *Trends Cell Biol* **14**(7): 377-385.

Bernatik, O., Ganji, R.S., Dijksterhuis, J., Konik, P., Cervenka, I., Polonio, T., Krejci, P., Schulte, G., and Bryja, V. 2011. Sequential activation and inactivation of dishevelled in the Wnt/{beta}-catenin pathway by casein kinases. *J Biol Chem*.

Berrier, A.L., Mastrangelo, A.M., Downward, J., Ginsberg, M., and LaFlamme, S.E. 2000. Activated R-ras, Rac1, PI 3-kinase and PKCepsilon can each restore cell spreading inhibited by isolated integrin beta1 cytoplasmic domains. *J Cell Biol* **151**(7): 1549-1560.

Bhanot, P., Brink, M., Samos, C.H., Hsieh, J.C., Wang, Y., Macke, J.P., Andrew, D., Nathans, J., and Nusse, R. 1996. A new member of the frizzled family from Drosophila functions as a Wingless receptor. *Nature* **382**(6588): 225-230.

Bi, D., Nishimura, J., Niiro, N., Hirano, K., and Kanaide, H. 2005. Contractile properties of the cultured vascular smooth muscle cells: the crucial role played by RhoA in the regulation of contractility. *Circ Res* **96**(8): 890-897.

Bilic, J., Huang, Y.L., Davidson, G., Zimmermann, T., Cruciat, C.M., Bienz, M., and Niehrs, C. 2007. Wnt induces LRP6 signalosomes and promotes dishevelled-dependent LRP6 phosphorylation. *Science* **316**(5831): 1619-1622.

Bisgrove, B.W. and Yost, H.J. 2006. The roles of cilia in developmental disorders and disease. *Development* **133**(21): 4131-4143.

Bishop, A.L. and Hall, A. 2000. Rho GTPases and their effector proteins. *Biochem J* **348 Pt 2**: 241-255.

Bivona, T.G., Perez De Castro, I., Ahearn, I.M., Grana, T.M., Chiu, V.K., Lockyer, P.J., Cullen, P.J., Pellicer, A., Cox, A.D., and Philips, M.R. 2003. Phospholipase Cgamma activates Ras on the Golgi apparatus by means of RasGRP1. *Nature* **424**(6949): 694-698.

Bivona, T.G. and Philips, M.R. 2003. Ras pathway signaling on endomembranes. *Current opinion in cell biology* **15**(2): 136-142.

Bivona, T.G., Quatela, S.E., Bodemann, B.O., Ahearn, I.M., Soskis, M.J., Mor, A., Miura, J., Wiener, H.H., Wright, L., Saba, S.G., Yim, D., Fein, A., Perez de Castro, I., Li, C., Thompson, C.B., Cox, A.D., and Philips, M.R. 2006. PKC regulates a farnesyl-electrostatic switch on K-Ras that promotes its association with Bcl-XL on mitochondria and induces apoptosis. *Molecular cell* **21**(4): 481-493.

Blacque, O.E., Reardon, M.J., Li, C., McCarthy, J., Mahjoub, M.R., Ansley, S.J., Badano, J.L., Mah, A.K., Beales, P.L., Davidson, W.S., Johnsen, R.C., Audeh, M., Plasterk, R.H., Baillie, D.L., Katsanis, N., Quarmby, L.M., Wicks, S.R., and Leroux, M.R. 2004. Loss of C. elegans BBS-7 and BBS-8 protein function results in cilia defects and compromised intraflagellar transport. *Genes & development* **18**(13): 1630-1642.

Blankesteijn, W.M., Essers-Janssen, Y.P., Ulrich, M.M., and Smits, J.F. 1996. Increased expression of a homologue of drosophila tissue polarity gene "frizzled" in left ventricular hypertrophy in the rat, as identified by subtractive hybridization. *J Mol Cell Cardiol* **28**(5): 1187-1191.

Blankesteijn, W.M., Essers-Janssen, Y.P., Verluyten, M.J., Daemen, M.J., and Smits, J.F. 1997. A homologue of Drosophila tissue polarity gene frizzled is expressed in migrating myofibroblasts in the infarcted rat heart. *Nat Med* **3**(5): 541-544.

Blitzer, J.T. and Nusse, R. 2006. A critical role for endocytosis in Wnt signaling. *BMC Cell Biol* **7**: 28.

Blomberg, N., Baraldi, E., Nilges, M., and Saraste, M. 1999. The PH superfold: a structural scaffold for multiple functions. *Trends Biochem Sci* **24**(11): 441-445.

Bohl, J., Brimer, N., Lyons, C., and Vande Pol, S.B. 2007. The stardust family protein MPP7 forms a tripartite complex with LIN7 and DLG1 that regulates the stability and localization of DLG1 to cell junctions. *J Biol Chem* **282**(13): 9392-9400.

Bos, J.L. 1989. ras oncogenes in human cancer: a review. *Cancer Res* **49**(17): 4682-4689.

Bos, J.L. and Pannekoek, W.J. 2012. Semaphorin signaling meets rap. *Sci Signal* **5**(212): pe6.

Boutros, M. and Mlodzik, M. 1999. Dishevelled: at the crossroads of divergent intracellular signaling pathways. *Mech Dev* **83**(1-2): 27-37.

Boutros, M., Paricio, N., Strutt, D.I., and Mlodzik, M. 1998. Dishevelled activates JNK and discriminates between JNK pathways in planar polarity and wingless signaling. *Cell* **94**(1): 109-118.

Bovolenta, P., Esteve, P., Ruiz, J.M., Cisneros, E., and Lopez-Rios, J. 2008. Beyond Wnt inhibition: new functions of secreted Frizzled-related proteins in development and disease. *Journal of cell science* **121**(Pt 6): 737-746.

Bradford, M.M. 1976. A rapid and sensitive method for the quantitation of microgram quantities of protein utilizing the principle of protein-dye binding. *Anal Biochem* **72**: 248-254.

Brown, K.E. and Freeman, M. 2003. Egfr signalling defines a protective function for ommatidial orientation in the Drosophila eye. *Development* **130**(22): 5401-5412.

Brown, S.D., Twells, R.C., Hey, P.J., Cox, R.D., Levy, E.R., Soderman, A.R., Metzker, M.L., Caskey, C.T., Todd, J.A., and Hess, J.F. 1998. Isolation and characterization of LRP6, a novel member of the low density lipoprotein receptor gene family. *Biochem Biophys Res Commun* **248**(3): 879-888.

Brtva, T.R., Drugan, J.K., Ghosh, S., Terrell, R.S., Campbell-Burk, S., Bell, R.M., and Der, C.J. 1995. Two distinct Raf domains mediate interaction with Ras. *The Journal of biological chemistry* **270**(17): 9809-9812.

Bryja, V., Andersson, E.R., Schambony, A., Esner, M., Bryjova, L., Biris, K.K., Hall, A.C., Kraft, B., Cajanek, L., Yamaguchi, T.P., Buckingham, M., and Arenas, E. 2009. The extracellular domain of Lrp5/6 inhibits noncanonical Wnt signaling in vivo. *Mol Biol Cell* **20**(3): 924-936.

Bryja, V., Schulte, G., and Arenas, E. 2007a. Wnt-3a utilizes a novel low dose and rapid pathway that does not require casein kinase 1-mediated phosphorylation of Dvl to activate beta-catenin. *Cell Signal* **19**(3): 610-616.

Bryja, V., Schulte, G., Rawal, N., Grahn, A., and Arenas, E. 2007b. Wnt-5a induces Dishevelled phosphorylation and dopaminergic differentiation via a CK1-dependent mechanism. *J Cell Sci* **120**(Pt 4): 586-595.

Buday, L. and Downward, J. 1993. Epidermal growth factor regulates the exchange rate of guanine nucleotides on p21ras in fibroblasts. *Mol Cell Biol* **13**(3): 1903-1910.

Buday, L. and Downward, J.. 2008. Many faces of Ras activation. *Biochimica et biophysica acta* **1786**(2): 178-187.

Butz, S., Okamoto, M., and Sudhof, T.C. 1998. A tripartite protein complex with the potential to couple synaptic vesicle exocytosis to cell adhesion in brain. *Cell* **94**(6): 773-782.

Cadigan, K.M. and Liu, Y.I. 2006. Wnt signaling: complexity at the surface. *J Cell Sci* **119**(Pt 3): 395-402.

Cain, R.J. and Ridley, A.J. 2009. Phosphoinositide 3-kinases in cell migration. *Biol Cell* **101**(1): 13-29.

Campbell, P.M. and Der, C.J. 2004. Oncogenic Ras and its role in tumor cell invasion and metastasis. *Semin Cancer Biol* **14**(2): 105-114.

Cantor, S.B., Urano, T., and Feig, L.A. 1995. Identification and characterization of Ral-binding protein 1, a potential downstream target of Ral GTPases. *Molecular and cellular biology* **15**(8): 4578-4584.

Cantrell, V.A. and Jessen, J.R. 2010. The planar cell polarity protein Van Gogh-Like 2 regulates tumor cell migration and matrix metalloproteinase-dependent invasion. *Cancer Lett* **287**(1): 54-61.

Capelluto, D.G., Kutateladze, T.G., Habas, R., Finkielstein, C.V., He, X., and Overduin, M. 2002. The DIX domain targets dishevelled to actin stress fibres and vesicular membranes. *Nature* **419**(6908): 726-729.

Capurro, M.I., Xiang, Y.Y., Lobe, C., and Filmus, J. 2005. Glypican-3 promotes the growth of hepatocellular carcinoma by stimulating canonical Wnt signaling. *Cancer Res* **65**(14): 6245-6254.

Carreira-Barbosa, F., Concha, M.L., Takeuchi, M., Ueno, N., Wilson, S.W., and Tada, M. 2003. Prickle 1 regulates cell movements during gastrulation and neuronal migration in zebrafish. *Development* **130**(17): 4037-4046.

Castellano, E. and Downward, J. 2010. Role of RAS in the regulation of PI 3-kinase. *Curr Top Microbiol Immunol* **346**: 143-169.

Castro, A.F., Rebhun, J.F., Clark, G.J., and Quilliam, L.A. 2003. Rheb binds tuberous sclerosis complex 2 (TSC2) and promotes S6 kinase activation in a rapamycin- and farnesylation-dependent manner. *The Journal of biological chemistry* **278**(35): 32493-32496.

Castro, A.F., Rebhun, J.F., and Quilliam, L.A. 2005. Measuring Ras-family GTP levels in vivo--running hot and cold. *Methods* **37**(2): 190-196.

Cecconi, F., Di Bartolomeo, S., Nardacci, R., Fuoco, C., Corazzari, M., Giunta, L., Romagnoli, A., Stoykova, A., Chowdhury, K., Fimia, G.M., and Piacentini, M.

2007. A novel role for autophagy in neurodevelopment. *Autophagy* **3**(5): 506-508.
Chae, J., Kim, M.J., Goo, J.H., Collier, S., Gubb, D., Charlton, J., Adler, P.N., and Park, W.J. 1999. The Drosophila tissue polarity gene starry night encodes a member of the protocadherin family. *Development* **126**(23): 5421-5429.
Chan, A.M., Miki, T., Meyers, K.A., and Aaronson, S.A. 1994. A human oncogene of the RAS superfamily unmasked by expression cDNA cloning. *Proc Natl Acad Sci U S A* **91**(16): 7558-7562.
Chan, D.W., Chan, C.Y., Yam, J.W., Ching, Y.P., and Ng, I.O. 2006. Prickle-1 negatively regulates Wnt/beta-catenin pathway by promoting Dishevelled ubiquitination/degradation in liver cancer. *Gastroenterology* **131**(4): 1218-1227.
Chang, E.H., Gonda, M.A., Ellis, R.W., Scolnick, E.M., and Lowy, D.R. 1982. Human genome contains four genes homologous to transforming genes of Harvey and Kirsten murine sarcoma viruses. *Proc Natl Acad Sci U S A* **79**(16): 4848-4852.
Chardin, P., Camonis, J.H., Gale, N.W., van Aelst, L., Schlessinger, J., Wigler, M.H., and Bar-Sagi, D. 1993. Human Sos1: a guanine nucleotide exchange factor for Ras that binds to GRB2. *Science* **260**(5112): 1338-1343.
Chen, H.C. 2005. Boyden chamber assay. *Methods Mol Biol* **294**: 15-22.
Chen, M., Gutierrez, G.J., and Ronai, Z.A. 2011. Ubiquitin-recognition protein Ufd1 couples the endoplasmic reticulum (ER) stress response to cell cycle control. *Proc Natl Acad Sci U S A* **108**(22): 9119-9124.
Chen, W., Hu, L.A., Semenov, M.V., Yanagawa, S., Kikuchi, A., Lefkowitz, R.J., and Miller, W.E. 2001. beta-Arrestin1 modulates lymphoid enhancer factor transcriptional activity through interaction with phosphorylated dishevelled proteins. *Proc Natl Acad Sci U S A* **98**(26): 14889-14894.
Chen, W., ten Berge, D., Brown, J., Ahn, S., Hu, L.A., Miller, W.E., Caron, M.G., Barak, L.S., Nusse, R., and Lefkowitz, R.J. 2003. Dishevelled 2 recruits beta-arrestin 2 to mediate Wnt5A-stimulated endocytosis of Frizzled 4. *Science* **301**(5638): 1391-1394.
Chen, W.S., Antic, D., Matis, M., Logan, C.Y., Povelones, M., Anderson, G.A., Nusse, R., and Axelrod, J.D. 2008. Asymmetric homotypic interactions of the atypical cadherin flamingo mediate intercellular polarity signaling. *Cell* **133**(6): 1093-1105.
Cheng, C.W., Yeh, J.C., Fan, T.P., Smith, S.K., and Charnock-Jones, D.S. 2008. Wnt5a-mediated non-canonical Wnt signalling regulates human endothelial cell proliferation and migration. *Biochem Biophys Res Commun* **365**(2): 285-290.
Cherfils, J. and Zeghouf, M. 2013. Regulation of small GTPases by GEFs, GAPs, and GDIs. *Physiol Rev* **93**(1): 269-309.
Cheyette, B.N., Waxman, J.S., Miller, J.R., Takemaru, K., Sheldahl, L.C., Khlebtsova, N., Fox, E.P., Earnest, T., and Moon, R.T. 2002. Dapper, a Dishevelled-associated antagonist of beta-catenin and JNK signaling, is required for notochord formation. *Dev Cell* **2**(4): 449-461.
Chiu, V.K., Bivona, T., Hach, A., Sajous, J.B., Silletti, J., Wiener, H., Johnson, R.L., 2nd, Cox, A.D., and Philips, M.R. 2002. Ras signalling on the endoplasmic reticulum and the Golgi. *Nature cell biology* **4**(5): 343-350.
Cho, E., Feng, Y., Rauskolb, C., Maitra, S., Fehon, R., and Irvine, K.D. 2006. Delineation of a Fat tumor suppressor pathway. *Nat Genet* **38**(10): 1142-1150.
Choy, E., Chiu, V.K., Silletti, J., Feoktistov, M., Morimoto, T., Michaelson, D., Ivanov, I.E., and Philips, M.R. 1999. Endomembrane trafficking of ras: the CAAX motif targets proteins to the ER and Golgi. *Cell* **98**(1): 69-80.
Chua, C.E., Lim, Y.S., and Tang, B.L. 2010. Rab35--a vesicular traffic-regulating small GTPase with actin modulating roles. *FEBS Lett* **584**(1): 1-6.
Ciani, L. and Salinas, P.C. 2005. WNTs in the vertebrate nervous system: from patterning to neuronal connectivity. *Nat Rev Neurosci* **6**(5): 351-362.
Ciechanover, A. 2005. Proteolysis: from the lysosome to ubiquitin and the proteasome. *Nature reviews Molecular cell biology* **6**(1): 79-87.
Cirone, P., Lin, S., Griesbach, H.L., Zhang, Y., Slusarski, D.C., and Crews, C.M. 2008. A role for planar cell polarity signaling in angiogenesis. *Angiogenesis* **11**(4): 347-360.
Ciruna, B., Jenny, A., Lee, D., Mlodzik, M., and Schier, A.F. 2006. Planar cell polarity signalling couples cell division and morphogenesis during neurulation. *Nature* **439**(7073): 220-224.

Clark, G.J., Kinch, M.S., Gilmer, T.M., Burridge, K., and Der, C.J. 1996. Overexpression of the Ras-related TC21/R-Ras2 protein may contribute to the development of human breast cancers. *Oncogene* **12**(1): 169-176.
Clark, R., Wong, G., Arnheim, N., Nitecki, D., and McCormick, F. 1985. Antibodies specific for amino acid 12 of the ras oncogene product inhibit GTP binding. *Proc Natl Acad Sci U S A* **82**(16): 5280-5284.
Clevers, H. and Nusse, R. 2012. Wnt/beta-catenin signaling and disease. *Cell* **149**(6): 1192-1205.
Cliffe, A., Hamada, F., and Bienz, M. 2003. A role of Dishevelled in relocating Axin to the plasma membrane during wingless signaling. *Curr Biol* **13**(11): 960-966.
Condeelis, J. 2001. How is actin polymerization nucleated in vivo? *Trends Cell Biol* **11**(7): 288-293.
Cong, F., Schweizer, L., and Varmus, H. 2004a. Casein kinase Iepsilon modulates the signaling specificities of dishevelled. *Mol Cell Biol* **24**(5): 2000-2011.
Cong, F., Schweizer, L., and Varmus, H. 2004b. Wnt signals across the plasma membrane to activate the beta-catenin pathway by forming oligomers containing its receptors, Frizzled and LRP. *Development* **131**(20): 5103-5115.
Conklin, M.W., Ada-Nguema, A., Parsons, M., Riching, K.M., and Keely, P.J. 2010. R-Ras regulates beta1-integrin trafficking via effects on membrane ruffling and endocytosis. *BMC cell biology* **11**: 14.
Corbeel, L. and Freson, K. 2008. Rab proteins and Rab-associated proteins: major actors in the mechanism of protein-trafficking disorders. *Eur J Pediatr* **167**(7): 723-729.
Corbit, K.C., Shyer, A.E., Dowdle, W.E., Gaulden, J., Singla, V., Chen, M.H., Chuang, P.T., and Reiter, J.F. 2008. Kif3a constrains beta-catenin-dependent Wnt signalling through dual ciliary and non-ciliary mechanisms. *Nat Cell Biol* **10**(1): 70-76.
Corte, M.D., Gonzalez, L.O., Corte, M.G., Quintela, I., Pidal, I., Bongera, M., and Vizoso, F. 2005. Collagenase-3 (MMP-13) expression in cutaneous malignant melanoma. *Int J Biol Markers* **20**(4): 242-248.
Costa, C., Barberis, L., Ambrogio, C., Manazza, A.D., Patrucco, E., Azzolino, O., Neilsen, P.O., Ciraolo, E., Altruda, F., Prestwich, G.D., Chiarle, R., Wymann, M., Ridley, A., and Hirsch, E. 2007. Negative feedback regulation of Rac in leukocytes from mice expressing a constitutively active phosphatidylinositol 3-kinase gamma. *Proc Natl Acad Sci U S A* **104**(36): 14354-14359.
Courbard, J.R., Djiane, A., Wu, J., and Mlodzik, M. 2009. The apical/basal-polarity determinant Scribble cooperates with the PCP core factor Stbm/Vang and functions as one of its effectors. *Dev Biol* **333**(1): 67-77.
Coussens, L.M., Fingleton, B., and Matrisian, L.M. 2002. Matrix metalloproteinase inhibitors and cancer: trials and tribulations. *Science* **295**(5564): 2387-2392.
Cox, A.D. and Der, C.J. 2010. Ras history: The saga continues. *Small GTPases* **1**(1): 2-27.
Coyle, R.C., Latimer, A., and Jessen, J.R. 2008. Membrane-type 1 matrix metalloproteinase regulates cell migration during zebrafish gastrulation: evidence for an interaction with non-canonical Wnt signaling. *Exp Cell Res* **314**(10): 2150-2162.
Cozier, G.E., Lockyer, P.J., Reynolds, J.S., Kupzig, S., Bottomley, J.R., Millard, T.H., Banting, G., and Cullen, P.J. 2000. GAP1IP4BP contains a novel group I pleckstrin homology domain that directs constitutive plasma membrane association. *J Biol Chem* **275**(36): 28261-28268.
Cruciat, C.M. and Niehrs, C. 2012. Secreted and transmembrane Wnt inhibitors and activators. *Cold Spring Harb Perspect Med* **3**(3): a015081.
Culhaci, N., Metin, K., Copcu, E., and Dikicioglu, E. 2004. Elevated expression of MMP-13 and TIMP-1 in head and neck squamous cell carcinomas may reflect increased tumor invasiveness. *BMC Cancer* **4**: 42.
Cullen, P.J., Hsuan, J.J., Truong, O., Letcher, A.J., Jackson, T.R., Dawson, A.P., and Irvine, R.F. 1995. Identification of a specific Ins(1,3,4,5)P4-binding protein as a member of the GAP1 family. *Nature* **376**(6540): 527-530.
Curtin, J.A., Quint, E., Tsipouri, V., Arkell, R.M., Cattanach, B., Copp, A.J., Henderson, D.J., Spurr, N., Stanier, P., Fisher, E.M., Nolan, P.M., Steel, K.P., Brown, S.D., Gray, I.C., and Murdoch, J.N. 2003. Mutation of Celsr1 disrupts planar polarity of inner ear hair cells and causes severe neural tube defects in the mouse. *Curr Biol* **13**(13): 1129-1133.
Dallol, A., Agathanggelou, A., Tommasi, S., Pfeifer, G.P., Maher, E.R., and Latif, F. 2005. Involvement of the RASSF1A tumor suppressor gene in controlling cell migration. *Cancer Res* **65**(17): 7653-7659.

Daneshmanesh, A.H., Porwit, A., Hojjat-Farsangi, M., Jeddi-Tehrani, M., Tamm, K.P., Grander, D., Lehmann, S., Norin, S., Shokri, F., Rabbani, H., Mellstedt, H., and Osterborg, A. 2013. Orphan receptor tyrosine kinases ROR1 and ROR2 in hematological malignancies. *Leuk Lymphoma* **54**(4): 843-850.

Dasgupta, B. and Gutmann, D.H. 2003. Neurofibromatosis 1: closing the GAP between mice and men. *Curr Opin Genet Dev* **13**(1): 20-27.

Dass, C.R., Ek, E.T., Contreras, K.G., and Choong, P.F. 2006. A novel orthotopic murine model provides insights into cellular and molecular characteristics contributing to human osteosarcoma. *Clinical & experimental metastasis* **23**(7-8): 367-380.

Daub, H., Olsen, J.V., Bairlein, M., Gnad, F., Oppermann, F.S., Korner, R., Greff, Z., Keri, G., Stemmann, O., and Mann, M. 2008. Kinase-selective enrichment enables quantitative phosphoproteomics of the kinome across the cell cycle. *Mol Cell* **31**(3): 438-448.

Daulat, A.M., Luu, O., Sing, A., Zhang, L., Wrana, J.L., McNeill, H., Winklbauer, R., and Angers, S. 2012. Mink1 regulates beta-catenin-independent Wnt signaling via Prickle phosphorylation. *Mol Cell Biol* **32**(1): 173-185.

Davidson, G., Wu, W., Shen, J., Bilic, J., Fenger, U., Stannek, P., Glinka, A., and Niehrs, C. 2005. Casein kinase 1 gamma couples Wnt receptor activation to cytoplasmic signal transduction. *Nature* **438**(7069): 867-872.

De, A. 2011. Wnt/Ca2+ signaling pathway: a brief overview. *Acta Biochim Biophys Sin (Shanghai)* **43**(10): 745-756.

De Cat, B., Muyldermans, S.Y., Coomans, C., Degeest, G., Vanderschueren, B., Creemers, J., Biemar, F., Peers, B., and David, G. 2003. Processing by proprotein convertases is required for glypican-3 modulation of cell survival, Wnt signaling, and gastrulation movements. *J Cell Biol* **163**(3): 625-635.

de Curtis, I. 2001. Cell migration: GAPs between membrane traffic and the cytoskeleton. *EMBO reports* **2**(4): 277-281.

de Lau, W.B., Snel, B., and Clevers, H.C. 2012. The R-spondin protein family. *Genome Biol* **13**(3): 242.

De Marco, P., Merello, E., Rossi, A., Piatelli, G., Cama, A., Kibar, Z., and Capra, V. 2012. FZD6 is a novel gene for human neural tube defects. *Hum Mutat* **33**(2): 384-390.

de Renzis, S., Sonnichsen, B., and Zerial, M. 2002. Divalent Rab effectors regulate the sub-compartmental organization and sorting of early endosomes. *Nature cell biology* **4**(2): 124-133.

de Rooij, J. and Bos, J.L. 1997. Minimal Ras-binding domain of Raf1 can be used as an activation-specific probe for Ras. *Oncogene* **14**(5): 623-625.

De Toledo, M., Colombo, K., Nagase, T., Ohara, O., Fort, P., and Blangy, A. 2000. The yeast exchange assay, a new complementary method to screen for Dbl-like protein specificity: identification of a novel RhoA exchange factor. *FEBS Lett* **480**(2-3): 287-292.

Debnath, J., Muthuswamy, S.K., and Brugge, J.S. 2003. Morphogenesis and oncogenesis of MCF-10A mammary epithelial acini grown in three-dimensional basement membrane cultures. *Methods* **30**(3): 256-268.

DeFeo, D., Gonda, M.A., Young, H.A., Chang, E.H., Lowy, D.R., Scolnick, E.M., and Ellis, R.W. 1981. Analysis of two divergent rat genomic clones homologous to the transforming gene of Harvey murine sarcoma virus. *Proc Natl Acad Sci U S A* **78**(6): 3328-3332.

Delgado, P., Cubelos, B., Calleja, E., Martinez-Martin, N., Cipres, A., Merida, I., Bellas, C., Bustelo, X.R., and Alarcon, B. 2009. Essential function for the GTPase TC21 in homeostatic antigen receptor signaling. *Nat Immunol* **10**(8): 880-888.

Deng, X., Zhao, H.S., Peng, Z., Deng, W.W., Li, N., Guo, S., and Shi, T.P. 2011. [Study on the mechanism of C17orf62 induced cell death]. *Beijing Da Xue Xue Bao* **43**(2): 168-172.

DerMardirossian, C. and Bokoch, G.M. 2005. GDIs: central regulatory molecules in Rho GTPase activation. *Trends Cell Biol* **15**(7): 356-363.

Descamps, B., Sewduth, R., Ferreira Tojais, N., Jaspard, B., Reynaud, A., Sohet, F., Lacolley, P., Allieres, C., Lamaziere, J.M., Moreau, C., Dufourcq, P., Couffinhal, T., and Duplaa, C. 2012. Frizzled 4 regulates arterial network organization through noncanonical Wnt/planar cell polarity signaling. *Circ Res* **110**(1): 47-58.

Destaing, O., Planus, E., Bouvard, D., Oddou, C., Badowski, C., Bossy, V., Raducanu, A., Fourcade, B., Albiges-Rizo, C., and Block, M.R. 2010. beta1A integrin is a master regulator of invadosome organization and function. *Mol Biol Cell* **21**(23): 4108-4119.

Devenport, D. and Fuchs, E. 2008. Planar polarization in embryonic epidermis orchestrates global asymmetric morphogenesis of hair follicles. *Nat Cell Biol* **10**(11): 1257-1268.

Diekmann, D., Brill, S., Garrett, M.D., Totty, N., Hsuan, J., Monfries, C., Hall, C., Lim, L., and Hall, A. 1991. Bcr encodes a GTPase-activating protein for p21rac. *Nature* **351**(6325): 400-402.

Diekmann, Y., Seixas, E., Gouw, M., Tavares-Cadete, F., Seabra, M.C., and Pereira-Leal, J.B. 2011. Thousands of rab GTPases for the cell biologist. *PLoS Comput Biol* **7**(10): e1002217.

Ding, Y., Zhang, Y., Xu, C., Tao, Q.H., and Chen, Y.G. 2013. HECT Domain-containing E3 ubiquitin ligase NEDD4L negatively regulates Wnt signaling by targeting Dishevelled for proteasomal degradation. *J Biol Chem*.

Dissanayake, S.K., Wade, M., Johnson, C.E., O'Connell, M.P., Leotlela, P.D., French, A.D., Shah, K.V., Hewitt, K.J., Rosenthal, D.T., Indig, F.E., Jiang, Y., Nickoloff, B.J., Taub, D.D., Trent, J.M., Moon, R.T., Bittner, M., and Weeraratna, A.T. 2007. The Wnt5A/protein kinase C pathway mediates motility in melanoma cells via the inhibition of metastasis suppressors and initiation of an epithelial to mesenchymal transition. *J Biol Chem* **282**(23): 17259-17271.

Doerks, T., Bork, P., Kamberov, E., Makarova, O., Muecke, S., and Margolis, B. 2000. L27, a novel heterodimerization domain in receptor targeting proteins Lin-2 and Lin-7. *Trends Biochem Sci* **25**(7): 317-318.

Dollar, G.L., Weber, U., Mlodzik, M., and Sokol, S.Y. 2005. Regulation of Lethal giant larvae by Dishevelled. *Nature* **437**(7063): 1376-1380.

Dow, L.E., Kauffman, J.S., Caddy, J., Zarbalis, K., Peterson, A.S., Jane, S.M., Russell, S.M., and Humbert, P.O. 2007. The tumour-suppressor Scribble dictates cell polarity during directed epithelial migration: regulation of Rho GTPase recruitment to the leading edge. *Oncogene* **26**(16): 2272-2282.

Downward, J. 2003. Targeting RAS signalling pathways in cancer therapy. *Nat Rev Cancer* **3**(1): 11-22.

Downward, J., Graves, J.D., Warne, P.H., Rayter, S., and Cantrell, D.A. 1990. Stimulation of p21ras upon T-cell activation. *Nature* **346**(6286): 719-723.

Drivas, G.T., Shih, A., Coutavas, E., Rush, M.G., and D'Eustachio, P. 1990. Characterization of four novel ras-like genes expressed in a human teratocarcinoma cell line. *Mol Cell Biol* **10**(4): 1793-1798.

Du, S.J., Purcell, S.M., Christian, J.L., McGrew, L.L., and Moon, R.T. 1995. Identification of distinct classes and functional domains of Wnts through expression of wild-type and chimeric proteins in Xenopus embryos. *Mol Cell Biol* **15**(5): 2625-2634.

Easty, D.J., Mitchell, P.J., Patel, K., Florenes, V.A., Spritz, R.A., and Bennett, D.C. 1997. Loss of expression of receptor tyrosine kinase family genes PTK7 and SEK in metastatic melanoma. *Int J Cancer* **71**(6): 1061-1065.

Ebinu, J.O., Bottorff, D.A., Chan, E.Y., Stang, S.L., Dunn, R.J., and Stone, J.C. 1998. RasGRP, a Ras guanyl nucleotide- releasing protein with calcium- and diacylglycerol-binding motifs. *Science* **280**(5366): 1082-1086.

Ehrhardt, A., Ehrhardt, G.R., Guo, X., and Schrader, J.W. 2002. Ras and relatives--job sharing and networking keep an old family together. *Exp Hematol* **30**(10): 1089-1106.

Eisenberg, S., Laude, A.J., Beckett, A.J., Mageean, C.J., Aran, V., Hernandez-Valladares, M., Henis, Y.I., and Prior, I.A. 2013. The role of palmitoylation in regulating Ras localization and function. *Biochem Soc Trans* **41**(1): 79-83.

Elbert, M., Cohen, D., and Musch, A. 2006. PAR1b promotes cell-cell adhesion and inhibits dishevelled-mediated transformation of Madin-Darby canine kidney cells. *Mol Biol Cell* **17**(8): 3345-3355.

Elnemr, A., Yonemura, Y., Bandou, E., Kinoshita, K., Kawamura, T., Takahashi, S., Tochiori, S., Endou, Y., and Sasaki, T. 2003. Expression of collagenase-3 (matrix metalloproteinase-13) in human gastric cancer. *Gastric Cancer* **6**(1): 30-38.

Endo, M., Doi, R., Nishita, M., and Minami, Y. 2012a. Ror family receptor tyrosine kinases regulate the maintenance of neural progenitor cells in the developing neocortex. *J Cell Sci* **125**(Pt 8): 2017-2029.

Endo, M., Nishita, M., and Minami, Y. 2012b. Analysis of Wnt/planar cell polarity pathway in cultured cells. *Methods Mol Biol* **839**: 201-214.

Endo, Y., Wolf, V., Muraiso, K., Kamijo, K., Soon, L., Uren, A., Barshishat-Kupper, M., and Rubin, J.S. 2005. Wnt-3a-dependent cell motility involves RhoA activation and is specifically regulated by dishevelled-2. *J Biol Chem* **280**(1): 777-786.

Enomoto, M., Hayakawa, S., Itsukushima, S., Ren, D.Y., Matsuo, M., Tamada, K., Oneyama, C., Okada, M., Takumi, T., Nishita, M., and Minami, Y. 2009. Autonomous regulation of osteosarcoma cell invasiveness by Wnt5a/Ror2 signaling. *Oncogene* **28**(36): 3197-3208.

Erdmann, J., Grosshennig, A., Braund, P.S., Konig, I.R., Hengstenberg, C., Hall, A.S., Linsel-Nitschke, P., Kathiresan, S., Wright, B., Tregouet, D.A., Cambien, F., Bruse, P., Aherrahrou, Z., Wagner, A.K., Stark, K., Schwartz, S.M., Salomaa, V., Elosua, R., Melander, O., Voight, B.F., O'Donnell, C.J., Peltonen, L., Siscovick, D.S., Altshuler, D., Merlini, P.A., Peyvandi, F., Bernardinelli, L., Ardissino, D., Schillert, A., Blankenberg, S., Zeller, T., Wild, P., Schwarz, D.F., Tiret, L., Perret, C., Schreiber, S., El Mokhtari, N.E., Schafer, A., Marz, W., Renner, W., Bugert, P., Kluter, H., Schrezenmeir, J., Rubin, D., Ball, S.G., Balmforth, A.J., Wichmann, H.E., Meitinger, T., Fischer, M., Meisinger, C., Baumert, J., Peters, A., Ouwehand, W.H., Deloukas, P., Thompson, J.R., Ziegler, A., Samani, N.J., and Schunkert, H. 2009. New susceptibility locus for coronary artery disease on chromosome 3q22.3. *Nat Genet* **41**(3): 280-282.

Erdogan, M., Pozzi, A., Bhowmick, N., Moses, H.L., and Zent, R. 2007. Signaling pathways regulating TC21-induced tumorigenesis. *J Biol Chem* **282**(38): 27713-27720.

Erdogan, M., Pozzi, A., Bhowmick, N., Moses, H.L., and Zent, R.. 2008. Transforming growth factor-beta (TGF-beta) and TGF-beta-associated kinase 1 are required for R-Ras-mediated transformation of mammary epithelial cells. *Cancer Res* **68**(15): 6224-6231.

Etheridge, S.L., Ray, S., Li, S., Hamblet, N.S., Lijam, N., Tsang, M., Greer, J., Kardos, N., Wang, J., Sussman, D.J., Chen, P., and Wynshaw-Boris, A. 2008. Murine dishevelled 3 functions in redundant pathways with dishevelled 1 and 2 in normal cardiac outflow tract, cochlea, and neural tube development. *PLoS Genet* **4**(11): e1000259.

Etienne-Manneville, S. 2006. In vitro assay of primary astrocyte migration as a tool to study Rho GTPase function in cell polarization. *Methods in enzymology* **406**: 565-578.

Erdogan, M., Pozzi, A., Bhowmick, N., Moses, H.L., and Zent, R. 2008. Polarity proteins in migration and invasion. *Oncogene* **27**(55): 6970-6980.

Etienne-Manneville, S. and Hall, A. 2001. Integrin-mediated activation of Cdc42 controls cell polarity in migrating astrocytes through PKCzeta. *Cell* **106**(4): 489-498.

Etienne-Manneville, S. and Hall, A. 2002. Rho GTPases in cell biology. *Nature* **420**(6916): 629-635.

Etienne-Manneville, S. and Hall, A. 2003. Cdc42 regulates GSK-3beta and adenomatous polyposis coli to control cell polarity. *Nature* **421**(6924): 753-756.

Falasca, M., Raimondi, C., and Maffucci, T. 2011. Boyden chamber. *Methods Mol Biol* **769**: 87-95.

Fan, W.T., Koch, C.A., de Hoog, C.L., Fam, N.P., and Moran, M.F. 1998. The exchange factor Ras-GRF2 activates Ras-dependent and Rac-dependent mitogen-activated protein kinase pathways. *Curr Biol* **8**(16): 935-938.

Fanto, M. and McNeill, H. 2004. Planar polarity from flies to vertebrates. *J Cell Sci* **117**(Pt 4): 527-533.

Fedorko, M. 1967. Effect of chloroquine on morphology of cytoplasmic granules in maturing human leukocytes--an ultrastructural study. *J Clin Invest* **46**(12): 1932-1942.

Feiguin, F., Hannus, M., Mlodzik, M., and Eaton, S. 2001. The ankyrin repeat protein Diego mediates Frizzled-dependent planar polarization. *Developmental cell* **1**(1): 93-101.

Feng, Y., Chen, M.H., Moskowitz, I.P., Mendonza, A.M., Vidali, L., Nakamura, F., Kwiatkowski, D.J., and Walsh, C.A. 2006. Filamin A (FLNA) is required for cell-cell contact in vascular development and cardiac morphogenesis. *Proc Natl Acad Sci U S A* **103**(52): 19836-19841.

Fernandez-Borja, M. 2012. A tale of three GTPases and a RIN in endothelial cell adhesion. *Cell Res* **22**(10): 1426-1428.

Fimia, G.M., Stoykova, A., Romagnoli, A., Giunta, L., Di Bartolomeo, S., Nardacci, R., Corazzari, M., Fuoco, C., Ucar, A., Schwartz, P., Gruss, P., Piacentini, M., Chowdhury, K., and Cecconi, F. 2007. Ambra1 regulates autophagy and development of the nervous system. *Nature* **447**(7148): 1121-1125.

Fliegauf, M., Benzing, T., and Omran, H. 2007. When cilia go bad: cilia defects and ciliopathies. *Nat Rev Mol Cell Biol* **8**(11): 880-893.

Foldynova-Trantirkova, S., Sekyrova, P., Tmejova, K., Brumovska, E., Bernatik, O., Blankenfeldt, W., Krejci, P., Kozubik, A., Dolezal, T., Trantirek, L., and Bryja, V. 2010. Breast cancer-specific mutations in CK1epsilon inhibit Wnt/beta-catenin and activate the Wnt/Rac1/JNK and NFAT pathways to decrease cell adhesion and promote cell migration. *Breast Cancer Res* **12**(3): R30.

Ford, C.E., Qian Ma, S.S., Quadir, A., and Ward, R.L. 2012. The dual role of the novel Wnt receptor tyrosine kinase, ROR2, in human carcinogenesis. *Int J Cancer*.

Forrester, W.C., Dell, M., Perens, E., and Garriga, G. 1999. A C. elegans Ror receptor tyrosine kinase regulates cell motility and asymmetric cell division. *Nature* **400**(6747): 881-885.

Fox, J.W., Lamperti, E.D., Eksioglu, Y.Z., Hong, S.E., Feng, Y., Graham, D.A., Scheffer, I.E., Dobyns, W.B., Hirsch, B.A., Radtke, R.A., Berkovic, S.F., Huttenlocher, P.R., and Walsh, C.A. 1998. Mutations in filamin 1 prevent migration of cerebral cortical neurons in human periventricular heterotopia. *Neuron* **21**(6): 1315-1325.

Fradkin, L.G., Dura, J.M., and Noordermeer, J.N. 2010. Ryks: new partners for Wnts in the developing and regenerating nervous system. *Trends Neurosci* **33**(2): 84-92.

Frank, S.R. and Hansen, S.H. 2008. The PIX-GIT complex: a G protein signaling cassette in control of cell shape. *Semin Cell Dev Biol* **19**(3): 234-244.

Franke, B., Akkerman, J.W., and Bos, J.L. 1997. Rapid Ca2+-mediated activation of Rap1 in human platelets. *The EMBO journal* **16**(2): 252-259.

Freije, J.M., Diez-Itza, I., Balbin, M., Sanchez, L.M., Blasco, R., Tolivia, J., and Lopez-Otin, C. 1994. Molecular cloning and expression of collagenase-3, a novel human matrix metalloproteinase produced by breast carcinomas. *J Biol Chem* **269**(24): 16766-16773.

Fuerer, C., Habib, S.J., and Nusse, R. 2010. A study on the interactions between heparan sulfate proteoglycans and Wnt proteins. *Dev Dyn* **239**(1): 184-190.

Fujimura, L., Watanabe-Takano, H., Sato, Y., Tokuhisa, T., and Hatano, M. 2009. Prickle promotes neurite outgrowth via the Dishevelled dependent pathway in C1300 cells. *Neurosci Lett* **467**(1): 6-10.

Fukuda, M. 2008. Regulation of secretory vesicle traffic by Rab small GTPases. *Cell Mol Life Sci* **65**(18): 2801-2813.

Fukuda, T., Chen, L., Endo, T., Tang, L., Lu, D., Castro, J.E., Widhopf, G.F., 2nd, Rassenti, L.Z., Cantwell, M.J., Prussak, C.E., Carson, D.A., and Kipps, T.J. 2008. Antisera induced by infusions of autologous Ad-CD154-leukemia B cells identify ROR1 as an oncofetal antigen and receptor for Wnt5a. *Proc Natl Acad Sci U S A* **105**(8): 3047-3052.

Furuhjelm, J. and Peranen, J. 2003. The C-terminal end of R-Ras contains a focal adhesion targeting signal. *Journal of cell science* **116**(Pt 18): 3729-3738.

Furushima, K., Yamamoto, A., Nagano, T., Shibata, M., Miyachi, H., Abe, T., Ohshima, N., Kiyonari, H., and Aizawa, S. 2007. Mouse homologues of Shisa antagonistic to Wnt and Fgf signalings. *Developmental biology* **306**(2): 480-492.

Gaengel, K. and Mlodzik, M. 2003. Egfr signaling regulates ommatidial rotation and cell motility in the Drosophila eye via MAPK/Pnt signaling and the Ras effector Canoe/AF6. *Development* **130**(22): 5413-5423.

Gan, X.Q., Wang, J.Y., Xi, Y., Wu, Z.L., Li, Y.P., and Li, L. 2008. Nuclear Dvl, c-Jun, beta-catenin, and TCF form a complex leading to stabilization of beta-catenin-TCF interaction. *J Cell Biol* **180**(6): 1087-1100.

Gao, B., Song, H., Bishop, K., Elliot, G., Garrett, L., English, M.A., Andre, P., Robinson, J., Sood, R., Minami, Y., Economides, A.N., and Yang, Y. 2011. Wnt signaling gradients establish planar cell polarity by inducing Vangl2 phosphorylation through Ror2. *Dev Cell* **20**(2): 163-176.

Gao, C., Cao, W., Bao, L., Zuo, W., Xie, G., Cai, T., Fu, W., Zhang, J., Wu, W., Zhang, X., and Chen, Y.G. 2010. Autophagy negatively regulates Wnt signalling by promoting Dishevelled degradation. *Nat Cell Biol* **12**(8): 781-790.

Gao, C. and Chen, Y.G. 2010. Dishevelled: The hub of Wnt signaling. *Cell Signal* **22**(5): 717-727.

Gawecka, J.E., Griffiths, G.S., Ek-Rylander, B., Ramos, J.W., and Matter, M.L. 2010. R-Ras regulates migration through an interaction with filamin A in melanoma cells. *PLoS One* **5**(6): e11269.

Giles, R.H., van Es, J.H., and Clevers, H. 2003. Caught up in a Wnt storm: Wnt signaling in cancer. *Biochim Biophys Acta* **1653**(1): 1-24.

Gobble, R.M., Qin, L.X., Brill, E.R., Angeles, C.V., Ugras, S., O'Connor, R.B., Moraco, N.H., Decarolis, P.L., Antonescu, C., and Singer, S. 2011. Expression profiling of

liposarcoma yields a multigene predictor of patient outcome and identifies genes that contribute to liposarcomagenesis. *Cancer Res* **71**(7): 2697-2705.
Goldfinger, L.E., Ptak, C., Jeffery, E.D., Shabanowitz, J., Han, J., Haling, J.R., Sherman, N.E., Fox, J.W., Hunt, D.F., and Ginsberg, M.H. 2007. An experimentally derived database of candidate Ras-interacting proteins. *Journal of proteome research* **6**(5): 1806-1811.
Goldfinger, L.E., Ptak, C., Jeffery, E.D., Shabanowitz, J., Hunt, D.F., and Ginsberg, M.H. 2006. RLIP76 (RalBP1) is an R-Ras effector that mediates adhesion-dependent Rac activation and cell migration. *J Cell Biol* **174**(6): 877-888.
Golubkov, V.S., Chekanov, A.V., Cieplak, P., Aleshin, A.E., Chernov, A.V., Zhu, W., Radichev, I.A., Zhang, D., Dong, P.D., and Strongin, A.Y. 2010. The Wnt/planar cell polarity protein-tyrosine kinase-7 (PTK7) is a highly efficient proteolytic target of membrane type-1 matrix metalloproteinase: implications in cancer and embryogenesis. *J Biol Chem* **285**(46): 35740-35749.
Gomez, G.A. and Daniotti, J.L. 2005. H-Ras dynamically interacts with recycling endosomes in CHO-K1 cells: involvement of Rab5 and Rab11 in the trafficking of H-Ras to this pericentriolar endocytic compartment. *The Journal of biological chemistry* **280**(41): 34997-35010.
Gonzalez-Sancho, J.M., Brennan, K.R., Castelo-Soccio, L.A., and Brown, A.M. 2004. Wnt proteins induce dishevelled phosphorylation via an LRP5/6- independent mechanism, irrespective of their ability to stabilize beta-catenin. *Mol Cell Biol* **24**(11): 4757-4768.
Goodrich, L.V. and Strutt, D. 2011. Principles of planar polarity in animal development. *Development* **138**(10): 1877-1892.
Gordon, M.D. and Nusse, R. 2006. Wnt signaling: multiple pathways, multiple receptors, and multiple transcription factors. *J Biol Chem* **281**(32): 22429-22433.
Gotoh, T., Niino, Y., Tokuda, M., Hatase, O., Nakamura, S., Matsuda, M., and Hattori, S. 1997. Activation of R-Ras by Ras-guanine nucleotide-releasing factor. *J Biol Chem* **272**(30): 18602-18607.
Graham, S.M., Oldham, S.M., Martin, C.B., Drugan, J.K., Zohn, I.E., Campbell, S., and Der, C.J. 1999. TC21 and Ras share indistinguishable transforming and differentiating activities. *Oncogene* **18**(12): 2107-2116.
Gravel, M., Iliescu, A., Horth, C., Apuzzo, S., and Gros, P. 2010. Molecular and cellular mechanisms underlying neural tube defects in the loop-tail mutant mouse. *Biochemistry* **49**(16): 3445-3455.
Gray, R.S., Roszko, I., and Solnica-Krezel, L. 2011. Planar cell polarity: coordinating morphogenetic cell behaviors with embryonic polarity. *Developmental cell* **21**(1): 120-133.
Green, J.L., Kuntz, S.G., and Sternberg, P.W. 2008. Ror receptor tyrosine kinases: orphans no more. *Trends Cell Biol* **18**(11): 536-544.
Griffiths, G.S., Grundl, M., Allen, J.S., 3rd, and Matter, M.L. 2011. R-Ras interacts with filamin a to maintain endothelial barrier function. *J Cell Physiol* **226**(9): 2287-2296.
Gubb, D. and Garcia-Bellido, A. 1982. A genetic analysis of the determination of cuticular polarity during development in Drosophila melanogaster. *J Embryol Exp Morphol* **68**: 37-57.
Gubb, D., Green, C., Huen, D., Coulson, D., Johnson, G., Tree, D., Collier, S., and Roote, J. 1999. The balance between isoforms of the prickle LIM domain protein is critical for planar polarity in Drosophila imaginal discs. *Genes & development* **13**(17): 2315-2327.
Guirao, B., Meunier, A., Mortaud, S., Aguilar, A., Corsi, J.M., Strehl, L., Hirota, Y., Desoeuvre, A., Boutin, C., Han, Y.G., Mirzadeh, Z., Cremer, H., Montcouquiol, M., Sawamoto, K., and Spassky, N. 2010. Coupling between hydrodynamic forces and planar cell polarity orients mammalian motile cilia. *Nat Cell Biol* **12**(4): 341-350.
Guo, Y., Rubin, E.M., Xie, J., Zi, X., and Hoang, B.H. 2008. Dominant negative LRP5 decreases tumorigenicity and metastasis of osteosarcoma in an animal model. *Clin Orthop Relat Res* **466**(9): 2039-2045.
Guyot, M.C., Bosoi, C.M., Kharfallah, F., Reynolds, A., Drapeau, P., Justice, M., Gros, P., and Kibar, Z. 2011. A novel hypomorphic Looptail allele at the planar cell polarity Vangl2 gene. *Dev Dyn* **240**(4): 839-849.
Habas, R., Dawid, I.B., and He, X. 2003. Coactivation of Rac and Rho by Wnt/Frizzled signaling is required for vertebrate gastrulation. *Genes Dev* **17**(2): 295-309.
Habas, R. and He, X. 2006. Activation of Rho and Rac by Wnt/frizzled signaling. *Methods Enzymol* **406**: 500-511.

Habas, R., Kato, Y., and He, X. 2001. Wnt/Frizzled activation of Rho regulates vertebrate gastrulation and requires a novel Formin homology protein Daam1. *Cell* **107**(7): 843-854.
Halford, M.M., Armes, J., Buchert, M., Meskenaite, V., Grail, D., Hibbs, M.L., Wilks, A.F., Farlie, P.G., Newgreen, D.F., Hovens, C.M., and Stacker, S.A. 2000. Ryk-deficient mice exhibit craniofacial defects associated with perturbed Eph receptor crosstalk. *Nat Genet* **25**(4): 414-418.
Hall-Glenn, F. and Lyons, K.M. 2011. Roles for CCN2 in normal physiological processes. *Cell Mol Life Sci* **68**(19): 3209-3217.
Hall, A. 1998. Rho GTPases and the actin cytoskeleton. *Science* **279**(5350): 509-514.
Hall, A. 2005. Rho GTPases and the control of cell behaviour. *Biochemical Society transactions* **33**(Pt 5): 891-895.
Hall, A. 2012. Rho family GTPases. *Biochem Soc Trans* **40**(6): 1378-1382.
Hamblet, N.S., Lijam, N., Ruiz-Lozano, P., Wang, J., Yang, Y., Luo, Z., Mei, L., Chien, K.R., Sussman, D.J., and Wynshaw-Boris, A. 2002. Dishevelled 2 is essential for cardiac outflow tract development, somite segmentation and neural tube closure. *Development* **129**(24): 5827-5838.
Hamel, B., Monaghan-Benson, E., Rojas, R.J., Temple, B.R., Marston, D.J., Burridge, K., and Sondek, J. 2011. SmgGDS is a guanine nucleotide exchange factor that specifically activates RhoA and RhoC. *J Biol Chem* **286**(14): 12141-12148.
Han, L. and Colicelli, J. 1995. A human protein selected for interference with Ras function interacts directly with Ras and competes with Raf1. *Mol Cell Biol* **15**(3): 1318-1323.
Hanahan, D. and Weinberg, R.A. 2000. The hallmarks of cancer. *Cell* **100**(1): 57-70.
Hanahan, D. and Weinberg, R.A. 2011. Hallmarks of cancer: the next generation. *Cell* **144**(5): 646-674.
Hancock, J.F. 2003. Ras proteins: different signals from different locations. *Nature reviews Molecular cell biology* **4**(5): 373-384.
Hancock, J.F. and Parton, R.G. 2005. Ras plasma membrane signalling platforms. *Biochem J* **389**(Pt 1): 1-11.
Hancock, J.F., Paterson, H., and Marshall, C.J. 1990. A polybasic domain or palmitoylation is required in addition to the CAAX motif to localize p21ras to the plasma membrane. *Cell* **63**(1): 133-139.
Hansen, M., Prior, I.A., Hughes, P.E., Oertli, B., Chou, F.L., Willumsen, B.M., Hancock, J.F., and Ginsberg, M.H. 2003. C-terminal sequences in R-Ras are involved in integrin regulation and in plasma membrane microdomain distribution. *Biochem Biophys Res Commun* **311**(4): 829-838.
Hansen, M., Rusyn, E.V., Hughes, P.E., Ginsberg, M.H., Cox, A.D., and Willumsen, B.M. 2002. R-Ras C-terminal sequences are sufficient to confer R-Ras specificity to H-Ras. *Oncogene* **21**(28): 4448-4461.
Hawkins, P.T., Anderson, K.E., Davidson, K., and Stephens, L.R. 2006. Signalling through Class I PI3Ks in mammalian cells. *Biochemical Society transactions* **34**(Pt 5): 647-662.
He, C. and Klionsky, D.J. 2009. Regulation mechanisms and signaling pathways of autophagy. *Annu Rev Genet* **43**: 67-93.
He, F., Xiong, W., Yu, X., Espinoza-Lewis, R., Liu, C., Gu, S., Nishita, M., Suzuki, K., Yamada, G., Minami, Y., and Chen, Y. 2008. Wnt5a regulates directional cell migration and cell proliferation via Ror2-mediated noncanonical pathway in mammalian palate development. *Development* **135**(23): 3871-3879.
He, X., Semenov, M., Tamai, K., and Zeng, X. 2004. LDL receptor-related proteins 5 and 6 in Wnt/beta-catenin signaling: arrows point the way. *Development* **131**(8): 1663-1677.
Heallen, T., Zhang, M., Wang, J., Bonilla-Claudio, M., Klysik, E., Johnson, R.L., and Martin, J.F. 2011. Hippo pathway inhibits Wnt signaling to restrain cardiomyocyte proliferation and heart size. *Science* **332**(6028): 458-461.
Heasman, S.J. and Ridley, A.J. 2008. Mammalian Rho GTPases: new insights into their functions from in vivo studies. *Nat Rev Mol Cell Biol* **9**(9): 690-701.
Heisenberg, C.P., Tada, M., Rauch, G.J., Saude, L., Concha, M.L., Geisler, R., Stemple, D.L., Smith, J.C., and Wilson, S.W. 2000. Silberblick/Wnt11 mediates convergent extension movements during zebrafish gastrulation. *Nature* **405**(6782): 76-81.
Hemsley, A., Arnheim, N., Toney, M.D., Cortopassi, G., and Galas, D.J. 1989. A simple method for site-directed mutagenesis using the polymerase chain reaction. *Nucleic Acids Res* **17**(16): 6545-6551.

Hendrickx, M. and Leyns, L. 2008. Non-conventional Frizzled ligands and Wnt receptors. *Dev Growth Differ* **50**(4): 229-243.
Herman, I.M. 1993. Actin isoforms. *Curr Opin Cell Biol* **5**(1): 48-55.
Herrmann, C., Martin, G.A., and Wittinghofer, A. 1995. Quantitative analysis of the complex between p21ras and the Ras-binding domain of the human Raf-1 protein kinase. *The Journal of biological chemistry* **270**(7): 2901-2905.
Hino, S., Michiue, T., Asashima, M., and Kikuchi, A. 2003. Casein kinase I epsilon enhances the binding of Dvl-1 to Frat-1 and is essential for Wnt-3a-induced accumulation of beta-catenin. *The Journal of biological chemistry* **278**(16): 14066-14073.
Hodkinson, P.S., Elliott, P.A., Lad, Y., McHugh, B.J., MacKinnon, A.C., Haslett, C., and Sethi, T. 2007. Mammalian NOTCH-1 activates beta1 integrins via the small GTPase R-Ras. *J Biol Chem* **282**(39): 28991-29001.
Holly, S.P., Larson, M.K., and Parise, L.V. 2005. The unique N-terminus of R-ras is required for Rac activation and precise regulation of cell migration. *Mol Biol Cell* **16**(5): 2458-2469.
Hovens, C.M., Stacker, S.A., Andres, A.C., Harpur, A.G., Ziemiecki, A., and Wilks, A.F. 1992. RYK, a receptor tyrosine kinase-related molecule with unusual kinase domain motifs. *Proc Natl Acad Sci U S A* **89**(24): 11818-11822.
Hsieh, J.C., Rattner, A., Smallwood, P.M., and Nathans, J. 1999. Biochemical characterization of Wnt-frizzled interactions using a soluble, biologically active vertebrate Wnt protein. *Proc Natl Acad Sci U S A* **96**(7): 3546-3551.
Huang, H.C. and Klein, P.S. 2004. The Frizzled family: receptors for multiple signal transduction pathways. *Genome Biol* **5**(7): 234.
Huang, Y., Saez, R., Chao, L., Santos, E., Aaronson, S.A., and Chan, A.M. 1995. A novel insertional mutation in the TC21 gene activates its transforming activity in a human leiomyosarcoma cell line. *Oncogene* **11**(7): 1255-1260.
Huff, S.Y., Quilliam, L.A., Cox, A.D., and Der, C.J. 1997. R-Ras is regulated by activators and effectors distinct from those that control Ras function. *Oncogene* **14**(2): 133-143.
Humbert, P.O., Grzeschik, N.A., Brumby, A.M., Galea, R., Elsum, I., and Richardson, H.E. 2008. Control of tumourigenesis by the Scribble/Dlg/Lgl polarity module. *Oncogene* **27**(55): 6888-6907.
Hurlstone, A. and Clevers, H. 2002. T-cell factors: turn-ons and turn-offs. *EMBO J* **21**(10): 2303-2311.
Ikeda, S., Kishida, S., Yamamoto, H., Murai, H., Koyama, S., and Kikuchi, A. 1998. Axin, a negative regulator of the Wnt signaling pathway, forms a complex with GSK-3beta and beta-catenin and promotes GSK-3beta-dependent phosphorylation of beta-catenin. *The EMBO journal* **17**(5): 1371-1384.
Iliescu, A., Gravel, M., Horth, C., Apuzzo, S., and Gros, P. 2011. Transmembrane topology of mammalian planar cell polarity protein Vangl1. *Biochemistry* **50**(12): 2274-2282.
Inoki, K., Ouyang, H., Zhu, T., Lindvall, C., Wang, Y., Zhang, X., Yang, Q., Bennett, C., Harada, Y., Stankunas, K., Wang, C.Y., He, X., MacDougald, O.A., You, M., Williams, B.O., and Guan, K.L. 2006. TSC2 integrates Wnt and energy signals via a coordinated phosphorylation by AMPK and GSK3 to regulate cell growth. *Cell* **126**(5): 955-968.
Iozzo, R.V., Eichstetter, I., and Danielson, K.G. 1995. Aberrant expression of the growth factor Wnt-5A in human malignancy. *Cancer Res* **55**(16): 3495-3499.
Ip, W., Wellman-Labadie, O., Tang, L., Su, M., Yu, R., Dutz, J., Wang, Y., Huang, S., Zhang, X., Huang, C., and Zhou, Y. 2011. Collagen triple helix repeat containing 1 promotes melanoma cell adhesion and survival. *J Cutan Med Surg* **15**(2): 103-110.
Ishitani, T., Kishida, S., Hyodo-Miura, J., Ueno, N., Yasuda, J., Waterman, M., Shibuya, H., Moon, R.T., Ninomiya-Tsuji, J., and Matsumoto, K. 2003. The TAK1-NLK mitogen-activated protein kinase cascade functions in the Wnt-5a/Ca(2+) pathway to antagonize Wnt/beta-catenin signaling. *Mol Cell Biol* **23**(1): 131-139.
Ishitani, T., Ninomiya-Tsuji, J., Nagai, S., Nishita, M., Meneghini, M., Barker, N., Waterman, M., Bowerman, B., Clevers, H., Shibuya, H., and Matsumoto, K. 1999. The TAK1-NLK-MAPK-related pathway antagonizes signalling between beta-catenin and transcription factor TCF. *Nature* **399**(6738): 798-802.
Itoh, K., Brott, B.K., Bae, G.U., Ratcliffe, M.J., and Sokol, S.Y. 2005. Nuclear localization is required for Dishevelled function in Wnt/beta-catenin signaling. *J Biol* **4**(1): 3.

Jaffe, A.B. and Hall, A. 2002. Rho GTPases in transformation and metastasis. *Adv Cancer Res* **84**: 57-80.
Jaffe, A.B. and Hall, A. 2005. Rho GTPases: biochemistry and biology. *Annu Rev Cell Dev Biol* **21**: 247-269.
Jenny, A. 2010. Planar cell polarity signaling in the Drosophila eye. *Curr Top Dev Biol* **93**: 189-227.
Jenny, A., Darken, R.S., Wilson, P.A., and Mlodzik, M. 2003. Prickle and Strabismus form a functional complex to generate a correct axis during planar cell polarity signaling. *EMBO J* **22**(17): 4409-4420.
Jeong, H.W., Nam, J.O., and Kim, I.S. 2005. The COOH-terminal end of R-Ras alters the motility and morphology of breast epithelial cells through Rho/Rho-kinase. *Cancer research* **65**(2): 507-515.
Jessen, J.R., Topczewski, J., Bingham, S., Sepich, D.S., Marlow, F., Chandrasekhar, A., and Solnica-Krezel, L. 2002. Zebrafish trilobite identifies new roles for Strabismus in gastrulation and neuronal movements. *Nature cell biology* **4**(8): 610-615.
Johansson, N., Airola, K., Grenman, R., Kariniemi, A.L., Saarialho-Kere, U., and Kahari, V.M. 1997. Expression of collagenase-3 (matrix metalloproteinase-13) in squamous cell carcinomas of the head and neck. *Am J Pathol* **151**(2): 499-508.
Jordan, J.D., Carey, K.D., Stork, P.J., and Iyengar, R. 1999. Modulation of rap activity by direct interaction of Galpha(o) with Rap1 GTPase-activating protein. *The Journal of biological chemistry* **274**(31): 21507-21510.
Jullien-Flores, V., Dorseuil, O., Romero, F., Letourneur, F., Saragosti, S., Berger, R., Tavitian, A., Gacon, G., and Camonis, J.H. 1995. Bridging Ral GTPase to Rho pathways. RLIP76, a Ral effector with CDC42/Rac GTPase-activating protein activity. *The Journal of biological chemistry* **270**(38): 22473-22477.
Jun, J.I. and Lau, L.F. 2011. Taking aim at the extracellular matrix: CCN proteins as emerging therapeutic targets. *Nat Rev Drug Discov* **10**(12): 945-963.
Jung, H., Kim, H.J., Lee, S.K., Kim, R., Kopachik, W., Han, J.K., and Jho, E.H. 2009. Negative feedback regulation of Wnt signaling by Gbetagamma-mediated reduction of Dishevelled. *Exp Mol Med* **41**(10): 695-706.
Junge, H.J., Yang, S., Burton, J.B., Paes, K., Shu, X., French, D.M., Costa, M., Rice, D.S., and Ye, W. 2009. TSPAN12 regulates retinal vascular development by promoting Norrin- but not Wnt-induced FZD4/beta-catenin signaling. *Cell* **139**(2): 299-311.
Jura, N., Scotto-Lavino, E., Sobczyk, A., and Bar-Sagi, D. 2006. Differential modification of Ras proteins by ubiquitination. *Molecular cell* **21**(5): 679-687.
Kabeya, Y., Mizushima, N., Ueno, T., Yamamoto, A., Kirisako, T., Noda, T., Kominami, E., Ohsumi, Y., and Yoshimori, T. 2000. LC3, a mammalian homologue of yeast Apg8p, is localized in autophagosome membranes after processing. *The EMBO journal* **19**(21): 5720-5728.
Kaech, S.M., Whitfield, C.W., and Kim, S.K. 1998. The LIN-2/LIN-7/LIN-10 complex mediates basolateral membrane localization of the C. elegans EGF receptor LET-23 in vulval epithelial cells. *Cell* **94**(6): 761-771.
Kagermeier-Schenk, B., Wehner, D., Ozhan-Kizil, G., Yamamoto, H., Li, J., Kirchner, K., Hoffmann, C., Stern, P., Kikuchi, A., Schambony, A., and Weidinger, G. 2011. Waif1/5T4 inhibits Wnt/beta-catenin signaling and activates noncanonical Wnt pathways by modifying LRP6 subcellular localization. *Developmental cell* **21**(6): 1129-1143.
Kalabis, J., Rosenberg, I., and Podolsky, D.K. 2006. Vangl1 protein acts as a downstream effector of intestinal trefoil factor (ITF)/TFF3 signaling and regulates wound healing of intestinal epithelium. *J Biol Chem* **281**(10): 6434-6441.
Karner, C.M., Chirumamilla, R., Aoki, S., Igarashi, P., Wallingford, J.B., and Carroll, T.J. 2009. Wnt9b signaling regulates planar cell polarity and kidney tubule morphogenesis. *Nature genetics* **41**(7): 793-799.
Karnoub, A.E. and Weinberg, R.A. 2008. Ras oncogenes: split personalities. *Nat Rev Mol Cell Biol* **9**(7): 517-531.
Katoh, M. 2002. Molecular cloning and characterization of Strabismus 2 (STB2). *Int J Oncol* **20**(5): 993-998.
Kazanskaya, O., Glinka, A., del Barco Barrantes, I., Stannek, P., Niehrs, C., and Wu, W. 2004. R-Spondin2 is a secreted activator of Wnt/beta-catenin signaling and is required for Xenopus myogenesis. *Dev Cell* **7**(4): 525-534.
Kazerounian, S., Gerald, D., Huang, M., Chin, Y.R., Udayakumar, D., Zheng, N., O'Donnell, R.K., Perruzzi, C., Mangiante, L., Pourat, J., Phung, T.L., Bravo-Nuevo, A., Shechter, S., McNamara, S., Duhadaway, J.B., Kocher, O.N., Brown, L.F., Toker, A., Prendergast, G.C., and Benjamin, L.E. 2013. RhoB differentially

controls Akt function in tumor cells and stromal endothelial cells during breast tumorigenesis. *Cancer Res* **73**(1): 50-61.
Keely, P.J., Rusyn, E.V., Cox, A.D., and Parise, L.V. 1999. R-Ras signals through specific integrin alpha cytoplasmic domains to promote migration and invasion of breast epithelial cells. *J Cell Biol* **145**(5): 1077-1088.
Keller, R. 2002. Shaping the vertebrate body plan by polarized embryonic cell movements. *Science* **298**(5600): 1950-1954.
Kelley, G.G., Reks, S.E., Ondrako, J.M., and Smrcka, A.V. 2001. Phospholipase C(epsilon): a novel Ras effector. *EMBO J* **20**(4): 743-754.
Kelly, O.G., Pinson, K.I., and Skarnes, W.C. 2004. The Wnt co-receptors Lrp5 and Lrp6 are essential for gastrulation in mice. *Development* **131**(12): 2803-2815.
Kho, D.H., Bae, J.A., Lee, J.H., Cho, H.J., Cho, S.H., Seo, Y.W., Ahn, K.Y., Chung, I.J., and Kim, K.K. 2009. KITENIN recruits Dishevelled/PKC delta to form a functional complex and controls the migration and invasiveness of colorectal cancer cells. *Gut* **58**(4): 509-519.
Khokhlatchev, A., Rabizadeh, S., Xavier, R., Nedwidek, M., Chen, T., Zhang, X.F., Seed, B., and Avruch, J. 2002. Identification of a novel Ras-regulated proapoptotic pathway. *Curr Biol* **12**(4): 253-265.
Khosravi-Far, R., Campbell, S., Rossman, K.L., and Der, C.J. 1998. Increasing complexity of Ras signal transduction: involvement of Rho family proteins. *Adv Cancer Res* **72**: 57-107.
Khosravi-Far, R., Solski, P.A., Clark, G.J., Kinch, M.S., and Der, C.J. 1995. Activation of Rac1, RhoA, and mitogen-activated protein kinases is required for Ras transformation. *Mol Cell Biol* **15**(11): 6443-6453.
Kibar, Z., Bosoi, C.M., Kooistra, M., Salem, S., Finnell, R.H., De Marco, P., Merello, E., Bassuk, A.G., Capra, V., and Gros, P. 2009. Novel mutations in VANGL1 in neural tube defects. *Hum Mutat* **30**(7): E706-715.
Kibar, Z., Salem, S., Bosoi, C.M., Pauwels, E., De Marco, P., Merello, E., Bassuk, A.G., Capra, V., and Gros, P. 2011. Contribution of VANGL2 mutations to isolated neural tube defects. *Clin Genet* **80**(1): 76-82.
Kibar, Z., Torban, E., McDearmid, J.R., Reynolds, A., Berghout, J., Mathieu, M., Kirillova, I., De Marco, P., Merello, E., Hayes, J.M., Wallingford, J.B., Drapeau, P., Capra, V., and Gros, P. 2007. Mutations in VANGL1 associated with neural-tube defects. *N Engl J Med* **356**(14): 1432-1437.
Kibar, Z., Underhill, D.A., Canonne-Hergaux, F., Gauthier, S., Justice, M.J., and Gros, P. 2001a. Identification of a new chemically induced allele (Lp(m1Jus)) at the loop-tail locus: morphology, histology, and genetic mapping. *Genomics* **72**(3): 331-337.
Kibar, Z., Vogan, K.J., Groulx, N., Justice, M.J., Underhill, D.A., and Gros, P. 2001b. Ltap, a mammalian homolog of Drosophila Strabismus/Van Gogh, is altered in the mouse neural tube mutant Loop-tail. *Nat Genet* **28**(3): 251-255.
Kikuchi, A., Demo, S.D., Ye, Z.H., Chen, Y.W., and Williams, L.T. 1994. ralGDS family members interact with the effector loop of ras p21. *Mol Cell Biol* **14**(11): 7483-7491.
Kikuchi, A. and Yamamoto, H. 2008. Tumor formation due to abnormalities in the beta-catenin-independent pathway of Wnt signaling. *Cancer Sci* **99**(2): 202-208.
Kikuchi, A., Yamamoto, H., and Kishida, S. 2007. Multiplicity of the interactions of Wnt proteins and their receptors. *Cell Signal* **19**(4): 659-671.
Kikuchi, A., Yamamoto, H., and Sato, A. 2009. Selective activation mechanisms of Wnt signaling pathways. *Trends Cell Biol* **19**(3): 119-129.
Kim, G.H., Her, J.H., and Han, J.K. 2008. Ryk cooperates with Frizzled 7 to promote Wnt11-mediated endocytosis and is essential for Xenopus laevis convergent extension movements. *J Cell Biol* **182**(6): 1073-1082.
Kim, H. and McCulloch, C.A. 2011. Filamin A mediates interactions between cytoskeletal proteins that control cell adhesion. *FEBS letters* **585**(1): 18-22.
Kim, K.A., Kakitani, M., Zhao, J., Oshima, T., Tang, T., Binnerts, M., Liu, Y., Boyle, B., Park, E., Emtage, P., Funk, W.D., and Tomizuka, K. 2005. Mitogenic influence of human R-spondin1 on the intestinal epithelium. *Science* **309**(5738): 1256-1259.
Kimmelman, A.C., Nunez Rodriguez, N., and Chan, A.M. 2002. R-Ras3/M-Ras induces neuronal differentiation of PC12 cells through cell-type-specific activation of the mitogen-activated protein kinase cascade. *Mol Cell Biol* **22**(16): 5946-5961.
Kimura, K., Tsuji, T., Takada, Y., Miki, T., and Narumiya, S. 2000. Accumulation of GTP-bound RhoA during cytokinesis and a critical role of ECT2 in this accumulation. *J Biol Chem* **275**(23): 17233-17236.

Kinashi, T., Katagiri, K., Watanabe, S., Vanhaesebroeck, B., Downward, J., and Takatsu, K. 2000. Distinct mechanisms of alpha 5beta 1 integrin activation by Ha-Ras and R-Ras. *J Biol Chem* **275**(29): 22590-22596.

Kinbara, K., Goldfinger, L.E., Hansen, M., Chou, F.L., and Ginsberg, M.H. 2003. Ras GTPases: integrins' friends or foes? *Nat Rev Mol Cell Biol* **4**(10): 767-776.

Kishida, M., Hino, S., Michiue, T., Yamamoto, H., Kishida, S., Fukui, A., Asashima, M., and Kikuchi, A. 2001. Synergistic activation of the Wnt signaling pathway by Dvl and casein kinase Iepsilon. *J Biol Chem* **276**(35): 33147-33155.

Kishida, S., Yamamoto, H., Ikeda, S., Kishida, M., Sakamoto, I., Koyama, S., and Kikuchi, A. 1998. Axin, a negative regulator of the wnt signaling pathway, directly interacts with adenomatous polyposis coli and regulates the stabilization of beta-catenin. *The Journal of biological chemistry* **273**(18): 10823-10826.

Kitagawa, M., Hatakeyama, S., Shirane, M., Matsumoto, M., Ishida, N., Hattori, K., Nakamichi, I., Kikuchi, A., and Nakayama, K. 1999. An F-box protein, FWD1, mediates ubiquitin-dependent proteolysis of beta-catenin. *The EMBO journal* **18**(9): 2401-2410.

Kiyono, M., Kaziro, Y., and Satoh, T. 2000. Induction of rac-guanine nucleotide exchange activity of Ras-GRF1/CDC25(Mm) following phosphorylation by the nonreceptor tyrosine kinase Src. *J Biol Chem* **275**(8): 5441-5446.

Kiyono, M., Satoh, T., and Kaziro, Y. 1999. G protein beta gamma subunit-dependent Rac-guanine nucleotide exchange activity of Ras-GRF1/CDC25(Mm). *Proc Natl Acad Sci U S A* **96**(9): 4826-4831.

Klein, P.S. and Melton, D.A. 1996. A molecular mechanism for the effect of lithium on development. *Proc Natl Acad Sci U S A* **93**(16): 8455-8459.

Klimowski, L.K., Garcia, B.A., Shabanowitz, J., Hunt, D.F., and Virshup, D.M. 2006. Site-specific casein kinase 1epsilon-dependent phosphorylation of Dishevelled modulates beta-catenin signaling. *FEBS J* **273**(20): 4594-4602.

Klingensmith, J., Yang, Y., Axelrod, J.D., Beier, D.R., Perrimon, N., and Sussman, D.J. 1996. Conservation of dishevelled structure and function between flies and mice: isolation and characterization of Dvl2. *Mech Dev* **58**(1-2): 15-26.

Klionsky, D.J. Abeliovich, H. Agostinis, P. Agrawal, D.K. Aliev, G. Askew, D.S. Baba, M. Baehrecke, E.H. Bahr, B.A. Ballabio, A. Bamber, B.A. Bassham, D.C. Bergamini, E. Bi, X. Biard-Piechaczyk, M. Blum, J.S. Bredesen, D.E. Brodsky, J.L. Brumell, J.H. Brunk, U.T. Bursch, W. Camougrand, N. Cebollero, E. Cecconi, F. Chen, Y. Chin, L.S. Choi, A. Chu, C.T. Chung, J. Clarke, P.G. Clark, R.S. Clarke, S.G. Clave, C. Cleveland, J.L. Codogno, P. Colombo, M.I. Coto-Montes, A. Cregg, J.M. Cuervo, A.M. Debnath, J. Demarchi, F. Dennis, P.B. Dennis, P.A. Deretic, V. Devenish, R.J. Di Sano, F. Dice, J.F. Difiglia, M. Dinesh-Kumar, S. Distelhorst, C.W. Djavaheri-Mergny, M. Dorsey, F.C. Droge, W. Dron, M. Dunn, W.A., Jr. Duszenko, M. Eissa, N.T. Elazar, Z. Esclatine, A. Eskelinen, E.L. Fesus, L. Finley, K.D. Fuentes, J.M. Fueyo, J. Fujisaki, K. Galliot, B. Gao, F.B. Gewirtz, D.A. Gibson, S.B. Gohla, A. Goldberg, A.L. Gonzalez, R. Gonzalez-Estevez, C. Gorski, S. Gottlieb, R.A. Haussinger, D. He, Y.W. Heidenreich, K. Hill, J.A. Hoyer-Hansen, M. Hu, X. Huang, W.P. Iwasaki, A. Jaattela, M. Jackson, W.T. Jiang, X. Jin, S. Johansen, T. Jung, J.U. Kadowaki, M. Kang, C. Kelekar, A. Kessel, D.H. Kiel, J.A. Kim, H.P. Kimchi, A. Kinsella, T.J. Kiselyov, K. Kitamoto, K. Knecht, E. Komatsu, M. Kominami, E. Kondo, S. Kovacs, A.L. Kroemer, G. Kuan, C.Y. Kumar, R. Kundu, M. Landry, J. Laporte, M. Le, W. Lei, H.Y. Lenardo, M.J. Levine, B. Lieberman, A. Lim, K.L. Lin, F.C. Liou, W. Liu, L.F. Lopez-Berestein, G. Lopez-Otin, C. Lu, B. Macleod, K.F. Malorni, W. Martinet, W. Matsuoka, K. Mautner, J. Meijer, A.J. Melendez, A. Michels, P. Miotto, G. Mistiaen, W.P. Mizushima, N. Mograbi, B. Monastyrska, I. Moore, M.N. Moreira, P.I. Moriyasu, Y. Motyl, T. Munz, C. Murphy, L.O. Naqvi, N.I. Neufeld, T.P. Nishino, I. Nixon, R.A. Noda, T. Nurnberg, B. Ogawa, M. Oleinick, N.L. Olsen, L.J. Ozpolat, B. Paglin, S. Palmer, G.E. Papassideri, I. Parkes, M. Perlmutter, D.H. Perry, G. Piacentini, M. Pinkas-Kramarski, R. Prescott, M. Proikas-Cezanne, T. Raben, N. Rami, A. Reggiori, F. Rohrer, B. Rubinsztein, D.C. Ryan, K.M. Sadoshima, J. Sakagami, H. Sakai, Y. Sandri, M. Sasakawa, C. Sass, M. Schneider, C. Seglen, P.O. Seleverstov, O. Settleman, J. Shacka, J.J. Shapiro, I.M. Sibirny, A. Silva-Zacarin, E.C. Simon, H.U. Simone, C. Simonsen, A. Smith, M.A. Spanel-Borowski, K. Srinivas, V. Steeves, M. Stenmark, H. Stromhaug, P.E. Subauste, C.S. Sugimoto, S. Sulzer, D. Suzuki, T. Swanson, M.S. Tabas, I. Takeshita, F. Talbot, N.J. Talloczy, Z. Tanaka, K. Tanida, I. Taylor, G.S. Taylor, J.P. Terman, A. Tettamanti, G. Thompson, C.B. Thumm, M. Tolkovsky, A.M. Tooze, S.A. Truant, R. Tumanovska, L.V. Uchiyama, Y. Ueno, T. Uzcategui, N.L.

van der Klei, I. Vaquero, E.C. Vellai, T. Vogel, M.W. Wang, H.G. Webster, P. Wiley, J.W. Xi, Z. Xiao, G. Yahalom, J. Yang, J.M. Yap, G. Yin, X.M. Yoshimori, T. Yu, L. Yue, Z. Yuzaki, M. Zabirnyk, O. Zheng, X. Zhu, X. and Deter, R.L. 2008. Guidelines for the use and interpretation of assays for monitoring autophagy in higher eukaryotes. *Autophagy* **4**(2): 151-175.

Klionsky, D.J., Cuervo, A.M., and Seglen, P.O. 2007. Methods for monitoring autophagy from yeast to human. *Autophagy* **3**(3): 181-206.

Kloog, Y. and Cox, A.D. 2000. RAS inhibitors: potential for cancer therapeutics. *Mol Med Today* **6**(10): 398-402.

Kohn, A.D. and Moon, R.T. 2005. Wnt and calcium signaling: beta-catenin-independent pathways. *Cell Calcium* **38**(3-4): 439-446.

Kolodkin, A.L., Matthes, D.J., and Goodman, C.S. 1993. The semaphorin genes encode a family of transmembrane and secreted growth cone guidance molecules. *Cell* **75**(7): 1389-1399.

Komatsu, M. and Ruoslahti, E. 2005. R-Ras is a global regulator of vascular regeneration that suppresses intimal hyperplasia and tumor angiogenesis. *Nat Med* **11**(12): 1346-1350.

Korinek, V., Barker, N., Willert, K., Molenaar, M., Roose, J., Wagenaar, G., Markman, M., Lamers, W., Destree, O., and Clevers, H. 1998. Two members of the Tcf family implicated in Wnt/beta-catenin signaling during embryogenesis in the mouse. *Mol Cell Biol* **18**(3): 1248-1256.

Kozian, D.H. and Augustin, H.G. 1997. Transcriptional regulation of the Ras-related protein TC21/R-Ras2 in endothelial cells. *FEBS Lett* **414**(2): 239-242.

Krapivinsky, G., Krapivinsky, L., Manasian, Y., Ivanov, A., Tyzio, R., Pellegrino, C., Ben-Ari, Y., Clapham, D.E., and Medina, I. 2003. The NMDA receptor is coupled to the ERK pathway by a direct interaction between NR2B and RasGRF1. *Neuron* **40**(4): 775-784.

Krecicki, T., Fraczek, M., Jelen, M., Podhorska, M., Szkudlarek, T., and Zatonski, T. 2003. Expression of collagenase-1 (MMP-1), collagenase-3 (MMP-13) and tissue inhibitor of matrix metalloproteinase-1 (TIMP-1) in laryngeal squamous cell carcinomas. *Eur Arch Otorhinolaryngol* **260**(9): 494-497.

Kroiher, M., Miller, M.A., and Steele, R.E. 2001. Deceiving appearances: signaling by "dead" and "fractured" receptor protein-tyrosine kinases. *Bioessays* **23**(1): 69-76.

Kruger, R.P., Aurandt, J., and Guan, K.L. 2005. Semaphorins command cells to move. *Nat Rev Mol Cell Biol* **6**(10): 789-800.

Kubota, S. and Takigawa, M. 2011. The role of CCN2 in cartilage and bone development. *J Cell Commun Signal* **5**(3): 209-217.

Kudo, Y., Iizuka, S., Yoshida, M., Tsunematsu, T., Kondo, T., Subarnbhesaj, A., Deraz, E.M., Siriwardena, S.B., Tahara, H., Ishimaru, N., Ogawa, I., and Takata, T. 2012. Matrix metalloproteinase-13 (MMP-13) directly and indirectly promotes tumor angiogenesis. *J Biol Chem* **287**(46): 38716-38728.

Kuhl, M. 2004. The WNT/calcium pathway: biochemical mediators, tools and future requirements. *Front Biosci* **9**: 967-974.

Kuhl, M., Geis, K., Sheldahl, L.C., Pukrop, T., Moon, R.T., and Wedlich, D. 2001. Antagonistic regulation of convergent extension movements in Xenopus by Wnt/beta-catenin and Wnt/Ca2+ signaling. *Mech Dev* **106**(1-2): 61-76.

Kuhl, M., Sheldahl, L.C., Malbon, C.C., and Moon, R.T. 2000a. Ca(2+)/calmodulin-dependent protein kinase II is stimulated by Wnt and Frizzled homologs and promotes ventral cell fates in Xenopus. *J Biol Chem* **275**(17): 12701-12711.

Kuhl, M., Sheldahl, L.C., Park, M., Miller, J.R., and Moon, R.T. 2000b. The Wnt/Ca2+ pathway: a new vertebrate Wnt signaling pathway takes shape. *Trends Genet* **16**(7): 279-283.

Kundu, M. and Thompson, C.B. 2008. Autophagy: basic principles and relevance to disease. *Annu Rev Pathol* **3**: 427-455.

Kurayoshi, M., Oue, N., Yamamoto, H., Kishida, M., Inoue, A., Asahara, T., Yasui, W., and Kikuchi, A. 2006. Expression of Wnt-5a is correlated with aggressiveness of gastric cancer by stimulating cell migration and invasion. *Cancer Res* **66**(21): 10439-10448.

Kuriyama, M., Harada, N., Kuroda, S., Yamamoto, T., Nakafuku, M., Iwamatsu, A., Yamamoto, D., Prasad, R., Croce, C., Canaani, E., and Kaibuchi, K. 1996. Identification of AF-6 and canoe as putative targets for Ras. *J Biol Chem* **271**(2): 607-610.

Kwong, L., Wozniak, M.A., Collins, A.S., Wilson, S.D., and Keely, P.J. 2003. R-Ras promotes focal adhesion formation through focal adhesion kinase and p130(Cas) by a novel mechanism that differs from integrins. *Mol Cell Biol* **23**(3): 933-949.

Laird, D.J., Altshuler-Keylin, S., Kissner, M.D., Zhou, X., and Anderson, K.V. 2011. Ror2 enhances polarity and directional migration of primordial germ cells. *PLoS Genet* **7**(12): e1002428.

Lajoie, P. and Nabi, I.R. 2010. Lipid rafts, caveolae, and their endocytosis. *Int Rev Cell Mol Biol* **282**: 135-163.

Lambert, J.M., Lambert, Q.T., Reuther, G.W., Malliri, A., Siderovski, D.P., Sondek, J., Collard, J.G., and Der, C.J. 2002. Tiam1 mediates Ras activation of Rac by a PI(3)K-independent mechanism. *Nat Cell Biol* **4**(8): 621-625.

Lander, H.M., Milbank, A.J., Tauras, J.M., Hajjar, D.P., Hempstead, B.L., Schwartz, G.D., Kraemer, R.T., Mirza, U.A., Chait, B.T., Burk, S.C., and Quilliam, L.A. 1996. Redox regulation of cell signalling. *Nature* **381**(6581): 380-381.

Lander, H.M., Ogiste, J.S., Pearce, S.F., Levi, R., and Novogrodsky, A. 1995a. Nitric oxide-stimulated guanine nucleotide exchange on p21ras. *The Journal of biological chemistry* **270**(13): 7017-7020.

Lander, H.M., Ogiste, J.S., Teng, K.K., and Novogrodsky, A. 1995b. p21ras as a common signaling target of reactive free radicals and cellular redox stress. *The Journal of biological chemistry* **270**(36): 21195-21198.

Langenhan, T., Promel, S., Mestek, L., Esmaeili, B., Waller-Evans, H., Hennig, C., Kohara, Y., Avery, L., Vakonakis, I., Schnabel, R., and Russ, A.P. 2009. Latrophilin signaling links anterior-posterior tissue polarity and oriented cell divisions in the C. elegans embryo. *Dev Cell* **17**(4): 494-504.

Larive, R.M., Abad, A., Cardaba, C.M., Hernandez, T., Canamero, M., de Alava, E., Santos, E., Alarcon, B., and Bustelo, X.R. 2012. The Ras-like protein R-Ras2/TC21 is important for proper mammary gland development. *Mol Biol Cell* **23**(12): 2373-2387.

Lawrence, P.A., Casal, J., and Struhl, G. 2004. Cell interactions and planar polarity in the abdominal epidermis of Drosophila. *Development* **131**(19): 4651-4664.

Lawrence, P.A. and Shelton, P.M. 1975. The determination of polarity in the developing insect retina. *J Embryol Exp Morphol* **33**(2): 471-486.

Lee, H.K., Chauhan, S.K., Kay, E., and Dana, R. 2011. Flt-1 regulates vascular endothelial cell migration via a protein tyrosine kinase-7-dependent pathway. *Blood* **117**(21): 5762-5771.

Lee, J.H., Cho, E.S., Kim, M.Y., Seo, Y.W., Kho, D.H., Chung, I.J., Kook, H., Kim, N.S., Ahn, K.Y., and Kim, K.K. 2005. Suppression of progression and metastasis of established colon tumors in mice by intravenous delivery of short interfering RNA targeting KITENIN, a metastasis-enhancing protein. *Cancer Res* **65**(19): 8993-9003.

Lee, J.H., Park, S.R., Chay, K.O., Seo, Y.W., Kook, H., Ahn, K.Y., Kim, Y.J., and Kim, K.K. 2004. KAI1 COOH-terminal interacting tetraspanin (KITENIN), a member of the tetraspanin family, interacts with KAI1, a tumor metastasis suppressor, and enhances metastasis of cancer. *Cancer Res* **64**(12): 4235-4243.

Lee, J.K., Bae, J.A., Sun, E.G., Kim, H.D., Yoon, T.M., Kim, K., Lee, J.H., Lim, S.C., and Kim, K.K. 2009. KITENIN increases invasion and migration of mouse squamous cancer cells and promotes pulmonary metastasis in a mouse squamous tumor model. *FEBS Lett* **583**(4): 711-717.

Lee, O.K., Frese, K.K., James, J.S., Chadda, D., Chen, Z.H., Javier, R.T., and Cho, K.O. 2003. Discs-Large and Strabismus are functionally linked to plasma membrane formation. *Nat Cell Biol* **5**(11): 987-993.

Lee, R.H., Iioka, H., Ohashi, M., Iemura, S., Natsume, T., and Kinoshita, N. 2007. XRab40 and XCullin5 form a ubiquitin ligase complex essential for the noncanonical Wnt pathway. *EMBO J* **26**(15): 3592-3606.

Leevers, S.J., Paterson, H.F., and Marshall, C.J. 1994. Requirement for Ras in Raf activation is overcome by targeting Raf to the plasma membrane. *Nature* **369**(6479): 411-414.

Lehto, M., Laitinen, S., Chinetti, G., Johansson, M., Ehnholm, C., Staels, B., Ikonen, E., and Olkkonen, V.M. 2001. The OSBP-related protein family in humans. *Journal of lipid research* **42**(8): 1203-1213.

Lehto, M., Mayranpaa, M.I., Pellinen, T., Ihalmo, P., Lehtonen, S., Kovanen, P.T., Groop, P.H., Ivaska, J., and Olkkonen, V.M. 2008. The R-Ras interaction partner ORP3 regulates cell adhesion. *Journal of cell science* **121**(Pt 5): 695-705.

Lejeune, S., Huguet, E.L., Hamby, A., Poulsom, R., and Harris, A.L. 1995. Wnt5a cloning, expression, and up-regulation in human primary breast cancers. *Clinical cancer research : an official journal of the American Association for Cancer Research* **1**(2): 215-222.

Leonoudakis, D., Conti, L.R., Anderson, S., Radeke, C.M., McGuire, L.M., Adams, M.E., Froehner, S.C., Yates, J.R., 3rd, and Vandenberg, C.A. 2004. Protein trafficking and anchoring complexes revealed by proteomic analysis of inward rectifier potassium channel (Kir2.x)-associated proteins. *J Biol Chem* **279**(21): 22331-22346.

Levental, I., Grzybek, M., and Simons, K. 2010. Greasing their way: lipid modifications determine protein association with membrane rafts. *Biochemistry* **49**(30): 6305-6316.

Lewis, J. and Davies, A. 2002. Planar cell polarity in the inner ear: how do hair cells acquire their oriented structure? *J Neurobiol* **53**(2): 190-201.

Li, C., Chen, H., Hu, L., Xing, Y., Sasaki, T., Villosis, M.F., Li, J., Nishita, M., Minami, Y., and Minoo, P. 2008. Ror2 modulates the canonical Wnt signaling in lung epithelial cells through cooperation with Fzd2. *BMC Mol Biol* **9**: 11.

Li, L., Hutchins, B.I., and Kalil, K. 2009a. Wnt5a induces simultaneous cortical axon outgrowth and repulsive axon guidance through distinct signaling mechanisms. *J Neurosci* **29**(18): 5873-5883.

Li, L., Yuan, H., Xie, W., Mao, J., Caruso, A.M., McMahon, A., Sussman, D.J., and Wu, D. 1999. Dishevelled proteins lead to two signaling pathways. Regulation of LEF-1 and c-Jun N-terminal kinase in mammalian cells. *J Biol Chem* **274**(1): 129-134.

Li, Q., Shen, L., Xin, T., Xiang, W., Chen, W., Gao, Y., Zhu, M., Yu, L., and Li, M. 2009b. Role of Scrib and Dlg in anterior-posterior patterning of the follicular epithelium during Drosophila oogenesis. *BMC Dev Biol* **9**: 60.

Li, X., Zhang, Y., Kang, H., Liu, W., Liu, P., Zhang, J., Harris, S.E., and Wu, D. 2005. Sclerostin binds to LRP5/6 and antagonizes canonical Wnt signaling. *J Biol Chem* **280**(20): 19883-19887.

Li, Z.D., Wu, Y., Bao, Y.L., Yu, C.L., Guan, L.L., Wang, Y.Z., Meng, X.Y., and Li, Y.X. 2009c. Identification and characterization of human ARIP2 and its relation to breast cancer. *Cytokine* **46**(2): 251-259.

Liang, C.C., Park, A.Y., and Guan, J.L. 2007. In vitro scratch assay: a convenient and inexpensive method for analysis of cell migration in vitro. *Nat Protoc* **2**(2): 329-333.

Lijam, N., Paylor, R., McDonald, M.P., Crawley, J.N., Deng, C.X., Herrup, K., Stevens, K.E., Maccaferri, G., McBain, C.J., Sussman, D.J., and Wynshaw-Boris, A. 1997. Social interaction and sensorimotor gating abnormalities in mice lacking Dvl1. *Cell* **90**(5): 895-905.

Lin, S., Baye, L.M., Westfall, T.A., and Slusarski, D.C. 2010. Wnt5b-Ryk pathway provides directional signals to regulate gastrulation movement. *J Cell Biol* **190**(2): 263-278.

Linder, S., Wiesner, C., and Himmel, M. 2011. Degrading devices: invadosomes in proteolytic cell invasion. *Annual review of cell and developmental biology* **27**: 185-211.

Lindqvist, M., Horn, Z., Bryja, V., Schulte, G., Papachristou, P., Ajima, R., Dyberg, C., Arenas, E., Yamaguchi, T.P., Lagercrantz, H., and Ringstedt, T. 2010. Vang-like protein 2 and Rac1 interact to regulate adherens junctions. *J Cell Sci* **123**(Pt 3): 472-483.

Liu, C., Li, Y., Semenov, M., Han, C., Baeg, G.H., Tan, Y., Zhang, Z., Lin, X., and He, X. 2002. Control of beta-catenin phosphorylation/degradation by a dual-kinase mechanism. *Cell* **108**(6): 837-847.

Liu, C., Lin, C., Whitaker, D.T., Bakeri, H., Bulgakov, O.V., Liu, P., Lei, J., Dong, L., Li, T., and Swaroop, A. 2013. Prickle1 is expressed in distinct cell populations of the central nervous system and contributes to neuronal morphogenesis. *Hum Mol Genet*.

Liu, W., Sato, A., Khadka, D., Bharti, R., Diaz, H., Runnels, L.W., and Habas, R. 2008a. Mechanism of activation of the Formin protein Daam1. *Proc Natl Acad Sci U S A* **105**(1): 210-215.

Liu, Y., Bhat, R.A., Seestaller-Wehr, L.M., Fukayama, S., Mangine, A., Moran, R.A., Komm, B.S., Bodine, P.V., and Billiard, J. 2007. The orphan receptor tyrosine kinase Ror2 promotes osteoblast differentiation and enhances ex vivo bone formation. *Mol Endocrinol* **21**(2): 376-387.

Liu, Y., Rubin, B., Bodine, P.V., and Billiard, J. 2008b. Wnt5a induces homodimerization and activation of Ror2 receptor tyrosine kinase. *J Cell Biochem* **105**(2): 497-502.
Lledo, P.M., Johannes, L., Vernier, P., Zorec, R., Darchen, F., Vincent, J.D., Henry, J.P., and Mason, W.T. 1994. Rab3 proteins: key players in the control of exocytosis. *Trends Neurosci* **17**(10): 426-432.
Lockyer, P.J., Bottomley, J.R., Reynolds, J.S., McNulty, T.J., Venkateswarlu, K., Potter, B.V., Dempsey, C.E., and Cullen, P.J. 1997. Distinct subcellular localisations of the putative inositol 1,3,4,5-tetrakisphosphate receptors GAP1IP4BP and GAP1m result from the GAP1IP4BP PH domain directing plasma membrane targeting. *Curr Biol* **7**(12): 1007-1010.
Lockyer, P.J., Kupzig, S., and Cullen, P.J. 2001. CAPRI regulates Ca(2+)-dependent inactivation of the Ras-MAPK pathway. *Current biology : CB* **11**(12): 981-986.
Logan, C.Y. and Nusse, R. 2004. The Wnt signaling pathway in development and disease. *Annu Rev Cell Dev Biol* **20**: 781-810.
Long, J.M., LaPorte, P., Paylor, R., and Wynshaw-Boris, A. 2004. Expanded characterization of the social interaction abnormalities in mice lacking Dvl1. *Genes Brain Behav* **3**(1): 51-62.
Lowe, D.G., Capon, D.J., Delwart, E., Sakaguchi, A.Y., Naylor, S.L., and Goeddel, D.V. 1987. Structure of the human and murine R-ras genes, novel genes closely related to ras proto-oncogenes. *Cell* **48**(1): 137-146.
Lu, K.P., Finn, G., Lee, T.H., and Nicholson, L.K. 2007. Prolyl cis-trans isomerization as a molecular timer. *Nature chemical biology* **3**(10): 619-629.
Lu, W., Yamamoto, V., Ortega, B., and Baltimore, D. 2004a. Mammalian Ryk is a Wnt coreceptor required for stimulation of neurite outgrowth. *Cell* **119**(1): 97-108.
Lu, X., Borchers, A.G., Jolicoeur, C., Rayburn, H., Baker, J.C., and Tessier-Lavigne, M. 2004b. PTK7/CCK-4 is a novel regulator of planar cell polarity in vertebrates. *Nature* **430**(6995): 93-98.
Luo, H., Hao, X., Ge, C., Zhao, F., Zhu, M., Chen, T., Yao, M., He, X., and Li, J. 2010. TC21 promotes cell motility and metastasis by regulating the expression of E-cadherin and N-cadherin in hepatocellular carcinoma. *Int J Oncol* **37**(4): 853-859.
Luukkaa, M., Vihinen, P., Kronqvist, P., Vahlberg, T., Pyrhonen, S., Kahari, V.M., and Grenman, R. 2006. Association between high collagenase-3 expression levels and poor prognosis in patients with head and neck cancer. *Head Neck* **28**(3): 225-234.
Luyten, A., Su, X., Gondela, S., Chen, Y., Rompani, S., Takakura, A., and Zhou, J. 2010. Aberrant regulation of planar cell polarity in polycystic kidney disease. *J Am Soc Nephrol* **21**(9): 1521-1532.
MacDonald, B.T., Tamai, K., and He, X. 2009. Wnt/beta-catenin signaling: components, mechanisms, and diseases. *Dev Cell* **17**(1): 9-26.
Macha, M.A., Matta, A., Sriram, U., Thakkar, A., Shukla, N.K., Datta Gupta, S., and Ralhan, R. 2010. Clinical significance of TC21 overexpression in oral cancer. *J Oral Pathol Med* **39**(6): 477-485.
Macheda, M.L., Sun, W.W., Kugathasan, K., Hogan, B.M., Bower, N.I., Halford, M.M., Zhang, Y.F., Jacques, B.E., Lieschke, G.J., Dabdoub, A., and Stacker, S.A. 2012. The Wnt receptor Ryk plays a role in mammalian planar cell polarity signaling. *J Biol Chem* **287**(35): 29312-29323.
Maestrini, E., Patrosso, C., Mancini, M., Rivella, S., Rocchi, M., Repetto, M., Villa, A., Frattini, A., Zoppe, M., Vezzoni, P., and et al. 1993. Mapping of two genes encoding isoforms of the actin binding protein ABP-280, a dystrophin like protein, to Xq28 and to chromosome 7. *Hum Mol Genet* **2**(6): 761-766.
Mak, B.C., Kenerson, H.L., Aicher, L.D., Barnes, E.A., and Yeung, R.S. 2005. Aberrant beta-catenin signaling in tuberous sclerosis. *Am J Pathol* **167**(1): 107-116.
Malbon, C.C. and Wang, H.Y. 2006. Dishevelled: a mobile scaffold catalyzing development. *Curr Top Dev Biol* **72**: 153-166.
Malliri, A., van der Kammen, R.A., Clark, K., van der Valk, M., Michiels, F., and Collard, J.G. 2002. Mice deficient in the Rac activator Tiam1 are resistant to Ras-induced skin tumours. *Nature* **417**(6891): 867-871.
Mandai, K., Nakanishi, H., Satoh, A., Obaishi, H., Wada, M., Nishioka, H., Itoh, M., Mizoguchi, A., Aoki, T., Fujimoto, T., Matsuda, Y., Tsukita, S., and Takai, Y. 1997. Afadin: A novel actin filament-binding protein with one PDZ domain localized at cadherin-based cell-to-cell adherens junction. *J Cell Biol* **139**(2): 517-528.
Marikawa, Y. and Elinson, R.P. 1998. beta-TrCP is a negative regulator of Wnt/beta-catenin signaling pathway and dorsal axis formation in Xenopus embryos. *Mechanisms of development* **77**(1): 75-80.

Marlow, F., Topczewski, J., Sepich, D., and Solnica-Krezel, L. 2002. Zebrafish Rho kinase 2 acts downstream of Wnt11 to mediate cell polarity and effective convergence and extension movements. *Curr Biol* **12**(11): 876-884.

Marte, B.M., Rodriguez-Viciana, P., Wennstrom, S., Warne, P.H., and Downward, J. 1997. R-Ras can activate the phosphoinositide 3-kinase but not the MAP kinase arm of the Ras effector pathways. *Curr Biol* **7**(1): 63-70.

Martin, D.D., Beauchamp, E., and Berthiaume, L.G. 2011. Post-translational myristoylation: Fat matters in cellular life and death. *Biochimie* **93**(1): 18-31.

Martinez-Martin, N., Fernandez-Arenas, E., Cemerski, S., Delgado, P., Turner, M., Heuser, J., Irvine, D.J., Huang, B., Bustelo, X.R., Shaw, A., and Alarcon, B. 2011. T cell receptor internalization from the immunological synapse is mediated by TC21 and RhoG GTPase-dependent phagocytosis. *Immunity* **35**(2): 208-222.

Masckauchan, T.N., Agalliu, D., Vorontchikhina, M., Ahn, A., Parmalee, N.L., Li, C.M., Khoo, A., Tycko, B., Brown, A.M., and Kitajewski, J. 2006. Wnt5a signaling induces proliferation and survival of endothelial cells in vitro and expression of MMP-1 and Tie-2. *Mol Biol Cell* **17**(12): 5163-5172.

Massimi, P., Zori, P., Roberts, S., and Banks, L. 2012. Differential regulation of cell-cell contact, invasion and anoikis by hScrib and hDlg in keratinocytes. *PLoS One* **7**(7): e40279.

Matern, H., Yang, X., Andrulis, E., Sternglanz, R., Trepte, H.H., and Gallwitz, D. 2000. A novel Golgi membrane protein is part of a GTPase-binding protein complex involved in vesicle targeting. *EMBO J* **19**(17): 4485-4492.

Matheny, S.A., Chen, C., Kortum, R.L., Razidlo, G.L., Lewis, R.E., and White, M.A. 2004. Ras regulates assembly of mitogenic signalling complexes through the effector protein IMP. *Nature* **427**(6971): 256-260.

Matheny, S.A. and White, M.A. 2009. Signaling threshold regulation by the Ras effector IMP. *J Biol Chem* **284**(17): 11007-11011.

Matsui, Y., Kikuchi, A., Araki, S., Hata, Y., Kondo, J., Teranishi, Y., and Takai, Y. 1990. Molecular cloning and characterization of a novel type of regulatory protein (GDI) for smg p25A, a ras p21-like GTP-binding protein. *Mol Cell Biol* **10**(8): 4116-4122.

Matsumoto, K., Asano, T., and Endo, T. 1997. Novel small GTPase M-Ras participates in reorganization of actin cytoskeleton. *Oncogene* **15**(20): 2409-2417.

Matsuzaki, T., Hanai, S., Kishi, H., Liu, Z., Bao, Y., Kikuchi, A., Tsuchida, K., and Sugino, H. 2002. Regulation of endocytosis of activin type II receptors by a novel PDZ protein through Ral/Ral-binding protein 1-dependent pathway. *J Biol Chem* **277**(21): 19008-19018.

Maurer-Stroh, S., Koranda, M., Benetka, W., Schneider, G., Sirota, F.L., and Eisenhaber, F. 2007. Towards complete sets of farnesylated and geranylgeranylated proteins. *PLoS Comput Biol* **3**(4): e66.

McCawley, L.J. and Matrisian, L.M. 2001. Matrix metalloproteinases: they're not just for matrix anymore! *Curr Opin Cell Biol* **13**(5): 534-540.

McCormick, F. 1992. Coupling of ras p21 signalling and GTP hydrolysis by GTPase activating proteins. *Philos Trans R Soc Lond B Biol Sci* **336**(1276): 43-47; discussion 47-48.

McNeill, H. 2010. Planar cell polarity: keeping hairs straight is not so simple. *Cold Spring Harbor perspectives in biology* **2**(2): a003376.

Meller, N., Merlot, S., and Guda, C. 2005. CZH proteins: a new family of Rho-GEFs. *J Cell Sci* **118**(Pt 21): 4937-4946.

Meng, L., Sefah, K., O'Donoghue, M.B., Zhu, G., Shangguan, D., Noorali, A., Chen, Y., Zhou, L., and Tan, W. 2010. Silencing of PTK7 in colon cancer cells: caspase-10-dependent apoptosis via mitochondrial pathway. *PLoS One* **5**(11): e14018.

Mercurio, S., Latinkic, B., Itasaki, N., Krumlauf, R., and Smith, J.C. 2004. Connective-tissue growth factor modulates WNT signalling and interacts with the WNT receptor complex. *Development* **131**(9): 2137-2147.

Merte, J., Jensen, D., Wright, K., Sarsfield, S., Wang, Y., Schekman, R., and Ginty, D.D. 2011. Sec24b selectively sorts Vangl2 to regulate planar cell polarity during neural tube closure. *Nat Cell Biol* **12**(1): 41-46; sup pp 41-48.

Mezzacappa, C., Komiya, Y., and Habas, R. 2012. Activation and function of small GTPases Rho, Rac, and Cdc42 during gastrulation. *Methods Mol Biol* **839**: 119-131.

Michaelis, U.R., Chavakis, E., Kruse, C., Jungblut, B., Kaluza, D., Wandzioch, K., Manavski, Y., Heide, H., Santoni, M.J., Potente, M., Eble, J.A., Borg, J.P., and

Brandes, R.P. 2013. The Polarity Protein Scrib is Essential for Directed Endothelial Cell Migration. *Circ Res*.

Mikels, A.J. and Nusse, R. 2006a. Purified Wnt5a protein activates or inhibits beta-catenin-TCF signaling depending on receptor context. *PLoS Biol* **4**(4): e115.

Mikels, A.J. and Nusse, R. 2006b. Wnts as ligands: processing, secretion and reception. *Oncogene* **25**(57): 7461-7468.

Milburn, M.V., Tong, L., deVos, A.M., Brunger, A., Yamaizumi, Z., Nishimura, S., and Kim, S.H. 1990. Molecular switch for signal transduction: structural differences between active and inactive forms of protooncogenic ras proteins. *Science* **247**(4945): 939-945.

Miller, J.R. 2002. The Wnts. *Genome Biol* **3**(1): REVIEWS3001.

Milner, J.M. and Cawston, T.E. 2005. Matrix metalloproteinase knockout studies and the potential use of matrix metalloproteinase inhibitors in the rheumatic diseases. *Curr Drug Targets Inflamm Allergy* **4**(3): 363-375.

Minami, Y., Oishi, I., Endo, M., and Nishita, M. 2010. Ror-family receptor tyrosine kinases in noncanonical Wnt signaling: their implications in developmental morphogenesis and human diseases. *Dev Dyn* **239**(1): 1-15.

Minden, A., Lin, A., McMahon, M., Lange-Carter, C., Derijard, B., Davis, R.J., Johnson, G.L., and Karin, M. 1994. Differential activation of ERK and JNK mitogen-activated protein kinases by Raf-1 and MEKK. *Science* **266**(5191): 1719-1723.

Mitchell, B., Stubbs, J.L., Huisman, F., Taborek, P., Yu, C., and Kintner, C. 2009. The PCP pathway instructs the planar orientation of ciliated cells in the Xenopus larval skin. *Curr Biol* **19**(11): 924-929.

Mitin, N., Rossman, K.L., and Der, C.J. 2006. Signaling interplay in Ras superfamily function. *Curr Biol* **15**(14): R563-574.

Mitin, N., Rossman, K.L., and Der, C.J. 2012. Identification of a novel actin-binding domain within the Rho guanine nucleotide exchange factor TEM4. *PLoS One* **7**(7): e41876.

Miyazaki, K., Fujita, T., Ozaki, T., Kato, C., Kurose, Y., Sakamoto, M., Kato, S., Goto, T., Itoyama, Y., Aoki, M., and Nakagawara, A. 2004. NEDL1, a novel ubiquitin-protein isopeptide ligase for dishevelled-1, targets mutant superoxide dismutase-1. *J Biol Chem* **279**(12): 11327-11335.

Mizuno-Yamasaki, E., Rivera-Molina, F., and Novick, P. 2012. GTPase networks in membrane traffic. *Annu Rev Biochem* **81**: 637-659.

Mizuno, T., Kaibuchi, K., Yamamoto, T., Kawamura, M., Sakoda, T., Fujioka, H., Matsuura, Y., and Takai, Y. 1991. A stimulatory GDP/GTP exchange protein for smg p21 is active on the post-translationally processed form of c-Ki-ras p21 and rhoA p21. *Proc Natl Acad Sci U S A* **88**(15): 6442-6446.

Mizushima, N. and Klionsky, D.J. 2007. Protein turnover via autophagy: implications for metabolism. *Annu Rev Nutr* **27**: 19-40.

Mizushima, N. and Yoshimori, T. 2007. How to interpret LC3 immunoblotting. *Autophagy* **3**(6): 542-545.

Mizushima, N., Yoshimori, T., and Ohsumi, Y. 2011. The role of Atg proteins in autophagosome formation. *Annual review of cell and developmental biology* **27**: 107-132.

Mlodzik, M. 2002. Planar cell polarization: do the same mechanisms regulate Drosophila tissue polarity and vertebrate gastrulation? *Trends Genet* **18**(11): 564-571.

Mohl, M., Winkler, S., Wieland, T., and Lutz, S. 2006. Gef10--the third member of a Rho-specific guanine nucleotide exchange factor subfamily with unusual protein architecture. *Naunyn Schmiedebergs Arch Pharmacol* **373**(5): 333-341.

Montcouquiol, M., Jones, J.M., and Sans, N. 2008. Detection of planar polarity proteins in mammalian cochlea. *Methods Mol Biol* **468**: 207-219.

Montcouquiol, M., Rachel, R.A., Lanford, P.J., Copeland, N.G., Jenkins, N.A., and Kelley, M.W. 2003. Identification of Vangl2 and Scrb1 as planar polarity genes in mammals. *Nature* **423**(6936): 173-177.

Montcouquiol, M., Sans, N., Huss, D., Kach, J., Dickman, J.D., Forge, A., Rachel, R.A., Copeland, N.G., Jenkins, N.A., Bogani, D., Murdoch, J., Warchol, M.E., Wenthold, R.J., and Kelley, M.W. 2006. Asymmetric localization of Vangl2 and Fz3 indicate novel mechanisms for planar cell polarity in mammals. *J Neurosci* **26**(19): 5265-5275.

Moodie, S.A., Willumsen, B.M., Weber, M.J., and Wolfman, A. 1993. Complexes of Ras.GTP with Raf-1 and mitogen-activated protein kinase kinase. *Science* **260**(5114): 1658-1661.

Moon, R.T., Brown, J.D., and Torres, M. 1997. WNTs modulate cell fate and behavior during vertebrate development. *Trends Genet* **13**(4): 157-162.
Mora, N., Rosales, R., and Rosales, C. 2007. R-Ras promotes metastasis of cervical cancer epithelial cells. *Cancer Immunol Immunother* **56**(4): 535-544.
Moran, M.F., Polakis, P., McCormick, F., Pawson, T., and Ellis, C. 1991. Protein-tyrosine kinases regulate the phosphorylation, protein interactions, subcellular distribution, and activity of p21ras GTPase-activating protein. *Mol Cell Biol* **11**(4): 1804-1812.
Morin, P.J., Sparks, A.B., Korinek, V., Barker, N., Clevers, H., Vogelstein, B., and Kinzler, K.W. 1997. Activation of beta-catenin-Tcf signaling in colon cancer by mutations in beta-catenin or APC. *Science* **275**(5307): 1787-1790.
Moskalenko, S., Henry, D.O., Rosse, C., Mirey, G., Camonis, J.H., and White, M.A. 2002. The exocyst is a Ral effector complex. *Nature cell biology* **4**(1): 66-72.
Moskalenko, S., Tong, C., Rosse, C., Mirey, G., Formstecher, E., Daviet, L., Camonis, J., and White, M.A. 2003. Ral GTPases regulate exocyst assembly through dual subunit interactions. *The Journal of biological chemistry* **278**(51): 51743-51748.
Mossie, K., Jallal, B., Alves, F., Sures, I., Plowman, G.D., and Ullrich, A. 1995. Colon carcinoma kinase-4 defines a new subclass of the receptor tyrosine kinase family. *Oncogene* **11**(10): 2179-2184.
Movilla, N., Crespo, P., and Bustelo, X.R. 1999. Signal transduction elements of TC21, an oncogenic member of the R-Ras subfamily of GTP-binding proteins. *Oncogene* **18**(43): 5860-5869.
Muller-Tidow, C., Schwable, J., Steffen, B., Tidow, N., Brandt, B., Becker, K., Schulze-Bahr, E., Halfter, H., Vogt, U., Metzger, R., Schneider, P.M., Buchner, T., Brandts, C., Berdel, W.E., and Serve, H. 2004. High-throughput analysis of genome-wide receptor tyrosine kinase expression in human cancers identifies potential novel drug targets. *Clin Cancer Res* **10**(4): 1241-1249.
Munoz, R., Moreno, M., Oliva, C., Orbenes, C., and Larrain, J. 2006. Syndecan-4 regulates non-canonical Wnt signalling and is essential for convergent and extension movements in Xenopus embryos. *Nat Cell Biol* **8**(5): 492-500.
Murakami, T., Maki, W., Cardones, A.R., Fang, H., Tun Kyi, A., Nestle, F.O., and Hwang, S.T. 2002. Expression of CXC chemokine receptor-4 enhances the pulmonary metastatic potential of murine B16 melanoma cells. *Cancer research* **62**(24): 7328-7334.
Murdoch, J.N., Henderson, D.J., Doudney, K., Gaston-Massuet, C., Phillips, H.M., Paternotte, C., Arkell, R., Stanier, P., and Copp, A.J. 2003. Disruption of scribble (Scrb1) causes severe neural tube defects in the circletail mouse. *Hum Mol Genet* **12**(2): 87-98.
Murphy, D.A. and Courtneidge, S.A. 2011. The 'ins' and 'outs' of podosomes and invadopodia: characteristics, formation and function. *Nature reviews Molecular cell biology* **12**(7): 413-426.
Muthuswamy, S.K. and Xue, B. 2012. Cell polarity as a regulator of cancer cell behavior plasticity. *Annu Rev Cell Dev Biol* **28**: 599-625.
Na, H.W., Shin, W.S., Ludwig, A., and Lee, S.T. 2012. The cytosolic domain of protein-tyrosine kinase 7 (PTK7), generated from sequential cleavage by a disintegrin and metalloprotease 17 (ADAM17) and gamma-secretase, enhances cell proliferation and migration in colon cancer cells. *J Biol Chem* **287**(30): 25001-25009.
Nagase, H., Enghild, J.J., Suzuki, K., and Salvesen, G. 1990. Stepwise activation mechanisms of the precursor of matrix metalloproteinase 3 (stromelysin) by proteinases and (4-aminophenyl)mercuric acetate. *Biochemistry* **29**(24): 5783-5789.
Nakamura, F., Stossel, T.P., and Hartwig, J.H. 2011. The filamins: organizers of cell structure and function. *Cell Adh Migr* **5**(2): 160-169.
Nakamura, N., Rabouille, C., Watson, R., Nilsson, T., Hui, N., Slusarewicz, P., Kreis, T.E., and Warren, G. 1995. Characterization of a cis-Golgi matrix protein, GM130. *J Cell Biol* **131**(6 Pt 2): 1715-1726.
Nam, J.S., Turcotte, T.J., Smith, P.F., Choi, S., and Yoon, J.K. 2006. Mouse cristin/R-spondin family proteins are novel ligands for the Frizzled 8 and LRP6 receptors and activate beta-catenin-dependent gene expression. *J Biol Chem* **281**(19): 13247-13257.
Narimatsu, M., Bose, R., Pye, M., Zhang, L., Miller, B., Ching, P., Sakuma, R., Luga, V., Roncari, L., Attisano, L., and Wrana, J.L. 2009. Regulation of planar cell polarity by Smurf ubiquitin ligases. *Cell* **137**(2): 295-307.
Neel, N.F., Lapierre, L.A., Goldenring, J.R., and Richmond, A. 2007. RhoB plays an essential role in CXCR2 sorting decisions. *J Cell Sci* **120**(Pt 9): 1559-1571.

Neel, N.F., Martin, T.D., Stratford, J.K., Zand, T.P., Reiner, D.J., and Der, C.J. 2011. The RalGEF-Ral Effector Signaling Network: The Road Less Traveled for Anti-Ras Drug Discovery. *Genes & cancer* **2**(3): 275-287.

Niehrs, C. 2012. The complex world of WNT receptor signalling. *Nat Rev Mol Cell Biol* **13**(12): 767-779.

Nimnual, A. and Bar-Sagi, D. 2002. The two hats of SOS. *Sci STKE* **2002**(145): pe36.

Nishigaki, M., Aoyagi, K., Danjoh, I., Fukaya, M., Yanagihara, K., Sakamoto, H., Yoshida, T., and Sasaki, H. 2005. Discovery of aberrant expression of R-RAS by cancer-linked DNA hypomethylation in gastric cancer using microarrays. *Cancer Res* **65**(6): 2115-2124.

Nishita, M., Enomoto, M., Yamagata, K., and Minami, Y. 2010a. Cell/tissue-tropic functions of Wnt5a signaling in normal and cancer cells. *Trends Cell Biol* **20**(6): 346-354.

Nishita, M., Itsukushima, S., Nomachi, A., Endo, M., Wang, Z., Inaba, D., Qiao, S., Takada, S., Kikuchi, A., and Minami, Y. 2010b. Ror2/Frizzled complex mediates Wnt5a-induced AP-1 activation by regulating Dishevelled polymerization. *Mol Cell Biol* **30**(14): 3610-3619.

Nishita, M., Yoo, S.K., Nomachi, A., Kani, S., Sougawa, N., Ohta, Y., Takada, S., Kikuchi, A., and Minami, Y. 2006. Filopodia formation mediated by receptor tyrosine kinase Ror2 is required for Wnt5a-induced cell migration. *J Cell Biol* **175**(4): 555-562.

Niu, L.J., Xu, R.X., Zhang, P., Du, M.X., and Jiang, X.D. 2012. Suppression of Frizzled-2-mediated Wnt/Ca(2)(+) signaling significantly attenuates intracellular calcium accumulation in vitro and in a rat model of traumatic brain injury. *Neuroscience* **213**: 19-28.

Nobes, C.D. and Hall, A. 1999. Rho GTPases control polarity, protrusion, and adhesion during cell movement. *J Cell Biol* **144**(6): 1235-1244.

Nola, S., Sebbagh, M., Marchetto, S., Osmani, N., Nourry, C., Audebert, S., Navarro, C., Rachel, R., Montcouquiol, M., Sans, N., Etienne-Manneville, S., Borg, J.P., and Santoni, M.J. 2008. Scrib regulates PAK activity during the cell migration process. *Human molecular genetics* **17**(22): 3552-3565.

Nomachi, A., Nishita, M., Inaba, D., Enomoto, M., Hamasaki, M., and Minami, Y. 2008. Receptor tyrosine kinase Ror2 mediates Wnt5a-induced polarized cell migration by activating c-Jun N-terminal kinase via actin-binding protein filamin A. *J Biol Chem* **283**(41): 27973-27981.

Nourry, C., Grant, S.G., and Borg, J.P. 2003. PDZ domain proteins: plug and play! *Sci STKE* **2003**(179): RE7.

Nunez Rodriguez, N., Lee, I.N., Banno, A., Qiao, H.F., Qiao, R.F., Yao, Z., Hoang, T., Kimmelman, A.C., and Chan, A.M. 2006. Characterization of R-ras3/m-ras null mice reveals a potential role in trophic factor signaling. *Mol Cell Biol* **26**(19): 7145-7154.

O'Shaughnessy, R.F., Yeo, W., Gautier, J., Jahoda, C.A., and Christiano, A.M. 2004. The WNT signalling modulator, Wise, is expressed in an interaction-dependent manner during hair-follicle cycling. *J Invest Dermatol* **123**(4): 613-621.

Oertli, B., Han, J., Marte, B.M., Sethi, T., Downward, J., Ginsberg, M., and Hughes, P.E. 2000. The effector loop and prenylation site of R-Ras are involved in the regulation of integrin function. *Oncogene* **19**(43): 4961-4969.

Oh, J.S., Manzerra, P., and Kennedy, M.B. 2004. Regulation of the neuron-specific Ras GTPase-activating protein, synGAP, by Ca2+/calmodulin-dependent protein kinase II. *J Biol Chem* **279**(17): 17980-17988.

Ohba, Y., Mochizuki, N., Yamashita, S., Chan, A.M., Schrader, J.W., Hattori, S., Nagashima, K., and Matsuda, M. 2000. Regulatory proteins of R-Ras, TC21/R-Ras2, and M-Ras/R-Ras3. *J Biol Chem* **275**(26): 20020-20026.

Ohkawara, B., Glinka, A., and Niehrs, C. 2011. Rspo3 binds syndecan 4 and induces Wnt/PCP signaling via clathrin-mediated endocytosis to promote morphogenesis. *Dev Cell* **20**(3): 303-314.

Ohkawara, B., Yamamoto, T.S., Tada, M., and Ueno, N. 2003. Role of glypican 4 in the regulation of convergent extension movements during gastrulation in Xenopus laevis. *Development* **130**(10): 2129-2138.

Ohta, Y., Hartwig, J.H., and Stossel, T.P. 2006. FilGAP, a Rho- and ROCK-regulated GAP for Rac binds filamin A to control actin remodelling. *Nat Cell Biol* **8**(8): 803-814.

Ohta, Y., Suzuki, N., Nakamura, S., Hartwig, J.H., and Stossel, T.P. 1999. The small GTPase RalA targets filamin to induce filopodia. *Proceedings of the National Academy of Sciences of the United States of America* **96**(5): 2122-2128.

Oinuma, I., Ishikawa, Y., Katoh, H., and Negishi, M. 2004. The Semaphorin 4D receptor Plexin-B1 is a GTPase activating protein for R-Ras. *Science* **305**(5685): 862-865.
Oinuma, I., Ito, Y., Katoh, H., and Negishi, M. 2010. Semaphorin 4D/Plexin-B1 stimulates PTEN activity through R-Ras GTPase-activating protein activity, inducing growth cone collapse in hippocampal neurons. *J Biol Chem* **285**(36): 28200-28209.
Oishi, I., Suzuki, H., Onishi, N., Takada, R., Kani, S., Ohkawara, B., Koshida, I., Suzuki, K., Yamada, G., Schwabe, G.C., Mundlos, S., Shibuya, H., Takada, S., and Minami, Y. 2003. The receptor tyrosine kinase Ror2 is involved in non-canonical Wnt5a/JNK signalling pathway. *Genes Cells* **8**(7): 645-654.
Oishi, I., Takeuchi, S., Hashimoto, R., Nagabukuro, A., Ueda, T., Liu, Z.J., Hatta, T., Akira, S., Matsuda, Y., Yamamura, H., Otani, H., and Minami, Y. 1999. Spatio-temporally regulated expression of receptor tyrosine kinases, mRor1, mRor2, during mouse development: implications in development and function of the nervous system. *Genes Cells* **4**(1): 41-56.
Okamoto, K., Narayanan, R., Lee, S.H., Murata, K., and Hayashi, Y. 2007. The role of CaMKII as an F-actin-bundling protein crucial for maintenance of dendritic spine structure. *Proc Natl Acad Sci U S A* **104**(15): 6418-6423.
Okino, K., Nagai, H., Hatta, M., Nagahata, T., Yoneyama, K., Ohta, Y., Jin, E., Kawanami, O., Araki, T., and Emi, M. 2003. Up-regulation and overproduction of DVL-1, the human counterpart of the Drosophila dishevelled gene, in cervical squamous cell carcinoma. *Oncol Rep* **10**(5): 1219-1223.
Oldridge, M., Fortuna, A.M., Maringa, M., Propping, P., Mansour, S., Pollitt, C., DeChiara, T.M., Kimble, R.B., Valenzuela, D.M., Yancopoulos, G.D., and Wilkie, A.O. 2000. Dominant mutations in ROR2, encoding an orphan receptor tyrosine kinase, cause brachydactyly type B. *Nat Genet* **24**(3): 275-278.
Osmani, N., Vitale, N., Borg, J.P., and Etienne-Manneville, S. 2006. Scrib controls Cdc42 localization and activity to promote cell polarization during astrocyte migration. *Current biology : CB* **16**(24): 2395-2405.
Ott, I., Fischer, E.G., Miyagi, Y., Mueller, B.M., and Ruf, W. 1998. A role for tissue factor in cell adhesion and migration mediated by interaction with actin-binding protein 280. *The Journal of cell biology* **140**(5): 1241-1253.
Otto, E.A., Schermer, B., Obara, T., O'Toole, J.F., Hiller, K.S., Mueller, A.M., Ruf, R.G., Hoefele, J., Beekmann, F., Landau, D., Foreman, J.W., Goodship, J.A., Strachan, T., Kispert, A., Wolf, M.T., Gagnadoux, M.F., Nivet, H., Antignac, C., Walz, G., Drummond, I.A., Benzing, T., and Hildebrandt, F. 2003. Mutations in INVS encoding inversin cause nephronophthisis type 2, linking renal cystic disease to the function of primary cilia and left-right axis determination. *Nat Genet* **34**(4): 413-420.
Park, M. and Moon, R.T. 2002. The planar cell-polarity gene stbm regulates cell behaviour and cell fate in vertebrate embryos. *Nat Cell Biol* **4**(1): 20-25.
Pasterkamp, R.J. 2005. R-Ras fills another GAP in semaphorin signalling. *Trends Cell Biol* **15**(2): 61-64.
Patthy, L. 2000. The WIF module. *Trends Biochem Sci* **25**(1): 12-13.
Pei, J. and Grishin, N.V. 2012. Unexpected diversity in Shisa-like proteins suggests the importance of their roles as transmembrane adaptors. *Cellular signalling* **24**(3): 758-769.
Pendas, A.M., Uria, J.A., Jimenez, M.G., Balbin, M., Freije, J.P., and Lopez-Otin, C. 2000. An overview of collagenase-3 expression in malignant tumors and analysis of its potential value as a target in antitumor therapies. *Clin Chim Acta* **291**(2): 137-155.
Peradziryi, H., Kaplan, N.A., Podleschny, M., Liu, X., Wehner, P., Borchers, A., and Tolwinski, N.S. 2011. PTK7/Otk interacts with Wnts and inhibits canonical Wnt signalling. *EMBO J* **30**(18): 3729-3740.
Peradziryi, H., Tolwinski, N.S., and Borchers, A. 2012. The many roles of PTK7: a versatile regulator of cell-cell communication. *Arch Biochem Biophys* **524**(1): 71-76.
Peters, J.M., McKay, R.M., McKay, J.P., and Graff, J.M. 1999. Casein kinase I transduces Wnt signals. *Nature* **401**(6751): 345-350.
Pfeffer, S.R. 2001. Rab GTPases: specifying and deciphering organelle identity and function. *Trends in cell biology* **11**(12): 487-491.
Phillips, H.M., Murdoch, J.N., Chaudhry, B., Copp, A.J., and Henderson, D.J. 2005. Vangl2 acts via RhoA signaling to regulate polarized cell movements during development of the proximal outflow tract. *Circ Res* **96**(3): 292-299.

Piccolo, S., Agius, E., Leyns, L., Bhattacharyya, S., Grunz, H., Bouwmeester, T., and De Robertis, E.M. 1999. The head inducer Cerberus is a multifunctional antagonist of Nodal, BMP and Wnt signals. *Nature* **397**(6721): 707-710.

Pinson, K.I., Brennan, J., Monkley, S., Avery, B.J., and Skarnes, W.C. 2000. An LDL-receptor-related protein mediates Wnt signalling in mice. *Nature* **407**(6803): 535-538.

Ponting, C.P. 1997. Evidence for PDZ domains in bacteria, yeast, and plants. *Protein Sci* **6**(2): 464-468.

Ponting, C.P. and Benjamin, D.R. 1996. A novel family of Ras-binding domains. *Trends in biochemical sciences* **21**(11): 422-425.

Pozzi, A., Coffa, S., Bulus, N., Zhu, W., Chen, D., Chen, X., Mernaugh, G., Su, Y., Cai, S., Singh, A., Brissova, M., and Zent, R. 2006. H-Ras, R-Ras, and TC21 differentially regulate ureteric bud cell branching morphogenesis. *Mol Biol Cell* **17**(4): 2046-2056.

Prebet, T., Lhoumeau, A.C., Arnoulet, C., Aulas, A., Marchetto, S., Audebert, S., Puppo, F., Chabannon, C., Sainty, D., Santoni, M.J., Sebbagh, M., Summerour, V., Huon, Y., Shin, W.S., Lee, S.T., Esterni, B., Vey, N., and Borg, J.P. 2010. The cell polarity PTK7 receptor acts as a modulator of the chemotherapeutic response in acute myeloid leukemia and impairs clinical outcome. *Blood* **116**(13): 2315-2323.

Prior, I.A., Harding, A., Yan, J., Sluimer, J., Parton, R.G., and Hancock, J.F. 2001. GTP-dependent segregation of H-ras from lipid rafts is required for biological activity. *Nature cell biology* **3**(4): 368-375.

Pukrop, T., Klemm, F., Hagemann, T., Gradl, D., Schulz, M., Siemes, S., Trumper, L., and Binder, C. 2006. Wnt 5a signaling is critical for macrophage-induced invasion of breast cancer cell lines. *Proc Natl Acad Sci U S A* **103**(14): 5454-5459.

Putz, U., Howitt, J., Lackovic, J., Foot, N., Kumar, S., Silke, J., and Tan, S.S. 2008. Nedd4 family-interacting protein 1 (Ndfip1) is required for the exosomal secretion of Nedd4 family proteins. *J Biol Chem* **283**(47): 32621-32627.

Pyagay, P., Heroult, M., Wang, Q., Lehnert, W., Belden, J., Liaw, L., Friesel, R.E., and Lindner, V. 2005. Collagen triple helix repeat containing 1, a novel secreted protein in injured and diseased arteries, inhibits collagen expression and promotes cell migration. *Circ Res* **96**(2): 261-268.

Qian, D., Jones, C., Rzadzinska, A., Mark, S., Zhang, X., Steel, K.P., Dai, X., and Chen, P. 2007. Wnt5a functions in planar cell polarity regulation in mice. *Dev Biol* **306**(1): 121-133.

Qin, Y., Capaldo, C., Gumbiner, B.M., and Macara, I.G. 2005a. The mammalian Scribble polarity protein regulates epithelial cell adhesion and migration through E-cadherin. *J Cell Biol* **171**(6): 1061-1071.

Qin, Y., Capaldo, C., Gumbiner, B.M., and Macara, I.G. 2005b. The mammalian Scribble polarity protein regulates epithelial cell adhesion and migration through E-cadherin. *The Journal of cell biology* **171**(6): 1061-1071.

Quilliam, L.A., Rebhun, J.F., and Castro, A.F. 2002. A growing family of guanine nucleotide exchange factors is responsible for activation of Ras-family GTPases. *Prog Nucleic Acid Res Mol Biol* **71**: 391-444.

Radhakrishna, H., Al-Awar, O., Khachikian, Z., and Donaldson, J.G. 1999. ARF6 requirement for Rac ruffling suggests a role for membrane trafficking in cortical actin rearrangements. *Journal of cell science* **112 (Pt 6)**: 855-866.

Raftopoulou, M. and Hall, A. 2004. Cell migration: Rho GTPases lead the way. *Dev Biol* **265**(1): 23-32.

Rajagopalan, H., Bardelli, A., Lengauer, C., Kinzler, K.W., Vogelstein, B., and Velculescu, V.E. 2002. Tumorigenesis: RAF/RAS oncogenes and mismatch-repair status. *Nature* **418**(6901): 934.

Rattner, A., Hsieh, J.C., Smallwood, P.M., Gilbert, D.J., Copeland, N.G., Jenkins, N.A., and Nathans, J. 1997. A family of secreted proteins contains homology to the cysteine-rich ligand-binding domain of frizzled receptors. *Proc Natl Acad Sci U S A* **94**(7): 2859-2863.

Rawls, A.S. and Wolff, T. 2003. Strabismus requires Flamingo and Prickle function to regulate tissue polarity in the Drosophila eye. *Development* **130**(9): 1877-1887.

Ren, X.D. and Schwartz, M.A. 2000. Determination of GTP loading on Rho. *Methods Enzymol* **325**: 264-272.

Repasky, G.A., Chenette, E.J., and Der, C.J. 2004. Renewing the conspiracy theory debate: does Raf function alone to mediate Ras oncogenesis? *Trends Cell Biol* **14**(11): 639-647.

Resat, H., Straatsma, T.P., Dixon, D.A., and Miller, J.H. 2001. The arginine finger of RasGAP helps Gln-61 align the nucleophilic water in GAP-stimulated hydrolysis of GTP. *Proc Natl Acad Sci U S A* **98**(11): 6033-6038.

Resh, M.D. 1999. Fatty acylation of proteins: new insights into membrane targeting of myristoylated and palmitoylated proteins. *Biochimica et biophysica acta* **1451**(1): 1-16.

Rey, I., Taylor-Harris, P., van Erp, H., and Hall, A. 1994. R-ras interacts with rasGAP, neurofibromin and c-raf but does not regulate cell growth or differentiation. *Oncogene* **9**(3): 685-692.

Reya, T. and Clevers, H. 2005. Wnt signalling in stem cells and cancer. *Nature* **434**(7035): 843-850.

Reynolds, A., McDearmid, J.R., Lachance, S., De Marco, P., Merello, E., Capra, V., Gros, P., Drapeau, P., and Kibar, Z. 2010. VANGL1 rare variants associated with neural tube defects affect convergent extension in zebrafish. *Mech Dev* **127**(7-8): 385-392.

Richardson, M.M., Jennings, L.K., and Zhang, X.A. 2011. Tetraspanins and tumor progression. *Clin Exp Metastasis* **28**(3): 261-270.

Rida, P.C. and Chen, P. 2009. Line up and listen: Planar cell polarity regulation in the mammalian inner ear. *Seminars in cell & developmental biology* **20**(8): 978-985.

Ridley, A.J. 1999. Rho family proteins and regulation of the actin cytoskeleton. *Prog Mol Subcell Biol* **22**: 1-22.

Ridley, A.J. 2001a. Rho family proteins: coordinating cell responses. *Trends Cell Biol* **11**(12): 471-477.

Ridley, A.J. 2001b. Rho GTPases and cell migration. *Journal of cell science* **114**(Pt 15): 2713-2722.

Ridley, A.J. 2001c. Rho proteins: linking signaling with membrane trafficking. *Traffic* **2**(5): 303-310.

Ridley, A.J. 2006. Rho GTPases and actin dynamics in membrane protrusions and vesicle trafficking. *Trends Cell Biol* **16**(10): 522-529.

Ridley, A.J. 2011. Life at the leading edge. *Cell* **145**(7): 1012-1022.

Ridley, A.J. and Hall, A. 1992. The small GTP-binding protein rho regulates the assembly of focal adhesions and actin stress fibers in response to growth factors. *Cell* **70**(3): 389-399.

Ridley, A.J., Schwartz, M.A., Burridge, K., Firtel, R.A., Ginsberg, M.H., Borisy, G., Parsons, J.T., and Horwitz, A.R. 2003. Cell migration: integrating signals from front to back. *Science* **302**(5651): 1704-1709.

Rincon-Arano, H., Rosales, R., Mora, N., Rodriguez-Castaneda, A., and Rosales, C. 2003. R-Ras promotes tumor growth of cervical epithelial cells. *Cancer* **97**(3): 575-585.

Rivera, C., Simonson, S.J., Yamben, I.F., Shatadal, S., Nguyen, M.M., Beurg, M., Lambert, P.F., and Griep, A.E. 2013. Requirement for Dlgh-1 in planar cell polarity and skeletogenesis during vertebrate development. *PLoS One* **8**(1): e54410.

Roberts, P.J. and Der, C.J. 2007. Targeting the Raf-MEK-ERK mitogen-activated protein kinase cascade for the treatment of cancer. *Oncogene* **26**(22): 3291-3310.

Robinson, A., Escuin, S., Doudney, K., Vekemans, M., Stevenson, R.E., Greene, N.D., Copp, A.J., and Stanier, P. 2011. Mutations in the planar cell polarity genes CELSR1 and SCRIB are associated with the severe neural tube defect craniorachischisis. *Hum Mutat* **33**(2): 440-447.

Robitaille, J., MacDonald, M.L., Kaykas, A., Sheldahl, L.C., Zeisler, J., Dube, M.P., Zhang, L.H., Singaraja, R.R., Guernsey, D.L., Zheng, B., Siebert, L.F., Hoskin-Mott, A., Trese, M.T., Pimstone, S.N., Shastry, B.S., Moon, R.T., Hayden, M.R., Goldberg, Y.P., and Samuels, M.E. 2002. Mutant frizzled-4 disrupts retinal angiogenesis in familial exudative vitreoretinopathy. *Nat Genet* **32**(2): 326-330.

Rodriguez-Viciana, P. and McCormick, F. 2006. Characterization of interactions between ras family GTPases and their effectors. *Methods in enzymology* **407**: 187-194.

Rodriguez-Viciana, P., Oses-Prieto, J., Burlingame, A., Fried, M., and McCormick, F. 2006. A phosphatase holoenzyme comprised of Shoc2/Sur8 and the catalytic subunit of PP1 functions as an M-Ras effector to modulate Raf activity. *Mol Cell* **22**(2): 217-230.

Rodriguez-Viciana, P., Sabatier, C., and McCormick, F. 2004. Signaling specificity by Ras family GTPases is determined by the full spectrum of effectors they regulate. *Mol Cell Biol* **24**(11): 4943-4954.

Rodriguez-Viciana, P., Tetsu, O., Oda, K., Okada, J., Rauen, K., and McCormick, F. 2005. Cancer targets in the Ras pathway. *Cold Spring Harb Symp Quant Biol* **70**: 461-467.

Rodriguez-Viciana, P., Warne, P.H., Dhand, R., Vanhaesebroeck, B., Gout, I., Fry, M.J., Waterfield, M.D., and Downward, J. 1994. Phosphatidylinositol-3-OH kinase as a direct target of Ras. *Nature* **370**(6490): 527-532.

Rodriguez-Viciana, P., Warne, P.H., Khwaja, A., Marte, B.M., Pappin, D., Das, P., Waterfield, M.D., Ridley, A., and Downward, J. 1997. Role of phosphoinositide 3-OH kinase in cell transformation and control of the actin cytoskeleton by Ras. *Cell* **89**(3): 457-467.

Roeb, E., Arndt, M., Jansen, B., Schumpelick, V., and Matern, S. 2004. Simultaneous determination of matrix metalloproteinase (MMP)-7, MMP-1, -3, and -13 gene expression by multiplex PCR in colorectal carcinomas. *Int J Colorectal Dis* **19**(6): 518-524.

Rojas, R.J. and Santos, E., ed. 2006. *Proteins and Cell Regulation*. Springer.

Rosenfeld, J., Capdevielle, J., Guillemot, J.C., and Ferrara, P. 1992. In-gel digestion of proteins for internal sequence analysis after one- or two-dimensional gel electrophoresis. *Anal Biochem* **203**(1): 173-179.

Rossman, K.L., Der, C.J., and Sondek, J. 2005. GEF means go: turning on RHO GTPases with guanine nucleotide-exchange factors. *Nature reviews Molecular cell biology* **6**(2): 167-180.

Rosso, S.B., Sussman, D., Wynshaw-Boris, A., and Salinas, P.C. 2005. Wnt signaling through Dishevelled, Rac and JNK regulates dendritic development. *Nat Neurosci* **8**(1): 34-42.

Roszko, I., Sawada, A., and Solnica-Krezel, L. 2009. Regulation of convergence and extension movements during vertebrate gastrulation by the Wnt/PCP pathway. *Seminars in cell & developmental biology* **20**(8): 986-997.

Rothbacher, U., Laurent, M.N., Deardorff, M.A., Klein, P.S., Cho, K.W., and Fraser, S.E. 2000. Dishevelled phosphorylation, subcellular localization and multimerization regulate its role in early embryogenesis. *EMBO J* **19**(5): 1010-1022.

Rowe, A. and Jackson, P. 2006. Expression of KITENIN, a KAI1/CD82 binding protein and metastasis enhancer, in bladder cancer cell lines: relationship to KAI1/CD82 levels and invasive behaviour. *Oncol Rep* **16**(6): 1267-1272.

Rubinstein, E. 2011. The complexity of tetraspanins. *Biochem Soc Trans* **39**(2): 501-505.

Rumenapp, U., Freichel-Blomquist, A., Wittinghofer, B., Jakobs, K.H., and Wieland, T. 2002. A mammalian Rho-specific guanine-nucleotide exchange factor (p164-RhoGEF) without a pleckstrin homology domain. *Biochem J* **366**(Pt 3): 721-728.

Ryu, H.S., Park, Y.L., Park, S.J., Lee, J.H., Cho, S.B., Lee, W.S., Chung, I.J., Kim, K.K., Lee, K.H., Kweon, S.S., and Joo, Y.E. 2010. KITENIN is associated with tumor progression in human gastric cancer. *Anticancer Res* **30**(9): 3479-3486.

Sabio, G., Arthur, J.S., Kuma, Y., Peggie, M., Carr, J., Murray-Tait, V., Centeno, F., Goedert, M., Morrice, N.A., and Cuenda, A. 2005. p38gamma regulates the localisation of SAP97 in the cytoskeleton by modulating its interaction with GKAP. *EMBO J* **24**(6): 1134-1145.

Saez, R., Chan, A.M., Miki, T., and Aaronson, S.A. 1994. Oncogenic activation of human R-ras by point mutations analogous to those of prototype H-ras oncogenes. *Oncogene* **9**(10): 2977-2982.

Saito, Y., Oinuma, I., Fujimoto, S., and Negishi, M. 2009. Plexin-B1 is a GTPase activating protein for M-Ras, remodelling dendrite morphology. *EMBO Rep* **10**(6): 614-621.

Sakanaka, C., Leong, P., Xu, L., Harrison, S.D., and Williams, L.T. 1999. Casein kinase iepsilon in the wnt pathway: regulation of beta-catenin function. *Proc Natl Acad Sci U S A* **96**(22): 12548-12552.

Sakane, H., Yamamoto, H., Matsumoto, S., Sato, A., and Kikuchi, A. 2012. Localization of glypican-4 in different membrane microdomains is involved in the regulation of Wnt signaling. *J Cell Sci* **125**(Pt 2): 449-460.

Sala-Valdes, M., Ailane, N., Greco, C., Rubinstein, E., and Boucheix, C. 2012. Targeting tetraspanins in cancer. *Expert Opin Ther Targets* **16**(10): 985-997.

Sanchez-Alvarez, L., Visanuvimol, J., McEwan, A., Su, A., Imai, J.H., and Colavita, A. 2011. VANG-1 and PRKL-1 cooperate to negatively regulate neurite formation in Caenorhabditis elegans. *PLoS Genet* **7**(9): e1002257.

Sandilands, E., Brunton, V.G., and Frame, M.C. 2007. The membrane targeting and spatial activation of Src, Yes and Fyn is influenced by palmitoylation and distinct RhoB/RhoD endosome requirements. *J Cell Sci* **120**(Pt 15): 2555-2564.

Sandri, C., Caccavari, F., Valdembri, D., Camillo, C., Veltel, S., Santambrogio, M., Lanzetti, L., Bussolino, F., Ivaska, J., and Serini, G. 2012. The R-Ras/RIN2/Rab5 complex controls endothelial cell adhesion and morphogenesis via active integrin endocytosis and Rac signaling. *Cell Res* **22**(10): 1479-1501.

Santy, L.C. and Casanova, J.E. 2001. Activation of ARF6 by ARNO stimulates epithelial cell migration through downstream activation of both Rac1 and phospholipase D. *The Journal of cell biology* **154**(3): 599-610.

Saras, J. and Heldin, C.H. 1996. PDZ domains bind carboxy-terminal sequences of target proteins. *Trends Biochem Sci* **21**(12): 455-458.

Sarkar, S., Perlstein, E.O., Imarisio, S., Pineau, S., Cordenier, A., Maglathlin, R.L., Webster, J.A., Lewis, T.A., O'Kane, C.J., Schreiber, S.L., and Rubinsztein, D.C. 2007. Small molecules enhance autophagy and reduce toxicity in Huntington's disease models. *Nat Chem Biol* **3**(6): 331-338.

Sasaki, A.T., Carracedo, A., Locasale, J.W., Anastasiou, D., Takeuchi, K., Kahoud, E.R., Haviv, S., Asara, J.M., Pandolfi, P.P., and Cantley, L.C. 2011. Ubiquitination of K-Ras enhances activation and facilitates binding to select downstream effectors. *Science signaling* **4**(163): ra13.

Sato, A., Yamamoto, H., Sakane, H., Koyama, H., and Kikuchi, A. 2010. Wnt5a regulates distinct signalling pathways by binding to Frizzled2. *EMBO J* **29**(1): 41-54.

Sawada, J., Urakami, T., Li, F., Urakami, A., Zhu, W., Fukuda, M., Li, D.Y., Ruoslahti, E., and Komatsu, M. 2012. Small GTPase R-Ras regulates integrity and functionality of tumor blood vessels. *Cancer Cell* **22**(2): 235-249.

Schlessinger, K., Hall, A., and Tolwinski, N. 2009. Wnt signaling pathways meet Rho GTPases. *Genes Dev* **23**(3): 265-277.

Schlessinger, K., McManus, E.J., and Hall, A. 2007. Cdc42 and noncanonical Wnt signal transduction pathways cooperate to promote cell polarity. *J Cell Biol* **178**(3): 355-361.

Schmidt, A. and Hall, A. 2002. Guanine nucleotide exchange factors for Rho GTPases: turning on the switch. *Genes Dev* **16**(13): 1587-1609.

Schulte, G. and Bryja, V. 2007. The Frizzled family of unconventional G-protein-coupled receptors. *Trends Pharmacol Sci* **28**(10): 518-525.

Schulte, G., Bryja, V., Rawal, N., Castelo-Branco, G., Sousa, K.M., and Arenas, E. 2005. Purified Wnt-5a increases differentiation of midbrain dopaminergic cells and dishevelled phosphorylation. *J Neurochem* **92**(6): 1550-1553.

Schwabe, G.C., Tinschert, S., Buschow, C., Meinecke, P., Wolff, G., Gillessen-Kaesbach, G., Oldridge, M., Wilkie, A.O., Komec, R., and Mundlos, S. 2000. Distinct mutations in the receptor tyrosine kinase gene ROR2 cause brachydactyly type B. *Am J Hum Genet* **67**(4): 822-831.

Schwarz-Romond, T., Fiedler, M., Shibata, N., Butler, P.J., Kikuchi, A., Higuchi, Y., and Bienz, M. 2007. The DIX domain of Dishevelled confers Wnt signaling by dynamic polymerization. *Nat Struct Mol Biol* **14**(6): 484-492.

Schwarz-Romond, T., Merrifield, C., Nichols, B.J., and Bienz, M. 2005. The Wnt signalling effector Dishevelled forms dynamic protein assemblies rather than stable associations with cytoplasmic vesicles. *J Cell Sci* **118**(Pt 22): 5269-5277.

Seglen, P.O. and Gordon, P.B. 1982. 3-Methyladenine: specific inhibitor of autophagic/lysosomal protein degradation in isolated rat hepatocytes. *Proceedings of the National Academy of Sciences of the United States of America* **79**(6): 1889-1892.

Seifert, J.R. and Mlodzik, M. 2007. Frizzled/PCP signalling: a conserved mechanism regulating cell polarity and directed motility. *Nat Rev Genet* **8**(2): 126-138.

Self, A.J., Caron, E., Paterson, H.F., and Hall, A. 2001. Analysis of R-Ras signalling pathways. *J Cell Sci* **114**(Pt 7): 1357-1366.

Self, A.J., Paterson, H.F., and Hall, A. 1993. Different structural organization of Ras and Rho effector domains. *Oncogene* **8**(3): 655-661.

Semenov, M., Tamai, K., and He, X. 2005. SOST is a ligand for LRP5/LRP6 and a Wnt signaling inhibitor. *J Biol Chem* **280**(29): 26770-26775.

Semenov, M.V., Tamai, K., Brott, B.K., Kuhl, M., Sokol, S., and He, X. 2001. Head inducer Dickkopf-1 is a ligand for Wnt coreceptor LRP6. *Curr Biol* **11**(12): 951-961.

Sethi, T., Ginsberg, M.H., Downward, J., and Hughes, P.E. 1999. The small GTP-binding protein R-Ras can influence integrin activation by antagonizing a Ras/Raf-initiated integrin suppression pathway. *Mol Biol Cell* **10**(6): 1799-1809.

Setou, M., Nakagawa, T., Seog, D.H., and Hirokawa, N. 2000. Kinesin superfamily motor protein KIF17 and mLin-10 in NMDA receptor-containing vesicle transport. *Science* **288**(5472): 1796-1802.

Shafer, B., Onishi, K., Lo, C., Colakoglu, G., and Zou, Y. 2011. Vangl2 promotes Wnt/planar cell polarity-like signaling by antagonizing Dvl1-mediated feedback inhibition in growth cone guidance. *Dev Cell* **20**(2): 177-191.

Shang, X., Cancelas, J.A., Li, L., Guo, F., Liu, W., Johnson, J.F., Ficker, A., Daria, D., Geiger, H., Ratner, N., and Zheng, Y. 2011. R-Ras and Rac GTPase cross-talk regulates hematopoietic progenitor cell migration, homing, and mobilization. *The Journal of biological chemistry* **286**(27): 24068-24078.

Sharma, R., Sud, N., Chattopadhyay, T.K., and Ralhan, R. 2005. TC21/R-Ras2 upregulation in esophageal tumorigenesis: potential diagnostic implications. *Oncology* **69**(1): 10-18.

Sheldahl, L.C., Park, M., Malbon, C.C., and Moon, R.T. 1999. Protein kinase C is differentially stimulated by Wnt and Frizzled homologs in a G-protein-dependent manner. *Curr Biol* **9**(13): 695-698.

Sheldahl, L.C., Slusarski, D.C., Pandur, P., Miller, J.R., Kuhl, M., and Moon, R.T. 2003. Dishevelled activates Ca2+ flux, PKC, and CamKII in vertebrate embryos. *J Cell Biol* **161**(4): 769-777.

Shibamoto, S., Higano, K., Takada, R., Ito, F., Takeichi, M., and Takada, S. 1998. Cytoskeletal reorganization by soluble Wnt-3a protein signalling. *Genes Cells* **3**(10): 659-670.

Shima, Y., Copeland, N.G., Gilbert, D.J., Jenkins, N.A., Chisaka, O., Takeichi, M., and Uemura, T. 2002. Differential expression of the seven-pass transmembrane cadherin genes Celsr1-3 and distribution of the Celsr2 protein during mouse development. *Dev Dyn* **223**(3): 321-332.

Shima, Y., Kawaguchi, S.Y., Kosaka, K., Nakayama, M., Hoshino, M., Nabeshima, Y., Hirano, T., and Uemura, T. 2007. Opposing roles in neurite growth control by two seven-pass transmembrane cadherins. *Nat Neurosci* **10**(8): 963-969.

Shimizu, H., Julius, M.A., Giarre, M., Zheng, Z., Brown, A.M., and Kitajewski, J. 1997. Transformation by Wnt family proteins correlates with regulation of beta-catenin. *Cell Growth Differ* **8**(12): 1349-1358.

Shin, W.S., Maeng, Y.S., Jung, J.W., Min, J.K., Kwon, Y.G., and Lee, S.T. 2008. Soluble PTK7 inhibits tube formation, migration, and invasion of endothelial cells and angiogenesis. *Biochem Biophys Res Commun* **371**(4): 793-798.

Shnitsar, I. and Borchers, A. 2008. PTK7 recruits dsh to regulate neural crest migration. *Development* **135**(24): 4015-4024.

Sibony-Benyamini, H. and Gil-Henn, H. 2012. Invadopodia: the leading force. *European journal of cell biology* **91**(11-12): 896-901.

Sidhu, R.S., Clough, R.R., and Bhullar, R.P. 2005. Regulation of phospholipase C-delta1 through direct interactions with the small GTPase Ral and calmodulin. *The Journal of biological chemistry* **280**(23): 21933-21941.

Simons, K. and Ikonen, E. 1997. Functional rafts in cell membranes. *Nature* **387**(6633): 569-572.

Simons, M., Gloy, J., Ganner, A., Bullerkotte, A., Bashkurov, M., Kronig, C., Schermer, B., Benzing, T., Cabello, O.A., Jenny, A., Mlodzik, M., Polok, B., Driever, W., Obara, T., and Walz, G. 2005. Inversin, the gene product mutated in nephronophthisis type II, functions as a molecular switch between Wnt signaling pathways. *Nat Genet* **37**(5): 537-543.

Simons, M. and Mlodzik, M. 2008. Planar cell polarity signaling: from fly development to human disease. *Annu Rev Genet* **42**: 517-540.

Slusarski, D.C., Corces, V.G., and Moon, R.T. 1997a. Interaction of Wnt and a Frizzled homologue triggers G-protein-linked phosphatidylinositol signalling. *Nature* **390**(6658): 410-413.

Slusarski, D.C., Yang-Snyder, J., Busa, W.B., and Moon, R.T. 1997b. Modulation of embryonic intracellular Ca2+ signaling by Wnt-5A. *Dev Biol* **182**(1): 114-120.

Small, J.V., Stradal, T., Vignal, E., and Rottner, K. 2002. The lamellipodium: where motility begins. *Trends Cell Biol* **12**(3): 112-120.

Song, C., Hu, C.D., Masago, M., Kariyai, K., Yamawaki-Kataoka, Y., Shibatohge, M., Wu, D., Satoh, T., and Kataoka, T. 2001. Regulation of a novel human phospholipase C, PLCepsilon, through membrane targeting by Ras. *J Biol Chem* **276**(4): 2752-2757.

Song, H., Hu, J., Chen, W., Elliott, G., Andre, P., Gao, B., and Yang, Y. 2010. Planar cell polarity breaks bilateral symmetry by controlling ciliary positioning. *Nature* **466**(7304): 378-382.

Song, H.H., Shi, W., Xiang, Y.Y., and Filmus, J. 2005. The loss of glypican-3 induces alterations in Wnt signaling. *J Biol Chem* **280**(3): 2116-2125.

Songyang, Z., Fanning, A.S., Fu, C., Xu, J., Marfatia, S.M., Chishti, A.H., Crompton, A., Chan, A.C., Anderson, J.M., and Cantley, L.C. 1997. Recognition of unique carboxyl-terminal motifs by distinct PDZ domains. *Science* **275**(5296): 73-77.

Sorkin, A. and von Zastrow, M. 2009. Endocytosis and signalling: intertwining molecular networks. *Nature reviews Molecular cell biology* **10**(9): 609-622.
Spaargaren, M. and Bischoff, J.R. 1994. Identification of the guanine nucleotide dissociation stimulator for Ral as a putative effector molecule of R-ras, H-ras, K-ras, and Rap. *Proc Natl Acad Sci U S A* **91**(26): 12609-12613.
Spaargaren, M., Martin, G.A., McCormick, F., Fernandez-Sarabia, M.J., and Bischoff, J.R. 1994. The Ras-related protein R-ras interacts directly with Raf-1 in a GTP-dependent manner. *Biochem J* **300 (Pt 2)**: 303-307.
St Croix, B., Rago, C., Velculescu, V., Traverso, G., Romans, K.E., Montgomery, E., Lal, A., Riggins, G.J., Lengauer, C., Vogelstein, B., and Kinzler, K.W. 2000. Genes expressed in human tumor endothelium. *Science* **289**(5482): 1197-1202.
Stacker, S.A., Hovens, C.M., Vitali, A., Pritchard, M.A., Baker, E., Sutherland, G.R., and Wilks, A.F. 1993. Molecular cloning and chromosomal localisation of the human homologue of a receptor related to tyrosine kinases (RYK). *Oncogene* **8**(5): 1347-1356.
Stambolic, V., Ruel, L., and Woodgett, J.R. 1996. Lithium inhibits glycogen synthase kinase-3 activity and mimics wingless signalling in intact cells. *Curr Biol* **6**(12): 1664-1668.
Stamos, J.L. and Weis, W.I. 2013. The beta-catenin destruction complex. *Cold Spring Harbor perspectives in biology* **5**(1): a007898.
Stearns, T., Evans, L., and Kirschner, M. 1991. Gamma-tubulin is a highly conserved component of the centrosome. *Cell* **65**(5): 825-836.
Steinert, S., Lee, E., Tresset, G., Zhang, D., Hortsch, R., Wetzel, R., Hebbar, S., Sundram, J.R., Kesavapany, S., Boschke, E., and Kraut, R. 2008. A fluorescent glycolipid-binding peptide probe traces cholesterol dependent microdomain-derived trafficking pathways. *PLoS One* **3**(8): e2933.
Stenmark, H. 2009. Rab GTPases as coordinators of vesicle traffic. *Nat Rev Mol Cell Biol* **10**(8): 513-525.
Sternlicht, M.D., Lochter, A., Sympson, C.J., Huey, B., Rougier, J.P., Gray, J.W., Pinkel, D., Bissell, M.J., and Werb, Z. 1999. The stromal proteinase MMP3/stromelysin-1 promotes mammary carcinogenesis. *Cell* **98**(2): 137-146.
Stokoe, D., Macdonald, S.G., Cadwallader, K., Symons, M., and Hancock, J.F. 1994. Activation of Raf as a result of recruitment to the plasma membrane. *Science* **264**(5164): 1463-1467.
Stone, J.C. 2011. Regulation and Function of the RasGRP Family of Ras Activators in Blood Cells. *Genes Cancer* **2**(3): 320-334.
Strutt, D.I. 2001. Asymmetric localization of frizzled and the establishment of cell polarity in the Drosophila wing. *Molecular cell* **7**(2): 367-375.
Strutt, H. and Strutt, D. 2003. EGF signaling and ommatidial rotation in the Drosophila eye. *Curr Biol* **13**(16): 1451-1457.
Stuebner, S., Faus-Kessler, T., Fischer, T., Wurst, W., and Prakash, N. 2010. Fzd3 and Fzd6 deficiency results in a severe midbrain morphogenesis defect. *Dev Dyn* **239**(1): 246-260.
Subbaiah, V.K., Kranjec, C., Thomas, M., and Banks, L. 2011. PDZ domains: the building blocks regulating tumorigenesis. *Biochem J* **439**(2): 195-205.
Sun, P., Watanabe, H., Takano, K., Yokoyama, T., Fujisawa, J., and Endo, T. 2006. Sustained activation of M-Ras induced by nerve growth factor is essential for neuronal differentiation of PC12 cells. *Genes Cells* **11**(9): 1097-1113.
Sun, T.Q., Lu, B., Feng, J.J., Reinhard, C., Jan, Y.N., Fantl, W.J., and Williams, L.T. 2001. PAR-1 is a Dishevelled-associated kinase and a positive regulator of Wnt signalling. *Nat Cell Biol* **3**(7): 628-636.
Sussman, D.J., Klingensmith, J., Salinas, P., Adams, P.S., Nusse, R., and Perrimon, N. 1994. Isolation and characterization of a mouse homolog of the Drosophila segment polarity gene dishevelled. *Dev Biol* **166**(1): 73-86.
Suzuki, J., Kaziro, Y., and Koide, H. 2000. Positive regulation of skeletal myogenesis by R-Ras. *Oncogene* **19**(9): 1138-1146.
Tada, M. and Kai, M. 2009. Noncanonical Wnt/PCP signaling during vertebrate gastrulation. *Zebrafish* **6**(1): 29-40.
Tada, M. and Kai, M. 2012. Planar cell polarity in coordinated and directed movements. *Curr Top Dev Biol* **101**: 77-110.
Takahashi, M., Fujita, M., Furukawa, Y., Hamamoto, R., Shimokawa, T., Miwa, N., Ogawa, M., and Nakamura, Y. 2002. Isolation of a novel human gene, APCDD1, as a direct target of the beta-Catenin/T-cell factor 4 complex with probable involvement in colorectal carcinogenesis. *Cancer research* **62**(20): 5651-5656.

Takai, Y., Sasaki, T., and Matozaki, T. 2001. Small GTP-binding proteins. *Physiol Rev* **81**(1): 153-208.

Takaya, A., Kamio, T., Masuda, M., Mochizuki, N., Sawa, H., Sato, M., Nagashima, K., Mizutani, A., Matsuno, A., Kiyokawa, E., and Matsuda, M. 2007. R-Ras regulates exocytosis by Rgl2/Rlf-mediated activation of RalA on endosomes. *Mol Biol Cell* **18**(5): 1850-1860.

Takeuchi, M., Nakabayashi, J., Sakaguchi, T., Yamamoto, T.S., Takahashi, H., Takeda, H., and Ueno, N. 2003. The prickle-related gene in vertebrates is essential for gastrulation cell movements. *Curr Biol* **13**(8): 674-679.

Tall, G.G., Barbieri, M.A., Stahl, P.D., and Horazdovsky, B.F. 2001. Ras-activated endocytosis is mediated by the Rab5 guanine nucleotide exchange activity of RIN1. *Dev Cell* **1**(1): 73-82.

Tamagnone, L., Artigiani, S., Chen, H., He, Z., Ming, G.I., Song, H., Chedotal, A., Winberg, M.L., Goodman, C.S., Poo, M., Tessier-Lavigne, M., and Comoglio, P.M. 1999. Plexins are a large family of receptors for transmembrane, secreted, and GPI-anchored semaphorins in vertebrates. *Cell* **99**(1): 71-80.

Tamai, K., Semenov, M., Kato, Y., Spokony, R., Liu, C., Katsuyama, Y., Hess, F., Saint-Jeannet, J.P., and He, X. 2000. LDL-receptor-related proteins in Wnt signal transduction. *Nature* **407**(6803): 530-535.

Tamai, K., Zeng, X., Liu, C., Zhang, X., Harada, Y., Chang, Z., and He, X. 2004. A mechanism for Wnt coreceptor activation. *Mol Cell* **13**(1): 149-156.

Tanegashima, K., Zhao, H., and Dawid, I.B. 2008. WGEF activates Rho in the Wnt-PCP pathway and controls convergent extension in Xenopus gastrulation. *EMBO J* **27**(4): 606-617.

Tardif, G., Reboul, P., Pelletier, J.P., and Martel-Pelletier, J. 2004. Ten years in the life of an enzyme: the story of the human MMP-13 (collagenase-3). *Mod Rheumatol* **14**(3): 197-204.

Taupin, D. and Podolsky, D.K. 2003. Trefoil factors: initiators of mucosal healing. *Nat Rev Mol Cell Biol* **4**(9): 721-732.

Tavares, A.T., Andrade, S., Silva, A.C., and Belo, J.A. 2007. Cerberus is a feedback inhibitor of Nodal asymmetric signaling in the chick embryo. *Development* **134**(11): 2051-2060.

Tawa, N.E., Jr., Odessey, R., and Goldberg, A.L. 1997. Inhibitors of the proteasome reduce the accelerated proteolysis in atrophying rat skeletal muscles. *J Clin Invest* **100**(1): 197-203.

Taylor, J., Abramova, N., Charlton, J., and Adler, P.N. 1998. Van Gogh: a new Drosophila tissue polarity gene. *Genetics* **150**(1): 199-210.

Theisen, H., Purcell, J., Bennett, M., Kansagara, D., Syed, A., and Marsh, J.L. 1994. dishevelled is required during wingless signaling to establish both cell polarity and cell identity. *Development* **120**(2): 347-360.

Tian, X., Gotoh, T., Tsuji, K., Lo, E.H., Huang, S., and Feig, L.A. 2004. Developmentally regulated role for Ras-GRFs in coupling NMDA glutamate receptors to Ras, Erk and CREB. *EMBO J* **23**(7): 1567-1575.

Tissir, F., Bar, I., Jossin, Y., De Backer, O., and Goffinet, A.M. 2005. Protocadherin Celsr3 is crucial in axonal tract development. *Nat Neurosci* **8**(4): 451-457.

Tissir, F. and Goffinet, A.M. 2005. Planar cell polarity signaling in neural development. *Curr Opin Neurobiol* **20**(5): 572-577.

Tissir, F. and Goffinet, A.M. 2006. Expression of planar cell polarity genes during development of the mouse CNS. *Eur J Neurosci* **23**(3): 597-607.

Tissir, F., Qu, Y., Montcouquiol, M., Zhou, L., Komatsu, K., Shi, D., Fujimori, T., Labeau, J., Tyteca, D., Courtoy, P., Poumay, Y., Uemura, T., and Goffinet, A.M. 2010. Lack of cadherins Celsr2 and Celsr3 impairs ependymal ciliogenesis, leading to fatal hydrocephalus. *Nat Neurosci* **13**(6): 700-707.

Tommasi, S., Dammann, R., Zhang, Z., Wang, Y., Liu, L., Tsark, W.M., Wilczynski, S.P., Li, J., You, M., and Pfeifer, G.P. 2005. Tumor susceptibility of Rassf1a knockout mice. *Cancer Res* **65**(1): 92-98.

Topol, L., Jiang, X., Choi, H., Garrett-Beal, L., Carolan, P.J., and Yang, Y. 2003. Wnt-5a inhibits the canonical Wnt pathway by promoting GSK-3-independent beta-catenin degradation. *J Cell Biol* **162**(5): 899-908.

Torban, E., Iliescu, A., and Gros, P. 2012. An expanding role of Vangl proteins in embryonic development. *Curr Top Dev Biol* **101**: 237-261.

Torban, E., Patenaude, A.M., Leclerc, S., Rakowiecki, S., Gauthier, S., Andelfinger, G., Epstein, D.J., and Gros, P. 2008. Genetic interaction between members of the

Vangl family causes neural tube defects in mice. *Proc Natl Acad Sci U S A* **105**(9): 3449-3454.
Torban, E., Wang, H.J., Groulx, N., and Gros, P. 2004. Independent mutations in mouse Vangl2 that cause neural tube defects in looptail mice impair interaction with members of the Dishevelled family. *J Biol Chem* **279**(50): 52703-52713.
Torban, E., Wang, H.J., Patenaude, A.M., Riccomagno, M., Daniels, E., Epstein, D., and Gros, P. 2007. Tissue, cellular and sub-cellular localization of the Vangl2 protein during embryonic development: effect of the Lp mutation. *Gene Expr Patterns* **7**(3): 346-354.
Torres, M.A., Yang-Snyder, J.A., Purcell, S.M., DeMarais, A.A., McGrew, L.L., and Moon, R.T. 1996. Activities of the Wnt-1 class of secreted signaling factors are antagonized by the Wnt-5A class and by a dominant negative cadherin in early Xenopus development. *J Cell Biol* **133**(5): 1123-1137.
Toyofuku, T., Zhang, H., Kumanogoh, A., Takegahara, N., Suto, F., Kamei, J., Aoki, K., Yabuki, M., Hori, M., Fujisawa, H., and Kikutani, H. 2004. Dual roles of Sema6D in cardiac morphogenesis through region-specific association of its receptor, Plexin-A1, with off-track and vascular endothelial growth factor receptor type 2. *Genes Dev* **18**(4): 435-447.
Traub, L.M. 2009. Tickets to ride: selecting cargo for clathrin-regulated internalization. *Nature reviews Molecular cell biology* **10**(9): 583-596.
Tree, D.R., Ma, D., and Axelrod, J.D. 2002. A three-tiered mechanism for regulation of planar cell polarity. *Seminars in cell & developmental biology* **13**(3): 217-224.
Tsai, I.C., Amack, J.D., Gao, Z.H., Band, V., Yost, H.J., and Virshup, D.M. 2007. A Wnt-CKIvarepsilon-Rap1 pathway regulates gastrulation by modulating SIPA1L1, a Rap GTPase activating protein. *Dev Cell* **12**(3): 335-347.
Tsang, M., Lijam, N., Yang, Y., Beier, D.R., Wynshaw-Boris, A., and Sussman, D.J. 1996. Isolation and characterization of mouse dishevelled-3. *Dev Dyn* **207**(3): 253-262.
Uematsu, K., He, B., You, L., Xu, Z., McCormick, F., and Jablons, D.M. 2003. Activation of the Wnt pathway in non small cell lung cancer: evidence of dishevelled overexpression. *Oncogene* **22**(46): 7218-7221.
Uitto, V.J., Airola, K., Vaalamo, M., Johansson, N., Putnins, E.E., Firth, J.D., Salonen, J., Lopez-Otin, C., Saarialho-Kere, U., and Kahari, V.M. 1998. Collagenase-3 (matrix metalloproteinase-13) expression is induced in oral mucosal epithelium during chronic inflammation. *Am J Pathol* **152**(6): 1489-1499.
Ulrich, F., Krieg, M., Schotz, E.M., Link, V., Castanon, I., Schnabel, V., Taubenberger, A., Mueller, D., Puech, P.H., and Heisenberg, C.P. 2005. Wnt11 functions in gastrulation by controlling cell cohesion through Rab5c and E-cadherin. *Dev Cell* **9**(4): 555-564.
Umbhauer, M., Djiane, A., Goisset, C., Penzo-Mendez, A., Riou, J.F., Boucaut, J.C., and Shi, D.L. 2000. The C-terminal cytoplasmic Lys-thr-X-X-X-Trp motif in frizzled receptors mediates Wnt/beta-catenin signalling. *EMBO J* **19**(18): 4944-4954.
Usui, T., Shima, Y., Shimada, Y., Hirano, S., Burgess, R.W., Schwarz, T.L., Takeichi, M., and Uemura, T. 1999. Flamingo, a seven-pass transmembrane cadherin, regulates planar cell polarity under the control of Frizzled. *Cell* **98**(5): 585-595.
Valster, A., Tran, N.L., Nakada, M., Berens, M.E., Chan, A.Y., and Symons, M. 2005. Cell migration and invasion assays. *Methods* **37**(2): 208-215.
van Amerongen, R. 2012. Alternative Wnt pathways and receptors. *Cold Spring Harb Perspect Biol* **4**(10).
van Amerongen, R., Mikels, A., and Nusse, R. 2008. Alternative wnt signaling is initiated by distinct receptors. *Sci Signal* **1**(35): re9.
van Bokhoven, H., Celli, J., Kayserili, H., van Beusekom, E., Balci, S., Brussel, W., Skovby, F., Kerr, B., Percin, E.F., Akarsu, N., and Brunner, H.G. 2000. Mutation of the gene encoding the ROR2 tyrosine kinase causes autosomal recessive Robinow syndrome. *Nat Genet* **25**(4): 423-426.
Van Keymeulen, A., Wong, K., Knight, Z.A., Govaerts, C., Hahn, K.M., Shokat, K.M., and Bourne, H.R. 2006. To stabilize neutrophil polarity, PIP3 and Cdc42 augment RhoA activity at the back as well as signals at the front. *J Cell Biol* **174**(3): 437-445.
Vanhaesebroeck, B., Stephens, L., and Hawkins, P. 2012. PI3K signalling: the path to discovery and understanding. *Nat Rev Mol Cell Biol* **13**(3): 195-203.
Varelas, X., Miller, B.W., Sopko, R., Song, S., Gregorieff, A., Fellouse, F.A., Sakuma, R., Pawson, T., Hunziker, W., McNeill, H., Wrana, J.L., and Attisano, L. 2010. The Hippo pathway regulates Wnt/beta-catenin signaling. *Dev Cell* **18**(4): 579-591.

Vavvas, D., Li, X., Avruch, J., and Zhang, X.F. 1998. Identification of Nore1 as a potential Ras effector. *J Biol Chem* **273**(10): 5439-5442.
Veeman, M.T., Axelrod, J.D., and Moon, R.T. 2003a. A second canon. Functions and mechanisms of beta-catenin-independent Wnt signaling. *Dev Cell* **5**(3): 367-377.
Veeman, M.T., Slusarski, D.C., Kaykas, A., Louie, S.H., and Moon, R.T. 2003b. Zebrafish prickle, a modulator of noncanonical Wnt/Fz signaling, regulates gastrulation movements. *Curr Biol* **13**(8): 680-685.
Vega, F.M., Colomba, A., Reymond, N., Thomas, M., and Ridley, A.J. 2012. RhoB regulates cell migration through altered focal adhesion dynamics. *Open Biol* **2**(5): 120076.
Vega, F.M. and Ridley, A.J. 2008. Rho GTPases in cancer cell biology. *FEBS Lett* **582**(14): 2093-2101.
Verkaar, F., van Rosmalen, J.W., Smits, J.F., Blankesteijn, W.M., and Zaman, G.J. 2009. Stably overexpressed human Frizzled-2 signals through the beta-catenin pathway and does not activate Ca2+-mobilization in Human Embryonic Kidney 293 cells. *Cell Signal* **21**(1): 22-33.
Verstreken, P., Koh, T.W., Schulze, K.L., Zhai, R.G., Hiesinger, P.R., Zhou, Y., Mehta, S.Q., Cao, Y., Roos, J., and Bellen, H.J. 2003. Synaptojanin is recruited by endophilin to promote synaptic vesicle uncoating. *Neuron* **40**(4): 733-748.
Vicente-Manzanares, M., Webb, D.J., and Horwitz, A.R. 2005. Cell migration at a glance. *J Cell Sci* **118**(Pt 21): 4917-4919.
Vigil, D., Cherfils, J., Rossman, K.L., and Der, C.J. 2010. Ras superfamily GEFs and GAPs: validated and tractable targets for cancer therapy? *Nature reviews Cancer* **10**(12): 842-857.
Vincent, J.P. and Beckett, K. 2011. Off-track takes Frizzled off the canonical path. *EMBO J* **30**(18): 3665-3666.
Vinson, C.R. and Adler, P.N. 1987. Directional non-cell autonomy and the transmission of polarity information by the frizzled gene of Drosophila. *Nature* **329**(6139): 549-551.
Vladar, E.K., Antic, D., and Axelrod, J.D. 2009. Planar cell polarity signaling: the developing cell's compass. *Cold Spring Harbor perspectives in biology* **1**(3): a002964.
Vojtek, A.B., Hollenberg, S.M., and Cooper, J.A. 1993. Mammalian Ras interacts directly with the serine/threonine kinase Raf. *Cell* **74**(1): 205-214.
Vonica, A. and Brivanlou, A.H. 2007. The left-right axis is regulated by the interplay of Coco, Xnr1 and derriere in Xenopus embryos. *Developmental biology* **303**(1): 281-294.
Vos, M.D., Martinez, A., Ellis, C.A., Vallecorsa, T., and Clark, G.J. 2003. The pro-apoptotic Ras effector Nore1 may serve as a Ras-regulated tumor suppressor in the lung. *J Biol Chem* **278**(24): 21938-21943.
Vu, T.H., Shipley, J.M., Bergers, G., Berger, J.E., Helms, J.A., Hanahan, D., Shapiro, S.D., Senior, R.M., and Werb, Z. 1998. MMP-9/gelatinase B is a key regulator of growth plate angiogenesis and apoptosis of hypertrophic chondrocytes. *Cell* **93**(3): 411-422.
Wada, H., Iwasaki, M., Sato, T., Masai, I., Nishiwaki, Y., Tanaka, H., Sato, A., Nojima, Y., and Okamoto, H. 2005. Dual roles of zygotic and maternal Scribble1 in neural migration and convergent extension movements in zebrafish embryos. *Development* **132**(10): 2273-2285.
Wada, H., Tanaka, H., Nakayama, S., Iwasaki, M., and Okamoto, H. 2006. Frizzled3a and Celsr2 function in the neuroepithelium to regulate migration of facial motor neurons in the developing zebrafish hindbrain. *Development* **133**(23): 4749-4759.
Wagner, G., Peradziryi, H., Wehner, P., and Borchers, A. 2010. PlexinA1 interacts with PTK7 and is required for neural crest migration. *Biochem Biophys Res Commun* **402**(2): 402-407.
Walker, S.A., Kupzig, S., Bouyoucef, D., Davies, L.C., Tsuboi, T., Bivona, T.G., Cozier, G.E., Lockyer, P.J., Buckler, A., Rutter, G.A., Allen, M.J., Philips, M.R., and Cullen, P.J. 2004. Identification of a Ras GTPase-activating protein regulated by receptor-mediated Ca2+ oscillations. *EMBO J* **23**(8): 1749-1760.
Wallingford, J.B. 2004. Closing in on vertebrate planar polarity. *Nat Cell Biol* **6**(8): 687-689.
Wallingford, J.B. 2010. Planar cell polarity signaling, cilia and polarized ciliary beating. *Curr Opin Cell Biol* **22**(5): 597-604.

Wallingford, J.B. 2012. Planar cell polarity and the developmental control of cell behavior in vertebrate embryos. *Annu Rev Cell Dev Biol* **28**: 627-653.
Wallingford, J.B., Fraser, S.E., and Harland, R.M. 2002. Convergent extension: the molecular control of polarized cell movement during embryonic development. *Dev Cell* **2**(6): 695-706.
Wallingford, J.B. and Habas, R. 2005. The developmental biology of Dishevelled: an enigmatic protein governing cell fate and cell polarity. *Development* **132**(20): 4421-4436.
Wallingford, J.B. and Mitchell, B. 2011. Strange as it may seem: the many links between Wnt signaling, planar cell polarity, and cilia. *Genes Dev* **25**(3): 201-213.
Wang, H., Zhang, W., Zhao, J., Zhang, L., Liu, M., Yan, G., Yao, J., Yu, H., and Yang, P. 2012. N-Glycosylation pattern of recombinant human CD82 (KAI1), a tumor-associated membrane protein. *J Proteomics* **75**(4): 1375-1385.
Wang, H.X., Li, Q., Sharma, C., Knoblich, K., and Hemler, M.E. 2011. Tetraspanin protein contributions to cancer. *Biochem Soc Trans* **39**(2): 547-552.
Wang, J., Mark, S., Zhang, X., Qian, D., Yoo, S.J., Radde-Gallwitz, K., Zhang, Y., Lin, X., Collazo, A., Wynshaw-Boris, A., and Chen, P. 2005. Regulation of polarized extension and planar cell polarity in the cochlea by the vertebrate PCP pathway. *Nat Genet* **37**(9): 980-985.
Wang, Q., Symes, A.J., Kane, C.A., Freeman, A., Nariculam, J., Munson, P., Thrasivoulou, C., Masters, J.R., and Ahmed, A. 2010. A novel role for Wnt/Ca2+ signaling in actin cytoskeleton remodeling and cell motility in prostate cancer. *PLoS One* **5**(5): e10456.
Wang, Y., Guo, N., and Nathans, J. 2006. The role of Frizzled3 and Frizzled6 in neural tube closure and in the planar polarity of inner-ear sensory hair cells. *J Neurosci* **26**(8): 2147-2156.
Wang, Y. and Nathans, J. 2007. Tissue/planar cell polarity in vertebrates: new insights and new questions. *Development* **134**(4): 647-658.
Wang, Z., Tseng, C.P., Pong, R.C., Chen, H., McConnell, J.D., Navone, N., and Hsieh, J.T. 2002. The mechanism of growth-inhibitory effect of DOC-2/DAB2 in prostate cancer. Characterization of a novel GTPase-activating protein associated with N-terminal domain of DOC-2/DAB2. *J Biol Chem* **277**(15): 12622-12631.
Wansleeben, C., Feitsma, H., Montcouquiol, M., Kroon, C., Cuppen, E., and Meijlink, F. 2011. Planar cell polarity defects and defective Vangl2 trafficking in mutants for the COPII gene Sec24b. *Development* **137**(7): 1067-1073.
Warne, P.H., Viciana, P.R., and Downward, J. 1993. Direct interaction of Ras and the amino-terminal region of Raf-1 in vitro. *Nature* **364**(6435): 352-355.
Wawrzak, D., Luyten, A., Lambaerts, K., and Zimmermann, P. 2009. Frizzled-PDZ scaffold interactions in the control of Wnt signaling. *Adv Enzyme Regul* **49**(1): 98-106.
Wawrzak, D., Metioui, M., Willems, E., Hendrickx, M., de Genst, E., and Leyns, L. 2007. Wnt3a binds to several sFRPs in the nanomolar range. *Biochem Biophys Res Commun* **357**(4): 1119-1123.
Weeraratna, A.T., Jiang, Y., Hostetter, G., Rosenblatt, K., Duray, P., Bittner, M., and Trent, J.M. 2002. Wnt5a signaling directly affects cell motility and invasion of metastatic melanoma. *Cancer Cell* **1**(3): 279-288.
Wehner, P., Shnitsar, I., Urlaub, H., and Borchers, A. 2011. RACK1 is a novel interaction partner of PTK7 that is required for neural tube closure. *Development* **138**(7): 1321-1327.
Wei, Q., Yokota, C., Semenov, M.V., Doble, B., Woodgett, J., and He, X. 2007. R-spondin1 is a high affinity ligand for LRP6 and induces LRP6 phosphorylation and beta-catenin signaling. *J Biol Chem* **282**(21): 15903-15911.
Wei, W., Li, M., Wang, J., Nie, F., and Li, L. 2012. The E3 ubiquitin ligase ITCH negatively regulates canonical Wnt signaling by targeting dishevelled protein. *Mol Cell Biol* **32**(19): 3903-3912.
Welch, H.C., Coadwell, W.J., Stephens, L.R., and Hawkins, P.T. 2003. Phosphoinositide 3-kinase-dependent activation of Rac. *FEBS Lett* **546**(1): 93-97.
Wellbrock, C., Karasarides, M., and Marais, R. 2004. The RAF proteins take centre stage. *Nature reviews Molecular cell biology* **5**(11): 875-885.
Wen, S., Zhu, H., Lu, W., Mitchell, L.E., Shaw, G.M., Lammer, E.J., and Finnell, R.H. 2010. Planar cell polarity pathway genes and risk for spina bifida. *Am J Med Genet A* **152A**(2): 299-304.
Wendeler, M.W., Paccaud, J.P., and Hauri, H.P. 2007. Role of Sec24 isoforms in selective export of membrane proteins from the endoplasmic reticulum. *EMBO Rep* **8**(3): 258-264.

Wennerberg, K. and Der, C.J. 2004. Rho-family GTPases: it's not only Rac and Rho (and I like it). *J Cell Sci* **117**(Pt 8): 1301-1312.
Wennerberg, K., Rossman, K.L., and Der, C.J. 2005. The Ras superfamily at a glance. *J Cell Sci* **118**(Pt 5): 843-846.
Westfall, T.A., Brimeyer, R., Twedt, J., Gladon, J., Olberding, A., Furutani-Seiki, M., and Slusarski, D.C. 2003. Wnt-5/pipetail functions in vertebrate axis formation as a negative regulator of Wnt/beta-catenin activity. *J Cell Biol* **162**(5): 889-898.
Wharton, K.A., Jr. 2003. Runnin' with the Dvl: proteins that associate with Dsh/Dvl and their significance to Wnt signal transduction. *Dev Biol* **253**(1): 1-17.
Wheeler, A.P. and Ridley, A.J. 2004. Why three Rho proteins? RhoA, RhoB, RhoC, and cell motility. *Exp Cell Res* **301**(1): 43-49.
Wheeler, A.P. and Ridley, A.J. 2007. RhoB affects macrophage adhesion, integrin expression and migration. *Exp Cell Res* **313**(16): 3505-3516.
White, M.A., Nicolette, C., Minden, A., Polverino, A., Van Aelst, L., Karin, M., and Wigler, M.H. 1995. Multiple Ras functions can contribute to mammalian cell transformation. *Cell* **80**(4): 533-541.
Willard, F.S., Willard, M.D., Kimple, A.J., Soundararajan, M., Oestreich, E.A., Li, X., Sowa, N.A., Kimple, R.J., Doyle, D.A., Der, C.J., Zylka, M.J., Snider, W.D., and Siderovski, D.P. 2009. Regulator of G-protein signaling 14 (RGS14) is a selective H-Ras effector. *PLoS One* **4**(3): e4884.
Willard, M.D., Willard, F.S., Li, X., Cappell, S.D., Snider, W.D., and Siderovski, D.P. 2007. Selective role for RGS12 as a Ras/Raf/MEK scaffold in nerve growth factor-mediated differentiation. *EMBO J* **26**(8): 2029-2040.
Willert, K. and Nusse, R. 1998. Beta-catenin: a key mediator of Wnt signaling. *Curr Opin Genet Dev* **8**(1): 95-102.
Williams, B.B., Cantrell, V.A., Mundell, N.A., Bennett, A.C., Quick, R.E., and Jessen, J.R. 2012a. VANGL2 regulates membrane trafficking of MMP14 to control cell polarity and migration. *J Cell Sci* **125**(Pt 9): 2141-2147.
Williams, B.B., Mundell, N., Dunlap, J., and Jessen, J. 2012b. The planar cell polarity protein VANGL2 coordinates remodeling of the extracellular matrix. *Commun Integr Biol* **5**(4): 325-328.
Williams, J.G., Pappu, K., and Campbell, S.L. 2003. Structural and biochemical studies of p21Ras S-nitrosylation and nitric oxide-mediated guanine nucleotide exchange. *Proceedings of the National Academy of Sciences of the United States of America* **100**(11): 6376-6381.
Winkler, S., Mohl, M., Wieland, T., and Lutz, S. 2005. GrinchGEF--a novel Rho-specific guanine nucleotide exchange factor. *Biochem Biophys Res Commun* **335**(4): 1280-1286.
Winter, C.G., Wang, B., Ballew, A., Royou, A., Karess, R., Axelrod, J.D., and Luo, L. 2001. Drosophila Rho-associated kinase (Drok) links Frizzled-mediated planar cell polarity signaling to the actin cytoskeleton. *Cell* **105**(1): 81-91.
Witte, F., Bernatik, O., Kirchner, K., Masek, J., Mahl, A., Krejci, P., Mundlos, S., Schambony, A., Bryja, V., and Stricker, S. 2010. Negative regulation of Wnt signaling mediated by CK1-phosphorylated Dishevelled via Ror2. *FASEB J* **24**(7): 2417-2426.
Witze, E.S., Litman, E.S., Argast, G.M., Moon, R.T., and Ahn, N.G. 2008. Wnt5a control of cell polarity and directional movement by polarized redistribution of adhesion receptors. *Science* **320**(5874): 365-369.
Wolff, T. and Rubin, G.M. 1998. Strabismus, a novel gene that regulates tissue polarity and cell fate decisions in Drosophila. *Development* **125**(6): 1149-1159.
Wong, G.T., Gavin, B.J., and McMahon, A.P. 1994. Differential transformation of mammary epithelial cells by Wnt genes. *Mol Cell Biol* **14**(9): 6278-6286.
Wong, H.C., Bourdelas, A., Krauss, A., Lee, H.J., Shao, Y., Wu, D., Mlodzik, M., Shi, D.L., and Zheng, J. 2003. Direct binding of the PDZ domain of Dishevelled to a conserved internal sequence in the C-terminal region of Frizzled. *Mol Cell* **12**(5): 1251-1260.
Wozniak, M.A., Kwong, L., Chodniewicz, D., Klemke, R.L., and Keely, P.J. 2005. R-Ras controls membrane protrusion and cell migration through the spatial regulation of Rac and Rho. *Mol Biol Cell* **16**(1): 84-96.
Wright, L.P. and Philips, M.R. 2006. Thematic review series: lipid posttranslational modifications. CAAX modification and membrane targeting of Ras. *J Lipid Res* **47**(5): 883-891.
Wright, T.M., Brannon, A.R., Gordan, J.D., Mikels, A.J., Mitchell, C., Chen, S., Espinosa, I., van de Rijn, M., Pruthi, R., Wallen, E., Edwards, L., Nusse, R., and Rathmell,

W.K. 2009. Ror2, a developmentally regulated kinase, promotes tumor growth potential in renal cell carcinoma. *Oncogene* **28**(27): 2513-2523.
Wu, C., Wei, W., Li, C., Li, Q., Sheng, Q., and Zeng, R. 2012. Delicate analysis of post-translational modifications on Dishevelled 3. *J Proteome Res* **11**(7): 3829-3837.
Wu, J. and Mlodzik, M. 2008. The frizzled extracellular domain is a ligand for Van Gogh/Stbm during nonautonomous planar cell polarity signaling. *Dev Cell* **15**(3): 462-469.
Wu, J. and Mlodzik, M. 2009. A quest for the mechanism regulating global planar cell polarity of tissues. *Trends in cell biology* **19**(7): 295-305.
Wu, Y.T., Tan, H.L., Shui, G., Bauvy, C., Huang, Q., Wenk, M.R., Ong, C.N., Codogno, P., and Shen, H.M. 2010. Dual role of 3-methyladenine in modulation of autophagy via different temporal patterns of inhibition on class I and III phosphoinositide 3-kinase. *The Journal of biological chemistry* **285**(14): 10850-10861.
Wynshaw-Boris, A. 2012. Dishevelled: in vivo roles of a multifunctional gene family during development. *Curr Top Dev Biol* **101**: 213-235.
Xu, K., Chong, D.C., Rankin, S.A., Zorn, A.M., and Cleaver, O. 2009. Rasip1 is required for endothelial cell motility, angiogenesis and vessel formation. *Developmental biology* **329**(2): 269-279.
Xu, K., Sacharidou, A., Fu, S., Chong, D.C., Skaug, B., Chen, Z.J., Davis, G.E., and Cleaver, O. 2011. Blood vessel tubulogenesis requires Rasip1 regulation of GTPase signaling. *Dev Cell* **20**(4): 526-539.
Xu, L., Lubkov, V., Taylor, L.J., and Bar-Sagi, D. 2010. Feedback regulation of Ras signaling by Rabex-5-mediated ubiquitination. *Current biology : CB* **20**(15): 1372-1377.
Xu, Q., Wang, Y., Dabdoub, A., Smallwood, P.M., Williams, J., Woods, C., Kelley, M.W., Jiang, L., Tasman, W., Zhang, K., and Nathans, J. 2004. Vascular development in the retina and inner ear: control by Norrin and Frizzled-4, a high-affinity ligand-receptor pair. *Cell* **116**(6): 883-895.
Yadav, K.K. and Bar-Sagi, D. 2010. Allosteric gating of Son of sevenless activity by the histone domain. *Proceedings of the National Academy of Sciences of the United States of America* **107**(8): 3436-3440.
Yagyu, R., Hamamoto, R., Furukawa, Y., Okabe, H., Yamamura, T., and Nakamura, Y. 2002. Isolation and characterization of a novel human gene, VANGL1, as a therapeutic target for hepatocellular carcinoma. *Int J Oncol* **20**(6): 1173-1178.
Yamagata, K., Li, X., Ikegaki, S., Oneyama, C., Okada, M., Nishita, M., and Minami, Y. 2012. Dissection of Wnt5a-Ror2 signaling leading to matrix metalloproteinase (MMP-13) expression. *J Biol Chem* **287**(2): 1588-1599.
Yamagishi, H., Garg, V., Matsuoka, R., Thomas, T., and Srivastava, D. 1999. A molecular pathway revealing a genetic basis for human cardiac and craniofacial defects. *Science* **283**(5405): 1158-1161.
Yamaguchi, T.P., Bradley, A., McMahon, A.P., and Jones, S. 1999. A Wnt5a pathway underlies outgrowth of multiple structures in the vertebrate embryo. *Development* **126**(6): 1211-1223.
Yamamoto, A., Nagano, T., Takehara, S., Hibi, M., and Aizawa, S. 2005. Shisa promotes head formation through the inhibition of receptor protein maturation for the caudalizing factors, Wnt and FGF. *Cell* **120**(2): 223-235.
Yamamoto, A., Tagawa, Y., Yoshimori, T., Moriyama, Y., Masaki, R., and Tashiro, Y. 1998. Bafilomycin A1 prevents maturation of autophagic vacuoles by inhibiting fusion between autophagosomes and lysosomes in rat hepatoma cell line, H-4-II-E cells. *Cell Struct Funct* **23**(1): 33-42.
Yamamoto, H., Oue, N., Sato, A., Hasegawa, Y., Matsubara, A., Yasui, W., and Kikuchi, A. 2010. Wnt5a signaling is involved in the aggressiveness of prostate cancer and expression of metalloproteinase. *Oncogene* **29**(14): 2036-2046.
Yamamoto, S., Nishimura, O., Misaki, K., Nishita, M., Minami, Y., Yonemura, S., Tarui, H., and Sasaki, H. 2008. Cthrc1 selectively activates the planar cell polarity pathway of Wnt signaling by stabilizing the Wnt-receptor complex. *Dev Cell* **15**(1): 23-36.
Yamamoto, T., Kaibuchi, K., Mizuno, T., Hiroyoshi, M., Shirataki, H., and Takai, Y. 1990. Purification and characterization from bovine brain cytosol of proteins that regulate the GDP/GTP exchange reaction of smg p21s, ras p21-like GTP-binding proteins. *J Biol Chem* **265**(27): 16626-16634.
Yamanaka, H., Moriguchi, T., Masuyama, N., Kusakabe, M., Hanafusa, H., Takada, R., Takada, S., and Nishida, E. 2002. JNK functions in the non-canonical Wnt pathway to regulate convergent extension movements in vertebrates. *EMBO Rep* **3**(1): 69-75.

Yamazaki, D., Kurisu, S., and Takenawa, T. 2005. Regulation of cancer cell motility through actin reorganization. *Cancer science* **96**(7): 379-386.
Yanagawa, S., Matsuda, Y., Lee, J.S., Matsubayashi, H., Sese, S., Kadowaki, T., and Ishimoto, A. 2002. Casein kinase I phosphorylates the Armadillo protein and induces its degradation in Drosophila. *EMBO J* **21**(7): 1733-1742.
Yanez-Mo, M., Barreiro, O., Gordon-Alonso, M., Sala-Valdes, M., and Sanchez-Madrid, F. 2009. Tetraspanin-enriched microdomains: a functional unit in cell plasma membranes. *Trends Cell Biol* **19**(9): 434-446.
Yang, S.H., Sharrocks, A.D., and Whitmarsh, A.J. 2013. MAP kinase signalling cascades and transcriptional regulation. *Gene* **513**(1): 1-13.
Ye, X., Wang, Y., Cahill, H., Yu, M., Badea, T.C., Smallwood, P.M., Peachey, N.S., and Nathans, J. 2009. Norrin, frizzled-4, and Lrp5 signaling in endothelial cells controls a genetic program for retinal vascularization. *Cell* **139**(2): 285-298.
Yokoyama, N. and Malbon, C.C. 2007. Phosphoprotein phosphatase-2A docks to Dishevelled and counterregulates Wnt3a/beta-catenin signaling. *J Mol Signal* **2**: 12.
Yokoyama, N., Markova, N.G., Wang, H.Y., and Malbon, C.C. 2012. Assembly of Dishevelled 3-based supermolecular complexes via phosphorylation and Axin. *Journal of molecular signaling* **7**(1): 8.
Yorimitsu, T. and Klionsky, D.J. 2005. Autophagy: molecular machinery for self-eating. *Cell Death Differ* **12 Suppl 2**: 1542-1552.
Yoshikawa, S., McKinnon, R.D., Kokel, M., and Thomas, J.B. 2003. Wnt-mediated axon guidance via the Drosophila Derailed receptor. *Nature* **422**(6932): 583-588.
Yost, C., Torres, M., Miller, J.R., Huang, E., Kimelman, D., and Moon, R.T. 1996. The axis-inducing activity, stability, and subcellular distribution of beta-catenin is regulated in Xenopus embryos by glycogen synthase kinase 3. *Genes Dev* **10**(12): 1443-1454.
Yu, H., Ye, X., Guo, N., and Nathans, J. 2012. Frizzled 2 and frizzled 7 function redundantly in convergent extension and closure of the ventricular septum and palate: evidence for a network of interacting genes. *Development* **139**(23): 4383-4394.
Zallen, J.A. 2007. Planar polarity and tissue morphogenesis. *Cell* **129**(6): 1051-1063.
Zeng, X., Tamai, K., Doble, B., Li, S., Huang, H., Habas, R., Okamura, H., Woodgett, J., and He, X. 2005. A dual-kinase mechanism for Wnt co-receptor phosphorylation and activation. *Nature* **438**(7069): 873-877.
Zhang, L., Gao, X., Wen, J., Ning, Y., and Chen, Y.G. 2006. Dapper 1 antagonizes Wnt signaling by promoting dishevelled degradation. *J Biol Chem* **281**(13): 8607-8612.
Zhang, X., Abreu, J.G., Yokota, C., MacDonald, B.T., Singh, S., Coburn, K.L., Cheong, S.M., Zhang, M.M., Ye, Q.Z., Hang, H.C., Steen, H., and He, X. 2012. Tiki1 is required for head formation via Wnt cleavage-oxidation and inactivation. *Cell* **149**(7): 1565-1577.
Zhang, X., Zhu, J., Yang, G.Y., Wang, Q.J., Qian, L., Chen, Y.M., Chen, F., Tao, Y., Hu, H.S., Wang, T., and Luo, Z.G. 2007. Dishevelled promotes axon differentiation by regulating atypical protein kinase C. *Nat Cell Biol* **9**(7): 743-754.
Zhang, X.A., He, B., Zhou, B., and Liu, L. 2003. Requirement of the p130CAS-Crk coupling for metastasis suppressor KAI1/CD82-mediated inhibition of cell migration. *J Biol Chem* **278**(29): 27319-27328.
Zhang, X.F., Settleman, J., Kyriakis, J.M., Takeuchi-Suzuki, E., Elledge, S.J., Marshall, M.S., Bruder, J.T., Rapp, U.R., and Avruch, J. 1993. Normal and oncogenic p21ras proteins bind to the amino-terminal regulatory domain of c-Raf-1. *Nature* **364**(6435): 308-313.
Zhang, Z., Vuori, K., Wang, H., Reed, J.C., and Ruoslahti, E. 1996. Integrin activation by R-ras. *Cell* **85**(1): 61-69.
Zheng, C.F., Ohmichi, M., Saltiel, A.R., and Guan, K.L. 1994. Growth factor induced MEK activation is primarily mediated by an activator different from c-raf. *Biochemistry* **33**(18): 5595-5599.
Zheng, C.Y., Seabold, G.K., Horak, M., and Petralia, R.S. 2011. MAGUKs, synaptic development, and synaptic plasticity. *Neuroscientist* **17**(5): 493-512.
Zheng, Y. 2001. Dbl family guanine nucleotide exchange factors. *Trends Biochem Sci* **26**(12): 724-732.
Zhou, W., Lin, L., Majumdar, A., Li, X., Zhang, X., Liu, W., Etheridge, L., Shi, Y., Martin, J., Van de Ven, W., Kaartinen, V., Wynshaw-Boris, A., McMahon, A.P., Rosenfeld, M.G., and Evans, S.M. 2007. Modulation of morphogenesis by noncanonical Wnt

signaling requires ATF/CREB family-mediated transcriptional activation of TGFbeta2. *Nat Genet* **39**(10): 1225-1234.
Zhu, L., Marvin, M.J., Gardiner, A., Lassar, A.B., Mercola, M., Stern, C.D., and Levin, M. 1999. Cerberus regulates left-right asymmetry of the embryonic head and heart. *Current biology : CB* **9**(17): 931-938.
Zhu, W., Shiojima, I., Ito, Y., Li, Z., Ikeda, H., Yoshida, M., Naito, A.T., Nishi, J., Ueno, H., Umezawa, A., Minamino, T., Nagai, T., Kikuchi, A., Asashima, M., and Komuro, I. 2008. IGFBP-4 is an inhibitor of canonical Wnt signalling required for cardiogenesis. *Nature* **454**(7202): 345-349.
Zhu, Y., Shen, T., Liu, J., Zheng, J., Zhang, Y., Xu, R., Sun, C., Du, J., Chen, Y., and Gu, L. 2013. Rab35 is required for Wnt5a/Dvl2-induced Rac1 activation and cell migration in MCF-7 breast cancer cells. *Cell Signal*.
Zhu, Y., Tian, Y., Du, J., Hu, Z., Yang, L., Liu, J., and Gu, L. 2012. Dvl2-dependent activation of Daam1 and RhoA regulates Wnt5a-induced breast cancer cell migration. *PLoS One* **7**(5): e37823.
Zou, J.X., Liu, Y., Pasquale, E.B., and Ruoslahti, E. 2002. Activated SRC oncogene phosphorylates R-ras and suppresses integrin activity. *J Biol Chem* **277**(3): 1824-1827.
Zou, J.X., Wang, B., Kalo, M.S., Zisch, A.H., Pasquale, E.B., and Ruoslahti, E. 1999. An Eph receptor regulates integrin activity through R-Ras. *Proc Natl Acad Sci U S A* **96**(24): 13813-13818.